The Intestinal Physiology of Bariatric Surgery

by

Jerry Dang

A thesis submitted in partial fulfillment of the requirements for the degree of

Doctor of Philosophy

Department of Surgery

University of Alberta

Abstract

Background

Evidence is emerging that the gut microbiome is an important contributor to the weight and metabolic effects of bariatric surgery. However, the microbial and intestinal physiological changes that occur with bariatric surgery are poorly understood. Developing this understanding potentially opens avenues for the development of targeted therapies to treat obesity and its metabolic diseases.

Aims

The aims of this study were to perform a comprehensive analysis of the physiological intestinal changes after bariatric surgery including microbial, metabolomic, gut hormonal, and morphological changes.

Methods

In the first study, we developed a protocol to perform Roux-en-Y gastric bypass (RYGB) in rats that had similar weight loss and metabolic changes to human RYGB. Secondly, we performed RYGB in rats to study changes in the distal ileum. The distal ileum demonstrates the most significant bile acid changes and is also the location where important gut hormones, such as glucagon-like-peptide-1, are produced. Thirdly, we conducted a three-arm prospective clinical trial in humans undergoing RYGB, sleeve gastrectomy (SG) and non-operative controls (CTRL)

to understand the microbial, metabolomic, and inflammatory changes that occur after bariatric surgery.

Results

In the first study, we developed an excellent RYGB surgical model in rats that had an overall survival of 88.9%. This model had significantly greater weight loss and better glucose tolerance compared to the sham surgery cohort. It was also an easily reproducible procedure that required no formal surgical training or experience.

In the second study, we performed RYGB and sham surgery in a cohort of rats and divided them into early (2 week) and late (14 week) cohorts. Ileal samples were comprehensively analyzed. At 14 weeks, there was increased L-cell density and increased villi height in the RYGB cohort. Bile acid analysis found lower concentrations of ileal bile acids following RYGB. Both early and late RYGB cohorts demonstrated higher abundances of *Escherichia-Shigella* and lower abundances of *Lactobacillus*. These shifts in microbial composition appeared to drive bile acid reductions as the loss of *Lactobacillus* and the increase in *Escherichia-Shigella* were both correlated with decreases in specific taurine and glycine conjugated bile acids.

Our three-arm human trial found significant microbial and metabolic shifts after RYGB and SG. We conducted integrated microbial-metabolomic analysis and identified three unique pathways that contribute to weight loss and metabolic improvement. In the first pathway, the abundance of

Romboutsia decreased after RYGB. This decrease was correlated to decreases in multiple different glycerophospholipids. This decrease in *Romboutsia* was correlated with lower weight and insulin resistance and appears to be a key pathway in RYGB.

After SG, the aminoacyl-tRNA pathway was significantly enriched in both the microbiome and metabolome. This enrichment was linked to a decreased abundance of a cluster of Firmicutes bacteria consisting of *Butyriciccocus*, *Eubacterium ventriosum* and *Monoglobus*. This Firmicutes shift was correlated with an increase in five amino acids which consequently enriched the aminoacyl-tRNA pathway. This pathway appears to be a driver of metabolic change as the loss of this Firmicutes cluster was correlated with lower weight, decreased insulin resistance, and decreased systemic inflammation.

When performing between group comparisons, SG demonstrated an enriched sphingolipid metabolism pathway at 9 months compared to RYGB. This pathway was enriched due to the loss of a cluster of Firmicutes bacteria (*Monoglobus*, *Eubacterium ventriosum*, *Eubacterium hallii*, *Dorea*, and *Lachnospira*) which correlated to increases in sphingomyelins and hydroxysphingomyelins and concurrently correlated to improved glucose tolerance. This appears to be a pathway in which SG, but not RYGB, improved glucose homeostasis.

Conclusions

In summary, this body of work identified pathways in which SG and RYGB induce weight loss and improved glucose metabolism. This occurred through various microbial-metabolomic pathways which included bile acids, glycerophospholipids, amino acids, and sphingolipids. Translational work building upon these findings by targeting and inducing shifts in microbial, metabolomic, or bile acid composition may lead to novel therapeutic options to treat obesity and its associated metabolic diseases.

Preface

This thesis is an original work by Jerry Dang. The human research project, of which this thesis is a part, received research ethics approval from the University of Alberta Research Ethics Board, Project Name "The Microbiology of Bariatric Surgery", No. PRO00071705, April 21, 2017. The rat research project, of which this thesis is a part, also received research ethics approval from the University of Alberta Research Ethics Board, Project Name "Bariatric Surgery in Rats", No. AUP00003000, January 8, 2019.

Chapter 2 of this thesis is published as: Dang JT, Mocanu V, Fang B, Laffin M, Karmali S, Madsen K, Birch DW. A Protocol for Roux-en-Y Gastric Bypass in Rats using Linear Staplers. *Journal of Visualized Experiments*. I was responsible for developing the surgical technique, writing the article, and filming the video. V. Mocanu assisted in developing the protocol and with filming. B. Fang helped narrate and edit the video. M. Laffin offered experience with murine surgical models.

Chapters 3 contains collaborative work with H. Park, V. Mocanu, M. Laffin and N.Hotte. I was responsible for performing rat procedures, rat husbandry, analyzing samples, statistical analysis and preparation of the manuscript. H. Park assisted with bioinformatics analysis. V. Mocanu and M. Laffin assisted with study design and reviewing the manuscript. N. Hotte assisted with analyzing samples.

Chapter 4 contains collaborative work with H. Park, V. Mocanu, M. Laffin, N.Hotte, and C. Tran. I was responsible for all patient consent, recruitment, follow-up and collection of samples for analysis. I performed laboratory analysis, statistical analysis, and preparation of the manuscript. H. Park assisted with bioinformatics analysis. V. Mocanu and M. Laffin assisted with study design and reviewing of the manuscript. N. Hotte assisted with analyzing samples. C. Tran assisted with counting L and K cells on immunofluorescence.

The remainder of the chapters in this thesis are original work performed by me in consultation with my supervisory committee.

Acknowledgements

I would like to thank my primary supervisor, Daniel Birch, for his mentorship, encouragement and support. I would like to thank my co-supervisor Karen Madsen for your endless advice, expertise and wisdom. I would also like to thank my co-supervisor Shahzeer Karmali for always looking out for me and providing me with countless opportunities.

Thank you to all members of the lab, especially Naomi, who was always there to make sure my experiments did not go haywire.

A special acknowledgement to my funding agencies that made this PhD possible through their generous financial support. Alberta Innovates, the University of Alberta, the Canadian Institutes of Health Research, the Centre of Excellence for Gastrointestinal Inflammation and Immunity Research, the Centre for the Advancement of Surgical Education and Simulation, the Society of American Gastrointestinal and Endoscopic Surgeons, and the American Society for Metabolic and Bariatric Surgery.

Finally, thank you to my loving wife Nhi, you have been incredibly patient and supportive of my goals and passions.

TABLE OF CONTENTS

LIST OF TABLES

LIST OF FIGURES

LIST OF SUPPLEMENTARY TABLES

LIST OF SUPPLEMENTARY FIGURES

CHAPTER 1. INTRODUCTION

1.1 OBESITY

1.1.1 INTRODUCTION

The prevalence of obesity has increased drastically over the past three decades and currently more than 600 million people worldwide are categorized as obese[1]. Obesity reduces quality of life and increases early mortality[2]. In the largest meta-analysis to date consisting of 230 cohort studies including over 30 million individuals, obesity was found to be associated with an increased risk of all-cause mortality[3]. It was associated with significant health risks including diabetes, coronary heart disease, hypertension and dyslipidemia[4,5]. Obesity has recently surpassed smoking as the leading cause of preventable diseases[6]. Given this, weight loss has been the primary focus for the treatment of obesity as higher body mass index (BMI) increases the risk of morbidity and mortality[7].

Weight loss has been demonstrated to be effective at reducing morbidity and mortality[8,9]. This includes reductions in the progression of diabetes[10,11] and improvements in hypertension[12]. Weight loss strategies have traditionally been focused on lifestyle interventions with a combination of diet, exercise, and behavioral modification. However, obesity is now recognized as a chronic, relapsing disease process[13] with complex physiological processes that lead to resistance to traditional weight loss strategies[14]. Studies have demonstrated that intensive lifestyle interventions typically only lead to weight loss of less than 10%[15]. To achieve better weight loss and metabolic outcomes, current treatment options for patients with severe obesity requires the inclusion of pharmacological therapy and bariatric surgery[15].

Pharmacological therapy is considered in patients with a BMI greater than 30 kg/m^2 or 27 to 30 kg/m^2 with associated comorbidities (i.e. diabetes, hypertension, obstructive sleep apnea, etc.). Bariatric surgery is considered for those who have severe obesity, defined as a BMI >40 kg/m^2 or >35 kg/m^2 with a comorbidity, and is the most effective means for achieving sustained weight loss with demonstrated improvement in morbidity and mortality[16–18].

1.1.2 Definition and Prevalence

The World Health Organization (WHO) defines overweight and obesity as abnormal or excessive fat accumulation that presents a risk to health[19]. A more objective measure of obesity uses BMI and considers a person as having obesity if their BMI is greater than 30 kg/m^2 and overweight as a BMI between 25 and 30 kg/m^2[19]. Classification of obesity by BMI are shown in Table 1.

Table 1. National Institutes of Health Classification of Overweight and Obesity by BMI, Waist Circumference, and Associated Disease Risks[20]

			Disease Risk* Relative to Normal Weight and Waist Circumference+	
	BMI (kg/m^2)	**Obesity Class**	**Men 102 cm (40 in) or less Women 88 cm (35 in) or less**	**Men > 102 cm (40 in) Women > 88 cm (35 in)**
Underweight	< 18.5		-	-
Normal	18.5–24.9		-	-
Overweight	25.0–29.9		Increased	High
Obesity	30.0–34.9	I	High	Very High
	35.0–39.9	II	Very High	Very High
Extreme Obesity	40.0 +	III	Extremely High	Extremely High

* Disease risk for type 2 diabetes, hypertension, and CVD.
+Increased waist circumference also can be a marker for increased risk, even in persons of normal weight.

The prevalence of obesity has been increasing at an alarming rate and has nearly doubled from 1980 to 2008. It is estimated that more than half a billion adults worldwide have obesity[21]. The WHO estimates that 2.8 million people die worldwide due to being overweight or obese and that 35.8 million of global disability-adjusted life years are caused by being overweight or obese[21]. The economic and societal costs of obesity are also staggering, estimated to be at 147 billion USD a year in the United States alone[22].

1.1.3 ETIOLOGY

Obesity is a chronic disease that affects children and adults. It is a multifactorial disease caused by a chronic surplus of energy in which energy intake exceeds expenditure[23]. This leads to the accumulation of adipose tissue[23]. Factors that contribute to obesity include lifestyle, diet, the environment, medications, socioeconomic factors, psychological factors, genetics, congenital disorders, neuroendocrine disorders, and the gut microbiome.

Regulation of energy homeostasis involves multiple, complex processes and is key to understanding the pathogenesis of obesity. Obesity is thought to stem from evolutionary mechanisms that promote fat accumulation when food is available so that humans may survive during periods of scarcity or famine. However, in an "obesogenic" environment, where high calorie food is available in abundance and periods of famine do not exist, this promotes obesity. Energy expenditure has also decreased in this pathogenic environment, due to an increase in sedentary occupations, which contributes to this imbalance in energy homeostasis[24]. This is supported by models of human energy homeostasis that suggest energy homeostasis is biased

towards weight gain since in the basal state, catabolic effector pathways are activated while anabolic pathways are inhibited[25].

Recent advances in gene sequencing have offered insights into the impact of the gut microbiome on obesity, specifically on its role in human metabolism and adiposity. The gastrointestinal microbiota has an impact on insulin resistance, inflammation and adiposity. Furthermore, large-scale changes in the gut microbiota are associated with obesity and respond to weight loss. Studies also demonstrate that restoration of the gut microbiota to a healthy state may reduce obesity and obesity-related diseases[26]. The impact of the human microbiome on obesity are discussed further in Section 1.7.

1.1.4 Health Consequences of Obesity

Obesity is associated with multiple health diseases. These include diabetes, dyslipidemia, hypertension, heart disease, stroke, venous thrombosis, osteoarthritis, gout, hepatobiliary disease, reflux, cancers, kidney stones, chronic kidney disease, urinary incontinence, depression, dementia, sleep apnea, infection and skin changes[27].

1.1.5 Treatments for Obesity

The long-term efficacy and effectiveness of obesity treatments has historically been poor. As obesity is a chronic and progressive condition, patients require long-term treatment[28]. Treatments focused on lifestyle modifications including changes to diet, exercise and behaviors lead to high

failure and usually lead to only minimal weight loss[10,29]. In severe obesity, many patients do not achieve significant weight loss goals with lifestyle interventions and drug therapy and surgery are typically needed.

1.1.5.1 DRUG THERAPY

Anti-obesity drugs can be useful as adjuncts to lifestyle interventions in patients with a BMI greater than 30 kg/m^2. There are currently multiple agents for achieving weight loss and most patients will achieve a 5 to 10 percent weight loss[30,31]. Two popular agents are Orlistat, which alters fat digestion by inhibiting pancreatic lipase[32], and liraglutide, a glucagon-like peptide-1 (GLP-1) analogue that suppresses appetite[33]. This amount of weight loss can significantly reduce the development of diabetes, hypertension or cardiovascular disease[34]. However, drug therapy does not cure obesity and a disruption of drug therapy typically results in weight regain, although long-term studies are lacking[31].

1.1.5.2 BARIATRIC SURGERY

While lifestyle interventions remain the mainstay of treatment in obesity, bariatric surgery has proven to be an effective therapy in treating severe obesity with sustained weight loss[9]. Current guidelines for the surgical management of obesity were first established by the National Institutes of Health (NIH) in 2004 and reviewed by the American Bariatric Society in 2004. Candidates for bariatric surgery must have a BMI $\geq$ 40 kg/m^2 without comorbid illness or a BMI of 35.0 to 39.9 kg/m^2 with at least one serious comorbidity. These include type 2 diabetes, obstructive sleep apnea (OSA), hypertension, hyperlipidemia, obesity-hypoventilation syndrome,

nonalcoholic fatty liver disease (NAFLD), pseudotumor cerebri, gastroesophageal reflux disease (GERD), asthma, venous stasis disease, severe urinary incontinence, debilitating arthritis, or impaired quality of life[35–37].

Bariatric surgery should be performed as part of a comprehensive assessment program. The American College of Surgeons (ACS) and the American Society of Metabolic and Bariatric Surgeons (ASMBS) have published standards on the preoperative assessment and postoperative care for bariatric patients. Part of these standards require patients receive assessment and care from a multidisciplinary team consisting of nurses, dieticians, psychologists, and physical therapists as well as the medical and surgical team[38].

The three most common bariatric procedures performed are laparoscopic adjustable gastric banding (AGB), sleeve gastrectomy (SG) and Roux-en-Y gastric bypass (RYGB). However, AGB is becoming less popular as recent studies have demonstrated frequent weight loss failure and long-term complications[39]. Bilio-intestinal bypass (BIB) is an uncommonly performed bariatric procedure where jejunum is divided 40 cm distal to the ligament of Treitz and then anastomosed 40 cm proximal to the ileocecal valve. An anastomosis is then performed between the blind jejunal limb and the gallbladder to modify bile flow which has been shown to affect the human intestinal microbiota[40,41]. Currently, RYGB is the most commonly performed bariatric procedure worldwide, while SG is the most common in the United States [42].

1.2 BARIATRIC SURGICAL PROCEDURES

1.2.1 SLEEVE GASTRECTOMY

SG was originally developed as the first part of a two-stage procedure for biliopancreatic diversion with duodenal switch[43]. However, it became an effective standalone procedure because of effective weight loss and remission of obesity-related comorbidities. This procedure entails resection of the greater curvature and fundus of the stomach (Figure 1). Sleeve gastrectomy induces weight loss by two mechanisms, by mechanical restriction and through an alteration in gut hormones involved in the central regulation of food intake[44].

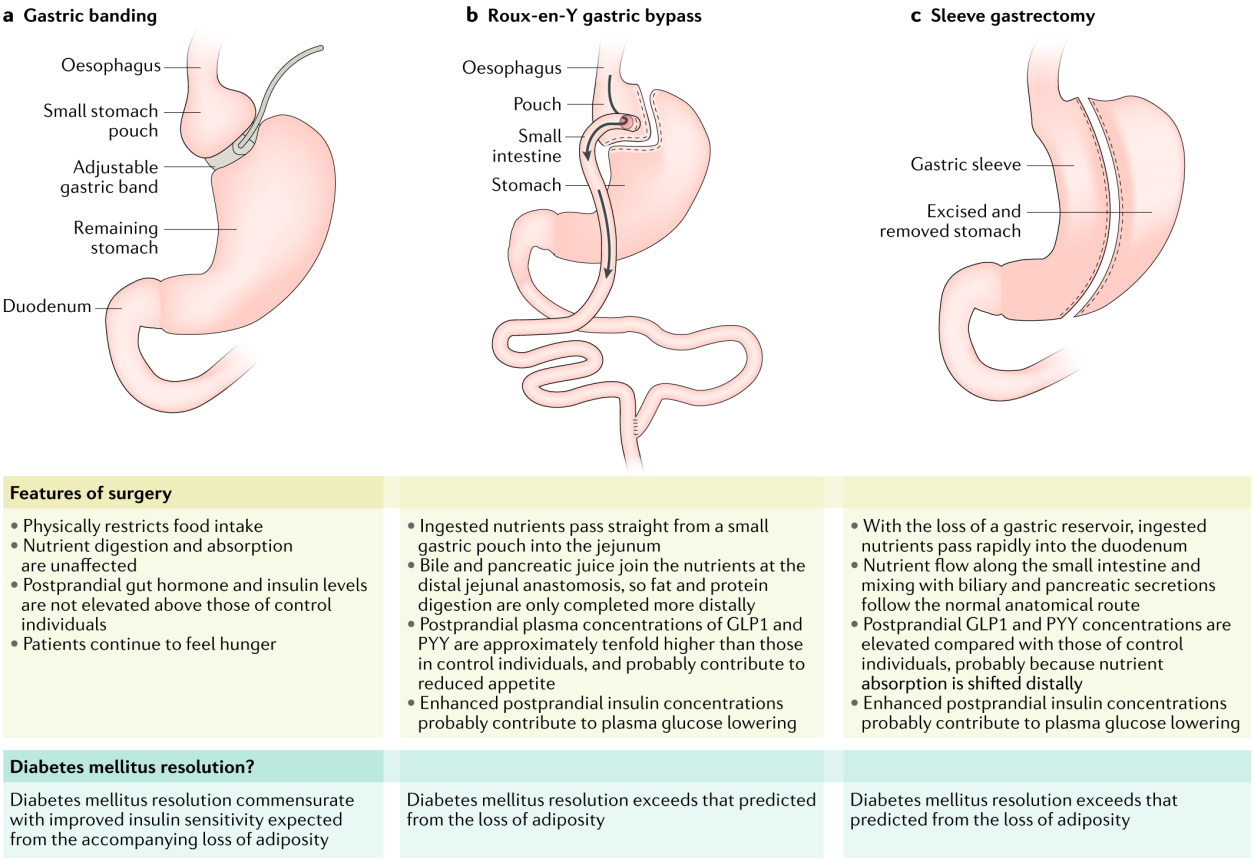

Figure 1. Bariatric surgical procedures for metabolic disease

Material from: Gribble FM, Reimann F. Function and mechanisms of enteroendocrine cells and gut hormones in metabolism. Nature Reviews Endocrinology. 2019 Apr;15(4):226-37. Reproduced with permission of Springer Nature via Copyright Clearance Center.[45]

After SG, the stomach volume is reduced in both volume and distensibility; overall volume is reduced by about 70 to 80 percent[46]. Removal of the stomach also removes ghrelin-producing cells, which function to stimulate appetite[44] and results in a reduction in appetite after surgery. Further, there is an increase in GLP-1, which is a hormone that increases insulin secretion as well as slows gastric emptying and intestinal motility. It is hypothesized that an increase in GLP-1 induces satiety, reduces hunger and improves glucose metabolism[47].

1.2.2 Roux-en-Y Gastric Bypass

As a bariatric procedure, RYGB was first described in 1966[48]. Compared to SG, it results in more durable weight loss and higher rates of remission of obesity-related comorbidities [16–18]. It is, however, associated with slightly higher rates of complications and mortality than SG[16].

RYGB involves the creation of a small gastric pouch (less than 30 mL), and the creation of a biliopancreatic limb and a Roux limb (Figure 1). The biliopancreatic limb is typically 30 to 50 cm and transports secretions from the gastric remnant, liver and pancreas. The Roux limb is typically 75 to 150 cm in length and is the primary channel for ingested food. The common channel is the remaining small bowel distal to where the two limbs join together and is where the majority of digestion and absorption occur, as pancreatic enzymes and bile mix with ingested food[49].

Like SG, the mechanism of weight loss in RYGB is multimodal. The small gastric pouch reduces food intake through mechanical restriction. The bypass results in a malabsorptive component as a significant portion of the small intestine is not absorbing calories and nutrients. More recently, studies have demonstrated that gut hormones play a significant role in weight loss after RYGB as well. These are primarily through ghrelin, peptide-YY, cholecystokinin (CCK), and GLP-1 hormone pathways[50].

Multiple studies demonstrate a suppressed ghrelin level, which likely contributes to the typical loss of appetite after RYGB[51–53]. Additionally, there is an increase in the response of peptide-YY and CCK to food intake, further suppressing appetite[51]. GLP-1 is an incretin hormone that is secreted by L-cells primarily in the distal intestine. GLP-1 rises dramatically after RYGB, and it is theorized that by bypassing the upper gut, nutrients are exposed earlier to the intestinal L-cells, causing an increase in GLP-1 release. GLP-1 likely plays a large role in the early improvement and remission of diabetes in patients after gastric bypass by potentiating the response of beta islet-cells in the pancreas which is ultimately responsible for secreting insulin. Thus, this rise in GLP-1 has been correlated with increased insulin secretion and insulin sensitivity after RYGB[54,55].

While weight loss through bariatric surgery has been shown to result from a combination of restrictive, malabsorptive and hormonal factors, the gut microbiota also plays a role in the effects of bariatric surgery, which will be discussed further in Section 1.7.2.

1.3 OUTCOMES OF BARIATRIC SURGERY

1.3.1 WEIGHT LOSS

Weight loss is most commonly reported as percentage of excess weight loss (EWL) in the bariatric surgery literature. EWL is defined as = (Weight loss)/(Baseline weight – Ideal weight) x 100[56]. At two years, the expected EWL after RYGB is typically about 70 percent[57] and after SG about 60 percent[58–60].

There is strong evidence that weight loss is sustained long term after bariatric surgery[16]. However, there are a certain proportion of patients who will fail at weight loss or even regain previous weight loss, referred to as weight recidivism. Magro et al.[61] followed RYGB patients prospectively for five years and found that 50 percent had weight regain, with a mean 8 percent increase from post-operative weight at one year. In a systematic review on weight recidivism after bariatric surgery, the cause of weight regain was multifactorial and included nutritional non-compliance, hormonal or metabolic imbalances, mental health disorders, physical inactivity and surgical or anatomic factors[62].

1.3.2 DIABETES

Bariatric surgery, especially RYGB, is effective at treating type 2 diabetes. Improvement in metabolic control typically occurs within days to weeks after RYGB, prior to significant weight loss. This is likely due to metabolic alterations that occur with RYGB, especially its effect on increasing GLP-1 release[63].

Diabetes remission or improvement was found to occur in 83 percent of patients in one large, prospective study. There have also been multiple randomized controlled trials comparing RYGB to medical management and have found that RYGB is superior in achieving diabetes remission. Diabetes remission rates after RYGB range from 40 to 83 percent, depending on the definition of remission, compared to zero percent with medical therapy[58,64–66]. However, two new randomized controlled trials, the SLEEVEPASS and SM-BOSS trials, demonstrate that diabetes remission is similar between RYGB and SG beyond five years postoperatively[67,68].

Diabetes remission rates are high for other bariatric procedures as well. In a large, prospective study by the American College of Surgeons Bariatric Surgery Center Network (ACS-BSCN), remission rates were found to be 83 percent for RYGB, 55 percent for SG, and 44 percent for AGB[58]. Factors that predict diabetes remission after bariatric surgery include young age, low glycosylated hemoglobin, and absence of preoperative need for diabetes medications or insulin.[69]

1.3.3 CARDIOVASCULAR

Cardiovascular risk factors such as hypertension and dyslipidemia have a well-established association with obesity[70,71]. Remission of hypertension with bariatric surgery is common. RYGB has higher remission rates than SG. In the ACS-BSCN study, remission of hypertension occurred in 79 percent of patients after RYGB, 68 percent after SG and 44 percent after AGB[58]. In another prospective study, remission rates were 59.9 percent for RYGB and 38.8 percent for SG[72].

Obesity-associated dyslipidemia also improves with bariatric surgery. The ACS-BSCN prospective study found highest rates of dyslipidemia remission after RYGB of 66 percent compared with 35 percent for SG and 33 percent for AGB[58].

1.3.4 Obstructive Sleep Apnea

There is an increased prevalence of OSA in obese populations[73]. Weight loss decreases the apnea hypopnea index, which is the number of apneic episodes or hypopneas per hour of sleep[74]. A recent systematic review found that after bariatric surgery, the majority of patients had resolution or improvement of OSA. Resolution or improvement after RYGB was 79 percent, SG was 86 percent and AGB was 77 percent[75].

1.3.5 Other Comorbidities

Bariatric surgery also improves polycystic ovarian syndrome, NAFLD, depression, quality of life and body image[76]. RYGB leads to improvement in GERD, but it is unclear whether SG improves or worsens symptoms. A systematic review on SG and GERD found seven studies that demonstrated a decrease in GERD prevalence but four studies that demonstrated an increase in severity of GERD[77].

1.3.6 Long-term Survival

Long-term survival is improved after bariatric surgery, primarily from a reduction in cardiovascular deaths. The Swedish Obese Subjects (SOS) study, a large, prospective study, demonstrated significantly lower numbers of cardiovascular deaths in the bariatric surgery group compared to the control group (1.4 vs 2.4 percent, respectively) and cardiovascular events (9.9 vs 11.5 percent, respectively) [78]. There were also less deaths from all causes in the surgery group than the control group overall (5.0 vs 6.3 percent, respectively)[16]. Weight loss was also shown to reduce lifetime cancer risk. In the SOS study, after bariatric surgery, the risk of all cancers was reduced from 6 to 3.9 percent over 20 years [79]. Cancer mortality was also lower after bariatric surgery. A study by Adams et al. demonstrate a cancer mortality reduction of 46 percent after bariatric surgery[80].

1.3.7 Complications

The 30-day mortality after bariatric surgery is low at 0.2 to 0.6 percent[81–83]. Serious complications include leak, bleeding, venous thromboembolism, marginal ulceration, internal herniation, stomal obstruction, and stenosis. Overall complication rates from the National Surgical Quality Improvement Program (NSQIP) have decreased from 4.6 percent in 2005 to 3.0 percent in 2013 with improvement in surgical technique, patient selection, preoperative and postoperative care[84]. There are two syndromes related to hyperinsulinemic hypoglycemia that may be related to changes in gut hormones after bariatric surgery and are relevant to the themes of this thesis. These are late dumping syndrome and hyperinsulinemic hypoglycemia with nesidioblastosis.

Dumping Syndrome

Neilsen et al. found that dumping syndrome occurs in 9.4% of patients after RYGB[85]. Dumping syndrome has two types, early and late. Early dumping syndrome usually occurs rapidly, within 15 minutes, and is due to rapid emptying of hyperosmolar food into the small bowel due to the changed intestinal configuration after RYGB. This causes a rapid fluid shift to occur in the small bowel and results in hypotension as well as a sympathetic nervous system response. Symptoms include abdominal pain, nausea, diarrhea, and tachycardia[86]. Late dumping syndrome, also referred to as postprandial hyperinsulinemic hypoglycemia is rare and occurs in approximately 0.1 to 0.3% of patients after RYGB. This syndrome occurs one to three hours after meals and results in hyperinsulinemic hypoglycemia. The pathophysiology is thought to occur due to an excessive release of insulin after high-carbohydrate meals[87]. An increased release of incretins such as GLP-1 and GIP are thought to play a role in late dumping syndrome but the pathophysiology remains incompletely understood[88]. Dumping syndrome is usually treated by dietary modifications with avoidance of foods high in simple sugars and with smaller, more frequent meals. However, refractory dumping syndrome may require medications such as calcium channel blockers or revisional bariatric surgery[89].

Hyperinsulinemic Hypoglycemia with Nesidioblastosis

Hyperinsulinemic hypoglycemia with nesidioblastosis (HHN) results in similar symptoms to late dumping syndrome due to postprandial hypoglycemia. However, the development of HHN is rare after RYGB and these patients demonstrate islet cell hyperplasia, histologically described as nesidioblastosis. Nesidioblastosis is defined as the proliferation of both ductular and islets cells,

with hypertrophy of beta cells within islets and formation of ductuloinsular complexes[90]. This hypertrophy of beta cells leads to increases in the secretion of insulin after meals. Diagnosis is made via selective arterial calcium stimulation since calcium is an insulin secretagogue. Most patients are successfully treated with partial pancreatic resection, however, some patients with recurrent symptoms may require completion pancreatectomy[91].

Hyperplasia of islet cells after RYGB appears to be driven by gut hormonal changes, primarily from hypersecretion of insulin-stimulating hormones such as GLP-1 and GIP[92]. Lee at al. attempted to treat nesidioblastosis with reversal of RYGB but this did not alleviate hypoglycemia despite large reductions in circulating GLP-1 levels. Instead, this study found dramatically higher levels of GIP after RYGB reversal and it appears that GIP plays an important role in persistent nesidioblastosis after RYGB reversal[93].

1.4 GUT HORMONES IN BARIATRIC SURGERY

1.4.1 GUT HORMONE FUNCTIONS

Gut hormones play key roles in bariatric surgery. Table 2 summarizes key gut hormones and their functions.

Table 2. Gut hormones involved in food intake or glucose homeostasis[45]

Hormone	Site Released	Organ	Functions
Cholecystokinin	I-cells	Proximal small intestine	• Stimulates gall bladder contraction • Stimulates bile and pancreatic secretions • Stimulates motility

Gastrin	G-cells	Stomach and Duodenum	• Stimulates gastric acid production
Ghrelin	X/A-cells	Stomach	• Increases appetite
Glucagon-like-peptide-1	L-cells	Distal small intestine and colon	• Stimulates insulin release • Inhibits gastric acid release and gastric emptying • Increases β-cell mass • Increases satiety
Gastric inhibitory polypeptide	K-cells	Duodenum and jejunum	• Stimulates insulin secretion • Influences fatty acid metabolism • Increases β-cell proliferation
Peptide YY	L-cells	Distal small intestine and colon	• Inhibits gastric motility • Increases satiety

GLP-1 is one of the most important gut hormones in bariatric surgery. It is released postprandially by intestinal endocrine L-cells[94] and has effects on a diverse set of pathways as demonstrated by Figure 2. After both RYGB and SG, there is an increase in postprandial GLP-1 that increases temporally with time from surgery[95]. It contributes to weight loss by inhibiting hunger, delaying gastric emptying and slowing intestinal motility. It also improves glucose homeostasis by stimulating insulin secretion and biosynthesis in the pancreas as well as peripherally mainly by increasing glucose uptake in white adipose tissue and skeletal muscle and by decreasing glucose production in the liver[95].

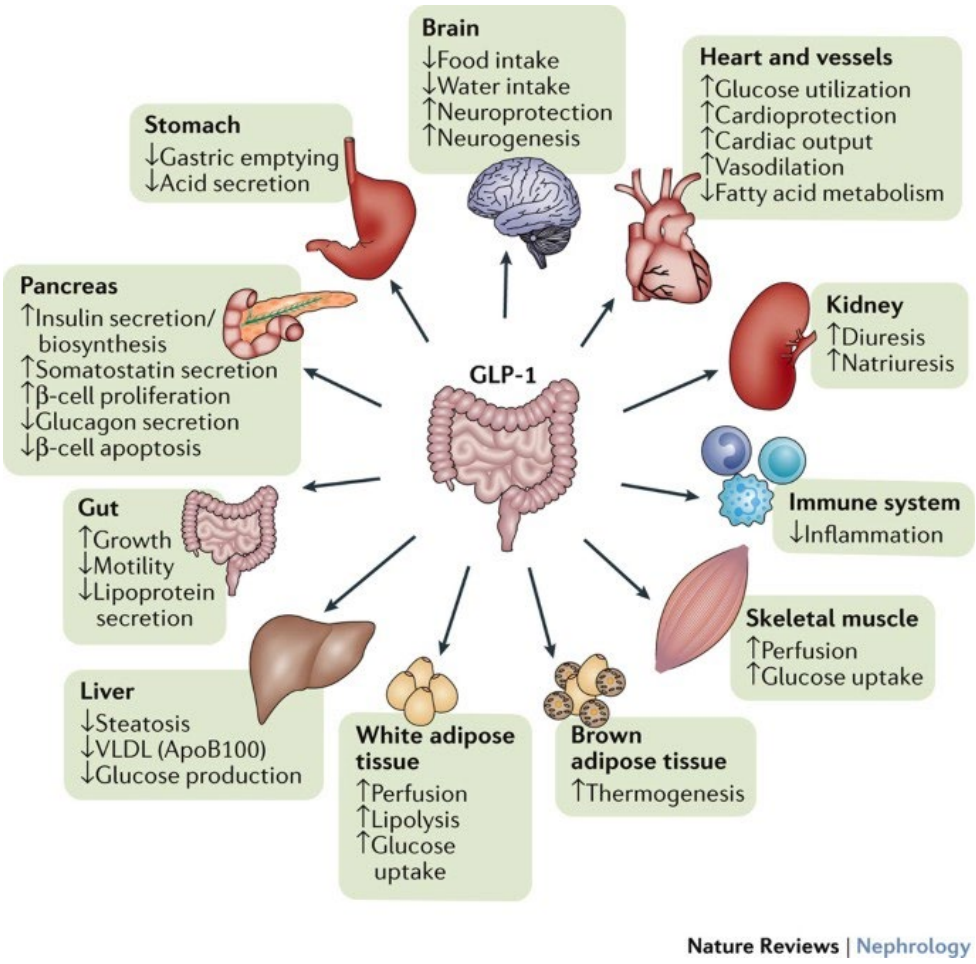

Figure 2. The multimodal effects of glucagon-like-peptide 1.

Material from: Muskiet, M., Tonneijck, L., Smits, M. *et al.* GLP-1 and the kidney: from physiology to pharmacology and outcomes in diabetes. *Nat Rev Nephrol* **13,** 605–628 (2017). https://doi.org/10.1038/nrneph.2017.123. Reproduced with permission of Springer Nature via Copyright Clearance Center. [94]

The regulation of GLP-1 release from L cells is regulated by nutritional, hormonal, and neural signals[94]. Proteins, lipids, electrolytes and carbohydrates are directly sensed on the luminal side of the L cell via G-protein-coupled receptors that function as chemosensors. This triggers the exocytosis of GLP-1 on the basolateral side of the L-cell (Figure 3). L cells also respond directly to proteins produced by gut microbiota such as *Akkermansia mucinaphila* to stimulate the release

of proglucagon (ie. the precursor to GLP-1)[96]. Short-chain fatty acids (SCFA), long chain fatty acids (LCFA) and deconjugated bile acids have also been shown to stimulate GLP-1 release from L cells[94].

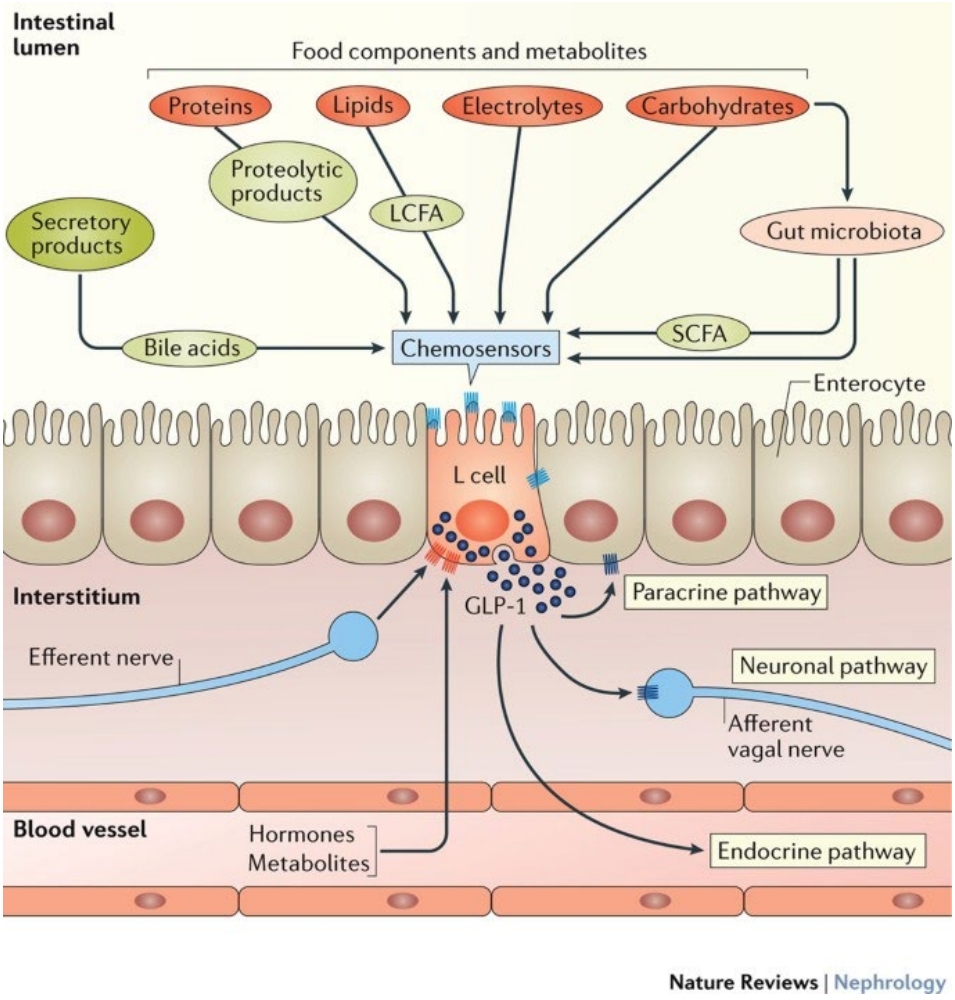

Figure 3. The sensory and secretory function of the L cell.

Material from: Muskiet, M., Tonneijck, L., Smits, M. *et al.* GLP-1 and the kidney: from physiology to pharmacology and outcomes in diabetes. *Nat Rev Nephrol* **13,** 605–628 (2017). https://doi.org/10.1038/nrneph.2017.123. Reproduced with permission of Springer Nature via Copyright Clearance Center.[94]

1.4.2 Gut Hormones and Glucose Metabolism

Sodium glucose cotransporters (i.e., SGLT1) drive glucose absorption across the small intestinal epithelium. This results in elevated plasma glucose concentrations and increasing plasma glucose triggers elevation of cellular calcium concentrations within pancreatic β-cells which consequently secrete insulin. Glucose also crosses via SGLT within K or L cells and this triggers release of glucose-dependent insulinotropic polypeptide (previously called gastric inhibitory polypeptide, GIP) and GLP-1, respectively. Pancreatic β-cells have GIP and GLP-1 receptors and concurrent rises in glucose concentration and binding by GIP and GLP-1 gut hormones results in increased insulin secretion. This process occurs via cAMP pathways[45] (Figure 4).

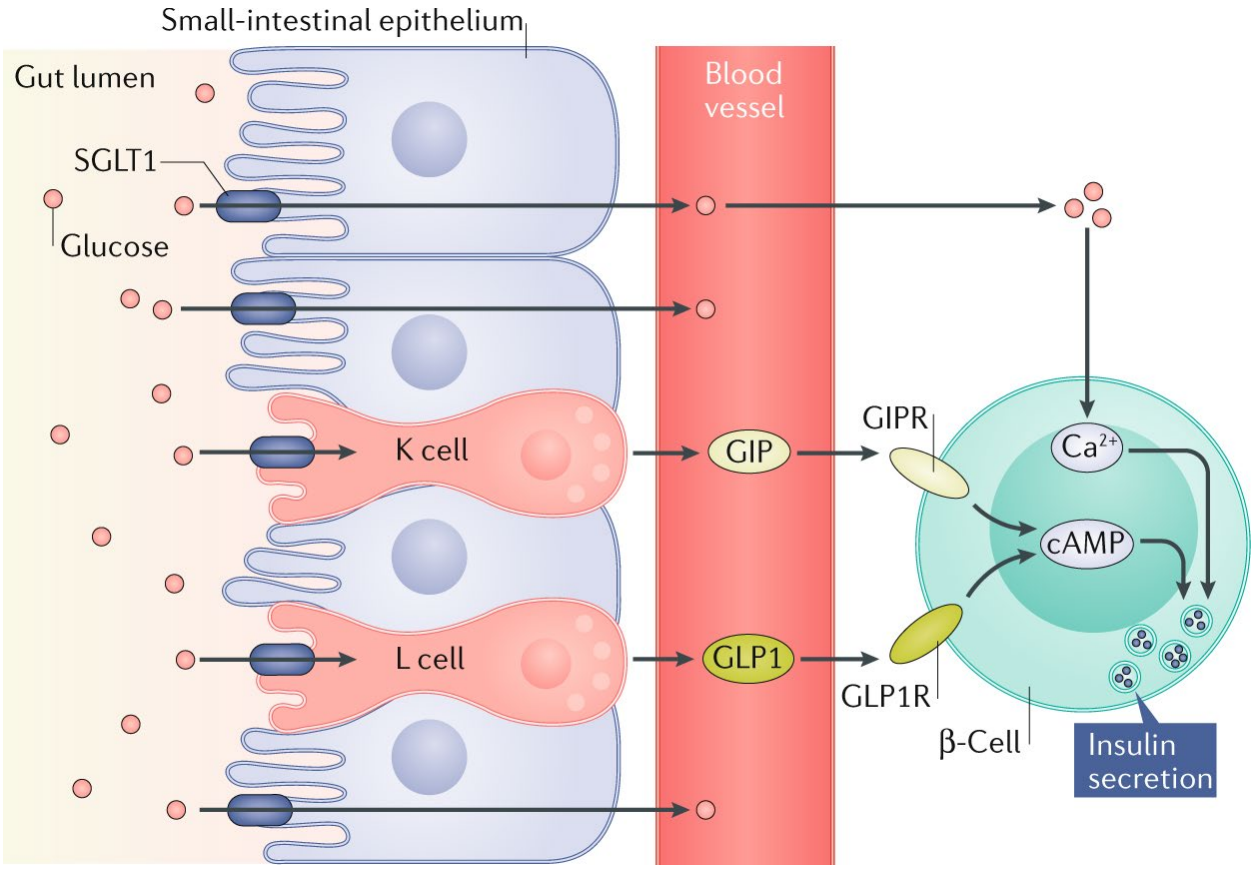

Figure 4. Glucose transport through intestinal epithelium and incretin effects.

Material from: Gribble FM, Reimann F. Function and mechanisms of enteroendocrine cells and gut hormones in metabolism. Nature Reviews Endocrinology. 2019 Apr;15(4):226-37. Reproduced with permission of Springer Nature via Copyright Clearance Center.[45]

1.4.3 Microbiota Interactions with Enteroendocrine Cells

There is emerging evidence demonstrating microbial pathways that stimulate secretion from enteroendocrine cells[45]. These occur mainly through deconjugated secondary bile acids, SCFAs, lipopolysaccharides (LPS), and indoles[45] (Figure 5). The gut microbiota produces these metabolites by fermentation or by other enzymatic pathways. Certain bacterial species participate in deconjugation of bile acids and these bile acids are permeable across the epithelium to trigger GPBAR1 which signals the L cell to secrete GLP-1, PYY, and glucagon-like-peptide-2 (GLP-2). SCFAs are the main metabolite produced in the colon by bacterial fermentation of dietary fibers and resistant starch. SCFAs can permeate through the epithelium and trigger gut hormone release via binding to the free-fatty-acid receptor. SCFAs also act on histone deacetylase to stimulate the release of PYY. Another trigger is LPS which is a component of the gram-negative bacterial cell wall. LPS does not normally permeate through the epithelium, however, in settings of dysbiosis and poor mucosal barrier integrity, LPS is able to reach the basolateral side and targets toll-like-receptor-4 (TLR4), which causes secretion of GLP-2 to promote intestinal repair. Indoles, which also act via TLR4, are organic compounds generated by bacterial aromatic amino acid catabolism. These compounds target voltage-gated (K_V) channels on L-cells resulting in membrane depolarization, calcium entry, and TLR4 signaling[45].

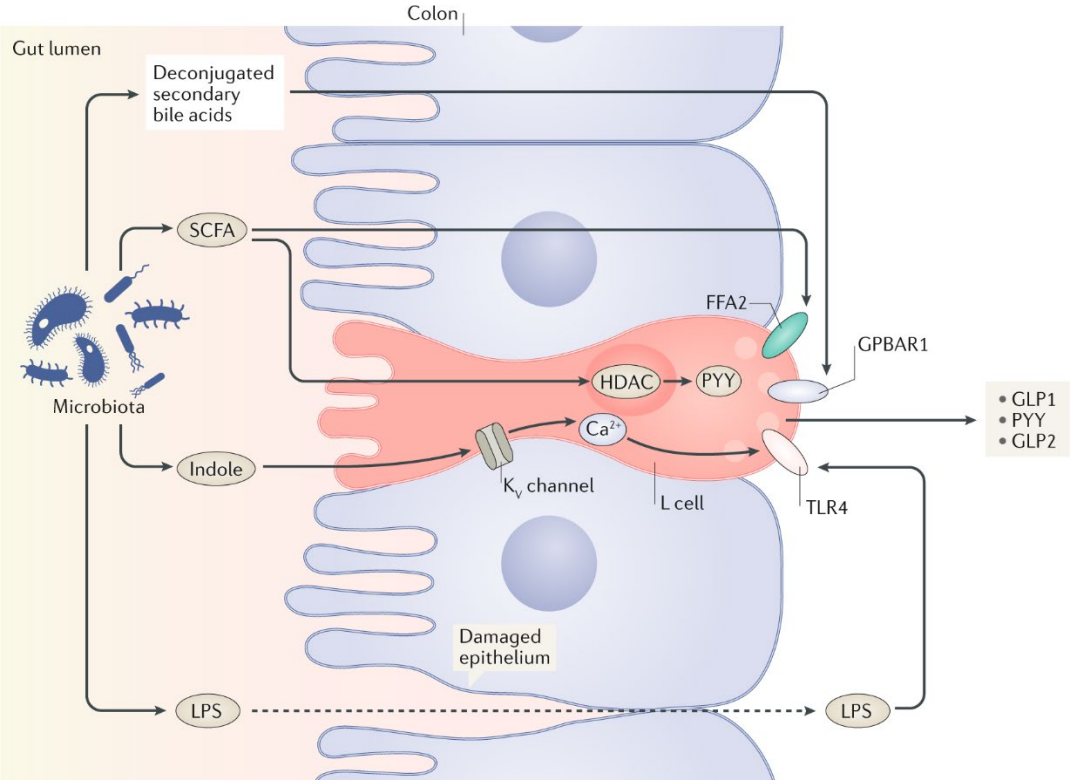

Figure 5. Microbiota interactions with enteroendocrine cells in the colon.

Material from: Gribble FM, Reimann F. Function and mechanisms of enteroendocrine cells and gut hormones in metabolism. Nature Reviews Endocrinology. 2019 Apr;15(4):226-37. Reproduced with permission of Springer Nature via Copyright Clearance Center.[45]

1.4.4 Gut Hormone Agonists

Gut hormones have been targeted as a treatment option of obesity and diabetes. These treatment modalities were inspired by the gut hormonal changes that occur after bariatric surgery, which result in an increase in GLP-1, GIP and glucagon. The first FDA approved medication for diabetes and weight loss was liraglutide, a GLP-1 analogue. In type 2 diabetes, liraglutide reduced HbA1c by up to 1.0%[97] with a mean weight loss of 7.2 kg[98]. Liraglutide also reduced mortality from cardiovascular events and death[15].

A longer-acting version, semaglutide was recently approved for diabetes and weight loss. It has similar efficacy to liraglutide but only requires subcutaneous injections once a week[99]. Tirzepatide was recently published in an open-label clinical trial and is a dual agonist which includes GLP-1 and GIP to mimic the effects of bariatric surgery. This dual agonist demonstrated greater weight loss and lowering of HbA1c than semaglutide, however side effects were more frequent[100]. Novel tri-agonists, which have GLP-1, GIP and glucagon, are currently being studied for the treatment of obesity and diabetes and studies in animal models have demonstrated greater effects than single- or dual- agonists[101].

1.5 ROLE OF BILE ACIDS IN BARIATRIC SURGERY

1.5.1 BILE ACID METABOLISM

Primary bile acids are produced in the liver and include chenodeoxycholic acid (CDCA) and cholic acid (CA) for humans while rodents produce CA and muricholic acids (MCA), primarily β-MCA. Before bile acids enter the duodenum, they are conjugated by glycine or taurine[102]. Conjugated bile acids are typically reabsorbed via the apical sodium dependent bile acid transporter (ASBT) in the ileum and recirculated to the liver via the portal vein. This process, called enterohepatic circulation, reabsorbs more than 95% of bile acids[102]. Bile acids are derived from cholesterol and its synthesis in the liver takes place via two pathways. The classical pathway contributes to 75% of bile acid production and starts with 7α-hydroxycholesterol and produces CA and CDCA. The alternative pathway occurs via 27-hydoxycholesterol but only produces CDCA (Figure 6).

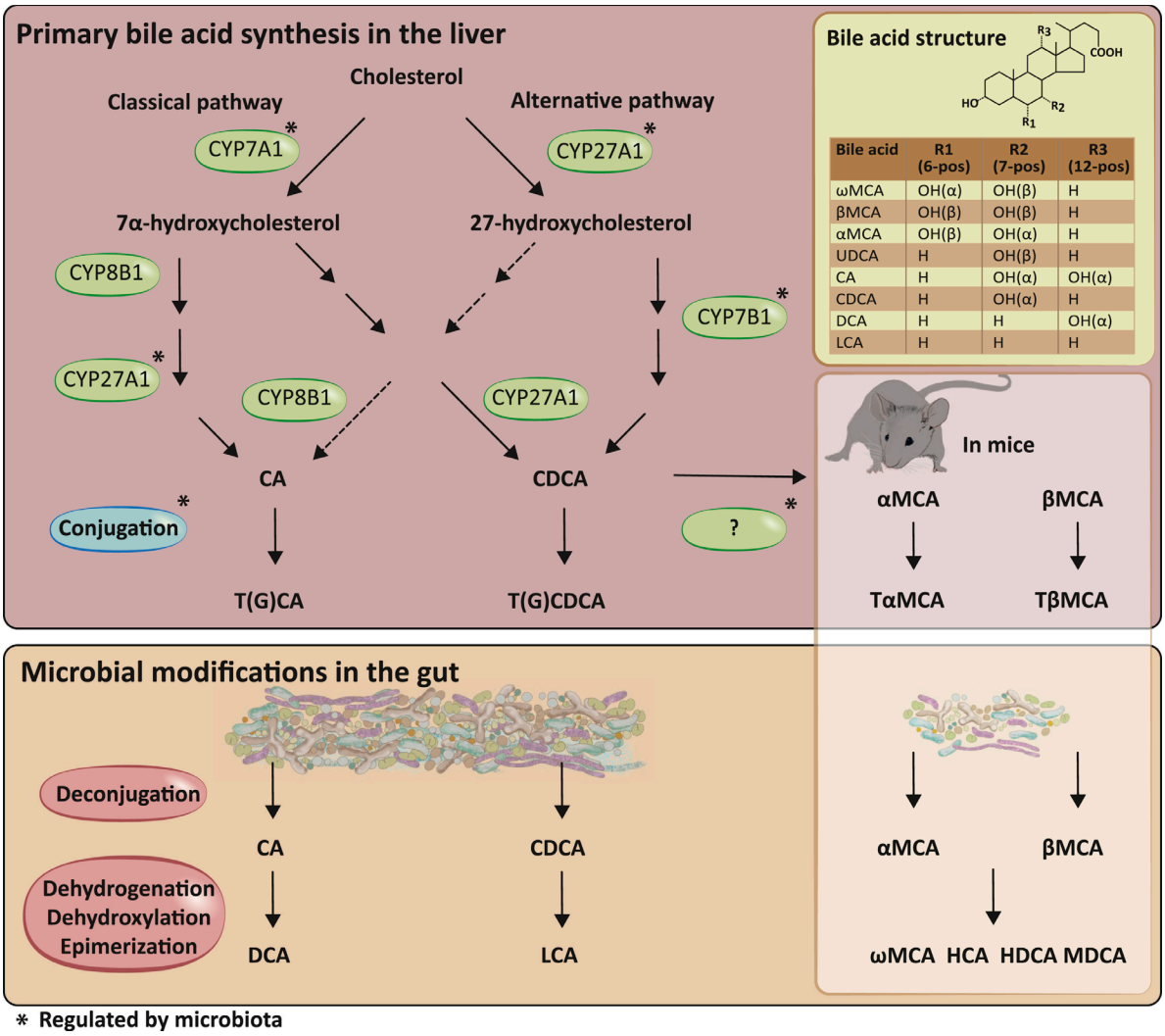

Figure 6. Bile acid metabolism in humans and rodents.

Material from: Wahlström A, Sayin SI, Marschall HU, Bäckhed F. Intestinal crosstalk between bile acids and microbiota and its impact on host metabolism. Cell metabolism. 2016 Jul 12;24(1):41-50. Reproduced with permission of Elsevier via Copyright Clearance Center.[102]

1.5.2 Microbiota and Bile Acids

Gut microbiota are responsible for deconjugating bile acids into secondary bile acids in the gut. Studies in germ-free mice or mice treated with antibiotics have found that the bile acid pool consists mainly of primary bile acids[103,104]. The ASBT, which is a brush-border protein where

conjugated bile acids are reabsorbed, has also been demonstrated to be regulated by gut microbiota[103].

When microbial deconjugation occurs, it prevents active reuptake via ASBT. Deconjugation is carried out by bacteria with bile salt hydrolase (BSH) activity. Functional BSH is present in multiple bacterial taxa including *Lactobacilli*, *Bifidobacteria*, *Clostridium*, and *Bacteroides*. However, there are some deconjugated primary bile acids that miss reuptake and enter the colon. Here they are metabolized through 7-dehydroxylation into secondary bile acids which include lithocholic acid and deoxycholic acid. In rodents, the same mechanism of 7-dehydroxylation occurs on α- and β-muricholic acid resulting in the formation of murideoxycholic acid. Notably, human and rodent have unique bile acid physiology, and this is important to consider when attempting to translate finding in rodents to humans.

1.5.3 FXR AND TGR5

Farnesoid X receptor (FXR) tightly regulates the synthesis of bile acids by negative inhibition[105]. FXR is expressed in multiple tissues with the liver and ileum being the most well studied although it is also expressed in the kidney, heart, ovary, thymus, eye, spleen, and testes[106]. In the liver, bile acids activate FXR which lead to the expression of SHP. SHP binds to liver receptor homolog-1 (LRH-1) which inhibits the Cyp7a1 gene to limit the classical pathway. FXR is also activated by bile acids in the distal ileum which induces expression of protein Fgf15/Fgf19. These proteins travel to hepatocytes via the portal vein, binds to FGF receptor 4/β-klotho heterodimer complex and triggers a JNK1/2 and ERK1/2 signaling cascade that also inhibits the

expression of Cyp7a1[102]. Within colonic L cells, FXR activation inhibits the synthesis of proglucagon, which is a precursor for GLP-1[107] (Figure 7).

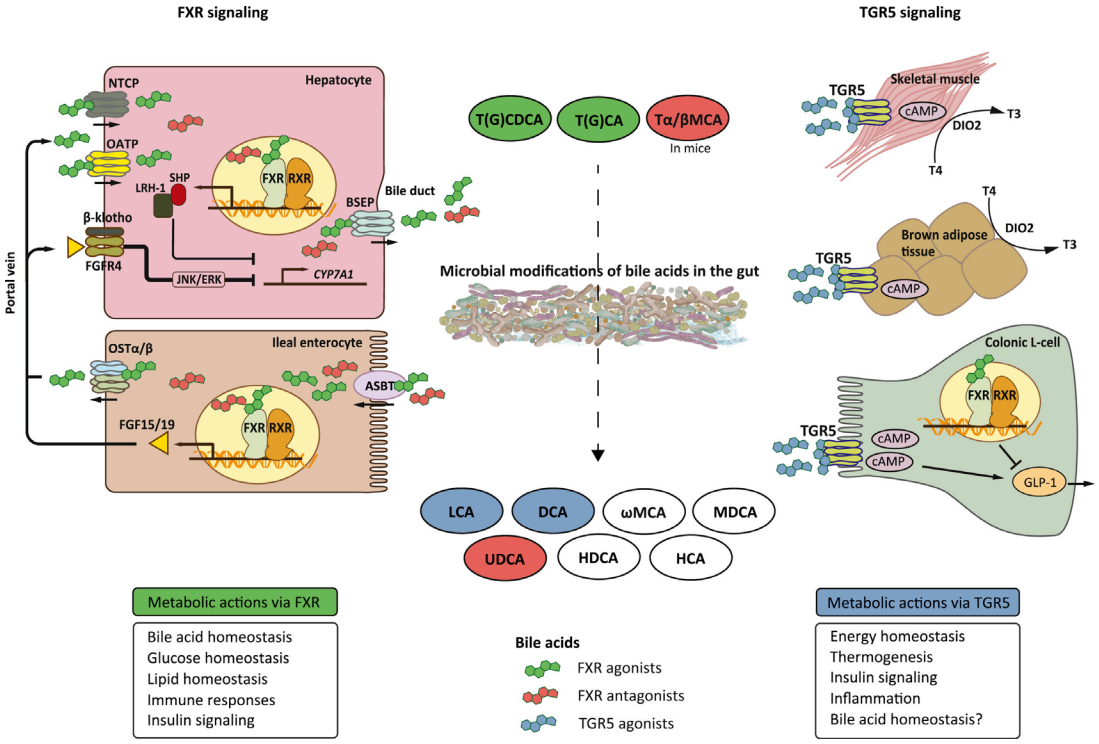

Figure 7. Microbial modification of bile acids and its effects through bile acid receptors FXR and TGR5.

Material from: Wahlström A, Sayin SI, Marschall HU, Bäckhed F. Intestinal crosstalk between bile acids and microbiota and its impact on host metabolism. Cell metabolism. 2016 Jul 12;24(1):41-50. Reproduced with permission of Elsevier via Copyright Clearance Center.[102]

Bile acids also act directly on L cells. Bile acids have demonstrated the ability to promote intestinal L-cell differentiation and increases in density. A study by Lund et al. found that both lithocholic acids and synthetic GPBAR1 agonists increased L-cell density and GLP-1 secretory capacity[108]. Bile acids also have direct effects on L cells through the FXR and TGR5 receptors[107,109,110]. For example, administration of TaMCA and TbMCA deactivated intestinal FXR which prevented diet-induced obesity and improved glucose metabolism[111,112]. Trabelsi et

al. demonstrated that FXR activation in colonic L cells inhibited the expression of proglucagon, which is a precursor to GLP-1. This occurred via interference of the carbohydrate-responsive element binding protein (ChREBP)[107].

1.6 THE HUMAN MICROBIOME

1.6.1 INTRODUCTION

The gastrointestinal microbiota is a complex community of microbes including bacteria, archaea, eukarya and viruses[113]. It contains approximately 100 trillion cells, far more than the number of human cells. Similar to the human genome, the collective genome of these microbes is defined as the microbiome[114]. The gut microbiota performs a variety of functions. These biological effects include the development of innate and adaptive immunity, maintenance of intestinal epithelial integrity, and acting as an energy source. It also provides vitamin biosynthesis, bile salt transformation, catabolism of dietary glycans and xenobiotic metabolism. The barrier function the gut microbiota provide is essential in preventing colonization by microbial pathogens[113].

The Human Microbiome Project was an initiative by the NIH to further understand the human microbiome. Its goals were to:

1) Utilize new technologies to characterize the human microbiome
2) Determine associations between the microbiome and health/disease
3) Provide a standard data resource and new technological approaches to enable studies by the scientific community[115,116]

Recent advances in gene sequencing technologies have made it possible to study the complex and abundant human microbiome.

1.6.2 Techniques for Analyzing Microbiota

1.6.2.1 CULTURE-BASED TECHNIQUES

Early studies on the gastrointestinal microbiota used anaerobic culture-based techniques and were only able to identify 400 to 500 distinct bacterial species[117]. Culture-based techniques require that organisms grow on culture media and limited the range in which organisms could be detected. It also selected for specific organisms, which does not reflect the true composition of the gut microbiota. Approximately 60 to 80 percent of gut microbes cannot be grown by conventional in-vitro methods[118].

1.6.2.2 16S rRNA SEQUENCING

In the late 1970s, Woese and Fox were the first to describe phylogenic analysis using ribosomal RNA sequence characterization[119]. The 16S rRNA is a molecule that is present in all bacteria and have highly conserved domains that can be used to identify bacterial groups. In the 1980s, molecular techniques based on 16S rRNA became available and have been used to understand prokaryotic communities. These techniques involved isolating the bacterial DNA followed by amplification by polymerase chain reaction using universal primers that targeted the conserved domains of the 16S rRNA genes. These amplicons were then subjected to electrophoresis or hybridization to produce the variable regions that describe specific bacterial communities[113].

Higher-resolution methods to study bacterial phylogeny have been developed that clone and sequence the 16S rRNA gene in automated capillary sequencers. This relies on Sanger sequencing which allows identification of bacteria at a higher phylogenic resolution and relies on bioinformatics tools such as the Ribosomal Database Project [120,121]. These technologies have advanced further with next-generation sequencing technologies that have both increased the speed and depth of resolution as well as decreased the cost by using massive parallel sequencing methods[120].

1.6.2.3 WHOLE GENOME SEQUENCING

The drawback of 16S rRNA sequencing is that it does not provide information about bacterial physiology or ecological significance[122]. A different approach is through whole genome shotgun sequencing of the community DNA. This approach sequences the entire genome of the microbes which are compared to previously described genes to determine the functional capability of the microbiota. This allows identification of genes that code for metabolic or biologic functions. The weakness of this technique is that large amounts of DNA are needed, contamination with host DNA can occur, and that many genes are identified that do not have a clear function.

1.7 THE HUMAN MICROBIOME AND OBESITY

Despite advances in the past few decades, the mechanisms underlying excessive fat mass accumulation and the development of obesity are not fully understood. There is evidence that the intestinal microbiome may play a central role in the development and perpetuation of obesity through regulation of energy homeostasis and fat storage[123]. Recent advancements in

metagenomic analysis, which allow for the rapid identification and quantification of these organisms, has increased our understanding of obesity and the microbiome.

The initial link between the gut microbiota and obesity was made in leptin-deficient mice by Ley et al[124]. Using 16S rRNA gene sequencing, Ley et al. revealed a greater representation of Firmicutes and fewer Bacteroidetes in obese mice microbiota. Ley et al. then performed shotgun sequencing which showed that genes involved in energy extraction were enriched in the obese mice[124]. The researchers then provided the luminal contents of the obese or lean mice to lean germ-free recipients and the mice receiving the microbes from obese donors gained more weight than their control cohort[125]. Studies in humans also reveal a higher proportion of Bacteroidetes in participants who had reductions in weight[126]. A study focused on twins by Turnbaugh et al. found that obesity was associated with a reduced representation of Bacteroidetes and decreased bacterial diversity[127]. These studies demonstrate that distinct microbial communities and metabolites are associated with lean body composition and that alterations to these communities can cause obesity and metabolic disease[128].

While a dysbiosis, defined as the imbalance of gut microbiota has been described in many studies of obesity, specific changes in gut microbes have not been as consistently present[129]. However, significant associations between diversity and richness indices and obesity have been described[129]. This lack of consistency highlights the need for a well-designed study to examine both microbial composition and the metabolic potential of the gut microbiota.

1.7.1 MECHANISMS LINKING THE MICROBIOTA TO OBESITY

Dysbiosis and decreases in diversity can be caused by changes in diet, oral antibiotic use, and changes in bile acids. Different mechanisms have been proposed to explain how dysbiosis and a lack of diversity causes obesity. These mechanisms include both a lack of and an increase in specific microbial products. These products use signaling pathways in the intestinal epithelial receptors to change gut hormonal expression. Gut microbiota and their interrelationships also create differences in their efficiency of caloric salvage. Further, chronic increased gut permeability has been associated with the development of obesity, diabetes and NAFLD[130].

1.7.1.1 INFLAMMATION AND INSULIN RESISTANCE

An increase in intestinal permeability with increased translocation of bacterial products resulting in chronic low-grade inflammation is recognized as an important component of obesity and metabolic syndrome[131]. Metabolic and immune systems are integrated and increases in pro-inflammatory cytokines have been shown to cause insulin resistance[132]. Lipopolysaccharide (LPS), an endotoxin and an essential component of the cell walls of Gram-negative bacteria, has been implicated in inflammation and insulin resistance. Cani et al. demonstrated this by infusing LPS subcutaneously in mice which induced both weight gain and insulin resistance[133]. Additionally, there is evidence that suggests high-fat diets aid in the transport of LPS out of the gut, resulting in metabolic inflammation. This mechanism is thought to be facilitated by triglycerides that form into chylomicrons which have a high affinity for LPS and thus move it from the gut into systemic circulation[134].

High-fat diets also increase LPS levels through changes in microbial composition. Studies on mice show that high-fat diets cause a reduction in the number of *Bifidobacteria*. Higher levels of *Bifidobacteria* have been associated with reduced inflammation and improved glucose tolerance. Lower levels, which may be caused by high-fat diets, result in higher gut permeability and higher LPS plasma levels[135]. This pattern has been seen in humans as well, with higher plasma LPS levels found in individuals with higher energy intake and in individuals with type 2 diabetes[136,137].

1.7.1.2 GUT HORMONES

The gut sends hormonal signals to the brain to control energy intake and expenditure. Enteroendocrine cells react to nutrient intake by secreting GLP-1 and GLP-2. GLP-1 is an incretin that stimulates the pancreas to release insulin, slows gastric emptying and promotes satiety and weight loss while GLP-2 increases intestinal glucose transport and reduces gut permeability[138]. Studies have demonstrated that gut microbiota can regulate enteroendocrine cells and mediate the release of gut hormones. Cani et al. administered oligofructose treatment to rats to increase the proportion of *Bifidobacteria* and found that this was associated with higher levels of GLP-1 and GLP-2[139]. Similarly, changes in gut hormones following RYGB are associated with the reduction in appetite and weight loss. Some evidence suggests that gut hormonal activity, especially GLP-1, may actually be caused by changes in the intestinal microbiome following bariatric surgery.

Samuel et al.[140] identified a specific pathway in which energy balance is dependent on enteroendocrine cells, gut hormones and gut microbiota. This pathway is through Gpr41, a receptor expressed by enteroendocrine cells in the gut epithelium. Samuel et al. compared germ-free, conventionalized, wild-type and knockout mice to reveal that Gpr41 is a regulator of host energy balance through PYY and that these effects were dependent on the gut microbiota.

1.7.2 Bariatric Surgery and the Human Microbiome

The underlying mechanism for weight loss following these operations is not completely understood though multiple factors are thought to play a role. These include reduced caloric intake, decreased nutrient absorption, increase satiety, release of satiety-promoting hormones (GLP-1, PYY) and shifts in bile acid metabolism[141,142].

Previous studies have found that the intestinal microbiome mediates a number of beneficial effects following bariatric surgery. Small studies have demonstrated changes in the composition and diversity of the gut microbiota after RYGB and SG in humans but findings were inconsistent[143–147]. One study also confirmed long-term microbial changes for RYGB and vertical banded gastroplasty (VBG) nine years after surgery[146]. A literature search was performed, and this identified 22 studies clinical studies on bariatric surgery and the gut microbiome. See Table 3 for study characteristics.

Table 3. Study characteristics[40,41,152–161,143,162,163,145–151]

Study	Country	Surgery	Sample Size	BMI ($kg/m^{2)}$	Microbiota analysis technique	Sampling times
Zhang 2009	China	RYGB	9	27.7 ± 4.1 (mean)	RT-PCR	-8 to 15M postop
Furet 2010	France	RYGB	43	≥ 40	RT-PCR	-Preop -3M postop -6M postop
Patil 2012	India	SG, AGB	5	≥ 35	Sanger sequencing	-3 to 12M postop
Kong 2013	France	RYGB	30	≥ 40	16S rRNA	-Preop -3M postop -6M postop
Graessler 2013	Germany	RYGB	6	≥ 40	Shotgun sequencing	-Preop -3M postop
Ward 2014	USA	RYGB	14	≥ 40	Shotgun sequencing	-Preop -6M postop
Damms-Machado 2015	Germany	SG	10	45.8 ± 0.9 (mean)	Shotgun sequencing	-Preop -3M postop -6M postop
Tremaroli 2015	Sweden	RYGB, VBG	14	42.2 for RYGB 43.0 for VBG (mean)	Shotgun sequencing	-9.4 years postop
Patrone 2016	Italy	BIB	11	≥ 35	16S rRNA	-6M postop
Palleja 2016	Denmark	RYGB	13	≥ 35	Shotgun sequencing	-Preop -3M postop -12M postop
Murphy 2016	New Zealand	RYGB, SG	14	RYGB 38.4 SG 36.9 (mean)	Shotgun sequencing	-12M postop
Federico 2016	Italy	BIB	11	≥ 35	PCR DGGE	-Preop -6M Postop
Ilhan 2017	USA	RYGB, AGB	38	RYGB 30.8 LAGB 36.6 (median)	16S rRNA	-RYGB 35M postop -LAGB 34 M postop (mean)
Sanmiguel 2017	USA	SG	8	44.1 (mean)	16S rRNA	-Preop -1M postop
Liu 2017	China	SG	23	44.5 (mean)	Shotgun sequencing	-Preop -1M postop -3M postop
Medina 2017	Chile	RYGB, SG	19	RYGB 37.1 SG 35.2	16S rRNA	-Preop -6M postop -12M postop
Chen 2017	China	RYGB	24	46.3	RT-PCR	-Preop -6M postop
Campisciano 2018	Italy	RYGB, SG	40	≥ 35	16S rRNA	-Preop -3M postop
Aron-Wisnewski 2018	France	SG, AGB	24	≥ 35	182 MB	-Preop -12M postop
Kikuchi 2018	Japan	SG, LAG-DJB, AGB	44	≥ 30	PCR	-Preop -3M postop

Kumar 2018	USA	RYGB, SG	34	≥ 35	150 bases	-Preop -24M postop
Cortez 2018	Brazil	DJBm	21	≥ 30	16S rRNA	-Preop -6M postop -12M postop

RYGB - Roux-en-Y gastric bypass; VBG - vertical banded gastroplasty; SG - sleeve gastrectomy; AGB – adjustable gastric banding; BIB – bilio-intestinal bypass; DJB – duodenal jejunal bypass; DJBm- duodenal-jejunal bypass with minimum gastric resection; preop - preoperative; postop - postoperative; M - months; PCR - polymerase chain reaction; USA - United States of America

Studies included a total of 455 participants and surgeries included RYGB, SG, AGB, VBG, bilio-intestinal bypass (BIB), duodenal jejunal bypass, and duodenal-jejunal bypass with minimum gastric resection. Interpreting these studies show inconsistent microbial changes that occur after bariatric surgery; however, some patterns emerge. Table 4 summarizes the microbial changes that occur after bariatric surgery in each study.

Table 4. Postoperative gut microbiota changes[40,41,152–161,143,162,163,145–151]

Study	Increased abundance	Decreased abundance
Zhang 2009	RYGB: *Enterobacteriaceae, Fusobacteriaceae, Verrucomicrobia, Gammaproteobacteria*	RYGB: *Clostridia*
Furet 2010	RYGB: *Bacteroides/Prevotella, E. coli*	RYGB: *Bifidobacterium, Lactobacillus, Leuconostoc, Pediococcus*
Patil 2012	No reported differences between obese and post-surgical cohorts	
Kong 2013	RYGB: *Bacteroides, Alistipes, Escherichia*	RYGB: Firmicutes *(Lactobacillus, Dorea, Blautia), Bifidobacterium*
Graessler 2013	RYGB: *Enterobacter, Citrobacter, Neurospora, Veillonella, Salmonella, Shigella* *E. coli tended to increase*	RYGB: *Faecalibacterium, Coprococcus, Helicobacter, Dictyostelium, Epidinium, Anaerostipes, Nakamurella, Methanospirillum, Thermomicrobium*
Ward 2014	Only compared PPI with no PPI either before or after RYGB	
Damms-Machado 2015	SG:Bacteroidetes	SG: Firmicutes (*Clostridium, Eubacterium, Faecalibacterium*, *Dorea*, *Coprococcu, Ruminococcus, Lachnospiraceae)*
Tremaroli 2015	RYGB: Gammaproteobacteria, several Proteobacteria *(Escherichia, Klebsiella, Pseudomonas)*	RYGB: 3 species of Firmicutes *(Clostridium difficile, Clostridium hiranonis, Gemella sanguinis)*
Patrone 2016	BIB: *Lactobacillus, Megasphaera, Acidaminococcus, Enterobacteriaceae*	BIB: *Lachnospiraceae, Clostridiaceae, Ruminococcaceae, Eubacteriaceae, Coriobacteriaceae*

Palleja 2016	RYGB: *Escherichia coli, Klebsiella pneumonia,* 10 species belonging to the genus *Streptococcus,* 4 from *Veillonella,* 2 from *Alistipes, Bifidobacterium dentium, Enterococcus faecalis, F. nucleatum, and Akkermansia muciniphila*	RYGB: *F. prausnitzii*
Murphy 2016	RYGB: Firmicutes, Actinobacteria SG: Bacteroidetes	RYGB: Bacteroidetes
Federico 2016	BIB: *Lactobacillus crispatus*	BIB: *Butyrivibrio fibrisolvens, Roseburia hominis/faecis, Dorea longicatena, Blautia sp./Ruminococcus sp., Ruminococcus obeum*
Ilhan 2017	RYGB: *Bacilli, Gammaproteobacteria, Fusobacteria, Flavobacteria* AGB: *Fusobacteria, Flavobacteria, Bacteriodaceae*	
Sanmiguel 2017	SG: Fusobacteria, Bacteroidetes, *Atopoium, TG5, Bulleidia, Epulopiscium*	SG: Firmicutes
Liu 2017	SG: *B. thetaiotaomicron, C. comes, D. longcatena, Clostridialis bacterium, Anaerotruncus colihominis, A. mucini phila*	
Medina 2017	RYGB: *Succiniclastum sp., Bacteroides, Citrobacter, Streptococcus luteciae, Bacteroides eggerthii, Bacteroides coprophilus and Lactobacillales sp.* SG: *Bulleidia, Escherichia coli, Akkermansia muciniphila, Streptococcus luteciae*	SG: *Bacteroides eggerthii, Bacteroides coprophilus, Lactobacillales sp.*
Chen 2017	RYGB: *Bacteroidetes, Bifidobacterium, Escherichia*	
Campisciano 2018	RYGB: *Proteobacteria, Prevotella, B.vulgatus*, *B. uniformis* SG: *B. uniformis*	SG: *Proteobacteria*
Aron-Wisnewski 2018	RYGB: Switched from Bacteroides B2 enterotype to Bacteroides B1 RYGB: Oscillibacter, Clostridium sp., Alistipes shahii, Butyricimonas, Butyricimonas virosa, Roseburia,	RYGB: *Coprobacillus, Anaerostipes hadrus,*
Kikuchi 2018	LSG: Bacteroidetes, Lactobacillales LSG-DJB: Enterobacteriales	LSG-DJB: *Bifidobacterium*
Kumar 2018	RYGB new strains: *Faecalibacterium prausnitzii, Bacteroides spp, Parabacteroides spD13* SG: new strains of *Bacteroides vulgatus*, *Akkermansia muciniphila*, *Bacteroides sp116*, *Ruminococcus torques ATCC*	RYGB: *Bacteroides stercoris, Bacteroides uniformis and Bacteroides vulgatu*
Cortez 2018	DJB: *Bacteroides, Akkermansia, Dialister*	

RYGB – Roux-en-Y gastric bypass; SG – sleeve gastrectomy; PPI – proton pump inhibitor
*Some data extracted from Magouliotis et al.[164]

1.7.2.1 BACTEROIDETES AND FIRMICUTES

Bacteroidetes and Firmicutes are two phyla that comprise 90% of the human distal gut microbiota[124]. Studies have demonstrated a higher ratio of Firmicutes to Bacteroidetes in obese mice[124,165]. After bariatric surgery, it appears that the ratio is reversed. Six studies demonstrated an increase in the abundance of Bacteroidetes after bariatric surgery [147,148,150,152,154,156] and five showed a decrease in Firmicutes [146–148,150,154]. Murphy et al.[152], however, demonstrated the opposite, with an increase in Firmicutes and decrease in Bacteroidetes after RYGB while Federico et al.[41] and Patrone et al.[40] also had an increase in Firmicutes after BIB. Unfortunately, the pathogenesis behind obesity and the Bacteroidetes-to-Firmicutes ratio is not clear. It is believed that the shift in the dominating bacterial phylum promotes more effective caloric intake[126].

Lactobacillus, within the Firmicutes phyla, decreased in two studies after RYGB [147,148] but increased in two studies after BIB[40,41]. Bacilli also increased after RYGB in Ilhan et al.[153] which includes the *Lactobacillus* species. *Lactobacillus* has been associated with weight loss in other studies[166] and long-term ingestion has been demonstrated to reduce body weight in animal studies[167,168]. It is not clear why *Lactobacillus* decreased in some studies and not others, but it is postulated that it may be related to surgical technique as RYGB and BIB result in different intestinal anatomical changes.

Liu et al.[156] performed shotgun sequencing before and after SG and noticed a significant increase in *Bacteroides thetaiotaomicron.*, within the Bacteroidetes phyla. In this study, abundance of *B. thetaiotaomicron* correlated well with weight reduction. Liu et al. also found that mice gavaged with live *B. thetaiotaomicron* had less adiposity. This is consistent with a study that demonstrated that *Bacteroidales*, which includes *B. thetaiotaomicron,* prevented increased adiposity in mice[169]. However, another study found an increased body fat content in germ-free mice colonized with *B. thetaiotaomicron*[170]. Liu et al. suggests that *B. thetaiotaomicron* may work synergistically with other bacteria to prevent fat adiposity, such as with *B. uniformis* or *Akkermansia*, both of which demonstrated an increased abundance with increased *B. thetaiotaomicron*. Sanmiguel et al.[154]. found that *Akkermansia* abundance was inversely correlated with the desire to eat sweet foods, which may contribute to its effect on promoting weight loss.

1.7.2.2 METABOLIC CHANGES AFTER BARIATRIC SURGERY

In addition to changing gut hormones, studies have shown that the gut microbiota also influences the serum metabolome. Pedersen et al.[171] demonstrates that a specific serum metabolome high in branched-chain amino acids (BCAAs) in insulin-resistant individuals correlates with a specific gut microbiome that has enriched biosynthetic potential for BCAAs. Eight of the studies in Table 1 measured metabolic changes [40,145–147,151–153,156] and two included metabolomic analysis[156,162] with microbial changes. There was a consistent reduction in blood glucose and insulin after bariatric surgery which was likely due to weight loss and reduced insulin resistance. There is likely a role of gut hormones, as GLP-1 and PYY were increased after bariatric surgery[164].

Liu et al.[156] specifically analyzed for correlations between the serum metabolome and gut microbiome after SG. They found that an increase in the abundance of *B. thetiaotaomicron* was associated with a decrease in circulating glutamate levels and that this correlated with an improvement in hyperglycemia, insulin resistance, serum concentration of leptin and inflammatory markers such as C-reactive protein. This suggests that weight-loss intervention restores a healthy microbiome and metabolome[156].

1.7.2.3 MECHANISM OF MICROBIOTA CHANGE AFTER BARIATRIC SURGERY

The mechanism in which bariatric surgery causes these microbial changes is not well understood. One explanation is that the rearrangement of the gastrointestinal tract after RYGB alters gut pH, oxygen content, bile acid concentrations and nutrient exposure which can affect bacterial composition and diversity[172]. However, significant microbial changes also occur after SG which does not have any intestinal rearrangement. These changes potentially are attributed to changes in diet, as a reduction in ghrelin secretion from the resected stomach has been demonstrated to induce reductions in volume of food intake as well as changes in food preference. Food choice tended towards less dietary fat and lower caloric-density foods[173].

1.8 METABOLOMICS

Our study utilizes metabolomics as part of a systems biology approach to understand the physiological changes that occur after bariatric surgery. Metabolomics is a powerful technique that allows for a comprehensive measurement of small molecules in biofluids[174]. These molecules encompass endogenous metabolites which include lipids, amino acids, peptides,

nucleic acids, organic acids, vitamins, thiols and carbohydrates[175]. Metabolite changes can be useful in understanding the pathophysiology of disease[176].

Metabolomic research has been primarily focused on its use as an early screening and diagnostic tool[177]. However, it can also be useful in understanding a pathological state, such as obesity, and the changes that occur after treatment[178]. It can be combined with genomics, transcriptomics, proteomics and metagenomics to provide information on metabolic pathways in pathological processes. However, the complexity of the metabolome makes interpretation difficult given its wide variety of chemically-diverse compounds[179].

1.8.1 Modern Analytical Techniques in Metabolomics

Modern techniques for metabolomic analysis include nuclear magnetic resonance spectrometry (NMR) and mass spectrometry (MS). NMR is the most common spectroscopic analytical technique and it provides a holistic view of the metabolome. It uses the magnetic properties of atomic nuclei to identify metabolites. Its advantages are that it is straightforward, largely automated and is non-destructive. However, it has limitations in detecting large numbers of low-abundance metabolites compared to MS[180].

MS ionizes chemical species and sorts ions based on mass-to-charge ratio and is increasingly used in high-throughput metabolomics. It has high sensitivity and covers a wide range of metabolites. MS is often performed in conjunction with gas chromatography, liquid

chromatography or capillary electrophoresis that first separates the compounds prior to metabolomic analysis.

1.8.2 Data Analysis and Bioinformatics Tools

The interpretation of complex metabolomics data is coupled with bioinformatics methods to identify the function of metabolites. One approach uses multivariate statistical analysis to determine which metabolites are expressed among groups in conjunction with a human metabolite database. Useful human metabolite databases include HMDB (http://www.hmdb.ca), METLIN (http://metlin.scripps.edu), MMCD (http://mmcd.nmrfam.wisc.edu), KEGG (http://www.genome.jp/kegg) and LIPID maps (http://www.lipidmaps.org)[179]. Recently, platforms have been released and are increasingly popular to consistently automate bioinformatics analysis: MetaboAnalyst[181] for the analysis of metabolites, MicrobiomeAnalyst[182] for the analysis of the microbiome, and M^2IA platform[183] for integrated analysis of the microbiome and metabolites. These platforms integrate a wide variety of bioinformatics analyses including univariate analysis, multivariate modeling, and functional network analysis[183].

1.9 TARGETED CHANGES IN GUT MICROBIOTA FOR OBESITY

There has been a recent interest and research in the use of prebiotics, probiotics, or fecal microbial transplantation (FMT) to alter the gut microbiota in the treatment of obesity and obesity-related comorbidities[184].

1.9.1 Effect of Prebiotics on Obesity

Prebiotics are substrates that selectively stimulate the growth or activity of specific gut microbiota to offer benefit to the host[185]. *Bifidobacteria*, a member of the Firmicutes phylum, was a target for prebiotics as it was demonstrated to be lower in obese compared to lean individuals[186]. Inulin-type fructans (ITFs), a prebiotic, induced an increase in *Bifidobacterium spp* in mice and reduced fat mass, glucose intolerance and LPS levels[187]. It also increased the number of L-cells in the jejunum resulting in higher levels of GLP-1 and GLP-2 hormones in mice, further suppressing appetite[188]. In humans, ITFs have also consistently increased the abundance of *Bifidobacterium* and *Faecalibacterium prausnitzii*, both of which appear to lower serum LPS levels. It also decreased fat mass but this decrease was not statistically significant[189].

1.9.2 Effect of Probiotics on obesity

Probiotics are viable strains of bacteria that promote health when consumed. *Lactobacillus* has been studied as a probiotic for its effect on obesity. The administration of *Lactobacillus* in obese individuals has been shown to decrease fat mass as well as decrease the risk of type 2 diabetes and insulin resistance[190,191]. A recent systematic review that included 115 studies and 957 subjects found that probiotics, the majority of which were *Lactobacillus*, in comparison to placebo had a significant, but small, effect on reduction of body weight, BMI and fat percentage but no significant effect on fat mass[192].

1.9.3 Fecal Microbial Transplantation

FMT has the potential to improve obesity and metabolic syndrome. Vrieze et al.[193] performed a study using FMT from lean individuals to individuals with metabolic syndrome and found an improvement in insulin sensitivity at six weeks. Vrieze et al. also found higher levels of butyrate-producing bacteria, suggesting a role of butyrate in regulating insulin sensitivity[193]. Kootte et al[194] completed a similar experiment that demonstrated improved insulin sensitivity at six weeks. However, this improvement did not persist to 18 weeks. Mocanu et al. performed a four-arm trial which included FMT with high- or low-fermentable fibers and found that FMT with low-fermentable fiber improved insulin sensitivity at 6 weeks but not at 12 weeks. This suggests that FMT promotes a change in the host's bacterial composition but that due to the hosts diet, lifestyle and personal core microbiome, the effect is transient as the host tends to have a return to their normal microbial composition[194].

Treating obesity by inducing a change in the gut microbiota has potential. However, being able to first truly understand the microbiota responsible for obesity and leanness and their associated interactions and pathways, are necessary to innovate and improve targeted microbial therapy.

1.10 AIMS AND HYPOTHESIS

The aim of this work was to understand the intestinal physiology of bariatric surgery. Chapter 2 describes a surgical protocol that we developed to perform RYGB in rats with low mortality and excellent representative metabolic outcomes. In Chapter 3, we describe a study where the terminal ileum of the rat is analyzed to determine physiological changes that occur after RYGB.

This study focuses on ileal microbiota, glucose metabolism, bile acids, intestinal morphology and L-cells to identify unique relationships. Chapter 4 is a three-arm prospective clinical trial that encompasses SG and RYGB and includes complex bioinformatics analysis of the microbial, metabolomic, inflammatory changes that occur after bariatric surgery in conjunction with clinical changes.

The intention of this work is to improve our understanding of the physiological changes that occur with bariatric surgery. This understanding may potentiate the development of approaches to modify the gut microbiome or metabolome through diet, prebiotics, probiotics, or fecal microbiota transplantation with the potential to improve metabolic syndromes or obesity, likely in conjunction with bariatric surgery.

CHAPTER 2. A PROTOCOL FOR ROUX-EN-Y GASTRIC BYPASS IN RATS USING LINEAR STAPLERS

2.1 ABSTRACT

Roux-en-Y gastric bypass (RYGB) is commonly performed for the treatment of severe obesity and type 2 diabetes. However, the mechanism of weight loss and metabolic changes are not well understood. Multiple factors are thought to play a role including reduced caloric intake, decreased nutrient absorption, increased satiety, release of satiety-promoting hormones, shifts in bile acid metabolism and alterations in the gut microbiota.

The rat RYGB model presents an ideal framework to study these mechanisms. Prior work on mouse models have had high mortality rates, ranging from 17 to 52%, limiting their adoption. Rat models demonstrate more physiologic reserve to surgical stimulus and are technically easier to adopt as they allow for the use of surgical staplers. One challenge with surgical staplers, however, is that they often leave a large gastric pouch which is not representative of RYGB in humans.

In this protocol, we present a RYGB protocol in rats that result in a small gastric pouch using surgical staplers. Utilizing two stapler fires which remove the forestomach of the rat, we obtain a smaller gastric pouch similar to that following a typical human RYGB. Surgical stapling also results in a better hemostasis than sharp division. Additionally, the forestomach of the rat does not contain any glands and its removal should not alter the physiology of RYGB.

Weight loss and metabolic changes in the RYGB cohort were significant compared to the sham cohort with significantly lower glucose tolerance at 14 weeks. Furthermore, this protocol has an excellent survival of 88.9% after RYGB. The skills described in this protocol can be acquired without previous microsurgical experience. Once mastered, this procedure will provide a reproducible tool for studying the mechanisms and effects of RYGB.

2.2 INTRODUCTION

Obesity and type 2 diabetes have become worldwide epidemics[1]. Although medical weight loss can improve diabetes in patients, those with severe diabetes benefit most from bariatric surgery. Bariatric surgery has proven to be safe and effective at weight loss and improving or curing type 2 diabetes[66,195], even in those with long-standing disease[196]. Metabolic bariatric procedures, such as the current gold-standard Roux-en-Y gastric bypass (RYGB) surgery, induce rapid and sustained improvements in glucose homeostasis while also reducing the need for diabetic medications[197–199].

After RYGB, glucose homeostasis improvement occurs rapidly and is independent of weight loss[200]. Two major theories have been proposed to explain the metabolic changes associated with diabetes remission that occur following metabolic surgery. First, the hindgut hypothesis postulates that, after bypass, higher concentrations of undigested nutrients reach the distal intestine enhancing the release of hormones such as GLP-1. On the other hand, the foregut

hypothesis suggests that bypassing the proximal intestine reduces secretion of anti-incretin hormones. Both of these effects could lead to early improvement of glucose metabolism[63].

Animal models have the potential to be a powerful tool to study these mechanisms. However, a major barrier in utilizing mouse or rat models is the technical difficulty in performing these procedures. Most studies have relied on mouse or rat models[201–203]. Mouse models have been difficult as the mouse stomach is too small to use stapler devices[202] and mortality rates are unacceptably high, ranging from 17 to 52%[204]. In rats, some protocols remain technically difficult to perform due to complex ligation of gastric vessels prior to dividing the stomach[203,205]. Other models divide the stomach using a stapler but leave a large pouch not consistent with the post RYGB human anatomy[202]. In this model, we provide detailed instructions on how to perform RYGB using linear staplers in a rat model resulting in a gastric pouch more in keeping with that of human anatomy. Overall, this procedure was associated with excellent survival rates and metabolic outcomes.

2.3 PROTOCOL

Animal use protocols were approved by the Health Science Animal Care and Use Committee at the University of Alberta (AUP00003000). See Figure 8 for a diagram demonstrating the RYGB anatomy. This protocol has also been published as a video: https://www.jove.com/t/62575/a-protocol-for-roux-en-y-gastric-bypass-in-rats-using-linear-staplers.

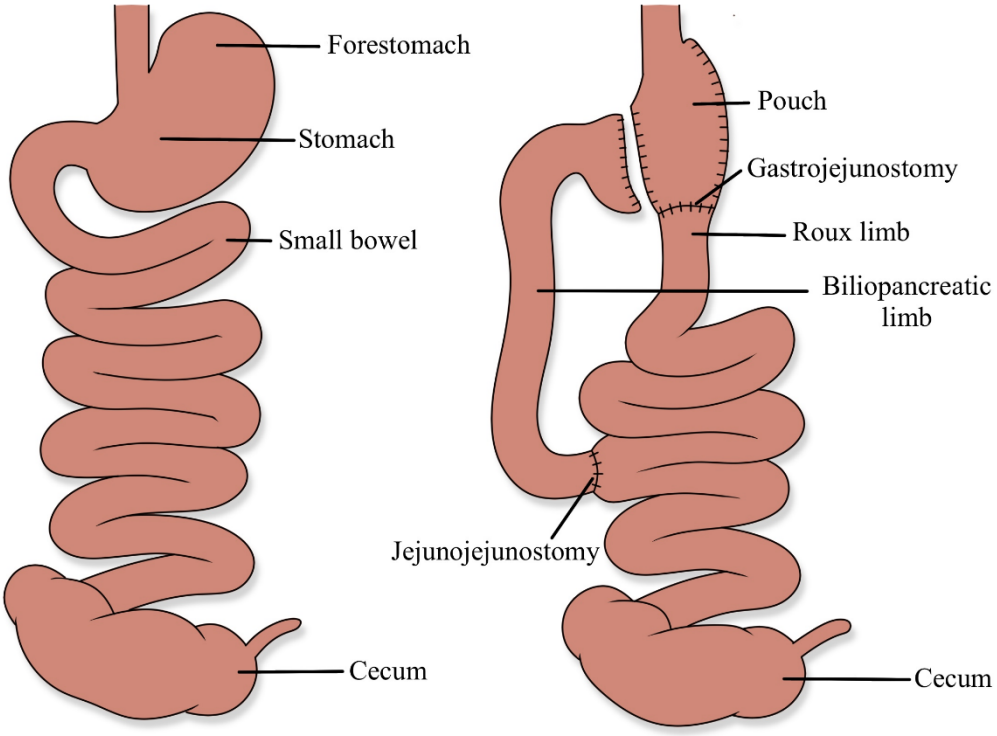

Figure 8. Roux-en-Y gastric bypass anatomy

2.3.1 ROUX-EN-Y GASTRIC BYPASS

1.1. Preparation of animals and operative setup

1.1.1. One week prior to the surgery, provide the rats with oral rehydration therapy and liquid diet in addition to their solid diet and water to acclimatize them to this new diet.

1.1.2. Fast rats with only access to water for 12-18 h prior to the surgery.

1.1.2.1. Ensure rats are fasted on a raised wire platform so that they cannot consume bedding material.

1.1.3. Inject rats with subcutaneous long buprenorphine sustained release (SR) at a dose of 1

mg/kg immediately before surgery.

1.1.4. Autoclave all surgical instruments, towels, and drapes.

1.1.5. Clean operating surface, heating pad and anesthetic nose cone with 70% ethanol.

1.1.6. Set up the operating surface with operating microscope, anesthetic machine and supplies in a manner which is ergonomic for the operating surgeon.

1.1.7. Use a temperature-regulated heating pad and set to 37 °C.

1.1.8. Place a sterile drape or towel over the heating pad.

1.1.9. Fill a 50 mL sterile conical tube with 0.9% saline.

1.2. Anesthetic induction and preparation

1.2.1. Induce anesthesia using 4% isoflurane as per previously established protocols[206].

1.2.2. Apply pressure to the hindfoot of all four limbs to ensure there is no pain response.

1.2.3. Check for adequate anesthesia and respiratory rate after every 5 min.

1.2.4. Apply lubricant to both eyes to prevent drying.

1.2.5. Shave hair from the abdomen.

1.2.6. Clean the abdomen with a povidone-iodine solution, allow the solution to dry, and change into sterile gloves.

1.2.7. Drape the rat with an opening in the drape to expose the abdomen.

1.2.8. Instruments, sutures, cotton swabs, and a 10 mL syringe are placed in a location that permits easy access during the procedure.

1.3. Median laparotomy

1.3.1. Make a 3 cm incision in the upper midline of the abdomen using a scalpel, just below the

xyphoid process as a landmark.

1.3.2. Using scissors, divide the fascia and peritoneum, with care to stay midline on the linea alba to reduce bleeding from the rectus abdominus. If there is bleeding, control it with thermal or electrocautery.

1.4. Mobilizing the stomach

1.4.1. Using two wet cotton swabs, bluntly dissect gastric attachments.

1.4.2. When encountering dense adhesions, use thermal cautery to divide gastric attachments, with care to avoid cauterizing the stomach. Sharply divide the ligament between the stomach and the accessory liver lobe to reduce the risk of liver tearing with stomach mobilization.

1.4.3. For larger blood vessels, especially at the short gastric arteries, ligate using 6-0 polypropylene suture.

1.4.4. Create a window on the right distal side of the esophagus but proximal to the left gastric artery. Ensure that a cotton swab can reach into this area posteriorly. The stomach is adequately mobilized when it can be exteriorized outside of the abdomen.

1.5. Identify and divide the jejunum

1.5.1. Identify the ligament of Treitz by following the jejunum proximally until observing it is attachment to the transverse mesocolon.

1.5.2. Measure 7 cm distally, identify a location between mesenteric vessels, and divide the bowel with micro scissors. Avoid Peyer's patches when dividing the bowel. Take care to only divide the bowel and not the mesentery.

1.5.3. Place a clean, saline soaked sponge prior to dividing the bowel to minimize contamination.

1.5.4. Check for the presence of a small crossing vessel in the mesentery at the border of the small bowel and divide this with cautery to avoid bleeding.

1.5.5. Continue to divide the mesentery 1 cm towards the mesenteric base.

1.5.6. Identify the proximal and distal jejunum. Place the proximal jejunum under a wet gauze on the rat's right and the distal jejunum on the rat's left.

1.6. Stapling the stomach

1.6.1. Insert a 45 mm linear cutting stapler with 3.5 mm staple height across the white line of the forestomach to create a smaller pouch. Wait for 10 s before firing the stapler.

1.6.2. Place pressure using gauze on the staple lines for 1 min to ensure hemostasis.

1.6.2.1. If hemostasis is not achieved with pressure alone, bleeding along the staple line is oversewn using 6-0 polypropylene figure of eight sutures.

1.6.3. Perform a second staple fire across the stomach into the window created previously. Wait for 10 s before firing the stapler.

1.6.3.1. Pressure is held along the staple line to ensure hemostasis and oversewing may be needed.

1.7. Gastrojejunostomy

1.7.1. A gastrotomy is made immediately after stapling the stomach. Delays in this can cause gastric distension and aspiration as the stomach is discontinuous after the second gastric staple.

1.7.2. Using an 11-blade scalpel, create a gastrotomy at the distal pouch. Express gastric contents through the gastrotomy. This is important to prevent gastric distension and aspiration. Lengthen this gastrotomy using micro scissors to approximately 5 mm. The gastrotomy is made large enough

for the cotton swab tip to just fit through.

1.7.3. Mobilize the distal end of the jejunum adjacent to the gastrotomy and place such that the mesentery is not twisted.

1.7.4. While suturing the anastomosis, ensure that the bowel is kept moist by covering it with saline-soaked gauze and reapplying saline regularly.

1.7.5. Using 6-0 polydioxanone or polypropylene suture, place a stay suture at the inferior margin of the anastomosis and gently retract using a snap. Tie with three knots.

1.7.6. Place a stay suture at the superior margin of the anastomosis and gently retract using a snap. Tie with six knots.

1.7.7. Suture the anterior side of the anastomosis in a continuous fashion, taking bites 1 mm wide and 1 mm apart with care to avoid taking the backside.

1.7.8. Once the suture has reached the inferior stay suture, tie these together with an additional six knots.

1.7.9. Once the anterior side is complete, flip the bowel and stomach over and pass the inferior stay suture through the mesenteric defect. Reapply the snap and retract inferiorly.

1.7.10. For the posterior side of the anastomosis, place full thickness interrupted 6-0 sutures, 1 mm wide and spaced 1 mm apart, with care to avoid taking the backside. These are tied with six knots each.

NOTE: The anterior side of the anastomosis is sutured in a continuous fashion while the posterior side is done in an interrupted fashion. This prevents potential stricture or stenosis associated with a circumferential continuous closure.

1.7.11. Check for the leakage by gently pushing luminal contents across the anastomosis. If there are areas with leakage, carefully reinforce them with interrupted sutures. Take care to avoid taking

the backwall when reinforcing with extra sutures.

1.8. Jejunojejunostomy

1.8.1. From the gastrojejunostomy, measure 20 cm distally.

1.8.2. Create a jejunotomy on the antimesenteric side using the 11-blade scalpel. Avoid making the jejunotomy over Peyer's patches.

1.8.3. Extend this jejunotomy using micro scissors, such that it is the same size as the biliopancreatic limb. Ensure that a cotton swab just fits inside.

1.8.4. Place the biliopancreatic limb such that there is no twisting of the mesentery.

1.8.5. Perform the anastomosis similarly to the gastrojejunostomy with 6-0 stay sutures on the superior and inferior sides. The anterior side is performed with continuous sutures while the posterior side is performed with interrupted sutures.

1.8.6. Ensure that the bowel is kept moist with saline during this anastomosis.

1.8.7. Check for leakage by gently pushing luminal contents through the anastomosis. If there are areas with leakage, reinforce them with interrupted sutures.

1.9. Reposition the bowel and stomach

1.9.1. Ensure that there is no twisting of the pouch, remnant stomach or liver. Ensure that the left lobe of the liver is anterior to the stomach and not trapped behind the pouch as this can cause compressive liver ischemia.

1.9.2. Position the bowel in the abdomen in its natural position such that there is no twisting.

1.10. Abdominal closure

1.10.1. Close the fascia with 3-0 polyglactin in a continuous fashion. 3-0 polydioxanone may also be used.

1.10.2. Close the skin with 2-0 silk in a continuous fashion.

1.11. Anesthetic emergence

1.11.1. Decrease isoflurane to zero but continue supplemental oxygen.

1.11.2. Administer a local anesthetic as a splash block to the incision.

1.11.3. Administer 10 mL of subcutaneous 5% dextrose in normal saline (D5NS) in the subcutaneous tissue behind the neck.

1.11.4. Place an Elizabethan rat collar before the rat is fully awake. Take care to fit it snugly but not too tight to cause discomfort.

NOTE: The collar is kept on until day 5 to prevent wound dehiscence.

2.3.2 SHAM SURGERY

NOTE: Sham surgery is performed similar to RYGB, however, no anastomoses are performed.

1.12. A gastrotomy is created and then closed with 6-0 polydioxanone or polypropylene sutures.

1.13. A jejunotomy is created 7 cm distal to the ligament of Treitz and then closed with 6-0 polydioxanone or polypropylene sutures.

2.3.3 POSTOPERATIVE CARE

1.14. Postoperative care

1.14.1. House rats individually and keep them on raised wire platforms until solid food is reintroduced to prevent consumption of bedding and luminal obstruction.

Note. Postoperative diet is resumed gradually as edema at the gastrojejunostomy can cause obstruction with the early resumption of solid diet.

1.14.2. Inspect the feet daily while rats are on raised wire platforms for any skin changes.

1.14.3. Keep rats on water and oral rehydration therapy diet for the first 72 hours.

1.14.4. Administer 10 mL of D5NS every 12 hours for the first 72 hours.

1.14.5. Administer subcutaneous short-acting buprenorphine at 0.01 mg/kg if rats appear to be in pain. The Rat Grimace Scale is used to assess for pain[207].

1.14.6. On postoperative day 3, add rodent liquid diet. Continue to provide water and oral rehydration therapy.

1.14.7. On postoperative day 5, restart high-fat diet. Continue to provide water and liquid diet. Remove the Elizabethan collar.

1.14.8. On postoperative day 7, discontinue liquid diet.

1.14.9. Remove skin sutures on postoperative day 10-14.

2.4 RESULTS

2.4.1 ANIMALS AND HOUSING

36 male Wistar rats were housed in pairs and were fed sterile rodent high-fat diet starting from six weeks of age. This diet has a caloric distribution that consists of 59% fat, 15% protein and 26% carbohydrates compared to 16% fat, 21% protein and 63% carbohydrates of normal chow. This diet was chosen to create a diet-induced obesity model as this is most representative of severe obesity in humans (Figure 9). At 16 weeks of age, they underwent RYGB or sham surgery. After the first postoperative week, rats were resumed on a high fat diet. Half of the rats were euthanized at 2 weeks post-operative and the other half were euthanized at 14 weeks

postoperative. This time points were chosen to demonstrate the early and late metabolic changes that occur with RYGB.

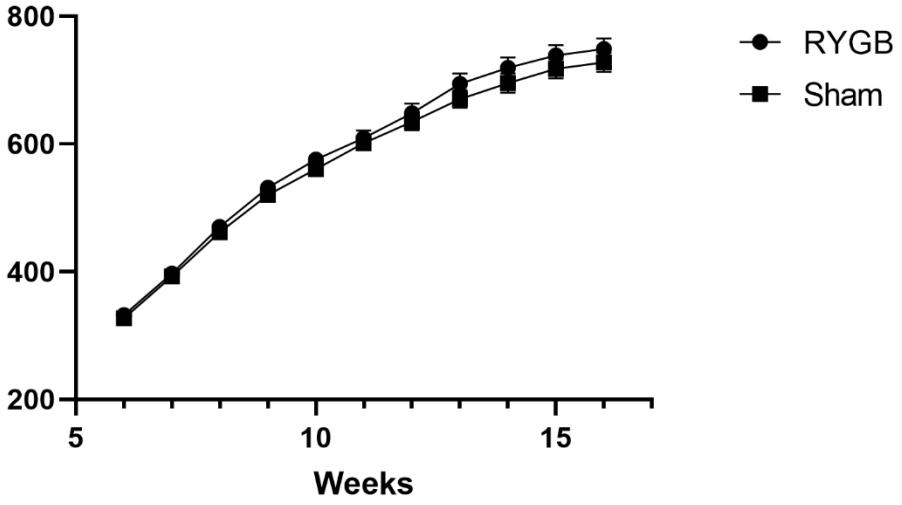

Figure 9. Preoperative absolute weight on high fat diet; RYGB, Roux-en-Y gastric bypass

2.4.2 MORTALITY

Overall, 33 (91.7%) rats survived to the planned study endpoint. All rats who underwent early euthanasia underwent necropsy by a veterinarian. Two rats were euthanized within 24 hours. One RYGB had aspiration pneumonitis and one sham rat had fascial dehiscence with unsalvageable bowel. Another RYGB rat was euthanized at two weeks due to anastomotic leak from the gastrojejunostomy. Overall, 88.9% of RYGB rats survived to study endpoint.

2.4.3 Body Weight

Rats undergoing RYGB had a lower postoperative weight than sham rats. Figure 10 demonstrates absolute weights for rats postoperatively while Figure 11 demonstrates postoperative percentage weight change which was statistically significant at all timepoints postoperatively. At 14 weeks, rats who had RYGB had a mean percentage weight change of 6.4% while rats with sham surgery had 23.7% ($p = 0.0001$).

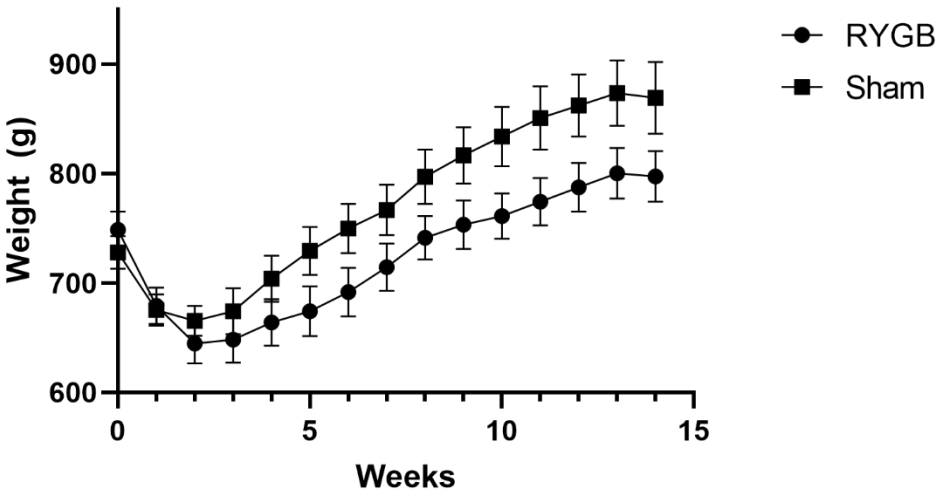

Figure 10. Postoperative absolute weight on high-fat diet; RYGB, Roux-en-Y gastric bypass

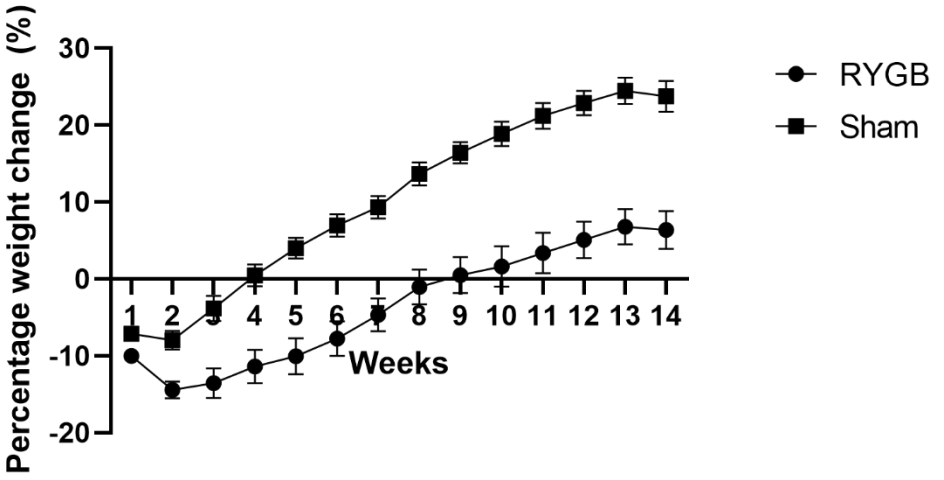

Figure 11. Postoperative percentage weight change on high-fat diet; RYGB, Roux-en-Y gastric bypass

2.4.4 Intraperitoneal glucose tolerance testing

Fasting blood glucose was not significantly different between any of the cohorts. However, the area under the curve was significantly lower in RYGB compared with sham at 13 weeks (18.1 vs 23.8 mmol-h/L, p=0.046, Figure 12) but was the same for RYGB vs sham at 1 week (20.8 vs 23.3 mmol-h/L, p=0.68).

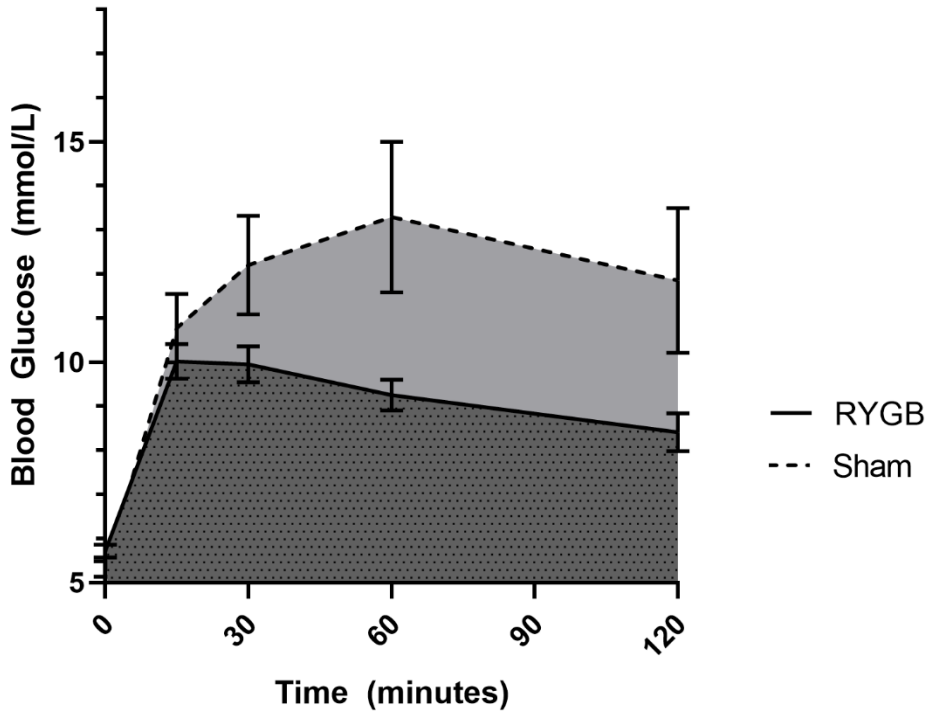

Figure 12. Intraperitoneal glucose tolerance testing in gastric bypass vs sham at 13 weeks. RYGB, Roux-en-Y gastric bypass

2.5 DISCUSSION

RYGB involves the creation of a small gastric pouch (less than 30 mL), and the creation of a biliopancreatic limb and a Roux limb (Figure 8). In humans, the biliopancreatic limb is typically 30 to 50 cm and transports secretions from the gastric remnant, liver, and pancreas. The Roux limb is typically 75 to 150 cm in length and is the primary channel for ingested food. The common channel is the remaining small bowel distal to where the two limbs join and is where the majority of digestion and absorption occur, as pancreatic enzymes and bile mix with ingested food[49].

The mechanism of weight loss in RYGB is multimodal. The small gastric pouch reduces food intake through mechanical restriction. The bypass results in a malabsorptive component as a significant portion of the small intestine is not absorbing calories and nutrients. More recently, studies have demonstrated that gut hormones play a significant role in weight loss after RYGB as well. These are primarily through ghrelin, peptide-YY, cholecystokinin (CCK), and GLP-1 hormone pathways[50].

Rat models provide a powerful method to study the mechanisms behind both the weight and metabolic effects of RYGB. In this paper, we present a RYGB protocol that has low mortality with significant weight loss and metabolic effects. Once the operator became familiar with the technique, the procedure took approximately 90 minutes to perform. The protocol can also be modified with longer biliopancreatic and Roux limb lengths to potentially increase weight loss and metabolic effect. Furthermore, it is technically more feasible than other models as it allows

the use of surgical staplers to achieve hemostasis and minimize operative time. Models that rely on sharp division of the stomach without stapling often result in higher mortality due to significant blood loss. The technical skills required to perform the procedure were relatively easy to acquire and learners were able to comfortably perform the procedure after approximately five to ten non-recovery procedures.

One of the critical steps of this protocol is to limit blood loss during mobilization of the stomach. Careful use of thermal cautery combined with suture ligation of vessels is important. It is also important to perform at least half the circumference of the anastomoses in an interrupted manner. This prevents excessive stricturing at the anastomoses. Furthermore, checking for leaks is crucial as these can lead to sepsis and death. Prior to closing the abdomen, it is essential that the left lobe of the liver is placed in its natural, anterior position and that there is no rotation in the bowel or the stomach as this can lead to visceral ischemia.

Postoperative care is vital to this protocol. Raised wire platforms are required during both fasting and postoperative periods as the consumption of solid material leads to anastomotic obstructions. It is vitally important to provide subcutaneous fluid as the rats may not tolerate oral fluids in the immediate postoperative period. The rats should be acclimatized to oral rehydration therapy and liquid diet as rats may avoid new diets due to associations with postoperative pain. This dietary protocol contributes to significant weight loss in the immediate postoperative period in both the RYGB and sham cohorts, and weight recovery in the sham group took about five weeks. However, strict adherence to this postoperative protocol is vital to reduce morbidity and

mortality after RYGB. Additionally, frequent examination of the rats using the Rat Grimace Scale is important to detect for morbidity. In our study, one rat developed a late anastomotic leak which was rapidly detected using this scale and allowed for early euthanasia to reduce suffering.

One of the advantages of this method is that it results in a smaller pouch through the use of surgical staplers to reduce gastric bleeding. When we attempted to sharply divide the stomach without staplers, it led to excessive bleeding and a much higher mortality rate. However, this also leads to removal of the forestomach and this may lead to physiologic changes that are different from that of human RYGB. However, the forestomach is unique to rodents and contains no glands and should not cause any changes to gut hormones.

The most important limitation of this method is that it requires two surgical stapler reloads per rat which can be costly. However, excellent survival outcomes potentially reduce cost by requiring less rats for a study, resulting in better utilization of husbandry facilities, surgical equipment and research personnel.

2.6 ACKNOWLEDGMENTS

This study was funded by the American Society for Metabolic and Bariatric Surgery Research Award. Ethicon graciously supplied sutures, staplers, and clips. The lead author's doctoral research was funded in by the University of Alberta Clinician Investigator Program and the Alberta Innovates Clinician Fellowship. We would also like to thank Michelle Tran for her medical illustration of the RYGB anatomy.

2.7 DISCLOSURES

Ethicon supplied two 45 mm linear cutting staplers, multiple 3.5 mm stapler reloads, and 6-0 polypropylene sutures. Authors have no other conflicts of interest to declare.

CHAPTER 3. MICROBIAL SHIFTS WITHIN THE ILEUM AFTER ROUX-EN-Y GASTRIC BYPASS ORCHESTRATE CHANGES IN GLUCOSE METABOLISM THROUGH MODULATION OF BILE ACIDS AND ENTEROENDOCRINE L-CELL ADAPTATION

3.1 ABSTRACT

Background

Roux-en-Y gastric bypass (RYGB)-induced glycemic improvement is associated with increases in glucagon-like-peptide-1 (GLP-1) secreted from L-cells in the ileum. Proposed mechanisms for GLP-1 changes include shifts in gut microbiota and bile acids, however these are poorly understood and have not been explored in the context of RYGB.

Objectives and Hypothesis

The objective of this study was to analyze changes in ileal bile acids and ileal microbial composition in diet-induced-obesity rats after RYGB to elucidate the early and late effects on L-cells and glucose homeostasis. We hypothesize that altered anatomy and bile acid physiology following RYGB leads to significant changes in gut microbial composition and function resulting in altered signaling to ileal L cells and increased release of GLP-1.

Methods

Rats underwent RYGB or sham surgery and were separated into early (2-week) or late (14-week) postoperative cohorts. Metabolic outcomes and ileal samples were analyzed.

Results

In early cohorts, there were no significant changes in L-cell density, serum GLP-1 or glucose tolerance. In late cohorts, RYGB rats demonstrated less weight regain and improved glucose tolerance. Following RYGB, there was increased L-cell density (45.0 vs 34.7 cells/mm^2, p=0.033) and increased villi height (507.7 vs 388.8 μm, p=0.0004) in the late RYGB cohort. No difference in the expression of GLP-1 relevant genes was observed at any timepoint. Bile acid analysis found lower concentrations of ileal bile acids (408.8 vs 144.7 μM, p=0.0052) following RYGB in the late cohort. Microbial analysis demonstrated decreased alpha diversity in early RYGB cohorts which normalized in the late group. In the early RYGB cohorts, there were higher abundances of *Escherichia-Shigella* but lower abundances of *Lactobacillus*, *Adlercreutzia*, and *Proteus* while the late cohorts demonstrated higher abundances of *Escherichia-Shigella* and lower abundances of *Lactobacillus*. *Lactobacillus* had positive correlations while *Escherichia-Shigella* had negative correlations with specific conjugated bile acids.

Conclusions

There were no differences in L-cells or glucose tolerance in the early cohorts. However, in the late cohorts, RYGB lead to an increase in L-cell density and villi height. Shifts in Lactobacillus and Escherichia-Shigella correlated with decreases in specific conjugated ileal bile acids.

3.2 INTRODUCTION

Roux-en-Y gastric bypass (RYGB) leads to rapid and sustained resolution of diabetes, however the mechanisms responsible for these dramatic corrections in maladaptive glucose homeostasis remain unclear[200]. Two major theories have been proposed to explain the metabolic changes associated with diabetes remission. First, the hindgut hypothesis postulates that higher concentrations of undigested nutrients reach the distal intestine enhancing the release of hormones such as glucagon-like-peptide-1 (GLP-1). Alternatively, the foregut hypothesis suggests that bypassing the proximal intestine reduces secretion of anti-incretin hormones. Intestinal enteroendocrine L-cells which secrete GLP-1 are thought to be key players underlying these two theories but little is known about how their post-operative adaptations influence metabolic improvement, nor the factors which may influence their translational capacity[63].

Enteroendocrine L-cells are present throughout the small and large bowel but are greatest in number within the distal ileum. Mechanisms by which RYGB influences L-cell changes that subsequently result in beneficial increases in GLP-1 are not entirely clear but emerging evidence has implicated several factors including surgical-induced changes in the gut microbiome and circulating bile acids. In a study of L-cell expression and gut microbes, Arora et al. found that colonization of germ-free mice with microbes from conventional mice resulted in transcriptional suppression of L-cells[208]. It is plausible that a rapid modulation of the enteric microbiome following RYGB alters gut microbial function with a resultant change in signaling to L-cells. Furthermore, studies consistently demonstrate profound RYGB-mediated changes to serum bile acid concentration and composition thought to occur due to intestinal adaptations that lead to increased intestinal absorption of nutrients[209]. These differences warrant further study as changes

to ileal bile acid composition modulate GLP-1 secretion through regulatory bile acid receptors TGR5[210] and FXR[211], and in turn also significantly influence gut microbial composition[143,145,212,213].

Ultimately, the complex changes that occur within the gut microbiota and enteric bile acid profiles after RYGB could lead to modulation of gene expression within L-cells with a subsequent increase in GLP-1 production and improvement in glucose homeostasis. We hypothesize that altered gut anatomy and bile acid physiology following RYGB leads to significant changes in gut microbial composition and function resulting in altered gene expression within ileal L-cells and increased release of GLP-1 and that early increases in GLP-1 will be modulated by transcriptional changes within L-cells and later through a proliferation in the quantity of L-cells.

3.3 METHODS

Study design

This study was approved by the Animal Research Ethics Board at the University of Alberta (AUP00003000). Thirty-six male Wistar rats were randomly assigned to four cohorts based on procedure and planned date of euthanasia: 2-week RYGB, 14-week RYGB, 2-week sham, or 14-week sham. Male rats were chosen to avoid estrous cycles of female rats which may affect hormone outcomes in the 2-week cohorts. The rats were doubly housed until six weeks of age after which they were separated into single cages to avoid cage effects biasing microbial analysis. Sterile high-fat-diet (HFD, Bio-Serv S3282, 60% calories from fat) was introduced at

six weeks of age and continued throughout the experiment, except during the perioperative period. Body weight was monitored weekly. RYGB or sham surgery were performed at 16 weeks of age. Study flowchart is detailed in Figure 13.

Rats were euthanized at 2 and 14 weeks after surgery to evaluate early and late post-RYGB L-cell and enteroendocrine changes. The two-week time point was chosen to evaluate early changes to allow for a one-week washout from postoperative liquid diet and to assess for metabolic changes while on HFD. The 14-week timepoint was chosen to allow for evaluation of late RYGB-adaptive L-cell changes. One week prior to euthanasia, intraperitoneal glucose tolerance testing (IPGTT) was performed. Rats were then euthanized with collection of blood for postprandial gut hormones, ileal tissue and ileal enteric contents. Ileal tissue underwent immunofluorescence staining to quantify the number of L and K cells. Intestinal morphology quantification was conducted with direct microscopy. Reverse transcription polymerase chain reaction (RT-PCR) was performed on ileal tissue for gene expression of GLP-1 and gastric inhibitory polypeptide (GIP) relevant genes. Ileal enteric contents underwent 16S rRNA sequencing for microbial composition and liquid chromatography-mass spectrometry for bile acid analysis.

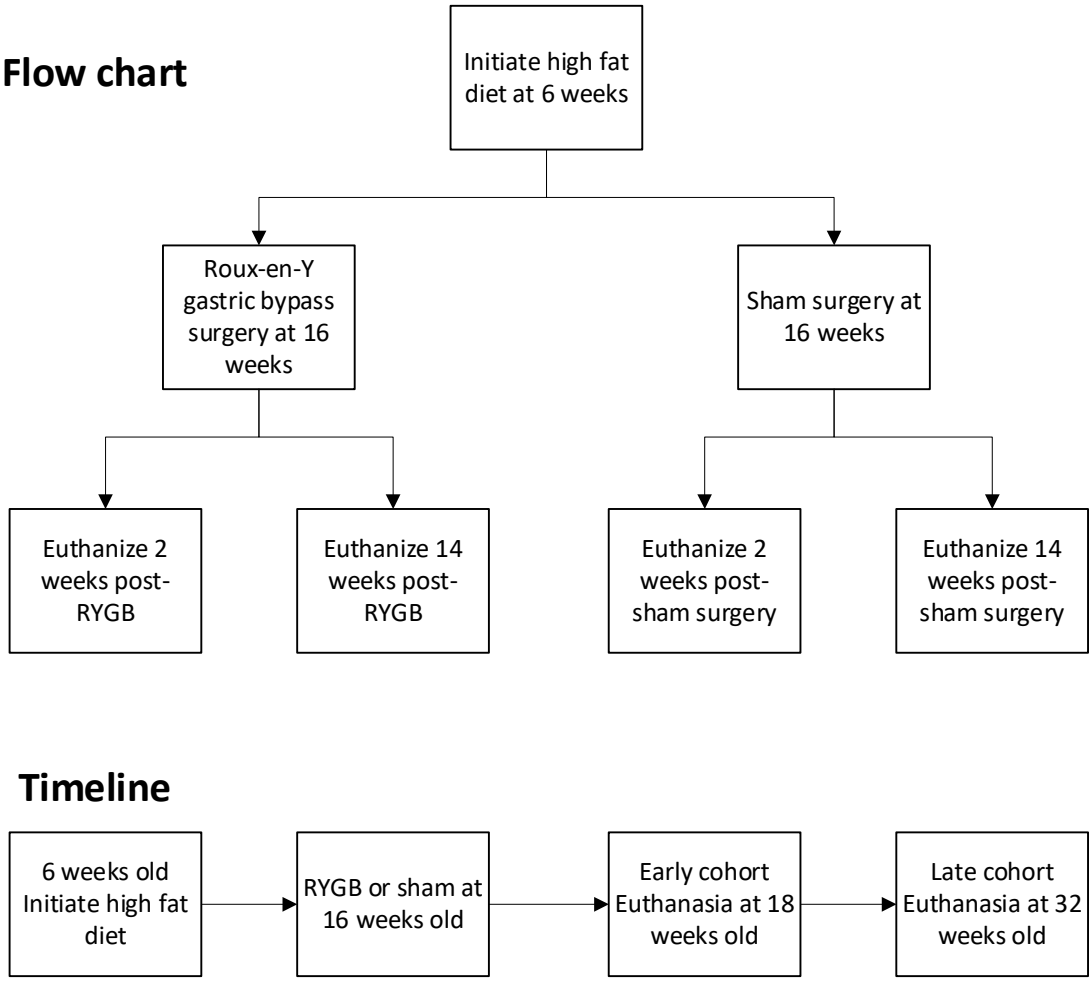

Figure 13. Study flowchart and timeline

Study objectives

The primary objective of this study was to determine early and late changes to L-cell quantity and GLP-1 gene expression of ileal L-cells between RYGB and sham surgery, defined as 2 weeks and 14 weeks, respectively.

Secondary objectives included determining changes in villi morphology, bile acid composition, and microbial composition within the ileum and identifying pathways in which these changes affect L-cell gene expression and quantity. Additionally, serum GLP-1 and glucose tolerance were compared between groups to determine the effects of RYGB on glucose metabolism.

Sample size calculation

Sample size calculations were designed to ensure GLP-1 changes induced by surgery would be adequately captured. In prior literature, rats had significantly increased GLP-1 after RYGB (25 vs 75 pmol/L, σ=30)[214]. Powering to detect a 25% GLP-1 difference between cohorts, with an alpha of 0.05 and a beta of 0.80, would require 8 rats per arm. Also accounting for a mortality of ~10%, this would require 9 rats per arm for a total of 36 rats.

Surgical procedure

After an overnight fast, RYGB (Figure 14) or sham surgery were performed based on previously published protocols[201,215]. In summary, anesthesia was induced using isoflurane and rats were given subcutaneous buprenorphine sustained release (1 mg/kg). A midline incision was made sharply, and the stomach was mobilized by dividing the gastric attachments using a combination of electrocautery and ligation with 6-0 polypropylene. A window was made in the gastrohepatic ligament superior to the left gastric artery to allow for stapling. The ligament of Treitz was located and the jejunum was divided 7 cm distally. The stomach was divided with a 45 mm laparoscopic linear stapler (Ethicon, ETS45) with 3.5 mm blue load staplers. Hemostasis at the staple line was achieved with pressure and suture ligation. A second stapler was deployed to

resect the gastric fundus (forestomach) to prevent retained food within a large pouch. A gastrotomy was created in the distal pouch. A circular gastrojejunostomy was created with 6-0 polypropylene (continuous on anterior side, interrupted on posterior). A leak check was performed by gently compressing enteric contents through the anastomosis. The jejunum was then measured 20 cm distally and an enterotomy was created. An end to side jejunojejunostomy was then performed using a similar technique to the gastrojejunostomy. The fascia was closed using 3-0 polyglactin and skin was closed with 2-0 silk.

The sham procedure was performed similarly except a gastrotomy was made in the distal anterior stomach and closed with 6-0 polypropylene. A jejunotomy was made 7 cm distal to ligament of Treitz and closed with 6-0 polypropylene.

Postoperatively, the rats were provided water and electrolyte replacement solution (Hydralyte) for 72 hours but given twice daily subcutaneous D5NS solution. On postoperative day 3, the rats were progressed to a liquid diet (Bio-Serv, F1259) and then resumed on high-fat diet on day 5.

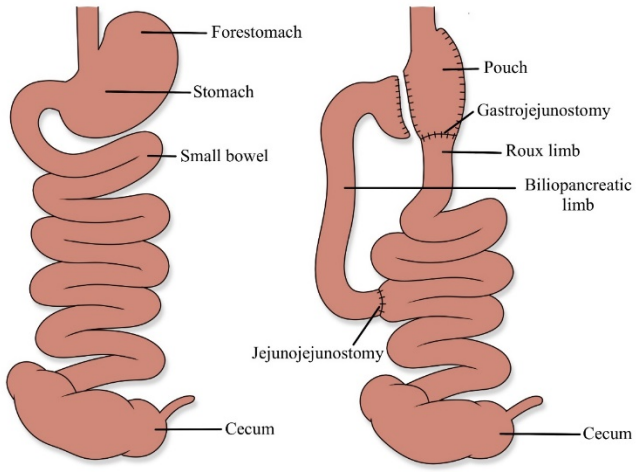

Figure 14. Roux-en-Y gastric bypass anatomy in the rat

Intraperitoneal glucose tolerance test (IPGTT)

An IPGTT was performed one week prior to euthanasia. After a 16-hour fast, blood glucose was measured from the lateral saphenous vein of unrestrained rats using a glucometer at baseline and following intraperitoneal dextrose injection at a dose of 2 g/kg of body weight. Post-injection glucose measurements occurred at 15, 30, 60, and 120 minutes.

Serum enzyme-linked immunosorbent assay (ELISA) analysis

Rats were fasted overnight for 12 hours prior to euthanasia and then given ad-lib access to high-fat diet for 3 hours. Blood was collected by cardiac puncture immediately prior to euthanasia for gut hormone testing. Serum was analyzed for total GLP-1 (Millipore, EZGLP1T-36K) and total GIP (Millipore, EZRMGIP-55K) using standard ELISA.

Isolation of intestinal cells, brightfield microscopy, and immunofluorescence

After rats were anesthetized, a 10-cm segment of ileum proximal to the cecum was removed. Intestinal tissue was opened longitudinally and rinsed with phosphate-buffered saline. Separate portions were flash frozen in a guanidinium thiocyanate solution (Thermo Fisher, Trizol) and cryopreserved in neutral buffered formalin (10% vol:vol) with sucrose[216]. These were fixed using a standard alcohol, xylene and paraffin process. Embedded tissue was cut to 16 μm and mounted on a slide.

Ileal morphology was examined using brightfield microscopy (Zeiss, Observer Z1) at 10x magnification. Twenty random villi and crypts were measured for villi height, villi width, crypt width, crypt depth and epithelial thickness. Only complete and vertically oriented villi and crypts were measured (Supplementary Figure 1).

Immunofluorescence staining was performed as per published protocols[217] using Polyclonal GIP (Thermo Fisher, PA5-76867, 1:800) and Anti-GLP1 (Abcam, ab26278, 1:800) primary antibodies with Alexa Fluor 488 (Thermo Fisher) and Alexa Fluor 647 (Thermo Fisher) secondary antibodies. This allowed visualization of L-, K- and L-cells which co-express GLP-1 and GIP. Nuclei staining was performed using diamidino-2-phenylindole (DAPI) solution (Thermo Fisher).

Forty random confocal images of epithelium were taken at 40x magnification using the WaveFX Confocal microscope. Images were manually counted for L-cells and K-cells. Cell density was calculated based on cells/mm^2. Supplementary Figure 2 is a representative image of resultant immunofluorescence staining.

Quantitative RT-PCR

RNA was extracted from ileal intestinal tissue using the TRIzol® Plus RNA Purification Kit (Thermo Fisher, 12183555). Reverse transcription was performed with the High-Capacity cDNA Reverse Transcription Kit (Thermo Fisher, 4368814). Quantitative PCR was performed with the TaqMan Gene Expression Master Mix and the following mRNA sequences:

- gcg (Proglucagon mRNA) for GLP-1 expression
- PC1/3 (Prohormone convertase 1/3 mRNA) – mediates posttranslational processing of proglucagon
- gip (Pro.GIP mRNA) for GIP expression
- Normalized to CgA (Chromogranin A) gene, specific for enteroendocrine cells
- Corrected against RPL32 (ribosomal protein 32) - housekeeping gene

Ileal microbial analysis

The microbial community compositions of ileal enteric contents were assessed using 16S rRNA gene sequencing. DNA was extracted from ileal homogenates combining enzymatic and mechanical cell lysis with the QIAamp DNA Stool Mini Kit (Qiagen, USA). Enteric microbiota

composition was characterized by 16S rRNA tag sequencing using the MiSeq Illumina technology (pair-end), targeting the V3-V5 regions. This analysis was performed by Genome Quebec (Montreal, Canada).

Demultiplexed FASTQ sequences were quality filtered, trimmed, dereplicated, and filtered for chimeric sequences using pair-ended DADA2 resulting in exact sequence variant (feature) tables[218]. The table was imported into R 3.6.1 to analyze for α-diversity (Shannon), β-diversity (wunifrac) and were performed using a function of the phyloseq v1.28.0 package[219]. Ordination plots for β-diversity metrics were generated by non-parametric multidimensional scaling ordination in R.

Ileal bile acid analysis

Bile acid analysis was performed for quantification of 20 rodent specific bile acids in rat ileal fecal matter using the AbsoluteIDQ bile acids kit (Biocrates) and liquid chromatography-mass spectrometry. This was performed at The Metabolomics Innovation Centre (Edmonton, Canada) and includes quantification of unconjugated, taurine- and glycine- conjugated bile acids.

Statistical Analysis

Descriptive categorical data were expressed as percentages and continuous data were expressed as mean ± standard deviation (SD). Baseline differences between groups were evaluated by univariate analyses using Fisher's exact test for categorical data and independent sample t-test

for continuous data. Multiple comparisons were adjusted using the Benjamini-Hochberg method to correct the false discovery rate. Error bars on figures represent standard error of the means. Analyses were conducted using STATA 15 (StataCorp 2017; College Station, TX). Figures were designed using Prism 9.0.0 (GraphPad Software, San Diego, CA). Statistical significance was defined using two-tailed tests with a p-value < 0.05.

Integrated microbial and bile acid analysis was performed using the M^2IA platform[183]. Microbial abundance counts were normalized by percentages. Differential bile acids and microbes between groups were selected using univariate analysis. Spearman's correlation coefficients were calculated between differential bile acids and microbes using a pairwise correlation analysis method with significance defined as $p < 0.05$ and $R > 0.3$ or < -0.3. Spearman's correlation was also performed between intestinal morphology, L-cell density and microbes.

3.4 RESULTS

Weight and Survival Outcomes

There was significant weight gain from weeks 6 to 16 in both the RYGB and sham cohorts after introduction of a HFD (%weight change, 125.1±3.9% vs 122.3±3.6%, p=0.6, Supplementary Figure 3). Following surgery, there was an initial loss of weight in the first two weeks due to post-operative dietary restrictions in both RYGB and sham animals. However, rats undergoing RYGB had significantly less weight gain at 14 weeks postoperatively compared to sham (6.4± 2.5 vs 23.7±2.0%, p=0.0001, Supplementary Figure 3).

Overall, 88.9% of RYGB rats and 93.8% of sham rats survived to study endpoints. All rats with unexpected mortality underwent necropsy by a veterinarian. Deaths were due to aspiration pneumonitis, fascial dehiscence and anastomotic leak at the gastrojejunostomy.

Ileal morphometric parameters

Early cohort RYGB rats had increases in ileal crypt width versus sham (48.3±3.9 vs 42.8 5.4 μm, p=0.04). When comparing the late cohorts, RYGB rats experienced additional significant morphological differences including increased villi height (507.7±64.7 vs 388.8±42.2 μm, p=0.0004), crypt width (50.3±9.1 vs 43.0±3.7 μm, p=0.04) and crypt depth (192.9±27.0 vs 165.3±21.4 μm, p=0.03, Figure 15). Villi width and epithelial thickness were similar amongst all groups.

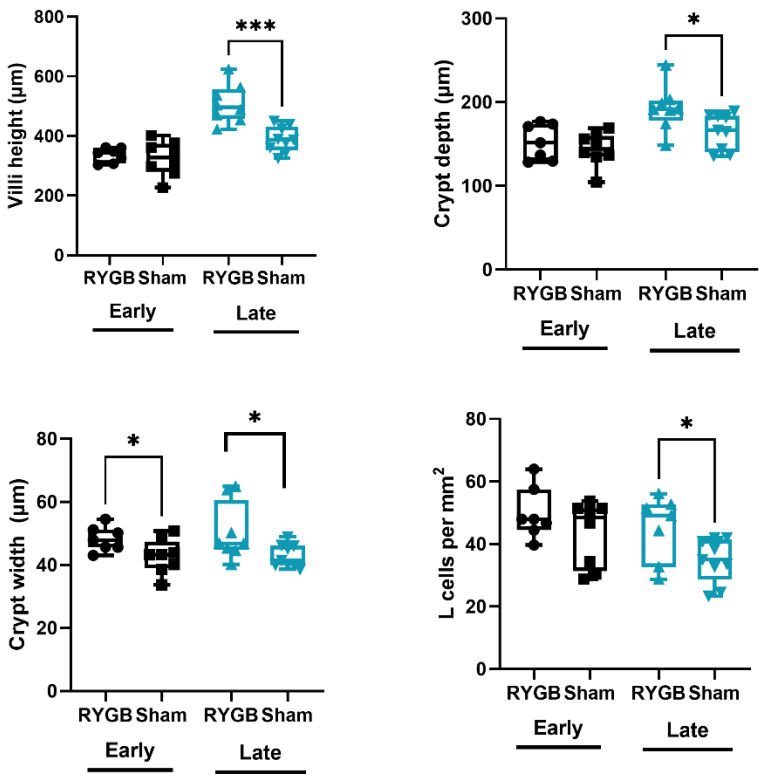

Figure 15. Ileal morphological changes and L-cell density amongst groups: early Roux-en-Y gastric bypass (RYGB) (n=7), early sham (n=8), late RYGB (n=8), late sham (n=9). Error bars on figures represent standard error of the means and asterisks represent statistical significance with * as $p<0.05$, ** as $p<0.01$, *** as $p<0.001$, **** as $p<0.0001$.

L-cell quantification and gene expression

Immunofluorescence demonstrated multiple L-cells within ileal tissue but only rare occurrences of K- or LK-cells. In the early cohorts, L-cell density was not significantly different but was significantly increased in the late RYGB cohort (45.0±10.5 vs 34.7±7.0 cells/mm^2, $p=0.03$, Figure 15). Despite increases in L-cell density, there were no significant differences in GLP-1 gene expression within L-cells between cohorts for *gcg* or *PC1/3* at either time point.

Glucose tolerance testing

There were no differences in glucose tolerance testing in the early groups. However, in the late groups, dynamic glycemic responses to an intraperitoneal glucose tolerance test revealed a significantly lower area under the curve after RYGB compared to sham (18.1±0.9 vs 23.8±3.9 mmol-h/L, p=0.046, Figure 16).

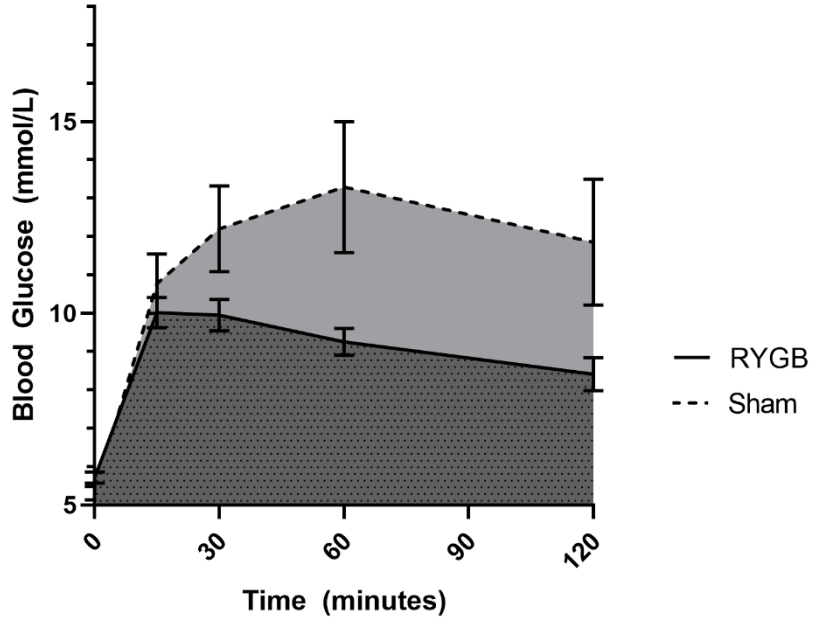

Figure 16. Intraperitoneal glucose tolerance testing in gastric bypass (n=8) vs sham (n=9) in the late cohorts; RYGB, Roux-en-Y gastric bypass.

L-cell enteroendocrine hormones

Post-prandial serum GLP-1 was similar between the early RYGB and early sham groups. However, GLP-1 was more than two times greater in the late RYGB compared to the late sham

cohort (45.4±48.2 vs 21.1±6.0 pM, p=0.12) but this did not reach statistical significance. Serum GIP did not differ between groups at either time point.

Microbial species alpha- and beta-diversity

Alpha-diversity analysis revealed that early RYGB animals had significantly decreased evenness (Shannon index) when compared to early sham cohorts (p=0.05). These differences were not present in the late cohorts due to restoration of diversity after RYGB (p=0.015). There were no statistical differences in richness (Chao1 index) between any cohorts (Figure 17b). Beta diversity approached statistical significance between the early RYGB cohort and early sham cohorts as determined by the Bray-Curtis dissimilarity index (p=0.052). However, in the late groups, beta diversity was significant between RYGB and sham (p=0.03, Figure 17c).

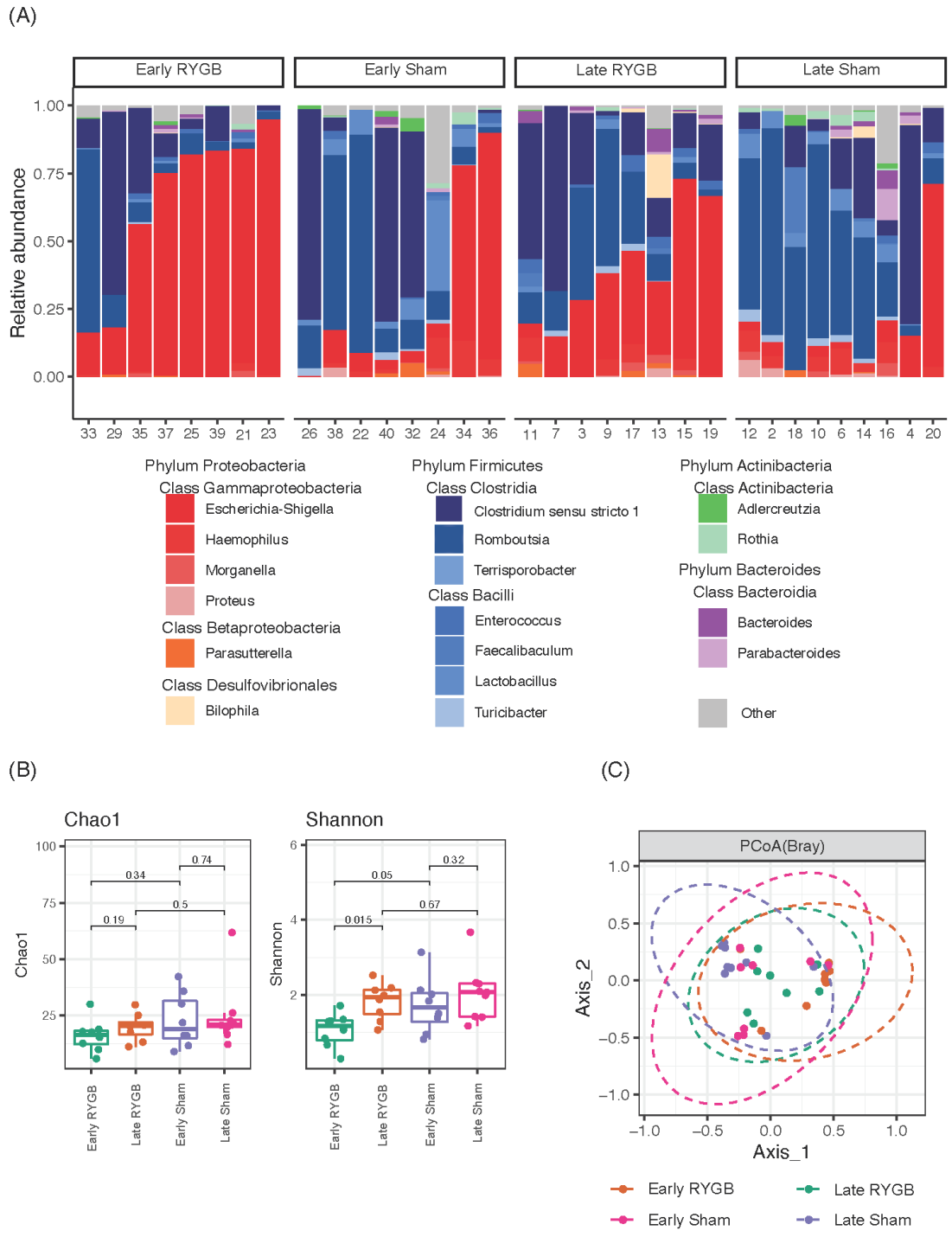

Figure 17. Differences in microbial abundance between Roux-en-Y gastric bypass and sham at early and late timepoints. (A) Taxonomic differences in relative microbial abundance between groups. (B) Between group differences in α diversity using the Chao1 and Shannon indices. (C) Between-group differences in β diversity using the Bray-Curtis dissimilarity index.

Microbial differences in abundances on univariate analysis

On the phylum level, there were higher Proteobacteria and lower Actinobacteriota in the early RYGB cohort compared to sham (Supplementary Figure 6). On a genus level, early RYGB had higher abundances of *Escherichia-Shigella* but lower abundances of *Lactobacillus*, *Adlercreutzia*, and *Proteus* (Supplementary Figure 5).

For the late cohorts, the higher abundance of Proteobacteria and lower Actinobacteriota became more significant with the addition of lower Firmicutes (Supplementary Figure 6). On a genus level, the only significant differences were higher abundances of *Escherichia-Shigella* and lower abundances of *Lactobacillus* (Supplementary Figure 7).

Ileal bile acids

Among 20 ileal bile acids analyzed, there were no significant differences in the early cohorts. The late cohorts demonstrated significantly lower levels of seven primary bile acids and four secondary bile acids after RYGB (Figure 18). Total bile acids were dramatically lower after RYGB compared to sham in the late groups (144.7±205.7 vs 408.8±122.5 vs μM, p=0.0052). In the late groups, there were also higher cholic-acid-derived to chenodeoxycholic-acid-derived bile acid ratios after RYGB compared to sham demonstrating significant shifts in bile acid composition (2.87±1.89 vs 0.77±0.15 μM, p=0.0045).

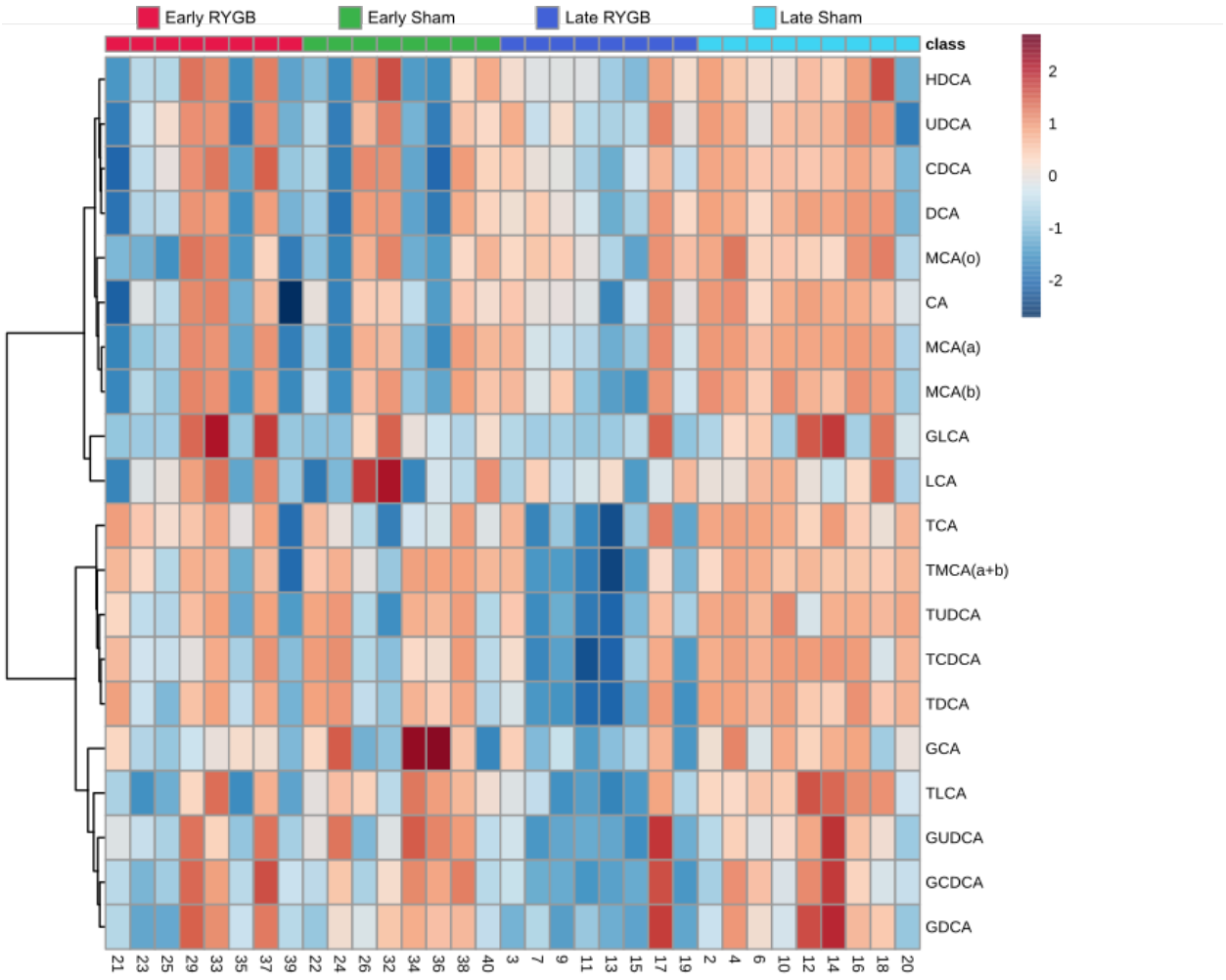

Figure 18. Heatmap of ileal bile acid concentrations after logarithmic transformation of data

Pairwise correlation analysis

Pairwise correlation analysis between microbial and bile acid shifts did not reveal any significant correlations when comparing early sham to early RYGB. However, the late sham and late RYGB cohorts demonstrated positive correlations between *Lactobacillus* with taurolithocholic acid and taurochenodeoxycholic acid as well as negative correlations between *Escherichia-Shigella* and taurolithocholic acid and glycodeoxycholic acid (Figure 19). Pairwise correlation between

intestinal morphology, L-cell density and microbes revealed negative correlations between Lactobacillus and villi height (R=-0.485, p=0.048).

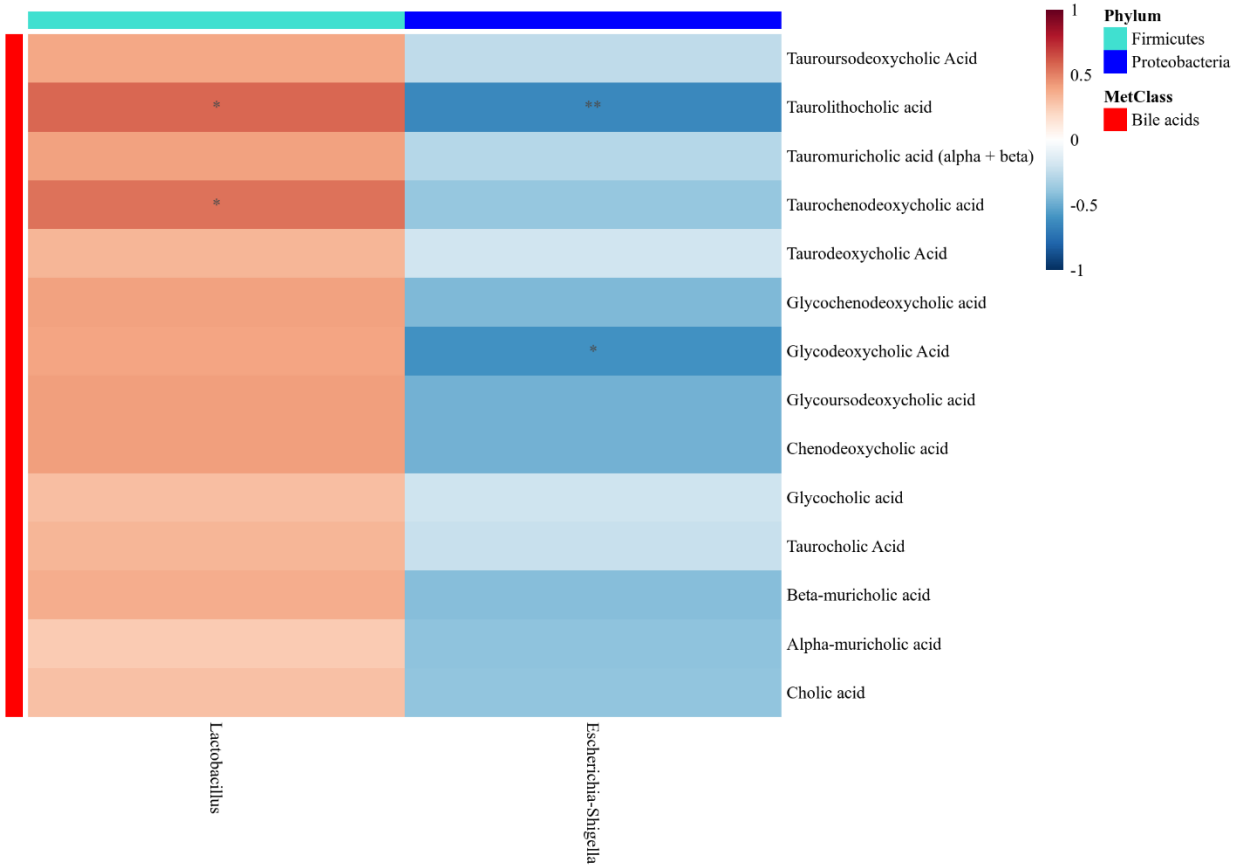

Figure 19. Heatmap of Spearman correlations of differential microbes and bile acids between late RYGB compared to late sham

3.5 DISCUSSION

To our knowledge, this is the first comprehensive analysis of metabolic changes assessed from the perspective of the terminal ileum following RYGB to evaluate the temporal relationships between bile acids, the gut microbiota, and L-cells. Our study found that early ileal and

metabolic changes were minimal after RYGB. However, late changes involved major shifts in bile acids and microbial composition which were associated with L-cell proliferation. In this discussion, we propose mechanisms to explain the changes observed in our study and present emerging evidence about the relationships between bile acids, the gut microbiota and L-cell proliferation.

Jejunal and ileal adaption occurring after RYGB was initially thought to occur due to compensatory mechanisms needed to overcome the decreased absorptive capacity of the alimentary limb[220,221]. However, an ileal interposition study suggested that these morphological processes are more complicated and may be mediated by increased nutrient and bile acid stimulation. Similarly, this study found intestinal hypertrophy and an increase in the total number of enteroendocrine cells[222]. Importantly, our study demonstrated no upregulation of GLP-1 associated gene expression suggesting that increased GLP-1 secretion is driven primarily by an increase in L-cell quantity rather than increased cellular production of GLP-1. Villi height was also negatively correlated with Lactobacillus in our study. This was unexpected as studies in broiler chicken show that Lactobacillus supplementation increases villi height[223]. It is possible that the modified ecological or microbial environment after RYGB that causes increased villi height is inadvertently driving a loss in Lactobacillus.

A number of human RYGB studies have demonstrated an increased proportion of systemic circulating bile acids after RYGB and there are suggestions that these increases may correlate with remission of diabetes[224–226]. Reductions in luminal bile acid concentration are due to

increased bile acid absorption after RYGB. Bhutta et al. demonstrated increased bile acid reabsorption in the proximal common jejunum but less reabsorption in the terminal ileum and colon. This may be related to the absence of bile in the Roux limb in conjunction with the absence of chyme in the biliopancreatic limb resulting in changes in the expression of genes related to bile acid absorption[227]. This is supported by an ileal interposition study which found increased bile acid reabsorption via apical sodium dependent bile acid transporter (ASBT) and an adaptive jejunization of the ileal segment due to its transposed location[228]. These findings are consistent with our study that found jejunization with lengthening of ileal villi as well as decreased concentrations of ileal bile acids.

There was a significant increase in Proteobacteria at a loss of Firmicutes in the late RYGB cohorts. One explanation is that phyla such as Firmicutes are more acid adaptive than Proteobacteria. RYGB leads to virtually absent acid secretion due to exclusion of the stomach and this leads to proportionally more alkaline pancreatic secretions flowing into the distal intestine[229,230]. This increased alkaline environment likely contributes to the shift towards Proteobacteria from Firmicutes that is occurring in our study. Increased oxygen within the intestinal lumen after RYGB may also contribute to the proliferation of Proteobacteria[231]. The Proteobacteria phylum includes many species that produce enzymes such as catalase and superoxide dismutase that can neutralize reactive oxygen species[232].

The late RYGB cohort had an increase in *Escherichia-Shigella* and a decrease in *Lactobacillus*. This is consistent with multiple studies that demonstrate an increase in Escherichia-Shigella and

decrease in Lactobacillus after RYGB[145,147,148]. Increases in *Escherichia-Shigella* correlated to decreases in taurolithocholic acid and glycodeoxycholic acid while decreases in *Lactobacillus* correlated to decreases in taurolithocholic acid and taurochenodeoxycholic acid. One mechanism in which *Lactobacillus* decreases bile acids is via its bile salt hydrolase (BSH) activity in the small bowel. Decreases in the abundance of *Lactobacillus* would lead to decreases in BSH activity, lowering levels of bile acid deconjugation, increasing the amount of bile acid reuptake, which may result in lower intraluminal bile acid levels[233]. Additionally, species such as *E. coli* exhibit bile salt oxidation and epimerization via hydroxysteroid dehydrogenase. Epimerization is a stereochemical change from an α to β configuration, with the formation of stable oxo-bile salt intermediates. Modified bile salts are typically reabsorbed and this contributes to reduced luminal concentrations of bile acids[234]. These processes potentially connect shifts in ileal bile acids to the microbial shifts that occur after RYGB through organism such as *Escherichia-Shigella* and *Lactobacillus*.

Lactobacillus was consistently decreased in both the early RYGB cohort and the late RYGB cohort. *Lactobacillus* is a gram-positive, aerotolerant anaerobic bacterial species often used as a probiotic. When used as a probiotic, there is emerging evidence that it has positive effects on glucose metabolism[235,236]. However, the role of *Lactobacillus* after RYGB is incongruent with these studies as its abundance after RYGB was found to be lower in our study as well as studies by Furet et al. and Kong et al.[147,148]. This decrease is thought to occur due to intraluminal increases in pH which tend to demote acidophilic genera such as *Lactobacillus*. *Lactobacillus* is also particularly adaptable to bile acids environments and reductions in luminal bile acids after RYGB may also contribute to decreases in its abundance[237].

One of the potential mechanisms for L-cell proliferation is through bile acid signaling. Bile acids have demonstrated the ability to directly cause intestinal L-cell differentiation and increases in density. A study by Lund et al. found that both lithocholic acids and synthetic GPBAR1 agonists increased L-cell density and GLP-1 secretory capacity[108]. Bile acids also have direct effects on L cells through the FXR and TGR5 receptors[107,109,110]. For example, TaMCA and TbMCA were demonstrated in two studies to inactivate intestinal FXR and prevent diet-induced obesity and improve glucose metabolism[111,112]. In our study, we found decreases in 11 bile acids in the late RYGB cohort and these shifts may contribute to signaling towards L-cell proliferation. Future studies directed at these bile acids may identify their effect on L-cells.

There is also emerging evidence that the gut microbiota within the ileum have rapid and pronounced effects on L-cells and GLP-1. Arora et al. studied germ-free mice and found that the recolonization of the ileal microbiota downregulated the production of GLP-1 through genes related to vesicular localization[208]. This occurred rapidly within one day of recolonization. Yoon et al. found that *Akkermansia muciniphila* secretes a protein that specifically induces the release of GLP-1 from intestinal L-cells[96]. Other studies have found that colonic *A. muciniphili* increases after RYGB [238,239]. However, high-fat diets have been demonstrated to significantly reduce the abundance of this bacteria and this could explain why our samples yielded sparse abundances of *A. municiphila* in all cohorts[240,241]. Our study primarily found increases in Escherichia-Shigella and decreases in Lactobacillus after RYGB and future studies directed at these species may identify if these species have effects on L-cells.

Limitations

Our study is the first to perform a comprehensive assessment of the rat ileum after RYGB to determine factors that may contribute to changes in L-cells. However, our study was not specifically designed to evaluate the underlying mechanisms responsible for the proliferation of L-cells and serves primarily as hypothesis generating. This study also did not demonstrate early improvement in glucose tolerance. This may be because our study used an obesity model and not a diabetic rat model which may have attenuated the early metabolic effects of RYGB. Another important limitation is that bile acid physiology has major differences between rats and humans.

3.6 CONCLUSIONS

There were no early changes to L-cells, bile acids, or glucose homeostasis after RYGB. However, RYGB caused a late and substantial increase in L-cell quantity with associated shifts in ileal bile acids which correlated to shifts in *Escherichia-Shigella* and *Lactobacillus*. This proliferation of L-cells contributed to increased GLP-1 secretion and improved glucose homeostasis. This study demonstrates that both foregut and hindgut theories are overly simplified and that the intestinal changes that contribute to L-cell proliferation are multimodal and complex. L-cells appear to be key players in the regulatory mechanisms associated with RYGB and more research is needed to elucidate the complex interplay between L-cells, bile acids and the gut microbiota.

3.7 SUPPLEMENTARY FIGURES

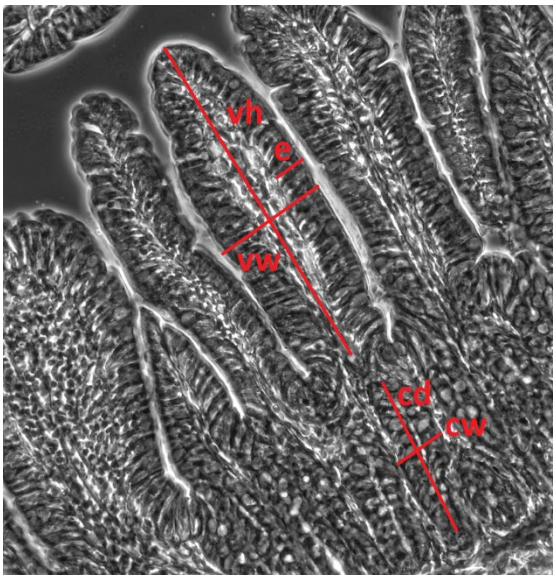

Supplementary Figure 1. Cross section of the ileum showing the measured parameters: villus height (vh), villus width (vw), crypt depth (cd) and crypt width (cw)

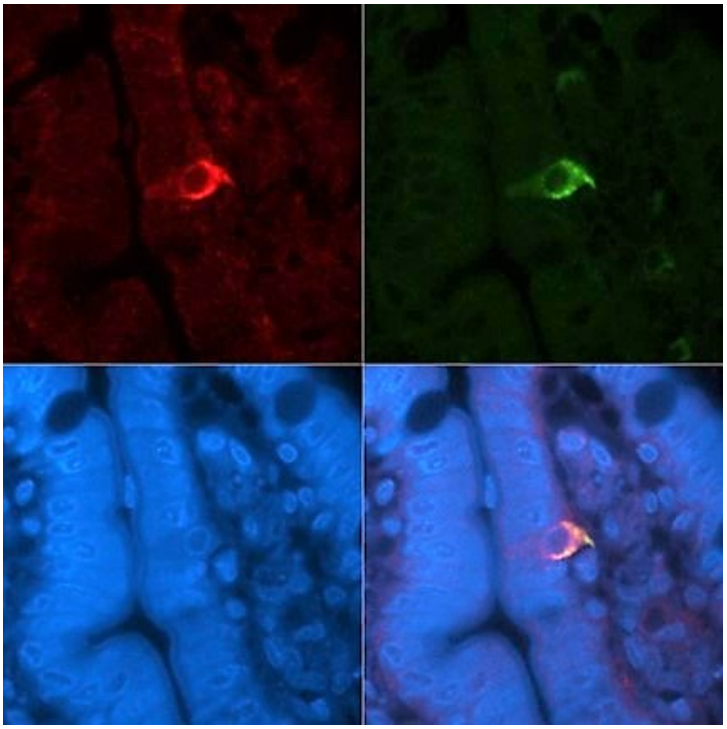

Supplementary Figure 2. Immunofluorescence staining of an LK cell. Red is GIP stain, green is GLP-1 stain and blue is DAPI stain for nuclei

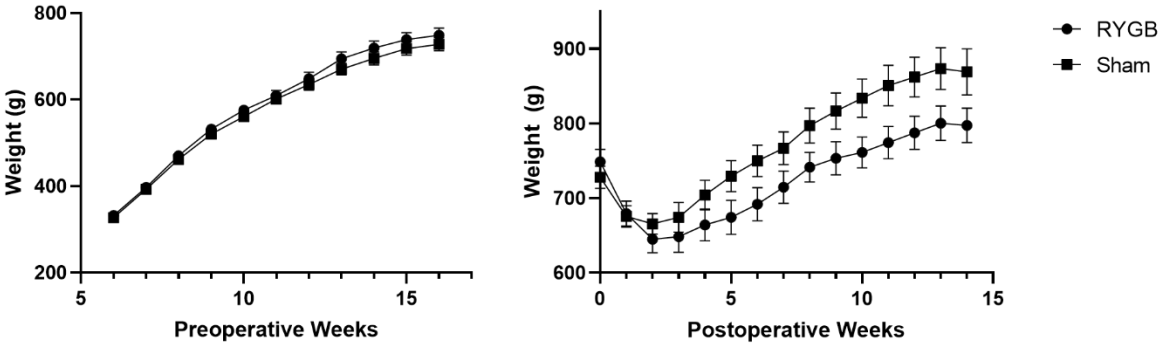

Supplementary Figure 3. Pre- and Post-operative absolute weight on high fat diet; RYGB, Roux-en-Y gastric bypass

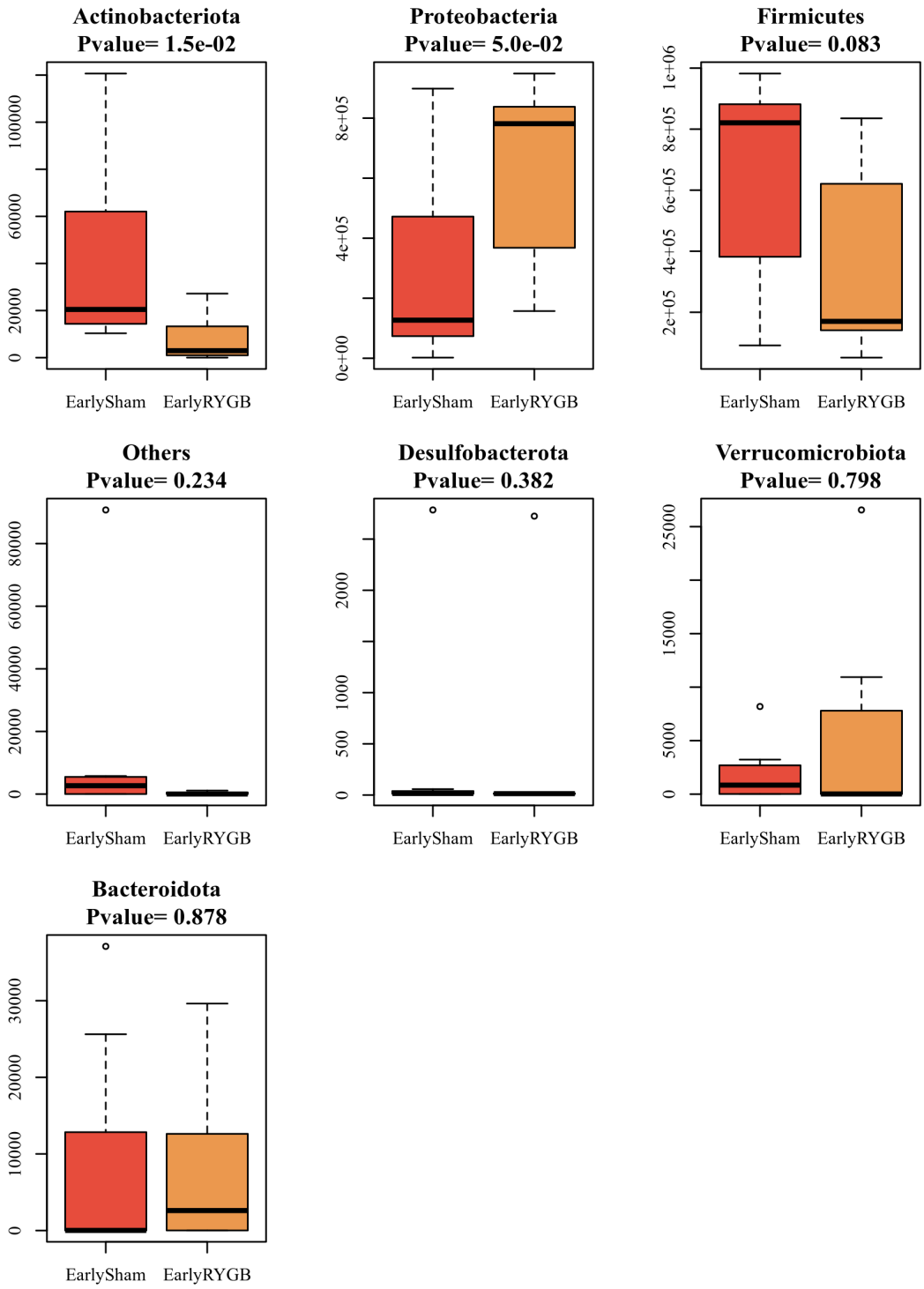

Supplementary Figure 4. Differential microbial taxa on univariate analysis at the phylum level between early sham cohorts and early Roux-en-Y gastric bypass cohorts

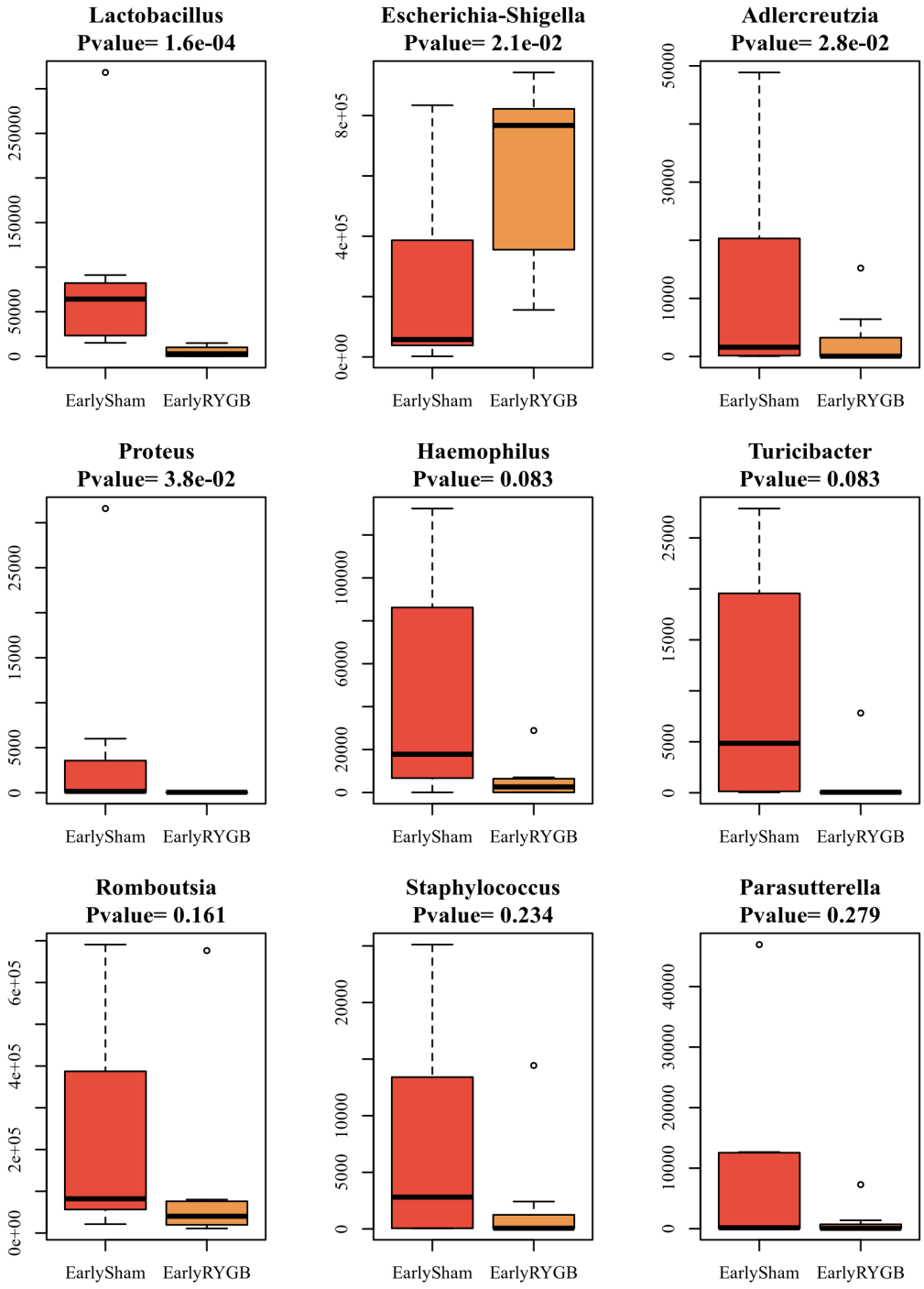

Supplementary Figure 5. Differential microbial taxa on univariate analysis at the genus level between early sham and early Roux-en-Y gastric bypass cohorts

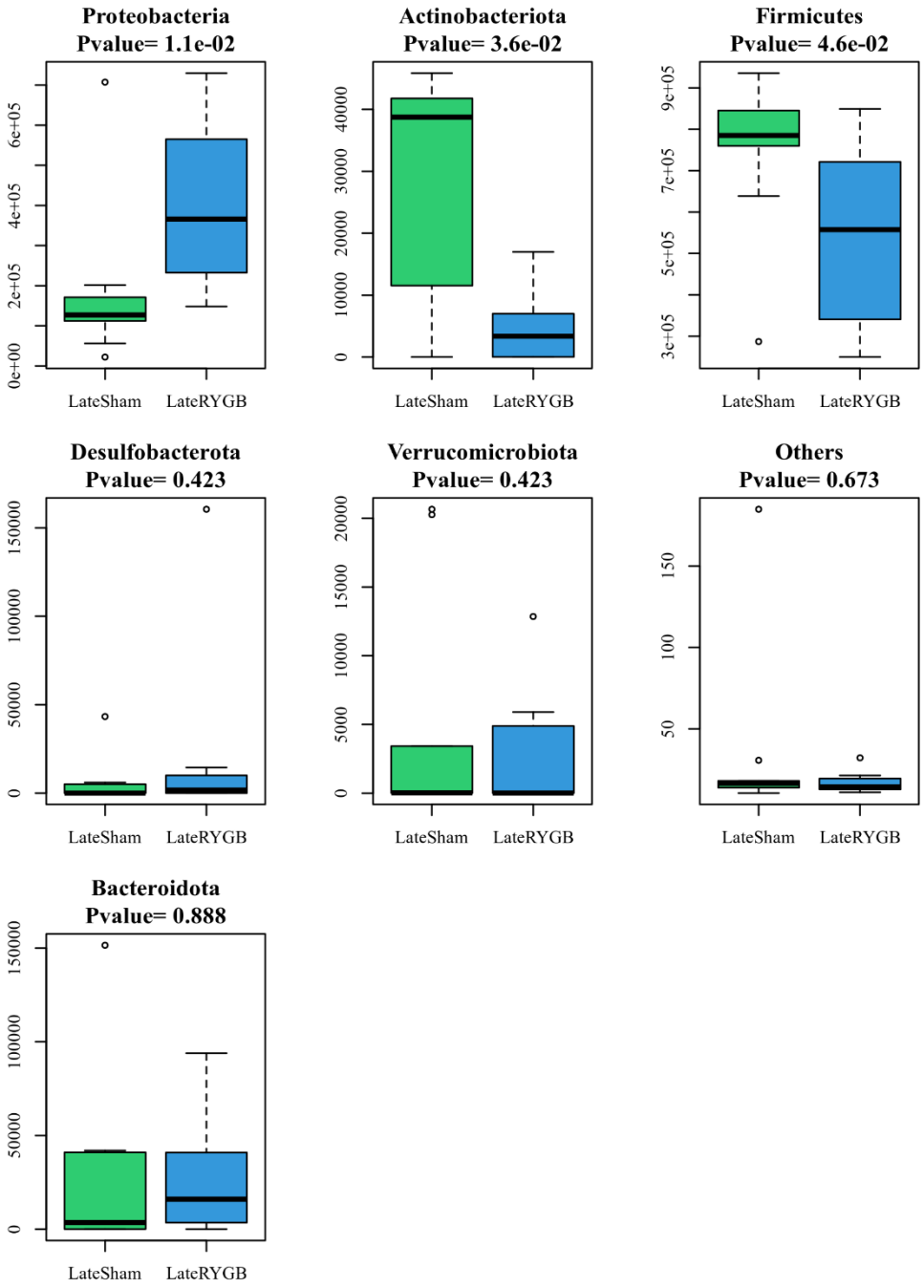

Supplementary Figure 6. Differential microbial taxa on univariate analysis at the phylum level between late sham and late Roux-en-Y gastric bypass cohorts

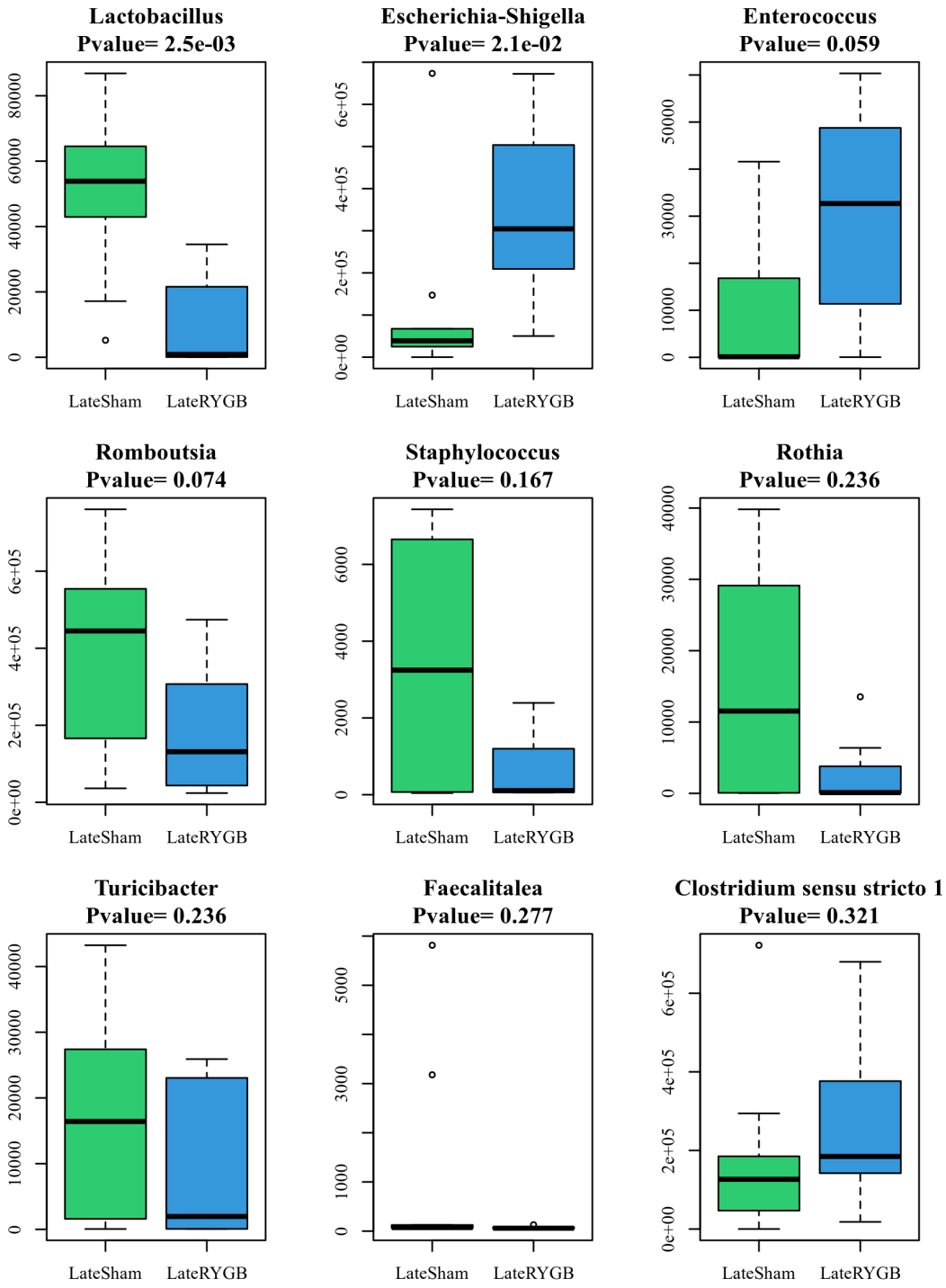

Supplementary Figure 7. Differential microbial taxa on univariate analysis at the genus level between late sham and late Roux-en-Y gastric bypass cohorts

CHAPTER 4. INTEGRATED FECAL MICROBIOME AND SERUM METABOLOMIC ANALYSIS REVEALS KEY METABOLIC PATHWAYS AFTER ROUX-EN-Y GASTRIC BYPASS AND SLEEVE GASTRECTOMY

4.1 ABSTRACT

Background

Bariatric surgery is the most effective modality for the treatment of severe obesity and metabolic syndrome. However, the underlying mechanisms for weight loss following Roux-en-Y gastric bypass (RYGB) and sleeve gastrectomy (SG) are not completely understood, and multiple mechanisms are thought to play a role. Evidence is emerging that the intestinal microbiome plays an important role in the development of obesity and microbial shifts may contribute to the effects of bariatric surgery.

Objectives and Hypothesis

The aim of this study was to investigate the microbial, metabolomic, and inflammatory changes that occur with RYGB and SG and compare them with patients who underwent dietary and behavioral interventions (CTRL). We hypothesize that altered intestinal physiology following RYGB and SG leads to specific changes microbial populations that contribute to metabolomic and inflammatory pathways that subsequently result in weight loss, reduced inflammation, and an improved metabolic profile.

Methods

This study a three-arm parallel prospective interventional clinical trial with participants in RYGB, SG, CTRL cohorts. Clinical parameters, blood samples and fecal samples were collected pre-intervention and 3 and 9 months after. A multi-omics approach was used to perform integrated microbial-metabolomic analysis to identify functional pathways in which weight loss and metabolic changes occur after bariatric surgery.

Results

A total of 80 patients were recruited (CTRL 28, SG 23, RYGB 28). RYGB demonstrated the most significant microbial changes with decreased alpha-diversity and significant beta-diversity between timepoints. Integrated microbial-metabolomic analysis revealed a unique pathway in which RYGB was associated with decreases in the abundance of *Romboutsia* which correlated to decreases in glycerophospholipids as well as lower weight and insulin resistance.

SG demonstrated a unique pathway linked to the decreased abundance of a cluster of three Firmicutes bacteria. This Firmicutes shift was correlated with an increase in five amino acids which consequently enriched the aminoacyl-tRNA pathway. The loss of this cluster also correlated with lower weight, decreased insulin resistance, and decreased systemic inflammation.

When performing between group comparisons, SG demonstrated an enriched pathway at 9 months compared to RYGB. This was the sphingolipid metabolism pathway which was enriched

due to the loss of a cluster of five Firmicutes bacteria which correlated to increases in sphingomyelins and hydroxysphingomyelins. This Firmicutes shift was also linked to improved glucose tolerance.

Conclusions

This prospective clinical trial provides a comprehensive analysis of the complex microbial-metabolomic relationships in bariatric surgery and identified pathways that may be the future target of therapeutic strategies for the treatment of obesity and metabolic disease.

4.2 BACKGROUND

Bariatric surgery is currently the most effective modality for treating severe obesity with evidence to support long-term sustained weight loss and improvement in obesity-related comorbidities[16]. The two most commonly performed bariatric surgical procedures are the Roux-en-Y gastric bypass (RYGB) and sleeve gastrectomy (SG)[242]. Patients with RYGB typically have more excess weight loss and, in diabetics, better glycemic control than those with SG[18]. The underlying mechanism for weight loss following these operations is not completely understood though multiple factors are thought to play a role. These include reduced caloric intake, decreased nutrient absorption, increased satiety, release of satiety-promoting gut hormones (glucagon-like peptide 1, peptide YY) and shifts in bile acid metabolism[141,142].

The prevalence of obesity and associated metabolic comorbidities is increasing worldwide[243]. Medical therapy for obesity has demonstrated only moderate success, and bariatric surgery is increasingly used for the treatment of severe obesity[244,245]. There is a need for novel strategies to promote weight loss and metabolic improvement and one potential target is the gut microbiome[246]. Increasing evidence suggests that the intestinal microbiome may play a central role in the development and perpetuation of obesity through regulation of energy homeostasis and fat storage[123]. However, the mechanisms underlying excessive fat mass accumulation, the development of obesity, and the complex microbial metabolic pathways are not fully understood.

The intestinal microbiome refers to the greater than 100 trillion bacteria that reside in the human intestine and comprise more genetic material than the entire human genome. Recent

advancements in metagenomic analysis, which allow for the rapid identification and quantification of these organisms, has increased our understanding of obesity and the microbiome. While a dysbiosis, defined as an imbalance of gut microbiota has been described in some, but not all, studies of obesity, specific changes in gut microbes remain inconsistent[129]. This lack of consistency highlights the need for well-designed studies which examine both microbial composition and metabolic potential of the gut microbiota in the context of obesity.

Recent evidence has linked the gut microbiota to the beneficial effects of bariatric surgery. Studies have demonstrated changes in the composition and diversity of the gut microbiota after RYGB and SG in humans[143,145,154–156,146–153]. One study also confirmed long-term microbial changes for RYGB[146]. However, comparative trials have been small and important differences between specific bacterial populations have not been well elucidated. Furthermore, no human study has examined the differences in bacterial composition following RYGB and SG in relation to metabolomic and inflammatory changes. It is essential to include these aspects to understand critical pathways in the physiology of bariatric surgery.

The aim of this study was to investigate the microbial, metabolomic, and inflammatory changes that occur with both RYGB and SG and compare them with non-operative controls. Specifically, we aimed to use a multi-omics approach to perform integrated microbial-metabolomic analysis to identify functional pathways in which metabolic changes occur after bariatric surgery. The intention is to improve our understanding of the physiological changes that occur with bariatric surgery. This understanding may potentiate the development of approaches to modify the gut

microbiota through diet, prebiotics, probiotics, or fecal microbial transplantation with the potential to improve obesity or diabetes, likely in conjunction with bariatric surgery. We hypothesize that altered intestinal physiology following RYGB and SG will lead to identifiable changes in specific microbial populations that contribute to metabolomic and inflammatory pathways that will subsequently result in weight loss, reduced inflammation, and an improved metabolic profile.

4.3 METHODS

Study design

This study was designed as a three-arm parallel prospective interventional clinical trial with patients in RYGB, SG and non-operative control (CTRL) cohorts. For the operative arms, subjects were enrolled at the time they were scheduled for surgery. Patient demographics including height, weight, BMI, and comorbidities were documented. Fecal, and blood samples were collected in clinic four weeks prior to surgery. In the post-operative period, blood and fecal collection took place at 3- and 9-months. All pre-operative samples were collected prior to subjects initiating a two to three-week pre-operative liquid diet designed to reduce hepatomegaly and ease in the technical surgical aspects of the procedure.

CTRL patients were treated with dietary and behavioral interventions for weight loss. This excludes meal replacement or pharmacologic interventions. For this cohort, subjects had initial sampling prior to initiating weight loss interventions. Further sampling occurred at 3 months and 9 months following initiation of the intervention.

Study objective

The primary objective of this study was to determine changes in microbial species and metabolites after SG and RYGB in relation to important metabolic parameters: weight, fasting blood glucose (FBG), hemoglobin A1c (HbA1c), fasting serum insulin (FSI), insulin resistance as estimated by the homeostatic model of insulin resistance (HOMA-IR), lipids, and C-reactive protein (CRP). This is a hypothesis generating study to identify microbial and metabolomic pathways that are associated with changes in clinical parameters after bariatric surgery.

Study population

This study was approved by the Health Research Ethics Board at the University of Alberta (PRO00071705) and registered with ClinicalTrials.gov (NCT03181347). Patients were recruited from the Edmonton Adult Specialty Bariatric Clinic at the Royal Alexandra Hospital from September 2017 to May 2019. The intent was to recruit 30 participants with a body mass index (BMI) greater than 35 kg/m^2 into each arm including 30 CTRL, 30 SG and 30 RYGB. Exclusion criteria included antibiotic, liraglutide, semaglutide or methotrexate usage within two months preceding enrollment as these have significant effects on the gut microbiota. Additionally, patients with meal replacement use within one month, previous bowel resection, inflammatory bowel disease or previous bariatric surgery were excluded.

Sample size calculation

Sample size calculations were performed a priori and designed to ensure we would adequately capture microbial changes induced by surgery. In prior literature, an important short-chain fatty acid-producing bacterial species' (*F. prausnitzii*) relative abundance was lower in a post-RYGB group compared to non-operative controls (0.031 v. 0.053 σ 0.024)[145]. With an alpha of 0.05 and a Beta of 0.90, this would require 26 subjects per arm. Including a dropout rate of 10%, this increases to 30 subjects per arm.

Bariatric surgery procedures

Primary laparoscopic bariatric surgery was performed by three fellowship-trained bariatric surgeons. Laparoscopic SG was performed using a 50 French bougie with stapling tight to the bougie as per the usual technique. Laparoscopic RYGB was performed with an approximately 110 cm Roux limb, 40 cm biliopancreatic limb, stapled jejunojejunostomy, and circular stapled gastrojejunostomy. The Roux limb was placed antecolic and the jejunostomy-jejunostomy mesenteric defect was routinely closed. Petersen's defect was closed routinely by two of the three surgeons.

Clinical biochemistry

Blood samples were collected after a 12-hour fast in heparinized collection tubes. Serum was isolated by centrifugation at 2000 g for 10 minutes following collection and stored at -80ºC.

Plasma and serum were tested using Alberta Health Services Laboratory Services, a public-health managed laboratory system that performs a comprehensive range of routine and

specialized lab testing. This included complete blood count with differential, ALT, ALP, bilirubin, creatinine, sodium, potassium, chloride, carbon dioxide, ferritin, thyroid stimulating hormone, free T4, FBG, HbA1c, FSI, and lipid panel. HOMA-IR was calculated from fasting blood glucose and insulin using the University of Oxford HOMA2 Calculator[247].

C-reactive protein, lipopolysaccharide, and inflammatory cytokines

Serum was assessed for CRP as a measurement of systemic inflammation, and lipopolysaccharide (LPS), as a measurement of bacterial translocation. Additionally, cytokines analyzed included IL-1β, IL-6, IL-8, IL-10, and TNF-α using enzyme-linked immunosorbent assays (R&D Systems, DuoSet for cytokines, Abbexa, abx514093 for LPS).

Serum metabolomics

Serum samples were analyzed for metabolomics profiling using liquid chromatography with tandem mass spectrometry targeting 143 metabolites. This was performed by the Metabolomics Innovation Center at the University of Alberta using the Biocrates AbsoluteIDQ p180 kit.

Fecal microbial analysis

Fecal sample collection was performed using a previous developed protocol used by our group for diet studies in inflammatory bowel disease. Collection cups were provided to participants, and they were instructed to collect fecal specimen the night prior or morning of their

appointment. Participants were instructed to store the specimen in the fridge in the interim and to transport them on ice to their appointment.

The microbial community composition of fecal samples was assessed using 16S rRNA gene analyses. DNA was extracted from ileal homogenates combining enzymatic and mechanical cell lysis with the QIAamp DNA Stool Mini Kit (Qiagen, Valencia, CA, USA). Enteric microbiota composition was characterized by 16S rRNA tag sequencing using the MiSeq Illumina technology (pair-end), targeting the V3-V5 regions. This analysis was performed by Genome Quebec (Montreal, Canada).

Demultiplexed FASTQ 16S rRNA sequences were quality filtered, trimmed, dereplicated, and filtered for chimeric sequences using pair-ended DADA2 resulting in exact sequence variant (feature) tables[218]. The table was imported into R 3.6.1 to analyze for α-diversity (Shannon/Chao1), β-diversity (wunifrac) and were performed using a function of the phyloseq v1.28.0 package[219]. Ordination plots for β-diversity metrics were generated by non-parametric multidimensional scaling ordination in R.

Statistical Analysis

Descriptive categorical data were expressed as percentages and continuous data were expressed as mean ± standard deviation (SD). Baseline differences between groups were evaluated by univariate analyses using Fisher's exact test for categorical data and one-way analysis of

variance (ANOVA) for continuous data. Multiple comparisons were adjusted using the Benjamin-Hochberg method to correct the false discovery rate. Analyses were conducted using STATA 15 (StataCorp 2017; College Station, TX). Figures were designed using Prism 9.0.2 (GraphPad Software, San Diego, CA). Statistical significance was defined using two-tailed tests with a p-value < 0.05. Error bars on figures represent standard error of the means and asterisks represent statistical significance with * as $p<0.05$, ** as $p<0.01$, *** as $p<0.001$, **** as $p<0.0001$.

Integrated microbiome-metabolomic analysis was performed using the M^2IA platform[183]. Microbial abundance counts were normalized by percentages and metabolites were normalized by log transformation. Differential metabolites and microbes between groups were selected using univariate analysis. Spearman's correlation coefficients were calculated between differential metabolites and microbes using a pairwise correlation analysis method with significance defined as $p < 0.05$ and $R > 0.3$ or < -0.3. Heatmaps were generated and visualized using a network plot. Spearman's correlation coefficients were also calculated between differential microbes and clinical parameters including weight, FBG, HbA1c, FSI, HOMA-IR, low-density lipoproteins (LDL), high-density lipoproteins (HDL), triglycerides (TG), total cholesterol (TC) and CRP.

Supervised multivariable analysis was conducted using sparse partial least squares discriminant analysis (sPLS-DA) to create score plots. Metabolic pathway enrichment analysis was performed on differential metabolites using univariate analysis. KEGG-based function of microbiome data were predicted using Tax4Fun2 following the linear discriminate analysis method[248].

Overlapping pathways were identified and interaction network plots were created demonstrating potential metabolites and microbes involved in these specific pathways.

4.4 RESULTS

Patient characteristics

A total of 80 patients were recruited, however, ten (3 CTRL, 5 SG, 2 RYGB) were lost to follow up at 3 months and an additional four patients from the control group were lost at 9 months because they underwent earlier bariatric surgery or were lost to follow-up (Figure 20). Recruitment was discontinued early due to increased use of liraglutide prior to surgery reducing the number of eligible participants. Overall, there were 28 CTRL, 23 SG and 29 RYGB patients included. Patient demographics are summarized in Table 5. There was a significantly lower baseline BMI in the surgical cohorts as they underwent an intensive pre-operative weight loss program prior to surgery.

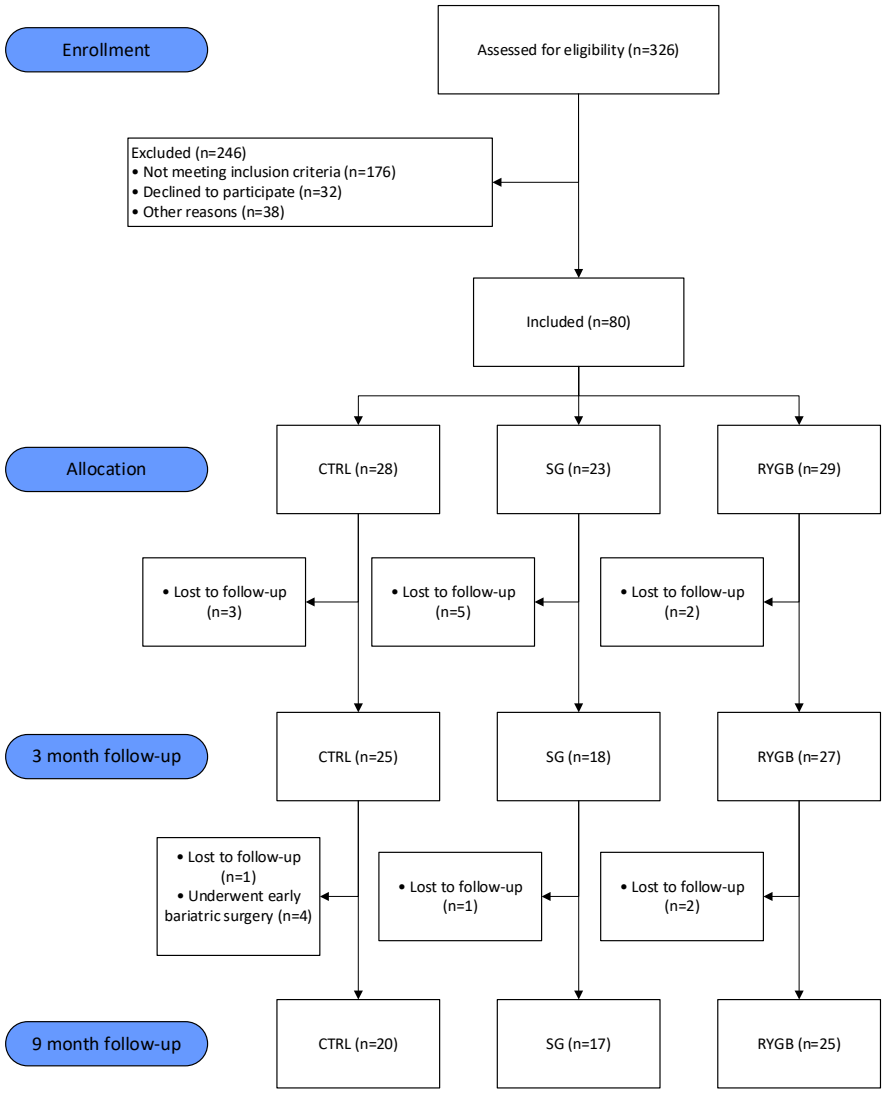

Figure 20. STROBE flow chart for observational studies

Table 5: Patient baseline demographics

Demographics mean (SD) or n (%)	**Non-operative controls** n = 25	**Sleeve gastrectomy** n = 18	**Roux-en-Y gastric bypass** n = 27	**p-value**
Number of patients (n)	25	18	27	-
Age at surgery (years)	47.7 (8.7)	47.9 (9.7)	47 (9.9)	0.940
Sex (female)	20 (80.0%)	17 (94.4%)	25 (92.6%)	0.356
Height (m)	1.67 (0.07)	1.69 (0.07)	1.67 (0.08)	0.725
Body mass index (kg/m^2)	47.1 (7.3)	40.8 (5.7)	42.9 (4.2)	0.002
General anxiety disorder	7 (28.0)	10 (55.6)	11 (40.7)	0.194
Coronary artery disease	0 (0.0)	0 (0.0)	0 (0.0)	1.000

Depression		13 (52.0)	10 (55.6)	15 (55.6)	0.982
Type 2 diabetes		2 (8.0)	1 (5.6)	3 (11.1)	0.877
Dyslipidemia		8 (32.0)	8 (44.4)	6 (22.2)	0.301
Gastroesophageal reflux		8 (32.0)	8 (44.4)	13 (48.2)	0.505
Hypertension		8 (32.0)	6 (33.3)	10 (37.0)	0.949
Hypothyroidism		4 (16.0)	5 (27.8)	6 (22.2)	0.661
Fatty liver disease		4 (16.0)	5 (27.8)	5 (18.5)	0.649
Osteoarthritis		12 (48.0)	9 (50.0)	9 (33.3)	0.444
Polycystic ovarian syndrome		1 (4.0)	3 (16.7)	2 (7.4)	0.428
Asthma		4 (16.0)	2 (11.1)	5 (18.5)	0.916
Obstructive sleep apnea		11 (44.0)	10 (55.6)	15 (55.6)	0.718
Ex-smoker		8 (32.0)	1 (5.6)	6 (22.2)	0.120
EOSS					
	0	0 (0.0)	0 (0.0)	3 (11.1)	
	1	2 (8.0)	1 (5.6)	3 (11.1)	0.625
	2	21 (84.0)	16 (88.9)	20 (74.1)	
	3	2 (8.0)	1 (5.6)	1 (3.7)	

EOSS, Edmonton obesity staging system

BMI decreased significantly after SG and RYGB at 3- and 9-month time points while CTRL did not demonstrate any significant weight loss (Figure 21).

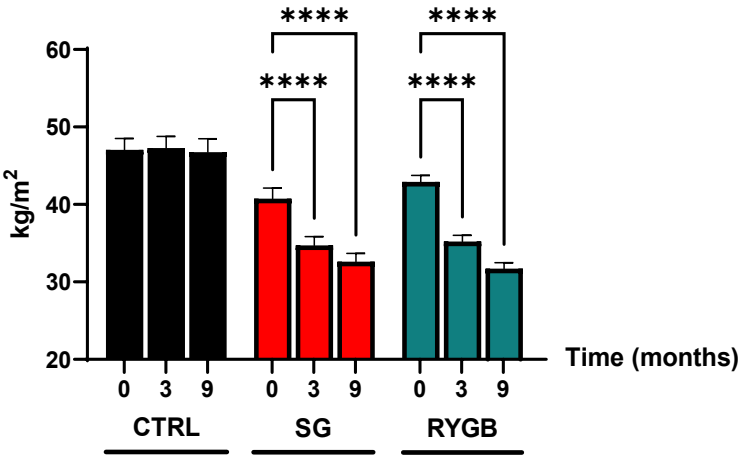

Figure 21. Body mass index. CTRL, non-operative control; SG, sleeve gastrectomy; RYGB, Roux-en-Y gastric bypass

Clinical biochemistry

Clinical biochemistry results are summarized in Supplementary Table 1. Clinical biochemistry results. There were significant improvements in lipid profiles after RYGB at both 3 and 9 months (Figure 22). There were also significant improvements in glucose metabolism after both SG and RYGB at 3 and 9 months. This included lower fasting blood glucose, hemoglobin A1c, insulin and HOMA-IR (Figure 22).

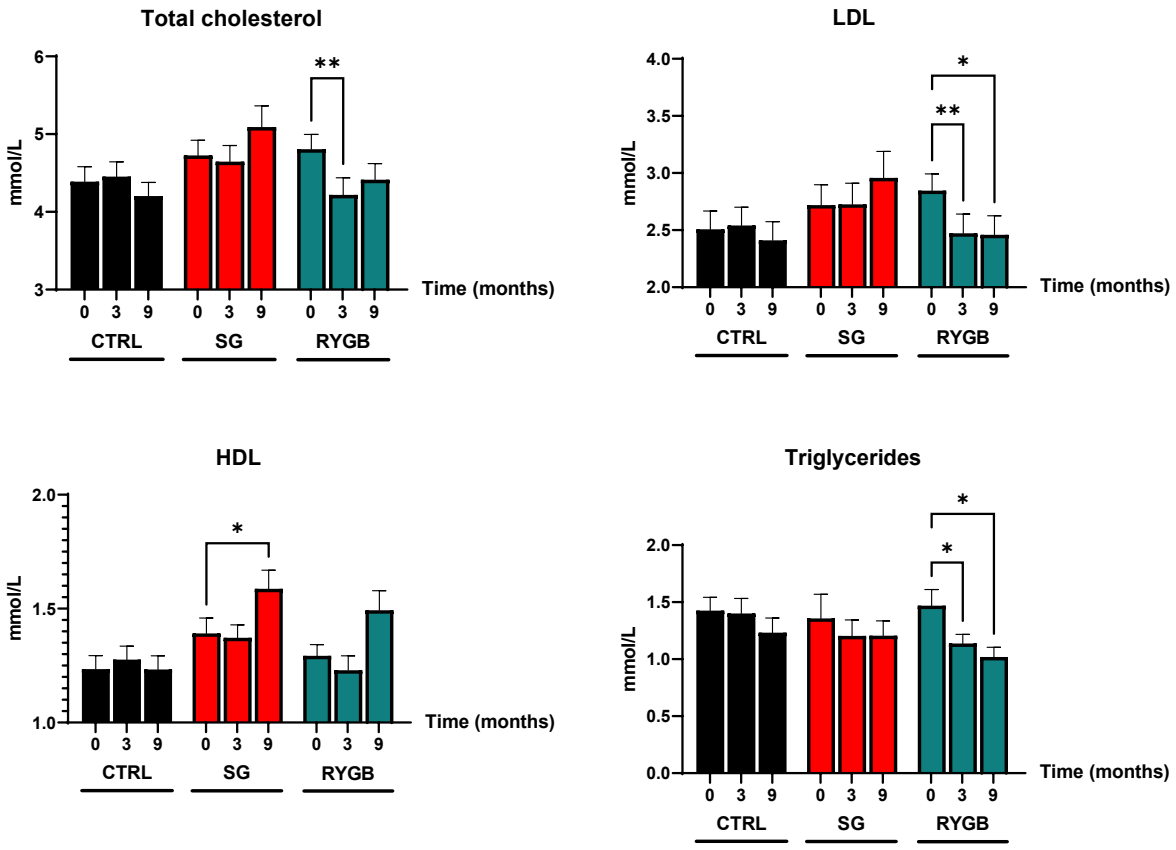

Figure 22. Lipid panel. CTRL, non-operative control (n=25); SG, sleeve gastrectomy (n=18); RYGB, Roux-en-Y gastric bypass (n=27); LDL, low-density lipoprotein; HDL, high-density lipoprotein. Error bars on figures represent standard error of the means and asterisks represent statistical significance with * as $p<0.05$, ** as $p<0.01$, *** as $p<0.001$, **** as $p<0.0001$.

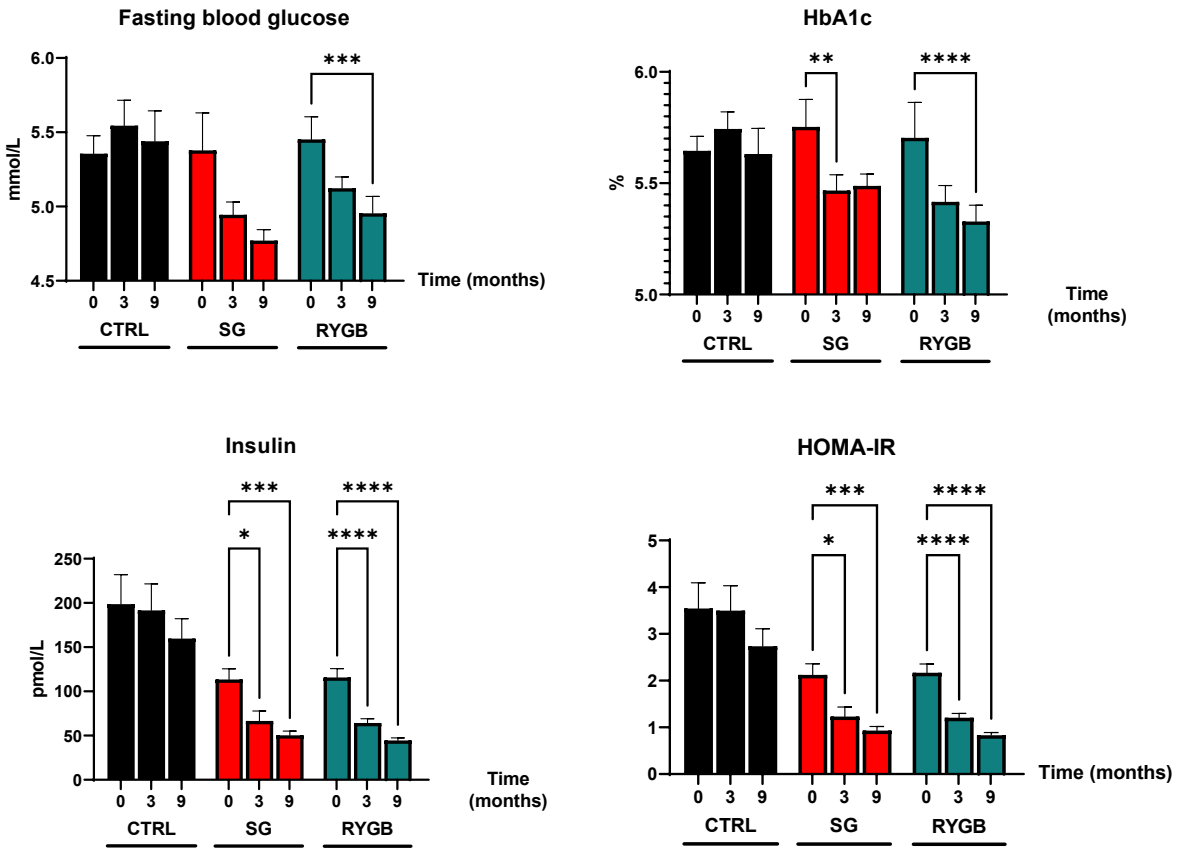

Figure 23. Metabolic parameters. CTRL, non-operative control (n=25); SG, sleeve gastrectomy (n=18); RYGB, Roux-en-Y gastric bypass (n=27); HbA1c, hemoglobin A1c; HOMA-IR, homeostatic model for the assessment of insulin resistance. Error bars on figures represent standard error of the means and asterisks represent statistical significance with * as $p<0.05$, ** as $p<0.01$, *** as $p<0.001$, **** as $p<0.0001$.

Inflammatory markers, LPS, and interleukins

There was a significant and progressive reduction in inflammatory markers after RYGB at 3 and 9 months. This included decreased C-reactive protein, white blood cells, and ferritin. SG did not have as definitive findings but did have a significant decrease in white blood cells at 9 months. However, LPS, as a measure of gut barrier integrity, did not show any significant changes at 3 or 9 months in any cohort (Figure 24, Supplementary Table 2).

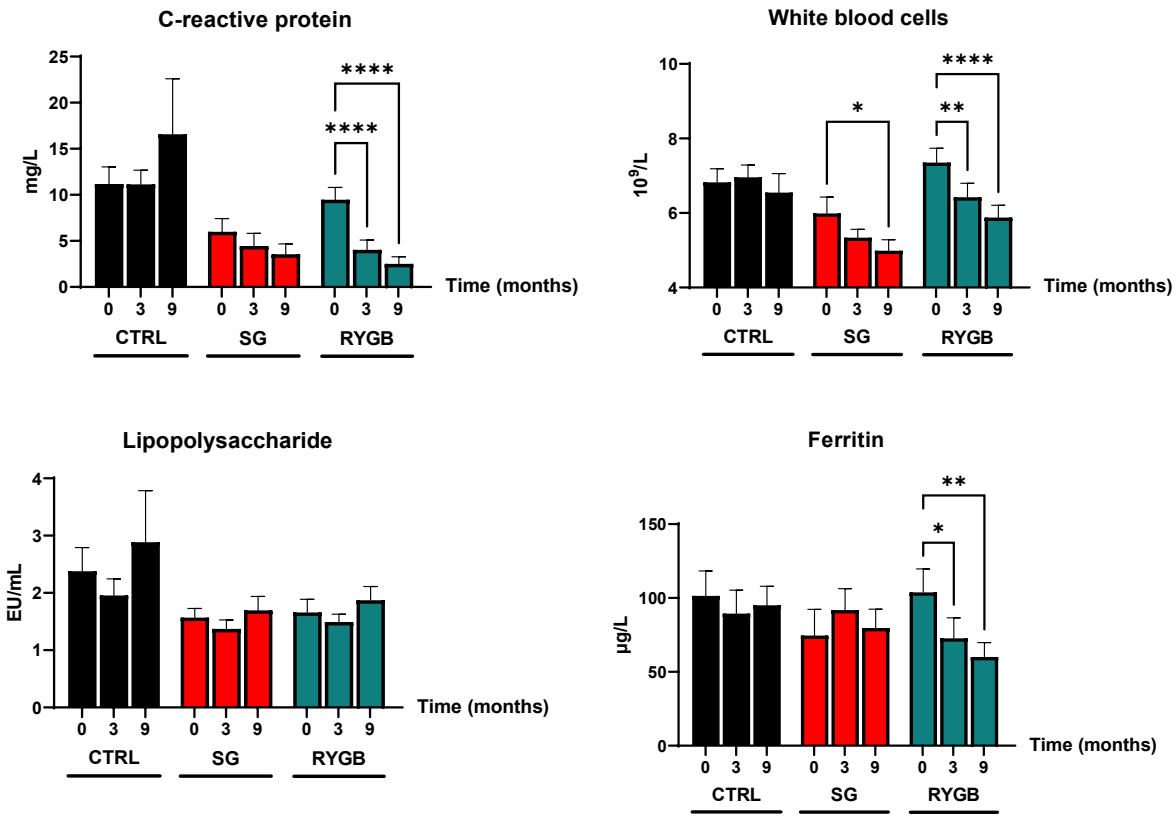

Figure 24. Inflammatory markers. CTRL, non-operative control (n=25); SG, sleeve gastrectomy (n=18); RYGB, Roux-en-Y gastric bypass (n=27). Error bars on figures represent standard error of the means and asterisks represent statistical significance with * as $p<0.05$, ** as $p<0.01$, *** as $p<0.001$, **** as $p<0.0001$.

There was no statistical significance with regards to interleukins IL-1β, IL-6, IL-8, IL-10 or TNF-α between timepoints in any of the groups (Supplementary Figure 8, Supplementary Table 2).

Microbial alpha- and beta-diversity between timepoints

Only the RYGB cohort had a statistically significant decrease in alpha-diversity at 9 months compared to baseline as demonstrated by lower Shannon and Chao1 indices (Figure 25a). CTRL and SG did not demonstrate any changes in alpha-diversity. Similarly, significant changes in beta-diversity (Bray-Curtis) were only present for the RYGB cohort when comparing baseline and 3-month (p=0.002) and 0 and 9-month (p=0.008) time points. Control and SG did not have significantly unique beta-diversity on the Bray-Curtis dissimilarity index (p>0.05) (Figure 25b).

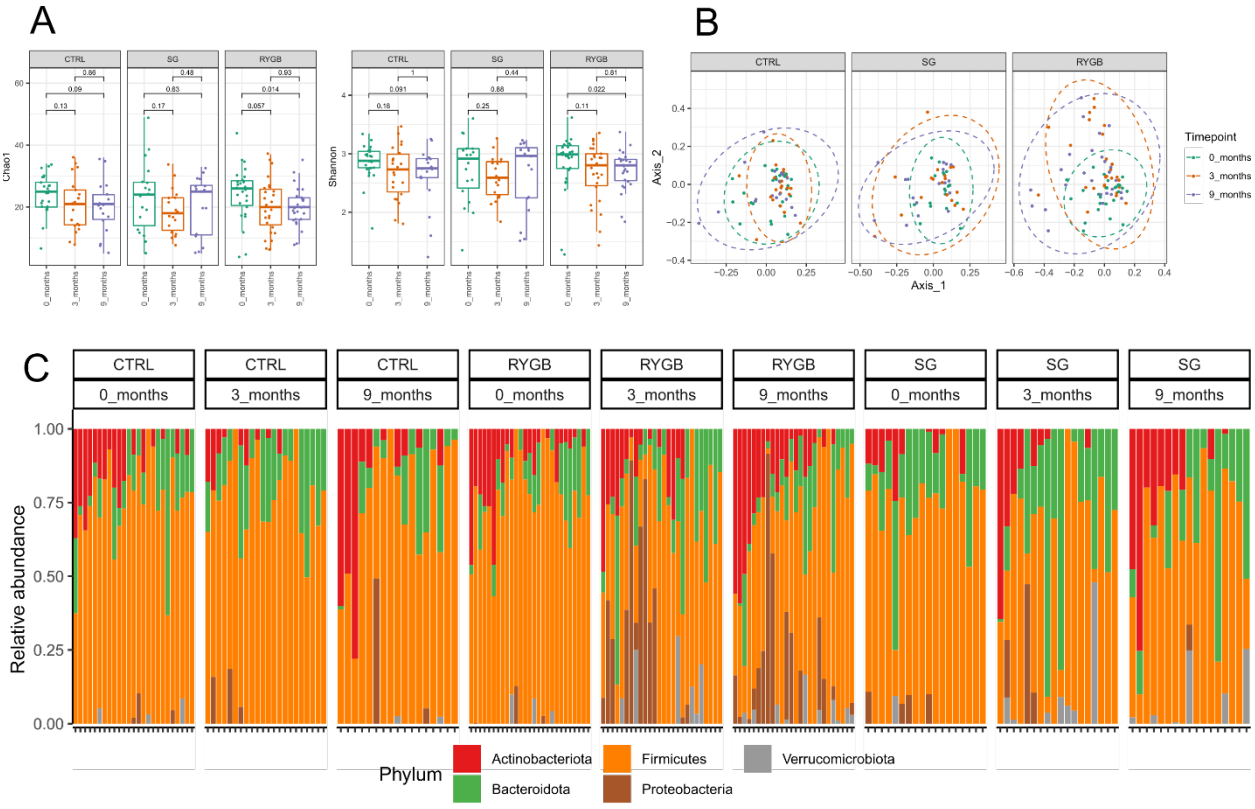

Figure 25. Differences in relative microbial abundance between non-operative control, sleeve gastrectomy and Roux-en-Y gastric bypass 0, 3 and 9 months. (A) Between timepoint differences in α diversity using the Chao1 and Shannon indices. (B) Between timepoint differences in β diversity using the Bray-Curtis dissimilarity index. (C) Taxa bar plots demonstrating phylum level differences in relative microbial abundance between groups.

Microbial differences in abundance between timepoints on univariate analysis

At the phylum level, CTRL demonstrated no significant differences at 3 and 9 months compared to baseline (Figure 25c). SG also did not have changes at 3 months but had an increase in the abundance of Actinobacteriota with a loss of Proteobacteria and Bacteroidota at 9 months. The RYGB cohorts demonstrated the most dramatic shifts microbial composition, with an increase in Proteobacteria and Verrucomicrobiota and a loss of Firmicutes at 3 months. At 9 months, these changes became more significant and included an increase in the abundance of Desulfobacterota.

At the genus level, after FDR correction, there were no significant changes in relative abundance for the CTRL at 3 and 9 months. The SG cohort only demonstrated genus level differences at 9 months, with increases in *Streptococcus* but decreases in *Monoglobus*, *Agathobacter*, *Butyricicoccus*, *Eubacterium hallii*, and *Lachnospiraceae UCG-010*. The RYGB cohort had the most substantial microbial shifts. At 3 months, there were increases in *Actinomyces*, *Streptococcus*, *Veillonella*, *Ruminococcaceae NK4A214*, *UCG-005*, *Akkermansia*, *Escherichia-Shigella* and decreases in *Dorea*, *Eubacterium ventriosum*, *Fusicatenibacter*, *Coprococcus*, *Erysipelotrichaceae*, *UCG-003*, *Anaerostipes*, *Eubacterium hallii*, *Christensenellaceae R-7* group, *Ruminococcus torques*, *UCG-002* and *Blautia*. At 9 months, there were increases in *Veillonella*, *NK4A214*, *Streptococcus*, *Anaerotruncus*, *Escherichia-Shigella*, *UCG-005*, *Akkermansia*, *Klebsiella* and decreases in *Anaerostipes*, *Oscillibacter*, *Dorea*, *Eubacterium ventriosum*, *Family XIII UCG-001*, *Romboutsia*, *Faecalibacterium*, *Lachnospira*, and *Dialister* (see Supplementary Figures).

Correlations between differential microbial taxa and clinical parameters

The SG cohort demonstrated positive correlations between multiple Firmicutes organisms including *Butyricicoccus*, *Lachnospiracaeae UCG-010*, *Eubacterium ventriosum*, *CAG-56* and metabolic parameters including higher weight, fasting blood glucose, insulin resistance and CRP but lower HDL. *Streptococcus* was the only Firmicutes bacteria with negative correlations to metabolic parameters and positive correlations to HDL (Figure 26a).

The RYGB cohort demonstrated mixed correlations between Firmicutes species and metabolic parameters. Among Firmicutes bacteria, *Butyricicoccus*, *Erysiplotrichaceae*, *UCG-003*, *Monoglobus*, *Dialister*, *Lachnospira*, *Oscillibacter*, *Romboutsia*, *Anaerostipes*, and *Eubacterium ventriosum* had positive correlations with metabolic parameters. Firmicutes bacteria that had negative correlations included *UCG-002*, *Veillonella*, *Christensenellaceae R-7* group, *NK4A214*, *Streptococcus*, *Alistipes* and *Collinsella*. Notably, the *Proteobacteria* genera were negatively associated with metabolic parameters and CRP. *Akkermansia* had negative correlations with weight, insulin resistance and CRP (Figure 26b).

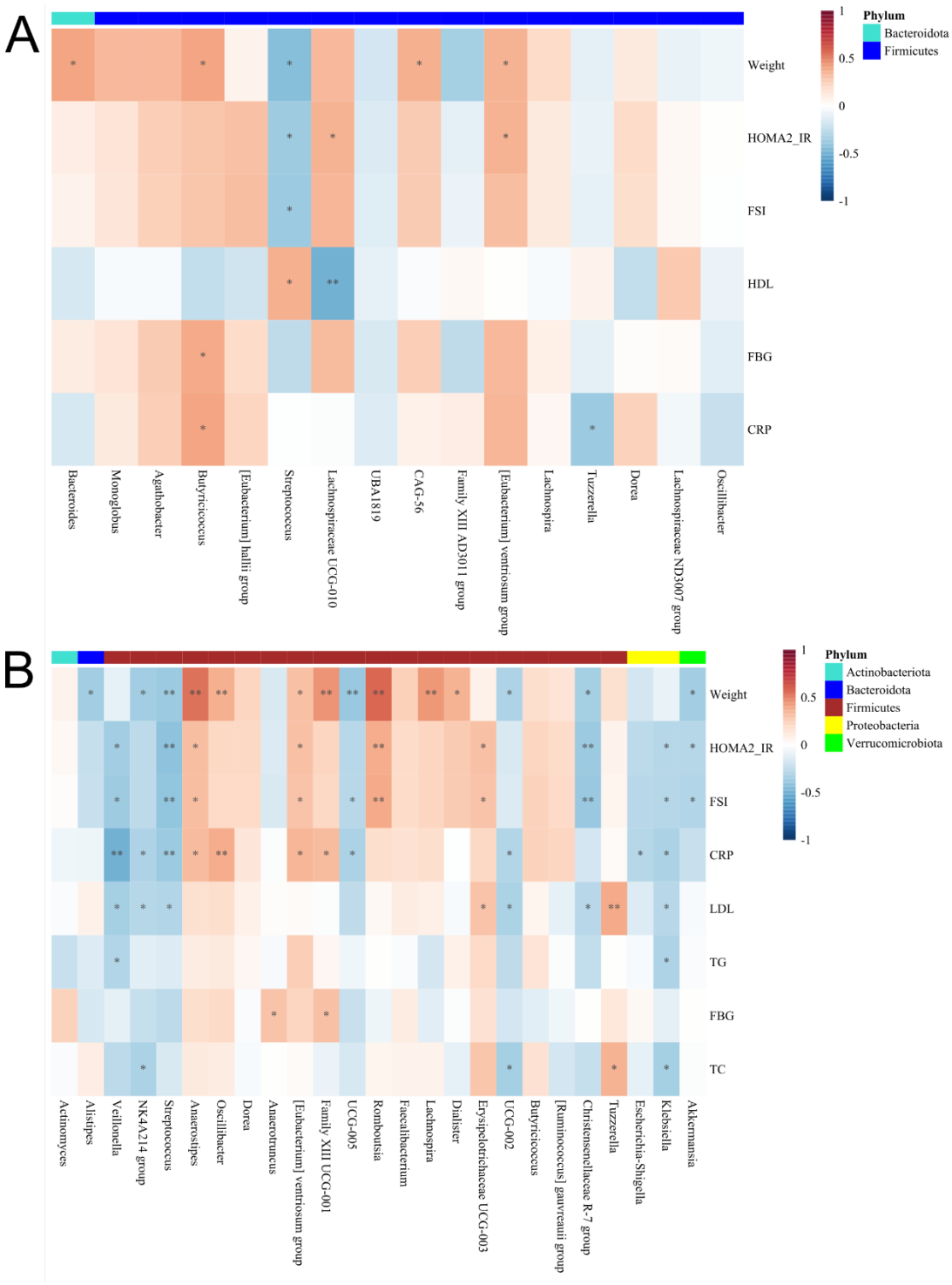

Figure 26. Heatmaps demonstrating Spearman correlations between differential microbial genera and clinical parameters at 9 months compared to baseline for (A) sleeve gastrectomy and (B) Roux-en-Y gastric bypass. FBG, fasting blood glucose, FSI; fasting serum insulin; HOMA2-IR, Homeostasis model for the assessment of insulin resistance; LDL low-density lipoprotein; HDL, high-density lipoprotein; TG, triglyceride; TC, total cholesterol; CRP, C-reactive protein.

Integrated microbiome-metabolome analysis

Integrated microbiome-metabolome analysis was conducted. sPLS-DA score plots demonstrated poor discrimination for CTRL at 0, 3 and 9 months. However, there was significant discrimination between 9 months and baseline for both SG and RYGB, with the most separation for the 9-month RYGB cohort (Figure 27).

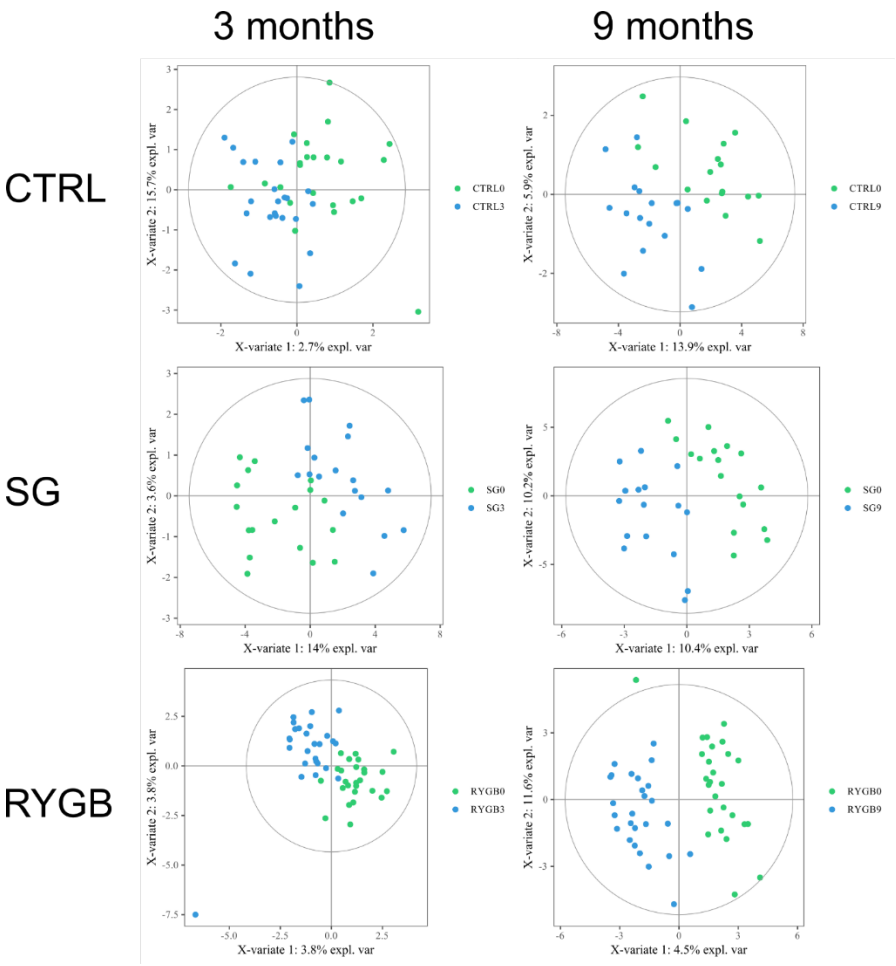

Figure 27. Sparse partial least squares discriminant analysis score plots including microbial and metabolomic variables for non-operative control (CTRL), sleeve gastrectomy (SG) and Roux-en-Y gastric bypass cohorts (RYGB) at 3 and 9 months compared to baseline.

Spearman's correlation was performed between differential microbial taxa and serum metabolites at 3 and 9 months compared to baseline. The CTRL group demonstrated minimal correlations, however, the SG and RYGB cohorts demonstrated an increasing number and complexity of interactions from 3 months to 9 months after bariatric surgery. The 9-month SG cohort demonstrated the most interactions, with a cluster of Firmicutes bacteria (*Butyricicoccus*, *Eubacterium ventriosum* and *Monoglobus*) having negative correlations with metabolites of various classes including amino acids, sphingolipids, and acylcarnitines (Figure 28). There were also negative correlations between sphingolipids and Firmicutes organisms including *Monoglobus*, *Eubacterium ventriosum*, *Eubacterium hallii*, *Dorea*, and *Lachnospira*. RYGB at 9 months was also dominated by interactions through Firmicutes bacteria with *Romboutsia* having positive correlations to multiple glycerophospholipid metabolites. (Figure 29).

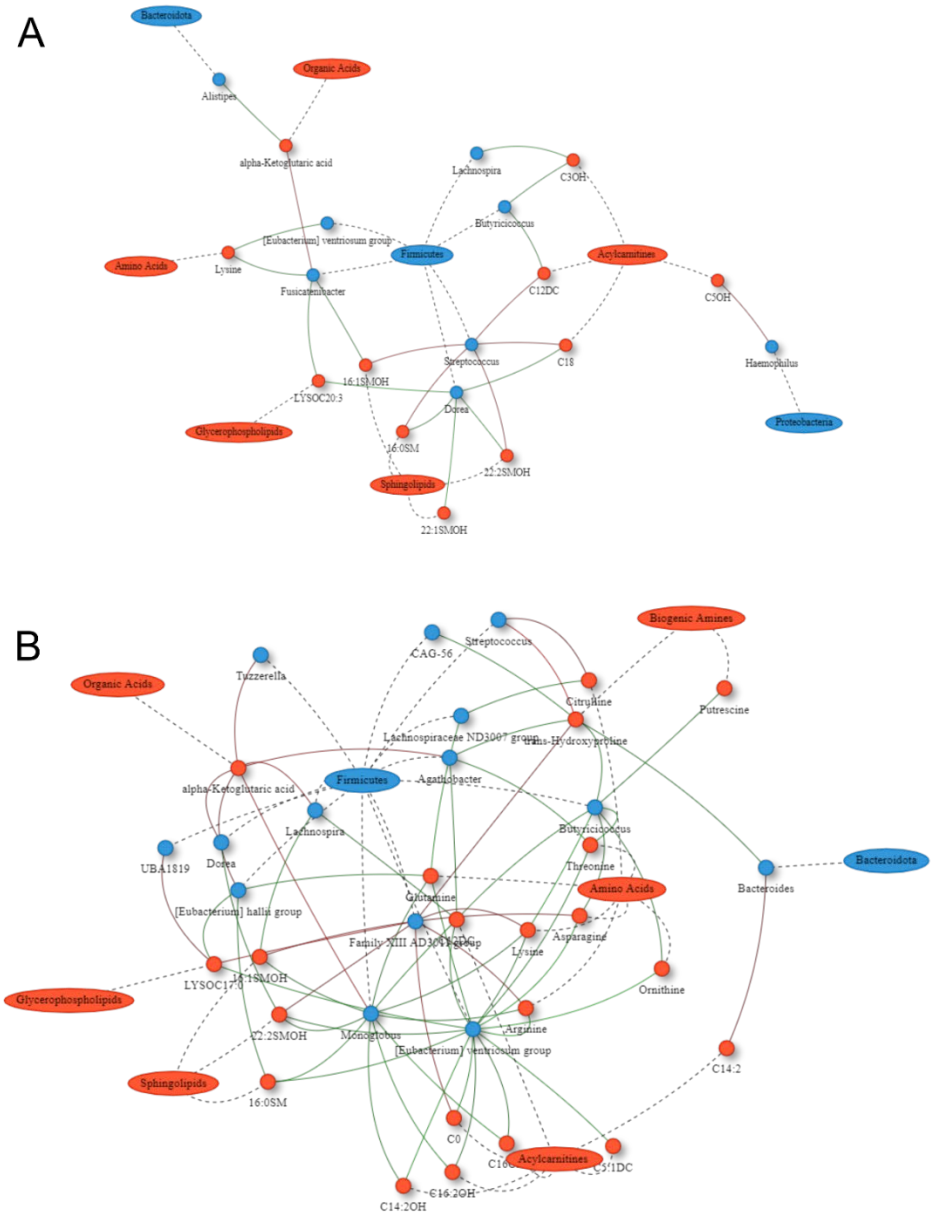

Figure 28. Network plot of Spearman correlations between differential microbes and metabolites at 3 and 9 months compared to baseline for sleeve gastrectomy. Metabolites are represented as red circles and metabolite classes as red ovals. Microbial genera are represented as blue circles and phyla as blue ovals. Positive and negative correlations are indicated using red and green colors, respectively. SM, sphingomyelins; SMOH, hydroxysphingomyelin; PC, phosphatidylcholine; LYSOC, lysophosphatidylcholine; C, carnitines.

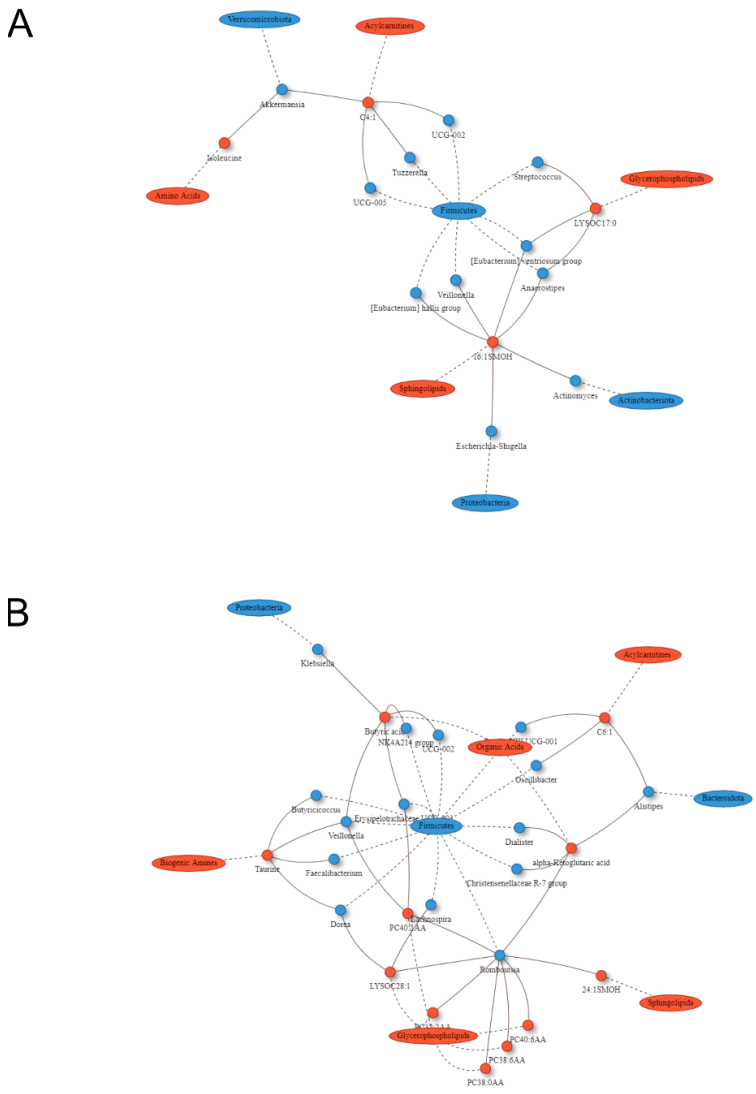

Figure 29. Network plot of Spearman correlations between differential microbes and metabolites at 3 and 9 months compared to baseline for Roux-en-Y gastric bypass. Metabolites are represented as red circles and metabolite classes as red ovals. Microbial genera are represented as blue circles and phyla as blue ovals. Positive and negative correlations are indicated using red and green colors, respectively. SM, sphingomyelins; SMOH, hydroxysphingomyelin; PC, phosphatidylcholine; LYSOC, lysophosphatidylcholine; C, carnitines.

Microbial functional prediction and metabolic pathway enrichment analysis (MPEA)

Differentially enriched and depleted KEGG-orthology functional pathways were identified between baseline and 9 months. In the CTRL cohort, this identified eleven and two significant microbial and metabolomic pathways, respectively. The SG cohort had differentially significant changes in eight microbial and six metabolic KO functional pathways while RYGB had the most significant changes with 20 microbial and four metabolomic functions identified (Figure 30 and Figure 31).

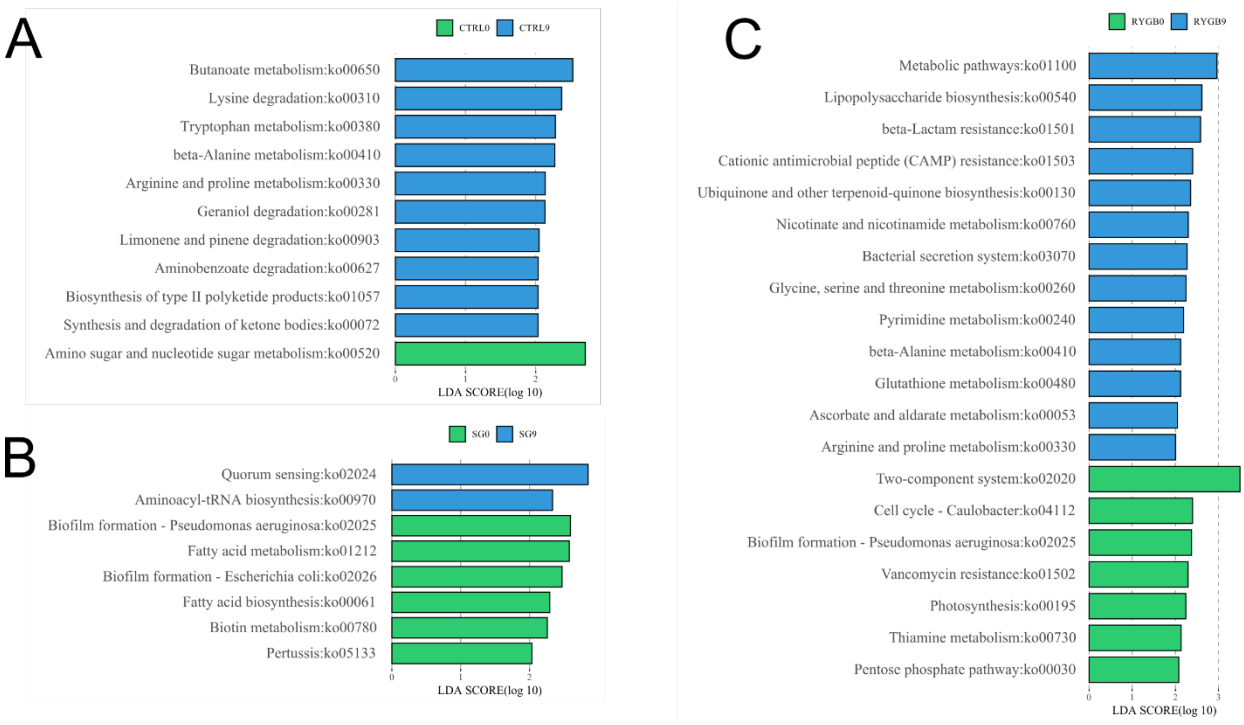

Figure 30. Microbial functional prediction of KEGG-based KO functions using linear discriminant analysis comparing 9 months to baseline for (A) non-operative control, (B) sleeve gastrectomy, and (C) Roux-en-Y gastric bypass. P-value < 0.05 is considered statistically significant.

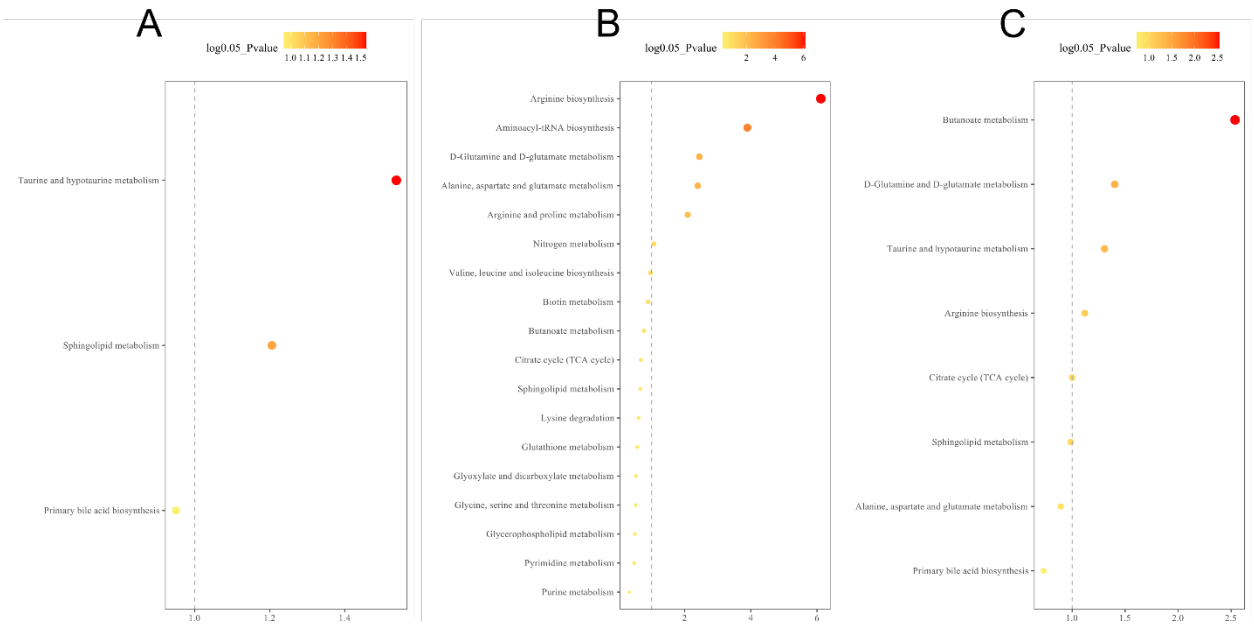

Figure 31. Differential metabolic pathway enrichment analysis comparing 9 months to baseline for (A) non-operative control, (B) sleeve gastrectomy, and (C) Roux-en-Y gastric bypass. P-value < 0.05 (or log0.05 p-value > 1.0) is considered statistically significant.

Among all group comparisons, only the 9-month SG cohort demonstrated a common enriched functional pathway on both microbial and metabolic functional analysis. The aminoacyl-transfer-RNA (aa-tRNA) biosynthesis pathway was significantly upregulated in both microbial and metabolomic functional pathways. This pathway was specifically enriched by five amino acids (arginine, asparagine, lysine, glutamine, threonine) and modified by potentially 79 unique bacterial genera (Figure 32).

hsa00970: Aminoacyl-tRNA biosynthesis

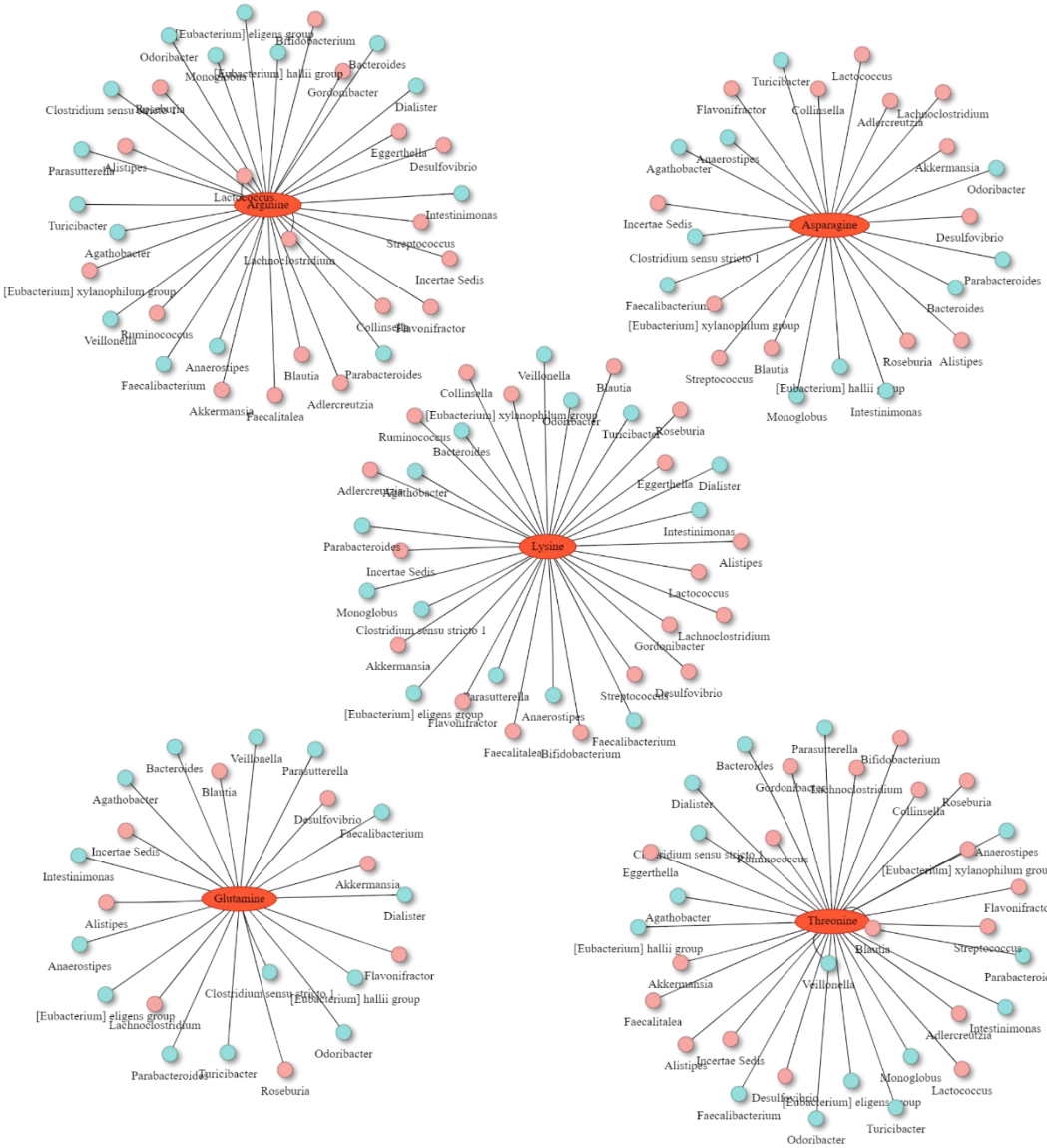

Figure 32. Venn diagram of significant differential pathways in functional network analysis implemented with the KEGG metabolic pathway database. Interaction network plots of enriched amino acids in the aminoacyl-transfer-RNA biosynthesis pathway with microbes that participate in its metabolism. Red colors indicate significantly up-regulated metabolites or microbes, while blue colors indicate significantly down-regulated metabolites or microbes.

Between group comparisons between SG and RYGB

On univariate microbial analysis, at 3 months, there were no significant microbial differences between RYGB or SG. However, at 9 months, RYGB had a higher abundance of Proteobacteria compared to SG but no differences at the genus level (Supplementary Figure 31). sPLS-DA score plots demonstrated significant discrimination between RYGB and SG at 3 months, however, this difference was not significant at 9 months (Figure 33).

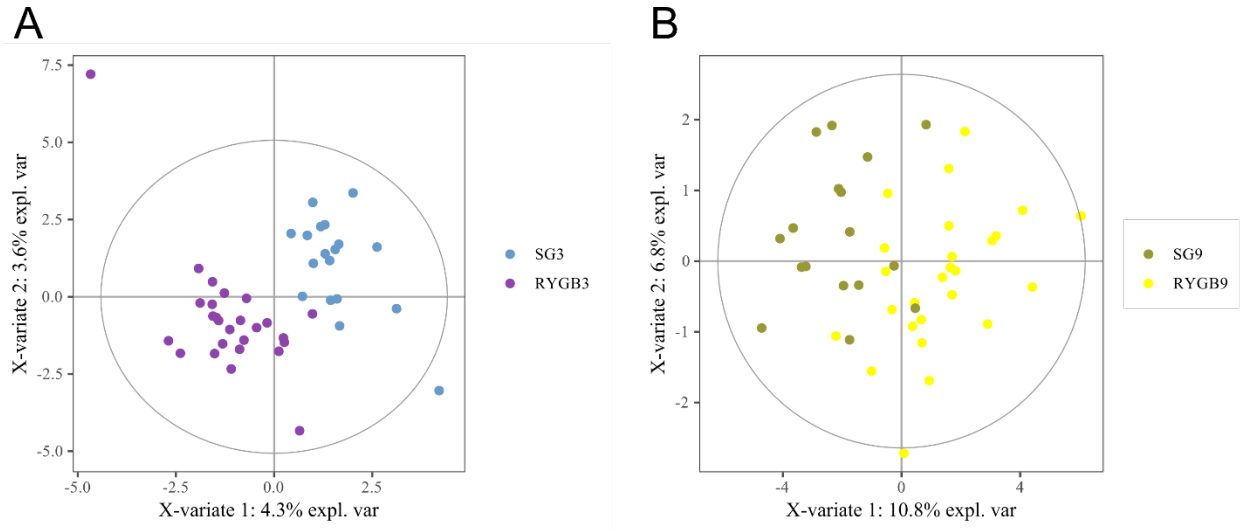

Figure 33. Sparse partial least squares discriminant analysis score plots including microbial and metabolomic variables between sleeve gastrectomy and Roux-en-Y gastric bypass cohorts at (A) 3 months and (B) 9 months.

Microbial functional pathway analysis revealed nine enriched pathways in SG and six enriched pathways in RYGB. In metabolomic pathway enrichment analysis, the aminoacyl-tRNA

biosynthesis pathway was the most significant metabolomic pathway enriched in SG compared to RYGB. Sphingolipid metabolism was significantly enriched in microbial functional analysis (p=0.03) and had near significance in metabolomic pathway enrichment analysis (p=0.09) in SG compared to RYGB.

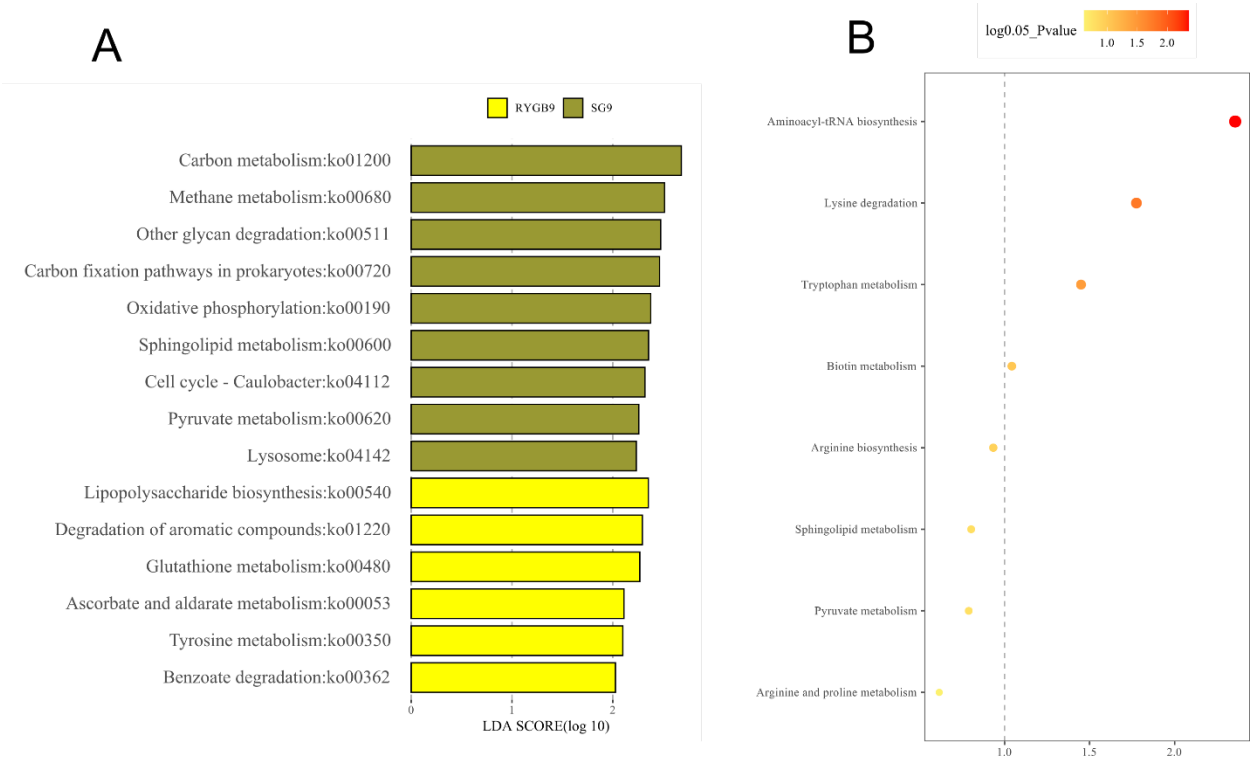

Figure 34. Functional analysis between sleeve gastrectomy and Roux-en-Y gastric bypass at 9 months for (A) microbial pathways and (B) metabolomic pathways. P-value < 0.05 (or log0.05 p-value > 1.0) is considered statistically significant.

4.5 DISCUSSION

In this study, we performed a comprehensive and integrated analysis of microbial, metabolomic, inflammatory and clinical changes between patients receiving aggressive medical intervention and those receiving the two most common bariatric surgical interventions – SG and RYGB. Consistent with the literature[67,68], RYGB and SG cohorts had significant postoperative weight loss with RYGB leading to greater improvements in metabolic and inflammatory measures.

Notably, RYGB resulted in the most significant microbial changes while SG had more pronounced metabolomic changes. In contrast, the CTRL cohort had minimal changes in clinical, inflammatory, microbial or metabolomic parameters. This prospective clinical trial and complex bioinformatics analysis revealed unique pathways in which weight loss and metabolic improvement occur after bariatric surgery.

RYGB had the most consistent decrease in markers of systemic inflammation as demonstrated by temporal decreases in CRP, WBC and ferritin. However, this decrease did not appear to be mediated by improvements in gut barrier integrity as serum LPS did not change despite significant microbial compositional shifts after RYGB. Our study also demonstrated an increase in pro-inflammatory, pathogenic Proteobacteria genera such as Escherichia-Shigella and Klebsiella[249] and a negative correlation between Proteobacteria and systemic inflammation. Tremaroli et al. demonstrated that although LPS synthesis increases in the gut microbiome after RYGB, this increase was not associated with an increase in systemic inflammation[146]. This may be due to improved mucosal tight-junction integrity after RYGB as demonstrated by Guo et al. This study also found reduced intestinal permeability and reduced systemic inflammation and metabolic endotoxemia after RYGB[250]. In the setting of RYGB, Proteobacteria appears to have a uniquely protective effects on systemic inflammation but explanations for this are not entirely clear.

The *Romboutsia* genus had the most microbial-metabolomic correlations and was decreased significantly after RYGB. This bacterium had positive correlations with six different

glycerophospholipids and its loss appears to mediate a decrease in serum quantities of glycerophospholipids. There is emerging evidence that glycerophospholipids are increased in the myotubes of obese patients and that membrane glycerophospholipids dynamics are linked to the development of diet-induced insulin resistance[251]. *Romboutsia* was positively correlated to higher weight and insulin resistance in our study which is consistent with previously described findings[252,253]. Furthermore, studies have linked *Romboutsia* to glycerophospholipids which have been implicated in obesity-induced fatty liver disease[254]. Given these correlations, it is suggestive that the modulatory effects of RYGB on glycerophospholipids may be mediated by changes in the abundance of *Romboutsia*.

The SG cohort had the most microbial-metabolomic correlations. These were predominantly from one Firmicutes cluster consisting of *Butyricicoccus*, *Eubacterium ventriosum* and *Monoglobus* (BEM) which had negative correlations with a wide array of metabolites. This cluster was decreased in abundance after SG and this change appears to increase various metabolites including amino acids, acylcarnitines, and sphingolipids. *Eubacterium ventriosum* has been associated with obesity[255,256] while butyrate-producing organisms such as *Butyricicoccus* appear to cause shifts in fermentation patterns which affect energy homeostasis[256]. In our study, this cluster was associated with higher weight, higher insulin resistance, higher fasting blood glucose and greater systemic inflammation.

The mechanism of this pathway appears to occur through the aa-tRNA biosynthesis pathway. The aa-tRNA biosynthesis pathway was the only significantly enriched pathway in both

microbial and metabolic functional analysis after SG. This pathway was mediated by five amino acids which were negatively correlated with the BEM cluster. After SG, it is likely that this pathway is driven by a reduction in the abundance of BEM bacteria resulting in increases in amino acids which contribute to the enrichment of aa-tRNA biosynthesis. Lower abundances of BEM bacteria were also correlated with improved glucose, lower weight and decreased inflammation which likely occurs through enrichment of the aa-tRNA biosynthesis pathway.

tRNAs are formed by direct aminoacylation of tRNAs which are catalyzed by aminoacyl-tRNA synthetases (aaRS)[257]. Alterations in tRNA biology have been associated with a large variety of diseases including cancer and metabolic disorders[258]. Specifically, mutations in aaRSs and variants in the tRNA-modifying enzyme CDKAL1 have been associated with an increased risk for obesity and type 2 diabetes[259–261]. Mutations in mitochondrial tRNA genes have also been associated with maternally inherited diabetes and deafness[262] and mutations in tRNA methyltransferase TRMT10A directly cause young onset diabetes and microcephaly[263]. aaRSs are also involved in intracellular amino acid signaling and recent studies support the notion that depletion or enrichment of amino acids modulate the activity of aa-tRNA biosynthesis[264]. Given the findings of our study, it is plausible that the loss of the BEM Firmicutes cluster after SG encourages the production of amino acids which concomitantly enriches the aa-tRNA biosynthesis pathway. Furthermore, this enrichment potentiates improved glucose, lower weight and decreased systemic inflammation.

When comparing SG to RYGB, there was a higher abundance of Proteobacteria after RYGB and this is thought to occur due to an increasing alkaline environment due to exclusion of the acid-producing stomach after RYGB. Proteobacteria are less acid adaptive than other phyla and increasingly alkaline environments potentially encourage their proliferation[265]. The increased abundance of Proteobacteria may also be related to increased oxygen within the intestinal lumen after RYGB[231]. Many members of the Proteobacteria phylum produce enzymes such as catalase and superoxide dismutase that can neutralize reactive oxygen species[232]. SG also had distinctive enrichment of the sphingolipid metabolism pathway within the microbiome and metabolome. SG induced the loss of a cluster of Firmicutes genera (*Monoglobus*, *Eubacterium ventriosum*, *Eubacterium hallii*, *Dorea*, and *Lachnospira*) that were correlated with increased serum sphingomyelins and hydroxysphingomyelins. Sphingomyelins are major phospholipids found in animal cell membranes and its metabolism creates products that play important roles in the cell. Lower serum sphingomyelins have been associated with prediabetes or diabetes[266] and inhibited sphingolipid metabolism has been linked to progression to type 2 diabetes through impairment of pancreatic β-cell function[267]. Our study links the decrease in five Firmicutes genera to an enrichment of sphingomyelins and the sphingolipid metabolism pathway, which is potentially a pathway contributing to improved glucose metabolism that is unique to SG, but not to RYGB.

Limitations of this study include relatively small sample sizes of patients in each group which may make it underpowered to detect smaller differences between timepoints. The study was prospective in design and differences in patient demographics may influence results. It is also possible that changes in medications, diet, and exercise may confound our findings as these can have effects on the microbiome and metabolome. However, patients were managed by the same

clinical team with standardized preoperative and postoperative care which should reduce confounding effects. There is also the possibility that performing multiple analyses can lead to false discovery, however, our control group underwent the same analysis and had minimal significant results. Recruitment was also prematurely discontinued, and this potentially increases our risk for a type II error. However, despite these limitations, our study provides the most comprehensive analysis of the complex microbial-metabolomic relationships in bariatric surgery to date and identified pathways that may be the future target of therapeutic strategies for the treatment of obesity and metabolic disease.

4.6 CONCLUSIONS

In this prospective clinical trial, we performed a comprehensive analysis on the microbial, metabolomic and inflammatory changes that occur with the two most common bariatric procedures, RYGB and SG. This trial identified unique pathways in which the effects of bariatric surgery occur via the gut microbiome. Specifically, for RYGB, we identified a clinically impactful pathway through *Romboutsia* and glycerophospholipids. For SG, enrichment of the aa-tRNA biosynthesis pathway occurred via the BEM Firmicutes cluster's effect on amino acids which lead to weight loss and improved glucose homeostasis. The loss of five specific Firmicutes bacteria (*Monoglobus*, *Eubacterium ventriosum*, *Eubacterium hallii*, *Dorea*, and *Lachnospira*) also enriched sphingolipid metabolism which may also contribute to better glucose control in SG but not in RYGB.

4.7 SUPPLEMENTARY MATERIAL

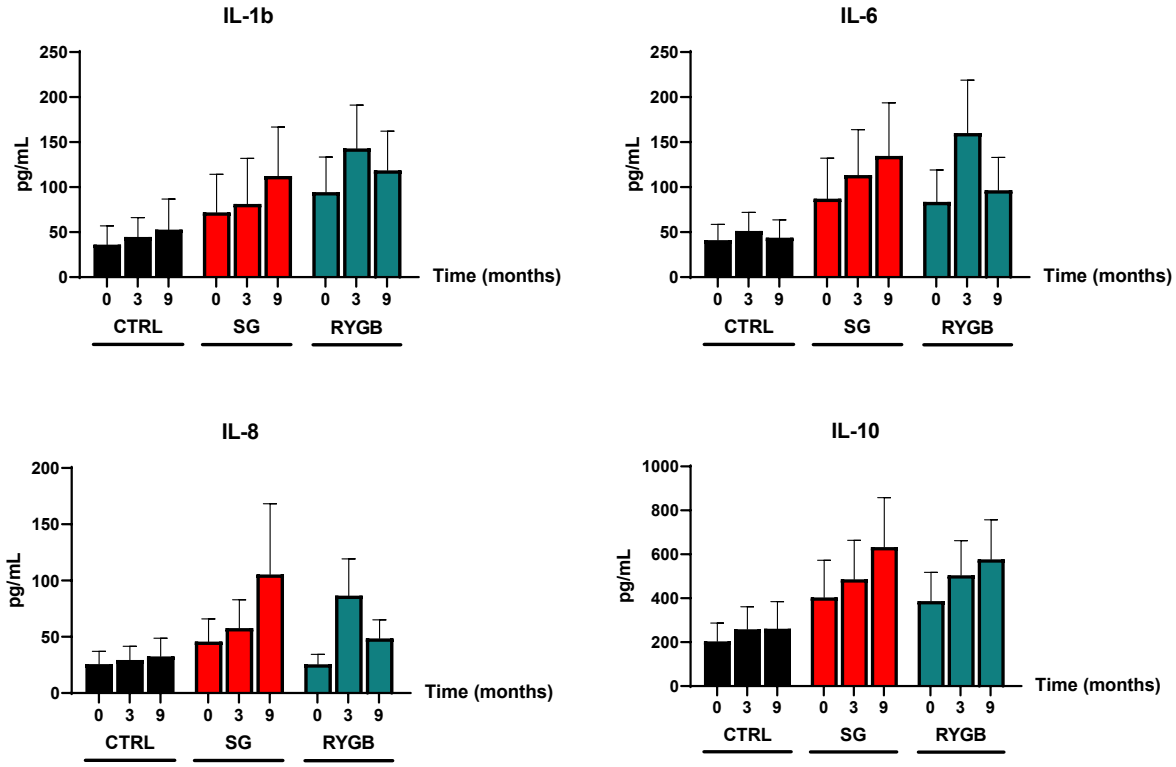

Supplementary Figure 8. Interleukins. CTRL, non-operative control; SG, sleeve gastrectomy; RYGB, Roux-en-Y gastric bypass.

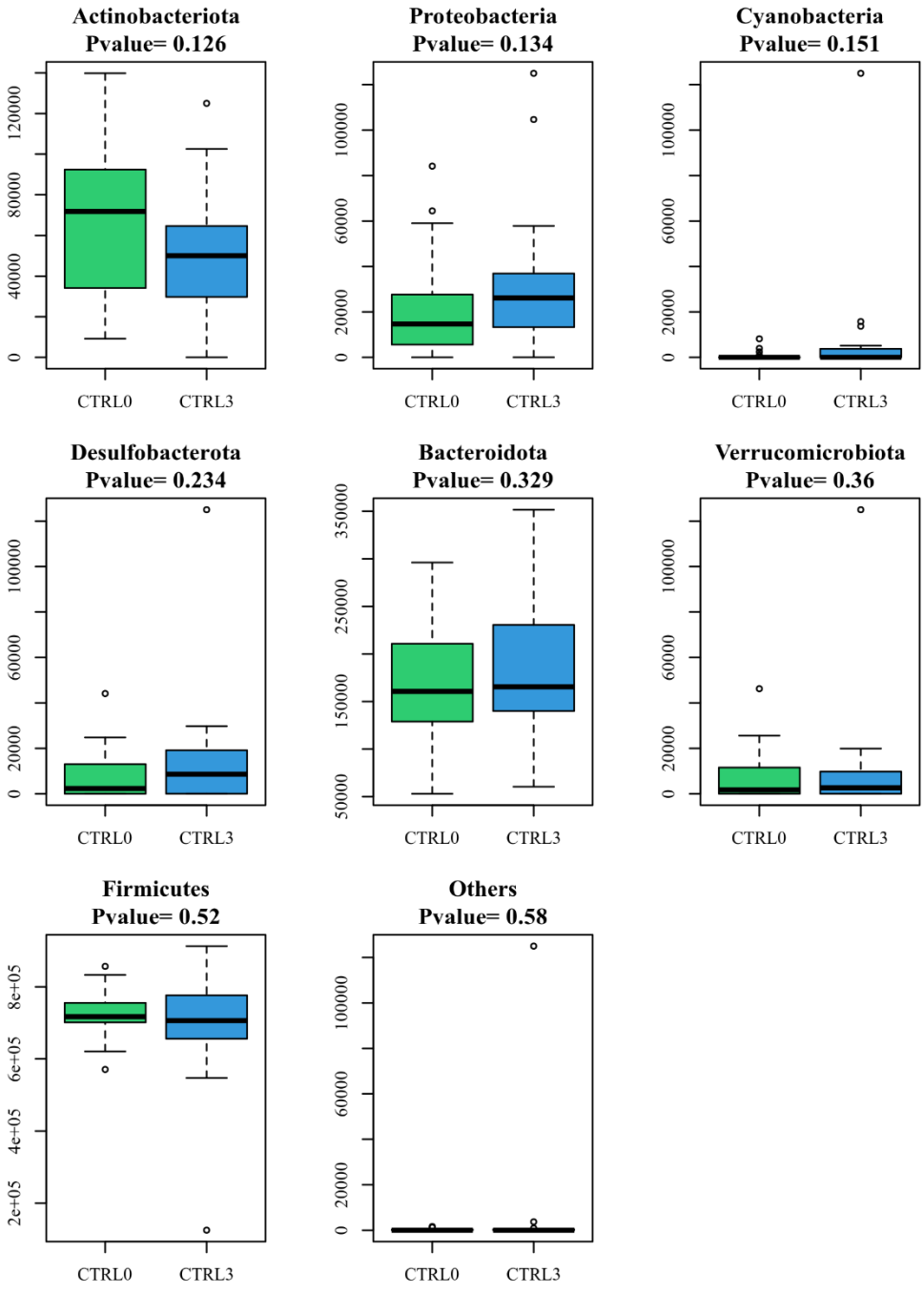

Supplementary Figure 9. Differential microbial taxa on univariate analysis at the phylum level between baseline and 3 months for non-operative control. Raw, non-corrected p-values are displayed.

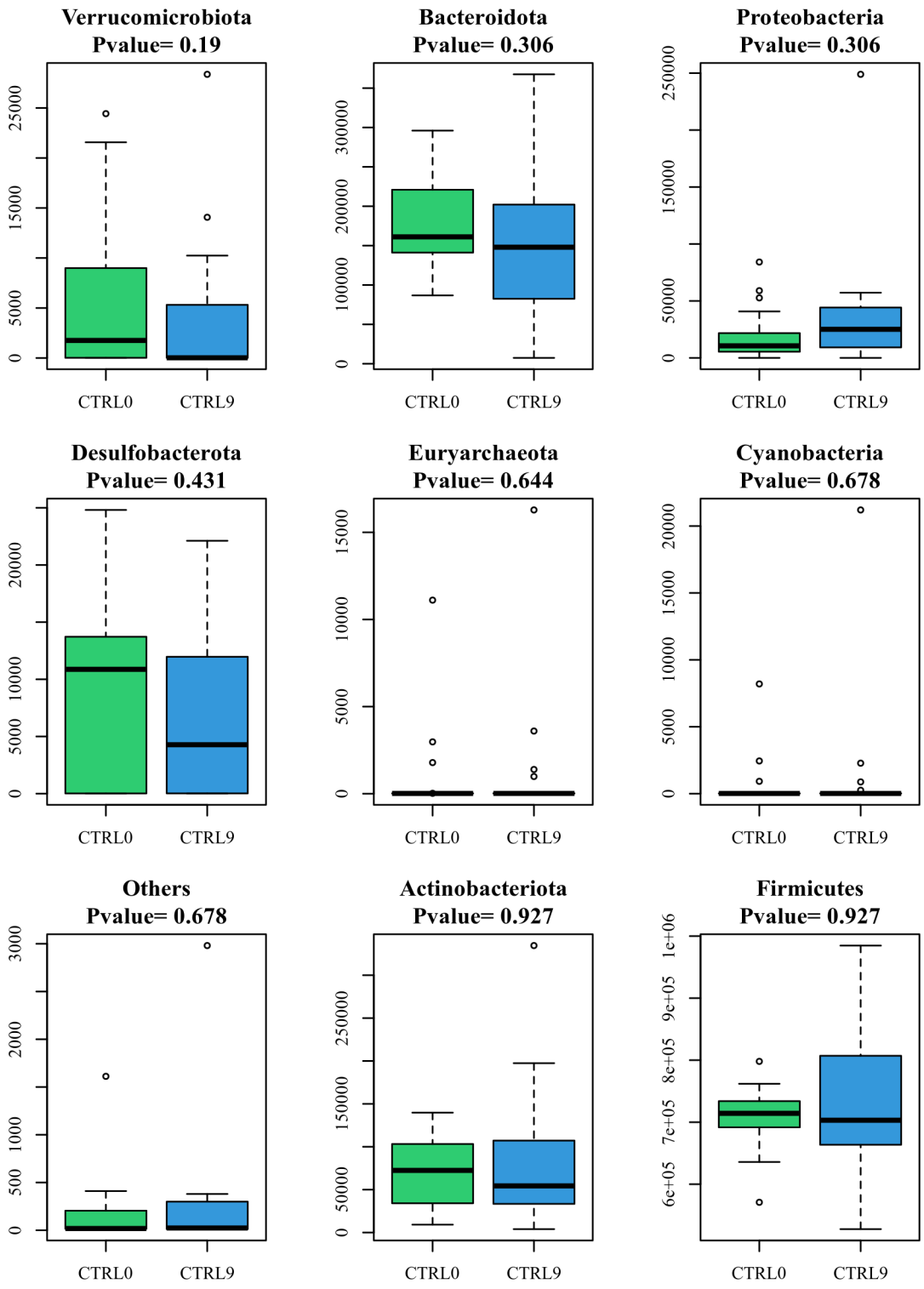

Supplementary Figure 10. Differential microbial taxa on univariate analysis at the phylum level between baseline and 9 months for non-operative control. Raw, non-corrected p-values are displayed.

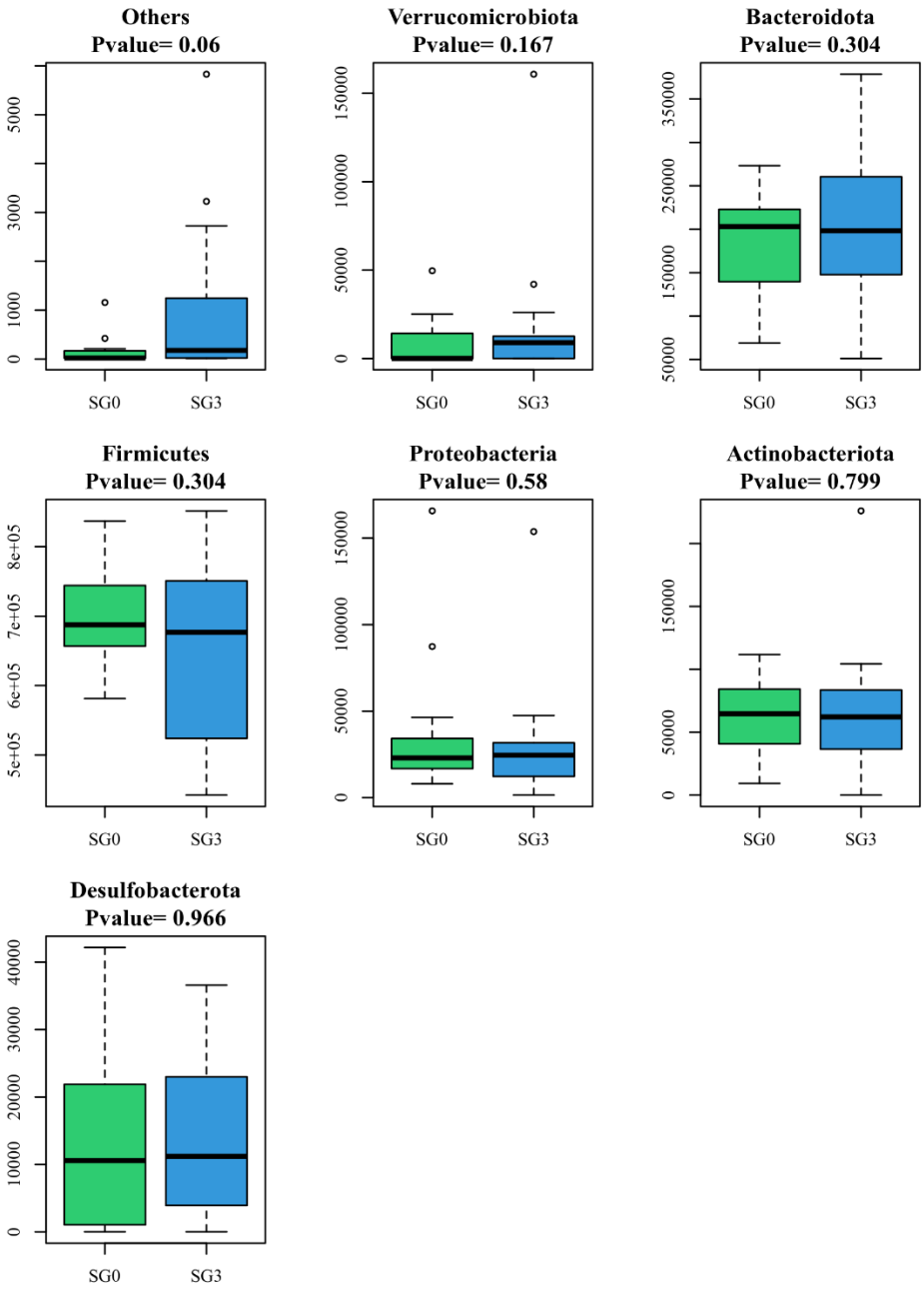

Supplementary Figure 11. Differential microbial taxa on univariate analysis at the phylum level between baseline and 3 months for sleeve gastrectomy. Raw, non-corrected p-values are displayed.

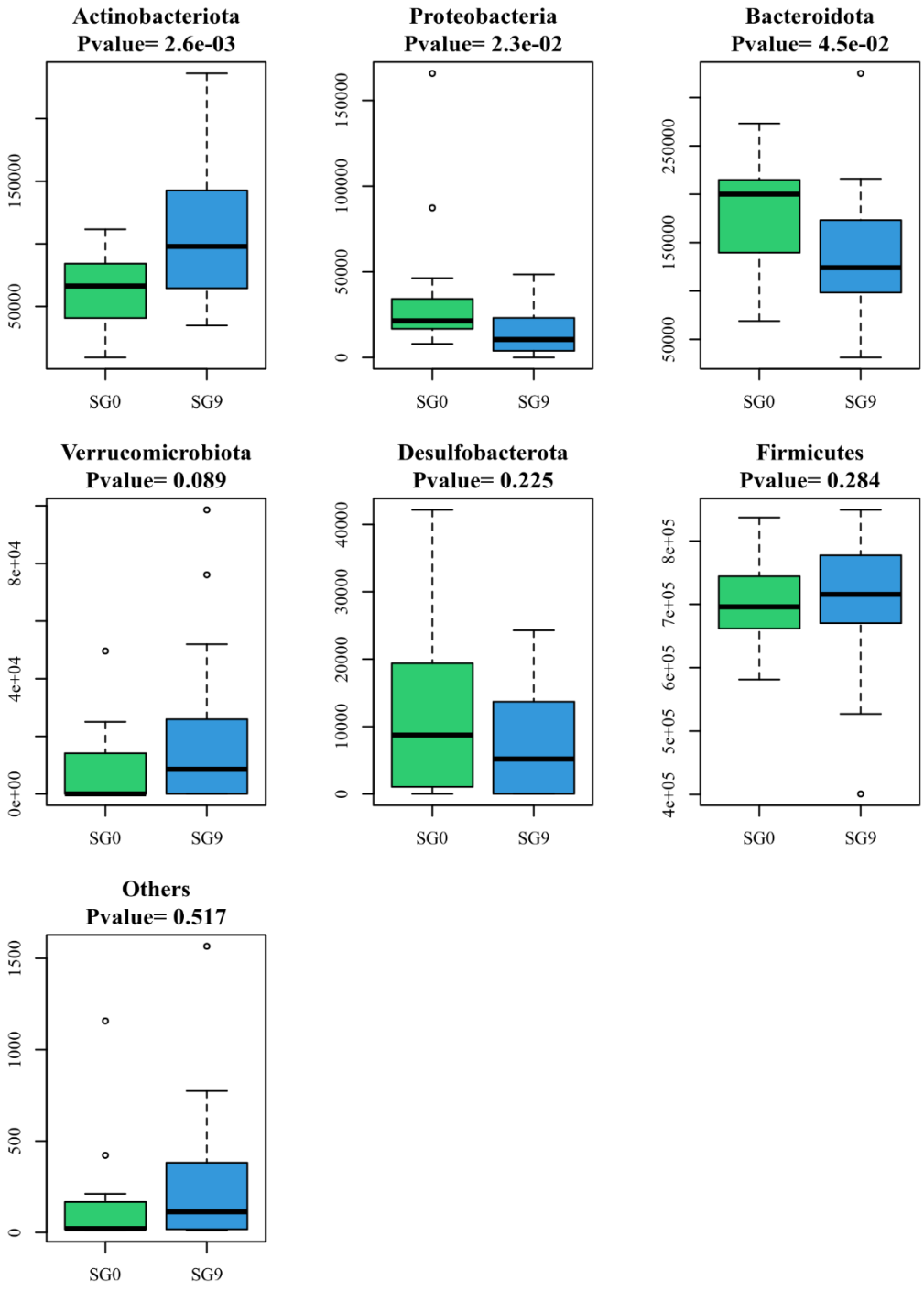

Supplementary Figure 12. Differential microbial taxa on univariate analysis at the phylum level between baseline and 9 months for sleeve gastrectomy. Raw, non-corrected p-values are displayed.

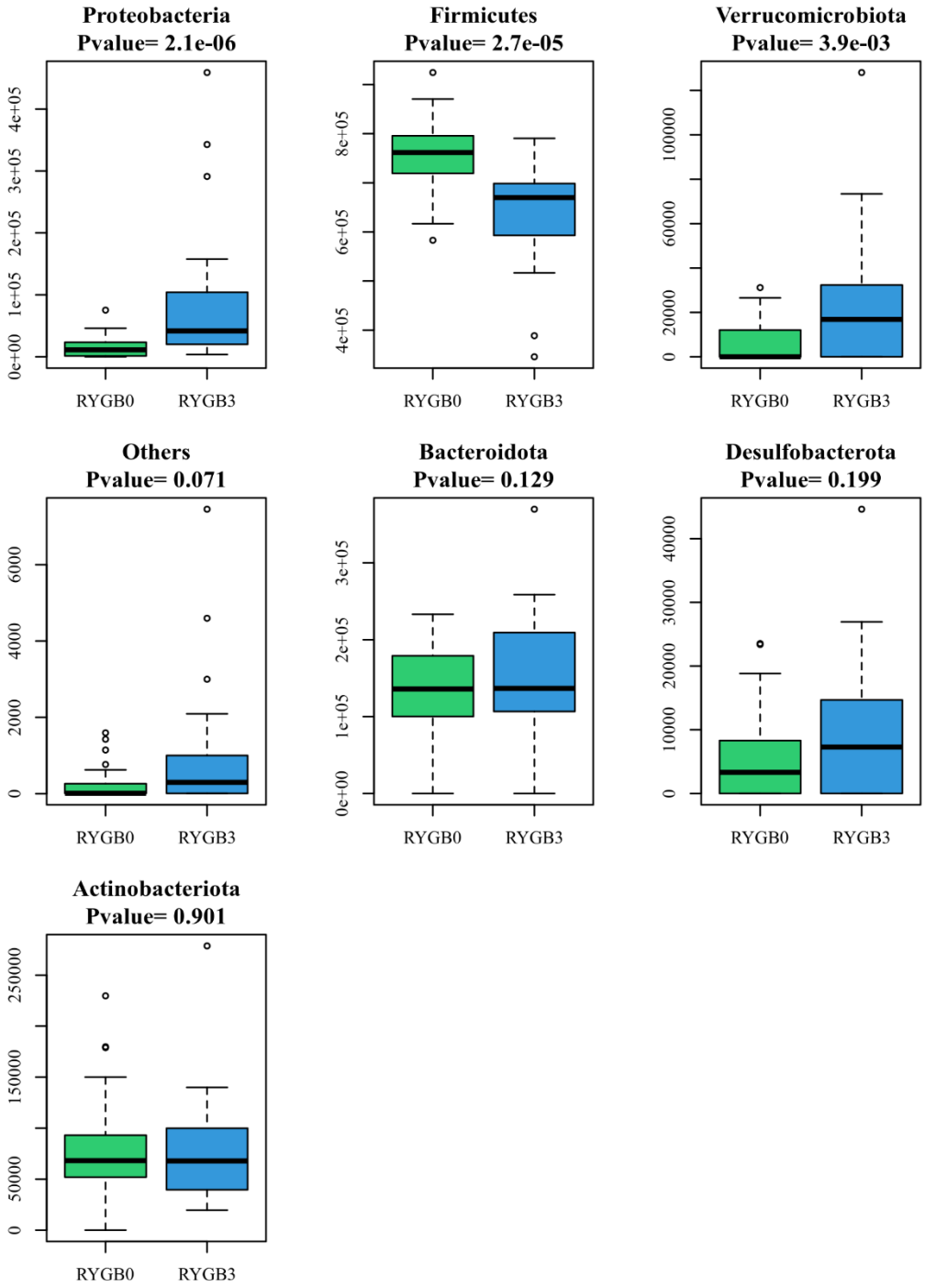

Supplementary Figure 13. Differential microbial taxa on univariate analysis at the phylum level between baseline and 3 months for Roux-en-Y gastric bypass. Raw, non-corrected p-values are displayed.

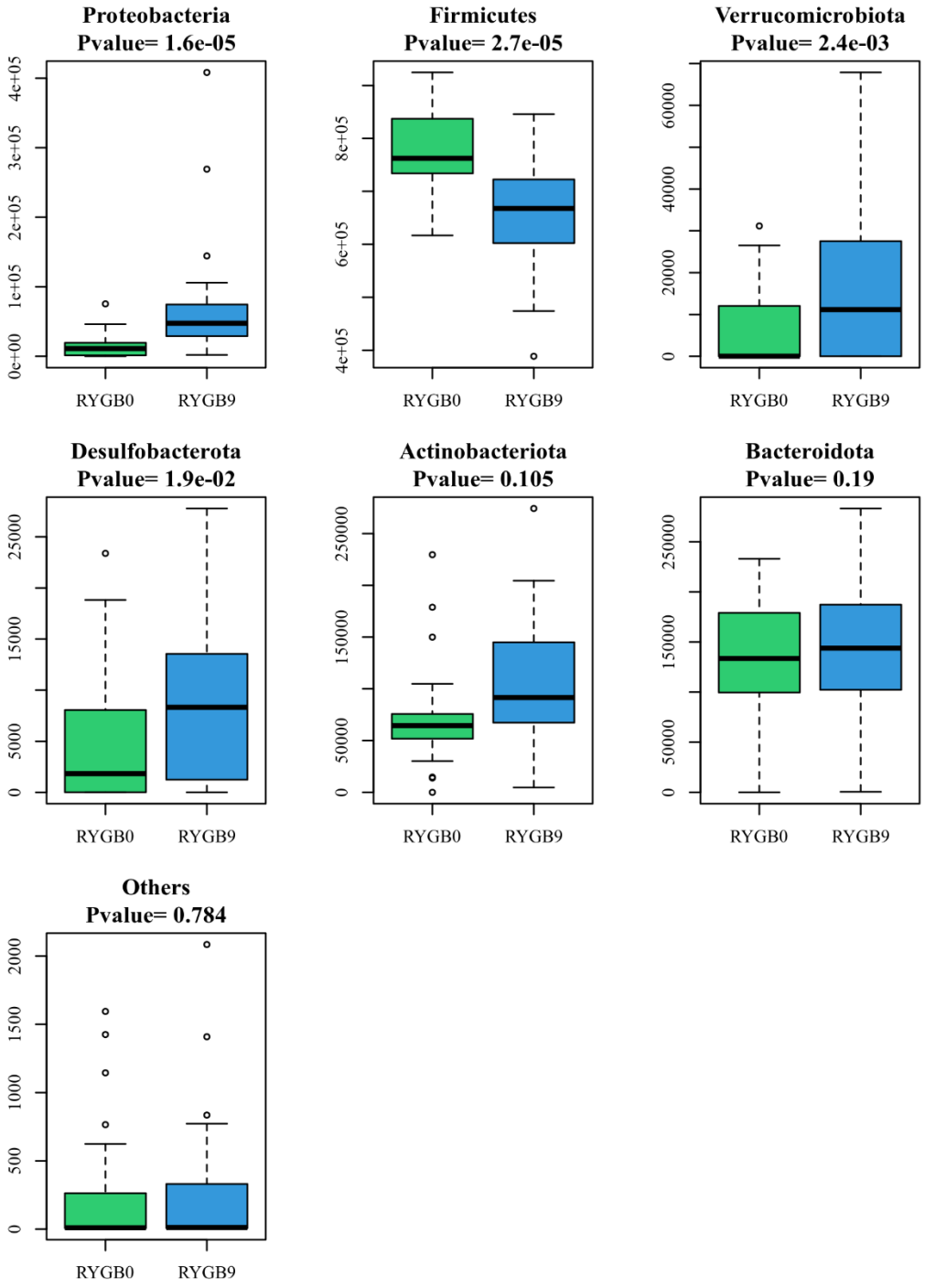

Supplementary Figure 14. Differential microbial taxa on univariate analysis at the phylum level between baseline and 9 months for Roux-en-Y gastric bypass. Raw, non-corrected p-values are displayed.

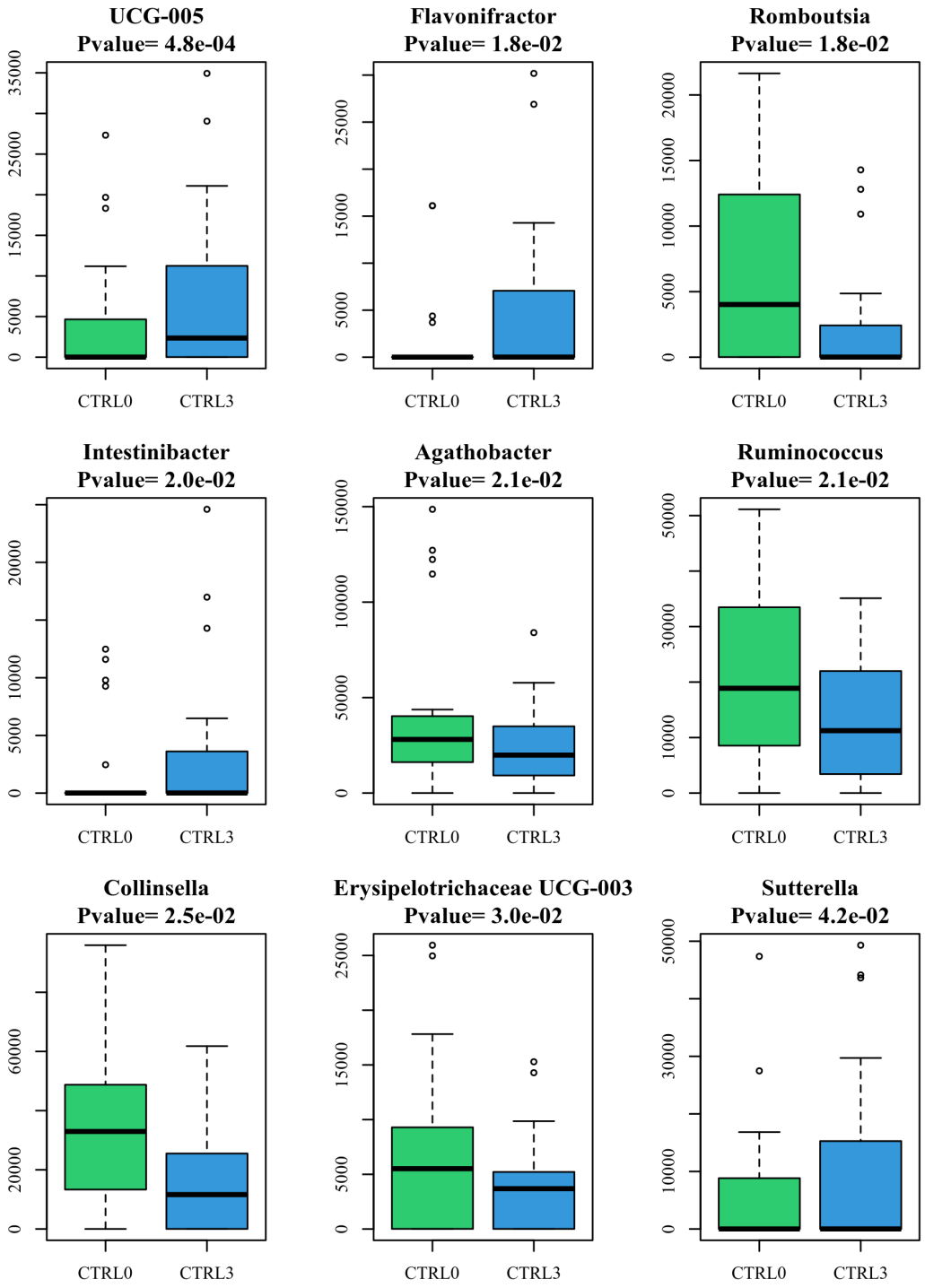

Supplementary Figure 15. Differential microbial taxa on univariate analysis at the genus level between baseline and 3 months for non-operative control. Raw, non-corrected p-values are displayed.

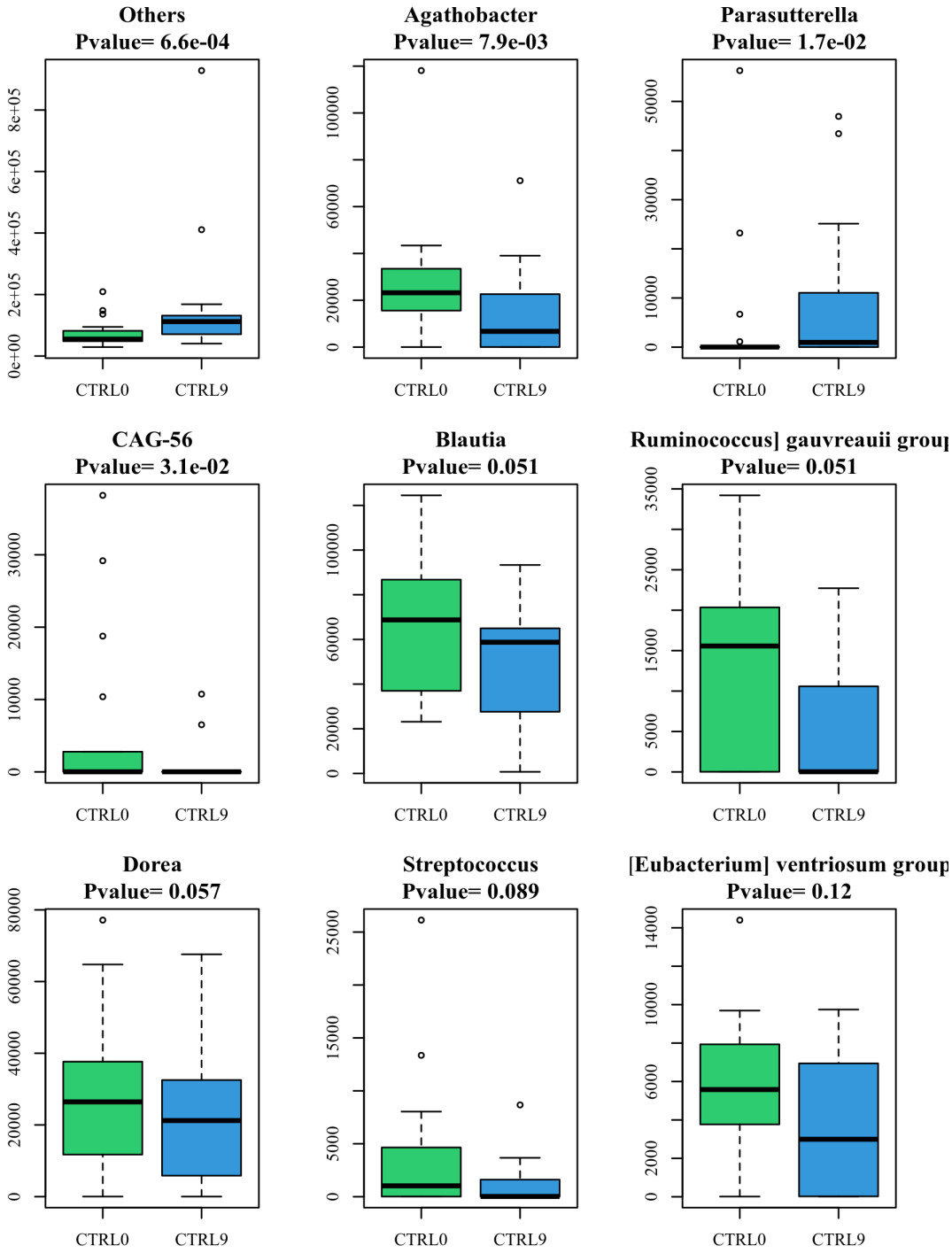

Supplementary Figure 16. Differential microbial taxa on univariate analysis at the genus level between baseline and 9 months for non-operative control. Raw, non-corrected p-values are displayed.

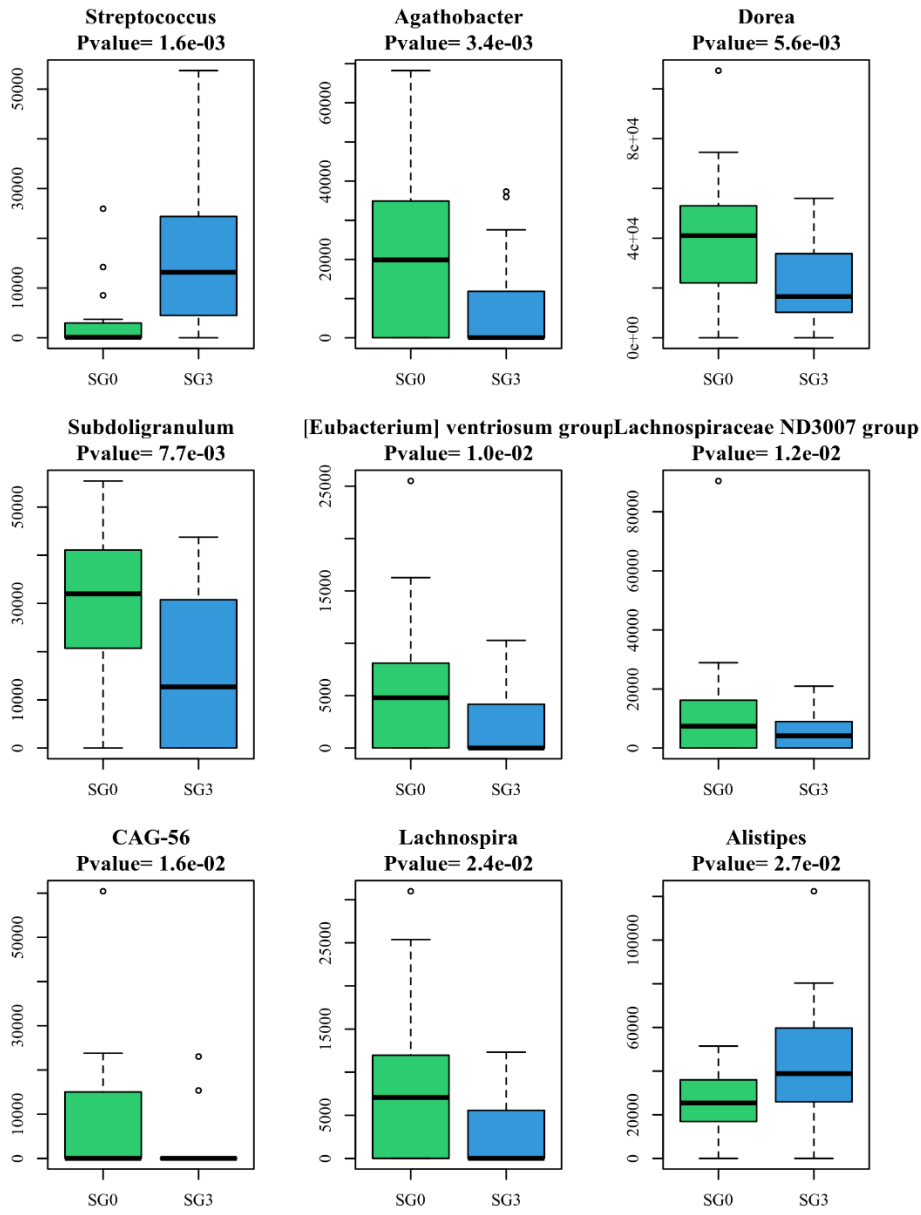

Supplementary Figure 17. Differential microbial taxa on univariate analysis at the genus level between baseline and 3 months for sleeve gastrectomy. Raw, non-corrected p-values are displayed.

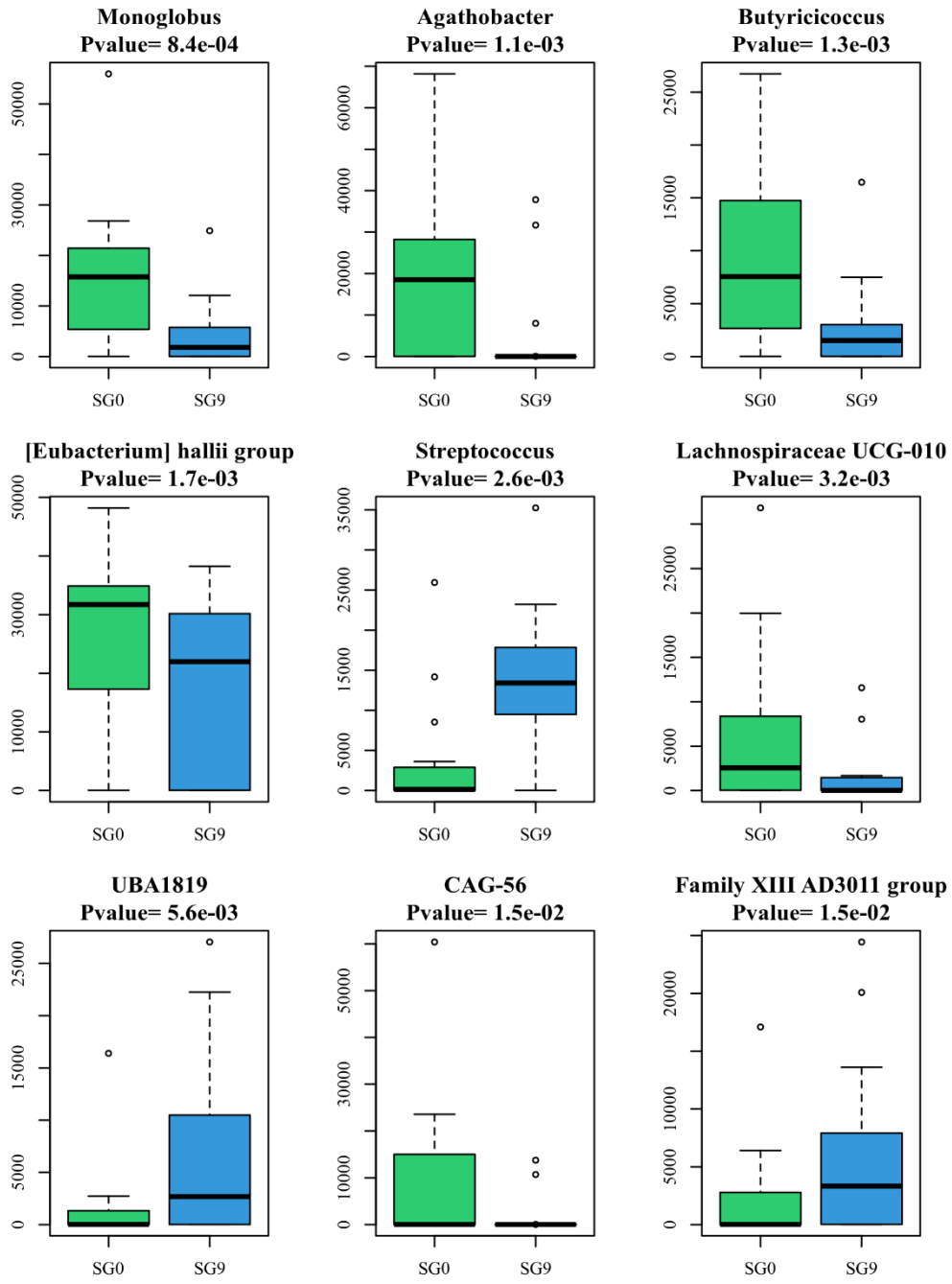

Supplementary Figure 18. Differential microbial taxa on univariate analysis at the genus level between baseline and 9 months for sleeve gastrectomy. Raw, non-corrected p-values are displayed.

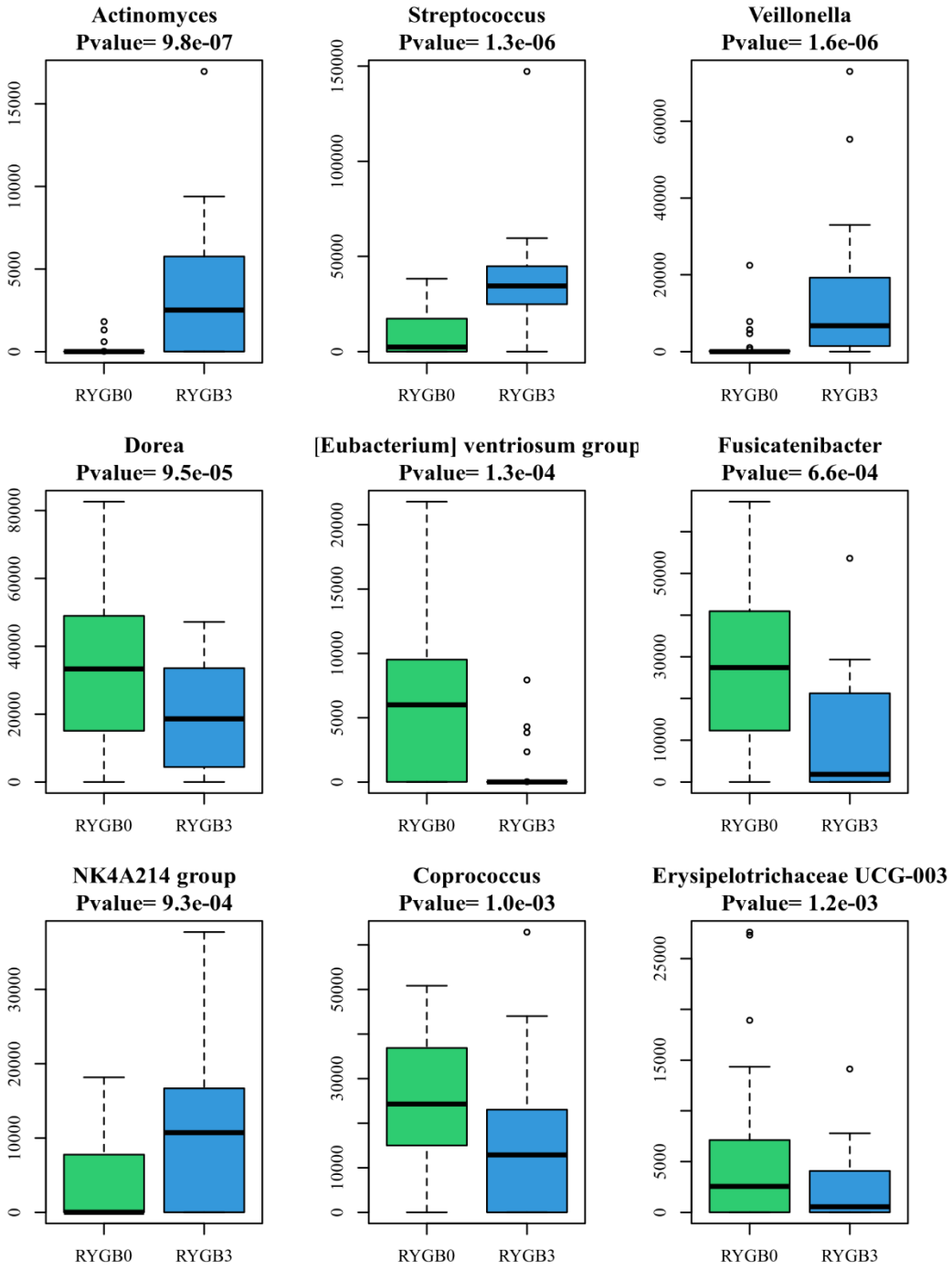

Supplementary Figure 19. Differential microbial taxa on univariate analysis at the genus level between baseline and 3 months for Roux-en-Y gastric bypass. Raw, non-corrected p-values are displayed.

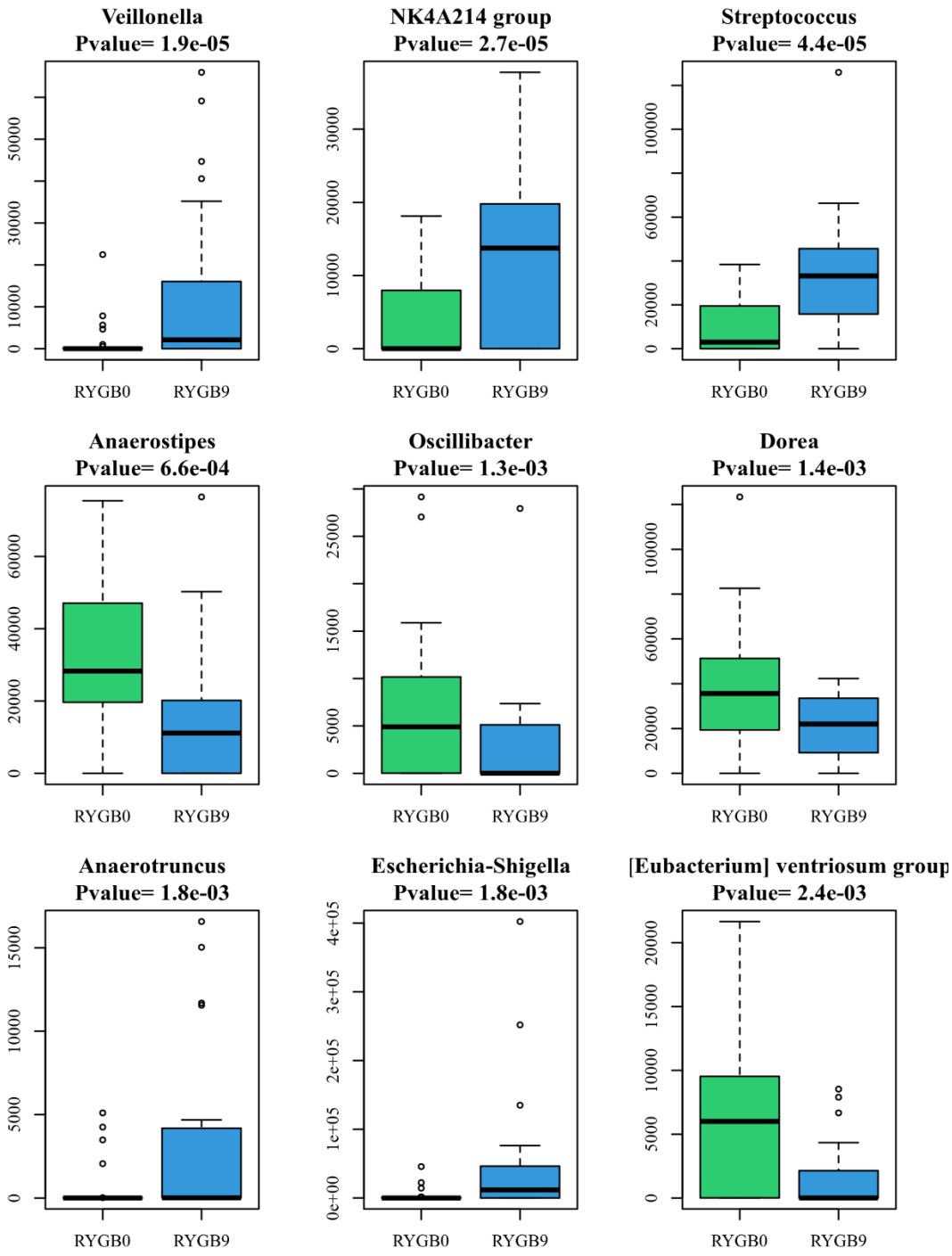

Supplementary Figure 20. Differential microbial taxa on univariate analysis at the genus level between baseline and 9 months for Roux-en-Y gastric bypass. Raw, non-corrected p-values are displayed.

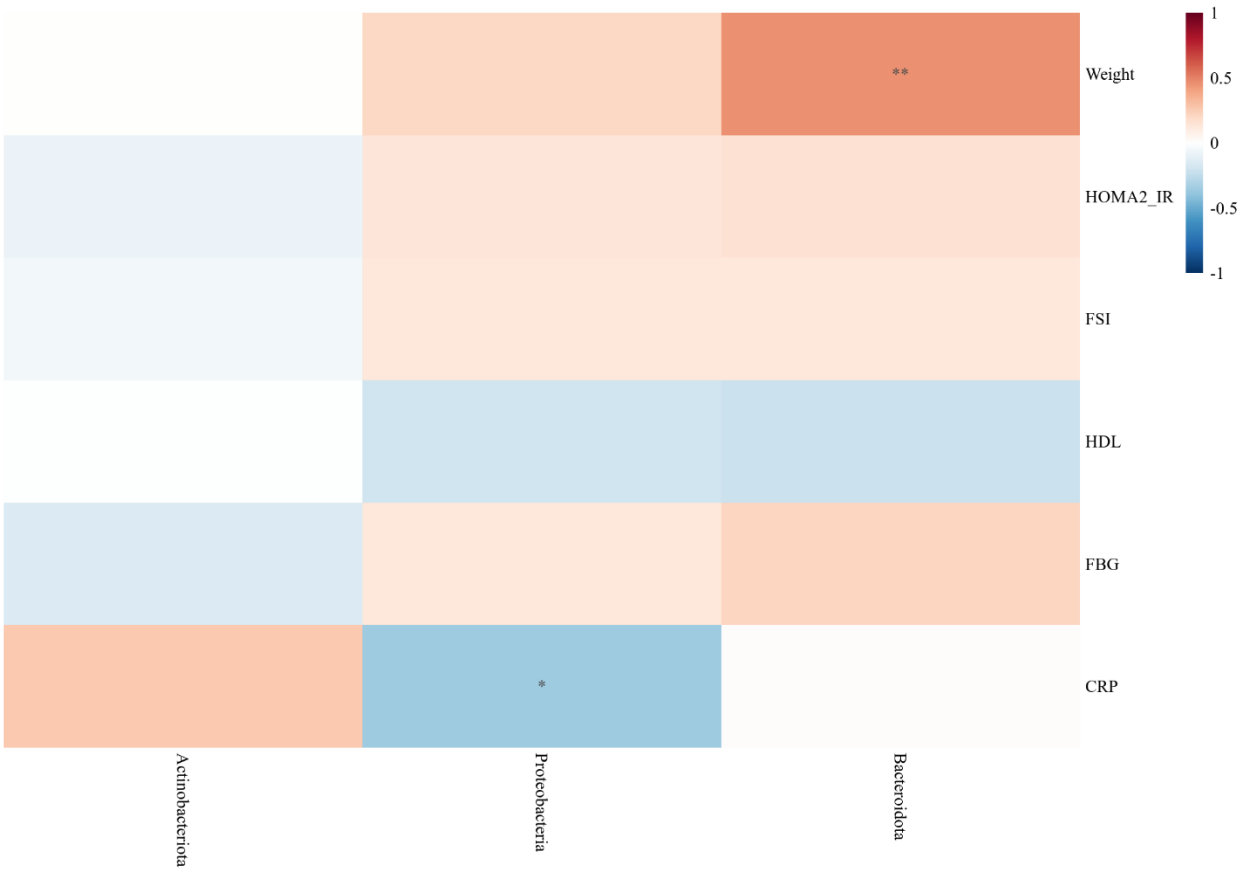

Supplementary Figure 21. Heatmap demonstrating Spearman correlations between differential microbial phlya and clinical parameters at 9 months compared to baseline for sleeve gastrectomy. FBG, fasting blood glucose, FSI; fasting serum insulin; HOMA2-IR, Homeostasis model for the assessment of insulin resistance; LDL low-density lipoprotein; HDL, high-density lipoprotein; TG, triglyceride; TC, total cholesterol; CRP, C-reactive protein.

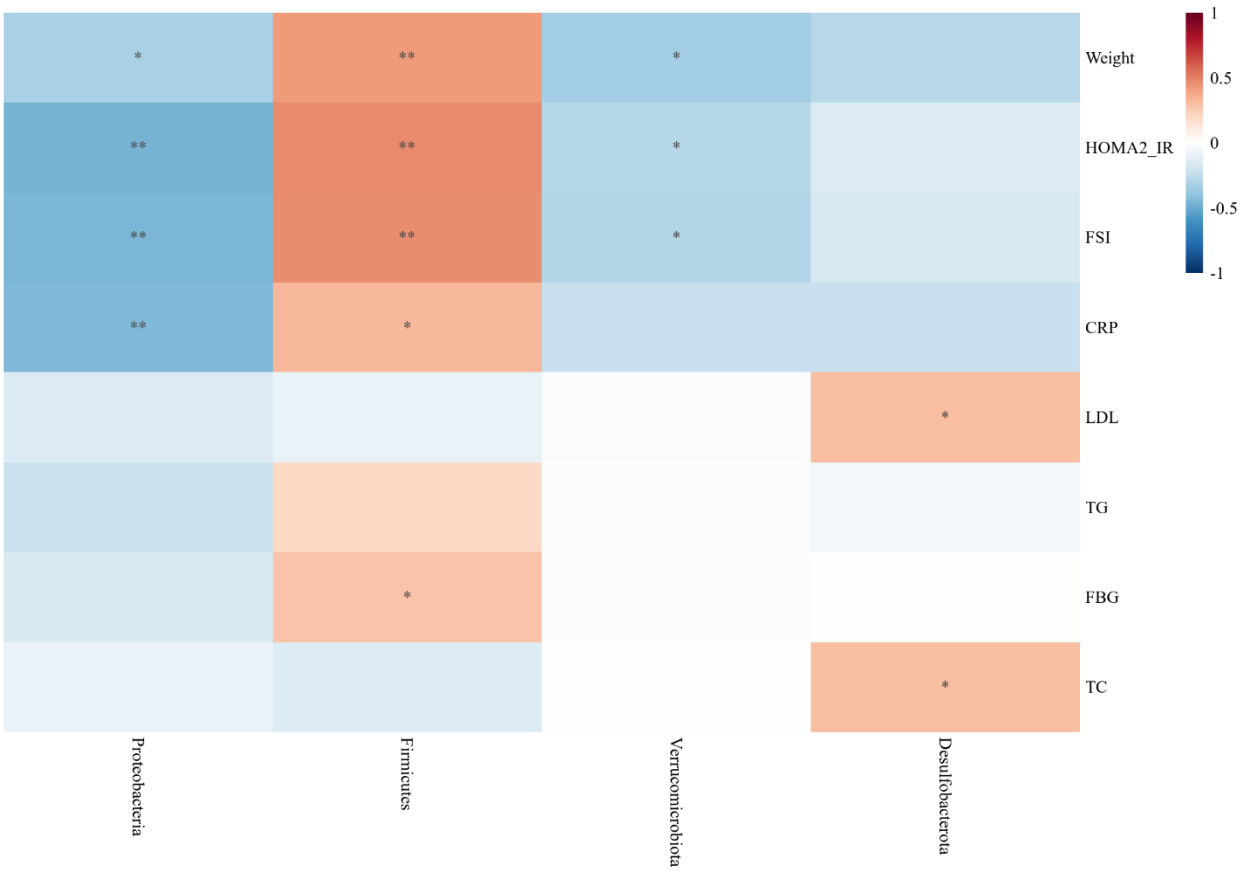

Supplementary Figure 22. Heatmap demonstrating Spearman correlations between differential microbial phlya and clinical parameters at 9 months compared to baseline for Roux-en-Y gastric bypass. FBG, fasting blood glucose, FSI; fasting serum insulin; HOMA2-IR, Homeostasis model for the assessment of insulin resistance; LDL low-density lipoprotein; HDL, high-density lipoprotein; TG, triglyceride; TC, total cholesterol; CRP, C-reactive protein.

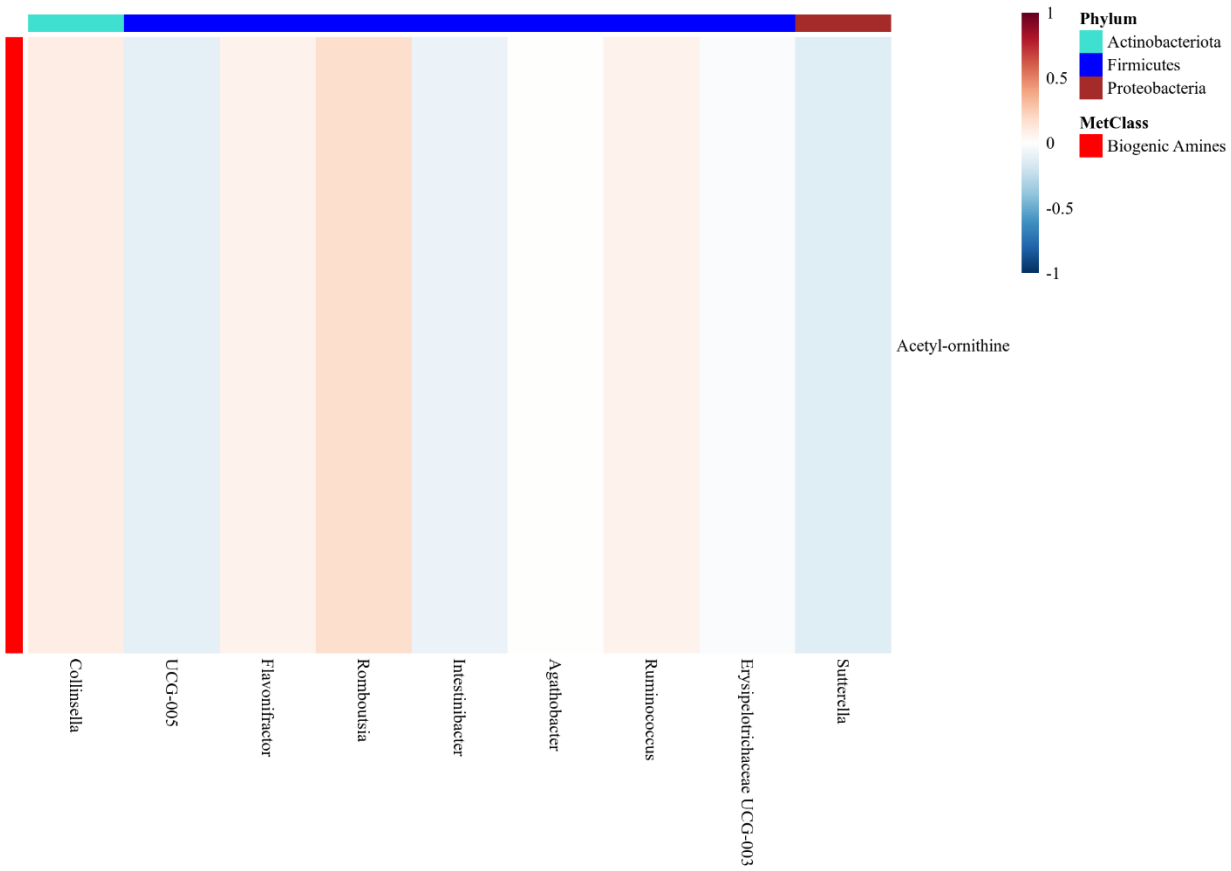

Supplementary Figure 23. Heatmap of Spearman correlations between differential microbes and metabolites at 3 months compared to baseline for non-operative control.

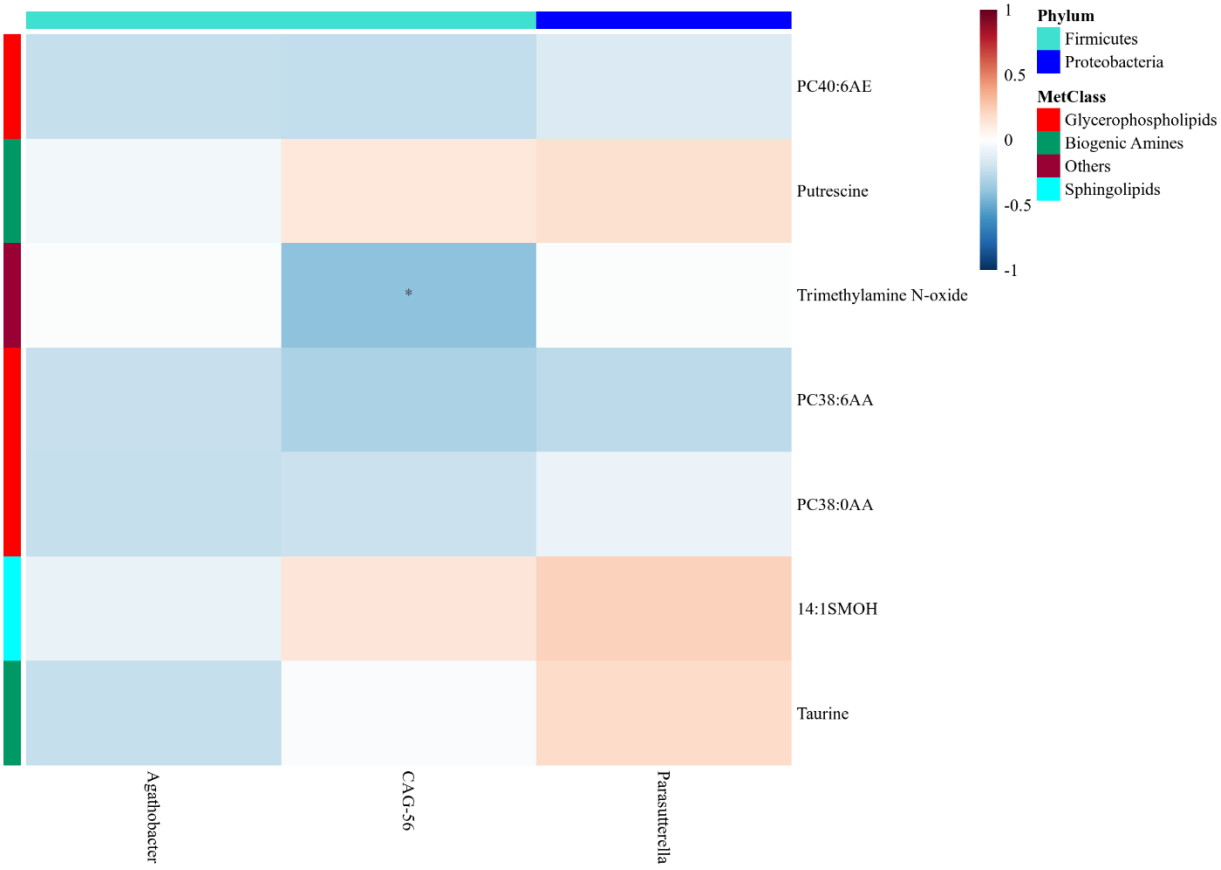

Supplementary Figure 24. Heatmap of Spearman correlations between differential microbes and metabolites at 9 months compared to baseline for non-operative control.

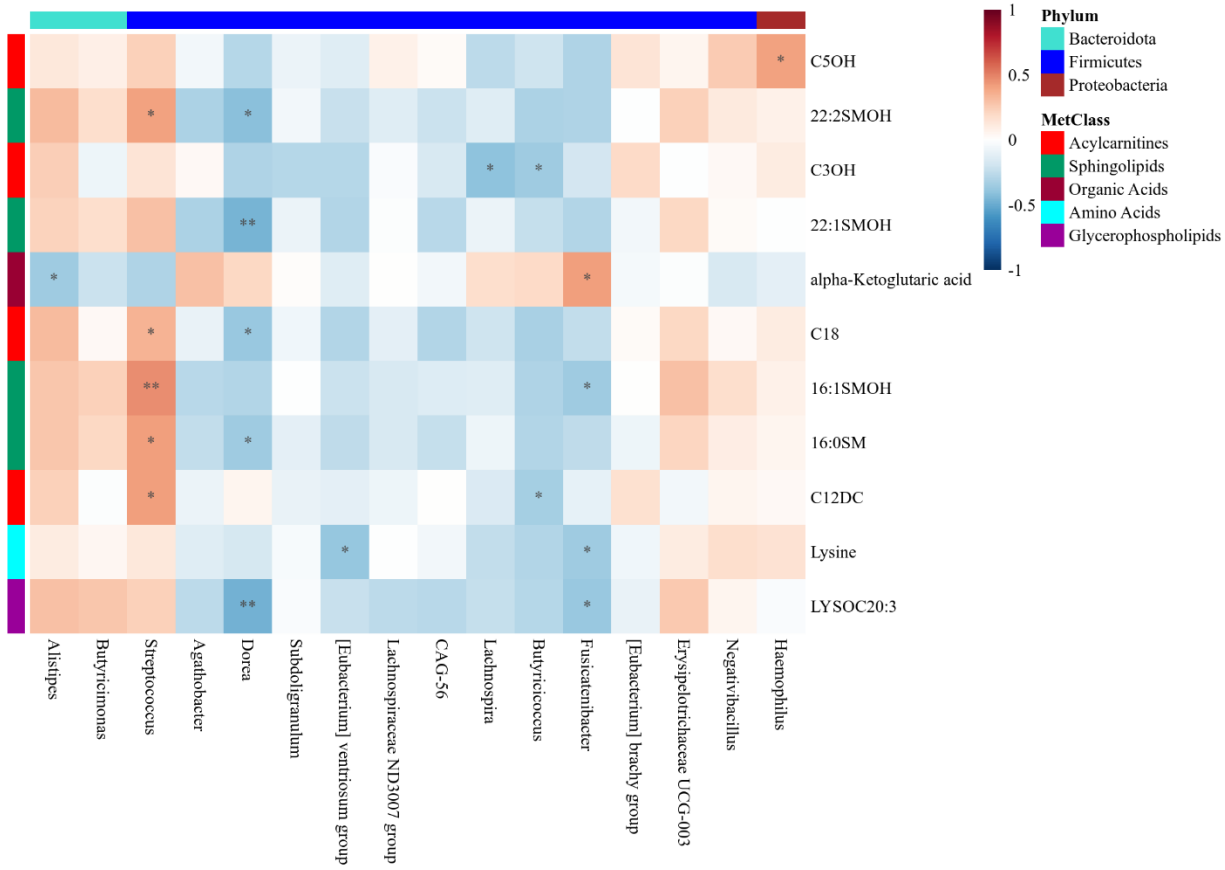

Supplementary Figure 25. Heatmap of Spearman correlations between differential microbes and metabolites at 3 months compared to baseline for sleeve gastrectomy.

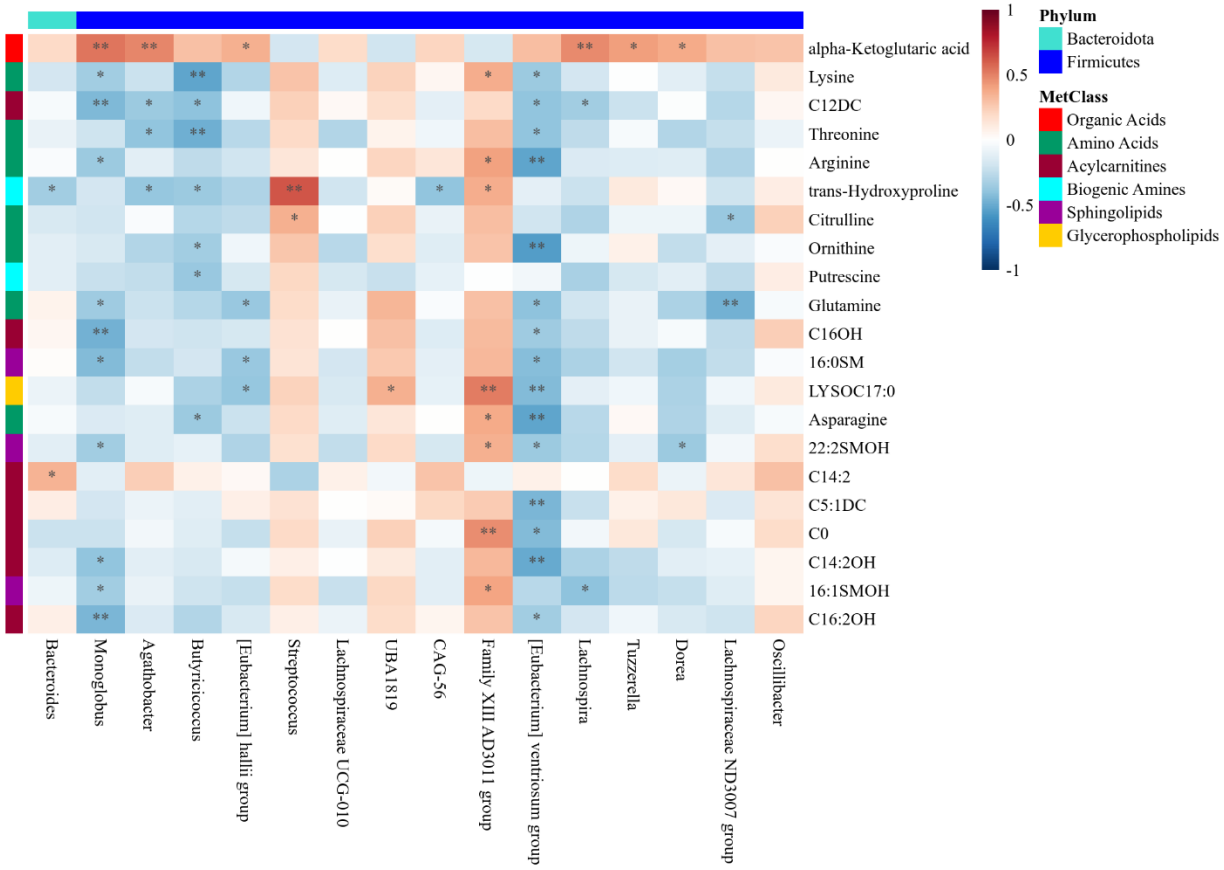

Supplementary Figure 26. Heatmap of Spearman correlations between differential microbes and metabolites at 9 months compared to baseline for sleeve gastrectomy.

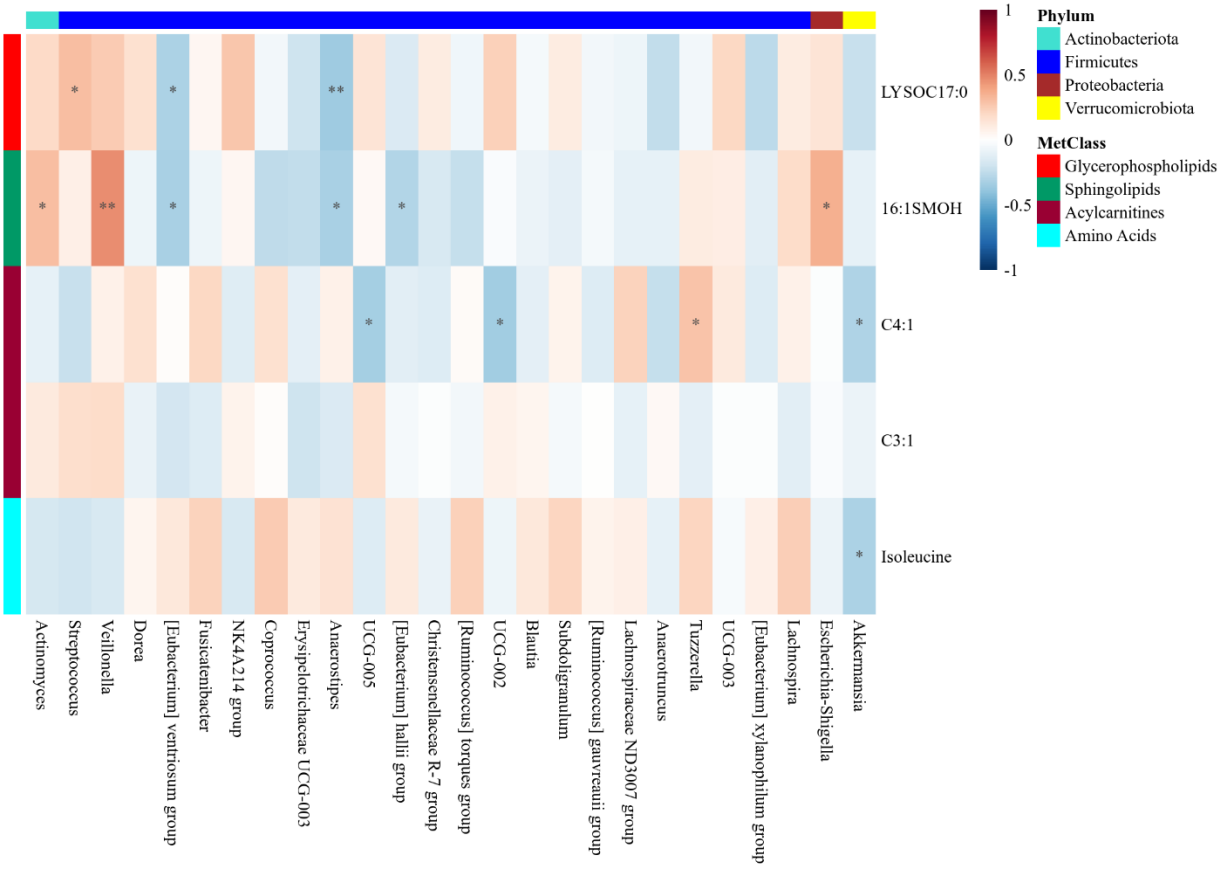

Supplementary Figure 27. Heatmap of Spearman correlations between differential microbes and metabolites at 3 months compared to baseline for Roux-en-Y gastric bypass.

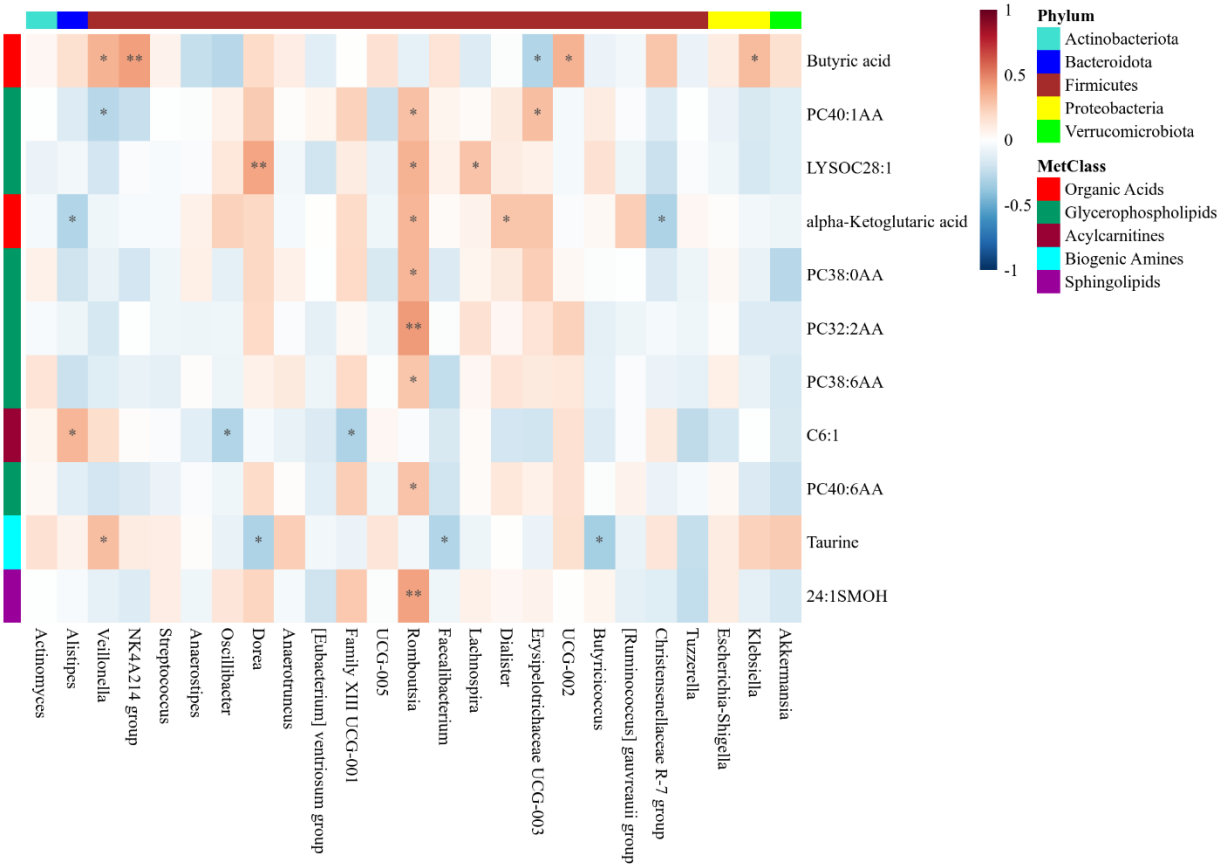

Supplementary Figure 28. Heatmap of Spearman correlations between differential microbes and metabolites at 9 months compared to baseline for Roux-en-Y gastric bypass.

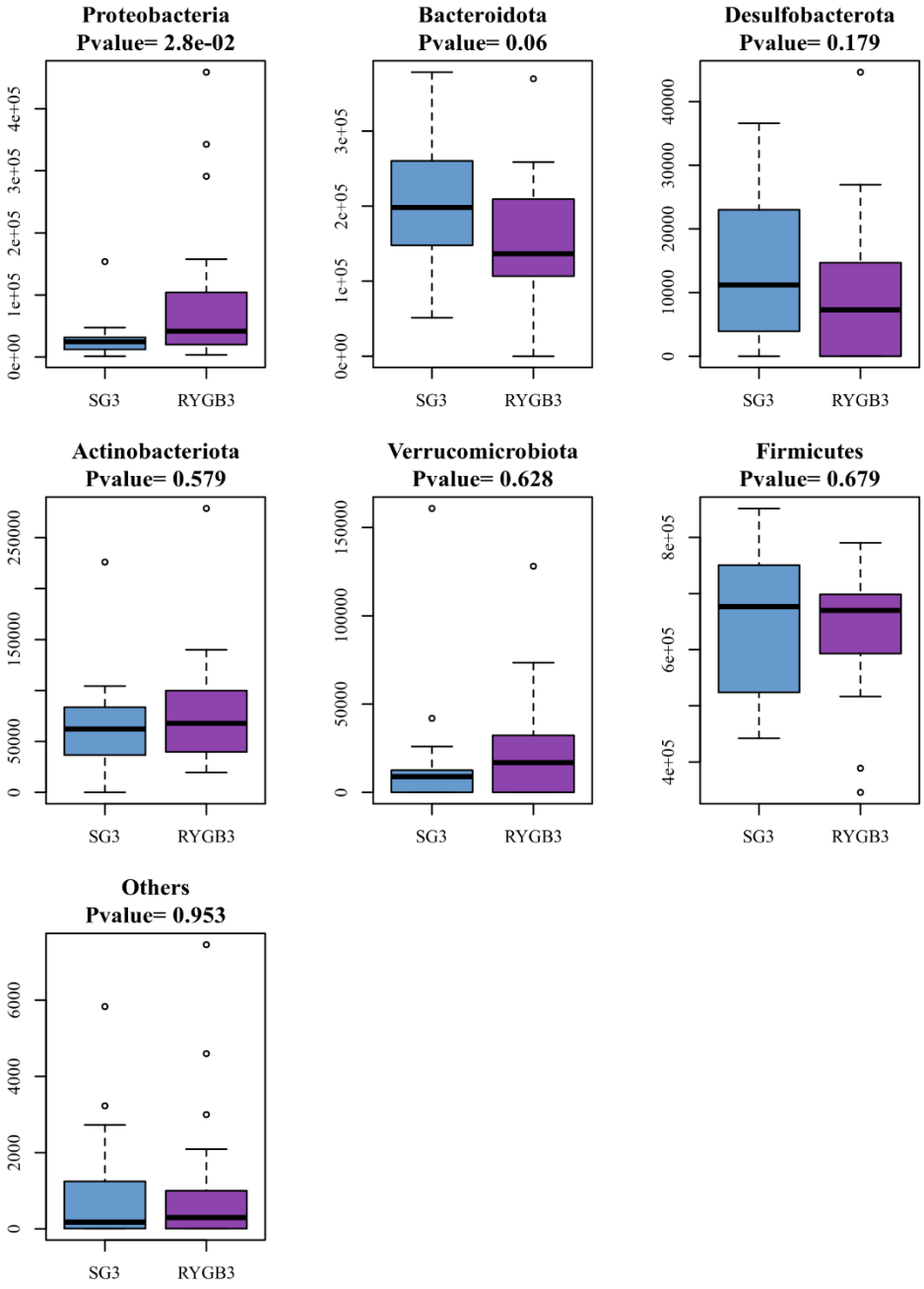

Supplementary Figure 29. Differential microbial taxa on univariate analysis at the phylum level between sleeve gastrectomy and Roux-en-Y gastric bypass at 3 months. Raw, non-corrected p-values are displayed.

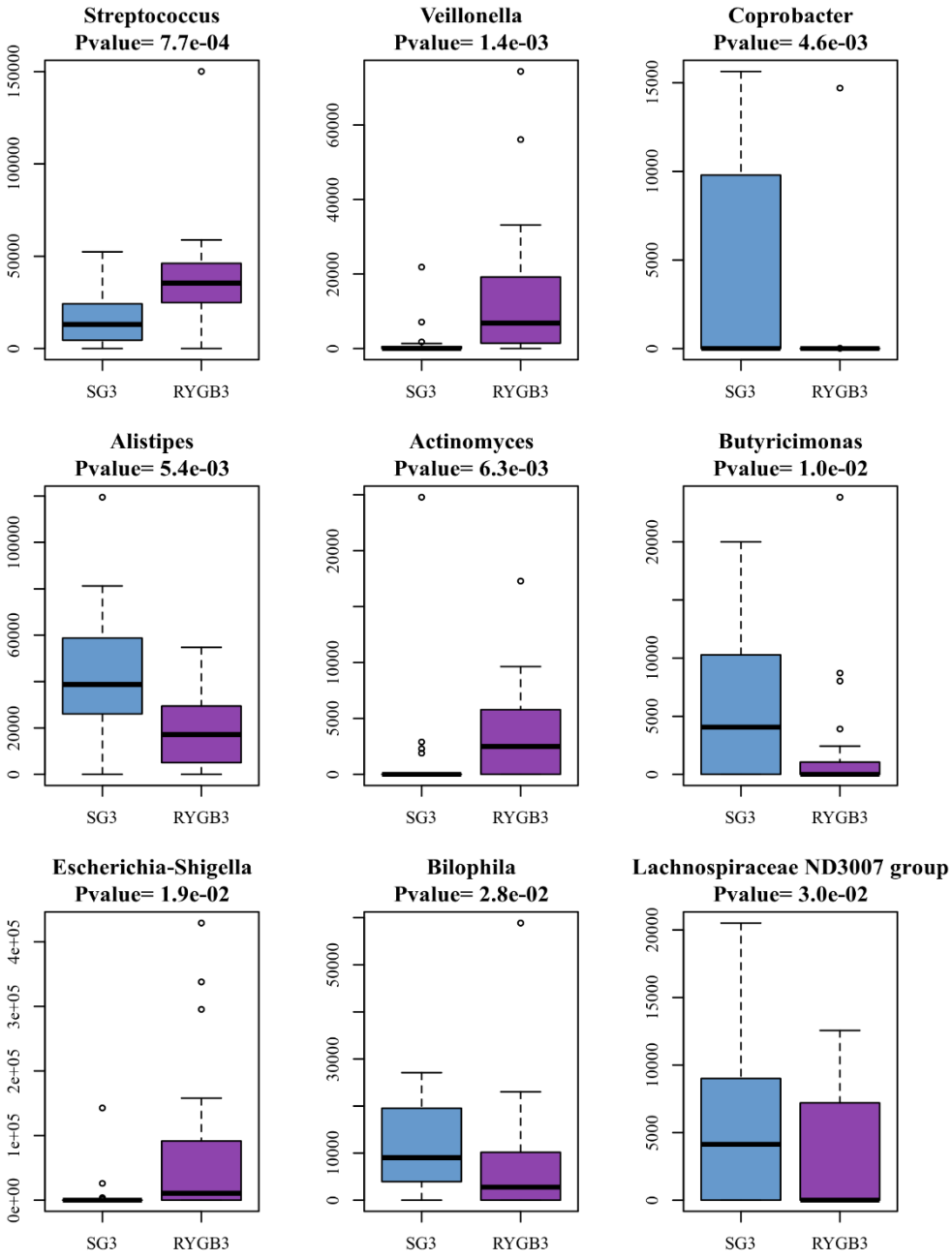

Supplementary Figure 30. Differential microbial taxa on univariate analysis at the genus level between sleeve gastrectomy and Roux-en-Y gastric bypass at 9 months. Raw, non-corrected p-values are displayed.

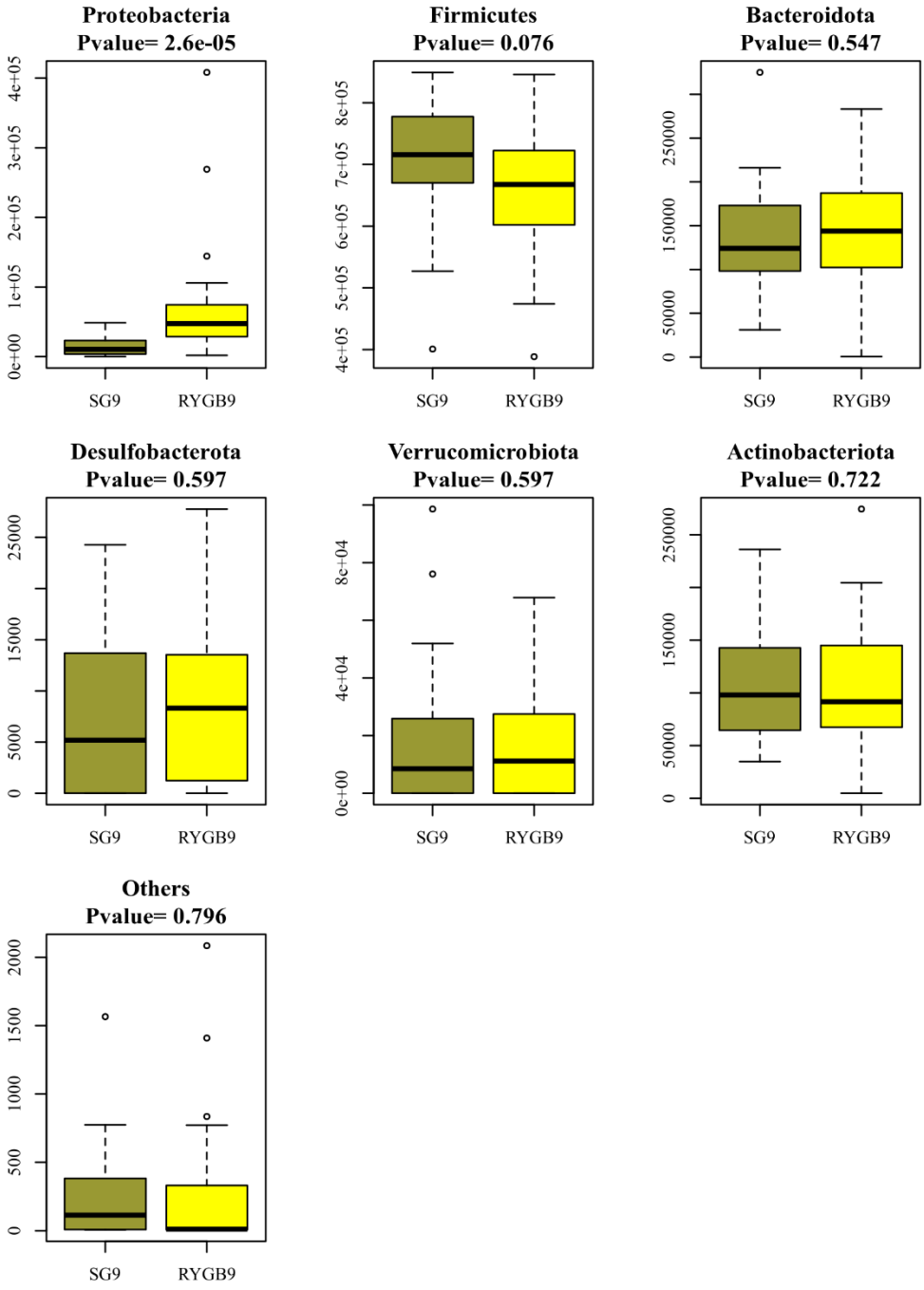

Supplementary Figure 31. Differential microbial taxa on univariate analysis at the phylum level between sleeve gastrectomy and Roux-en-Y gastric bypass at 9 months. Raw, non-corrected p-values are displayed.

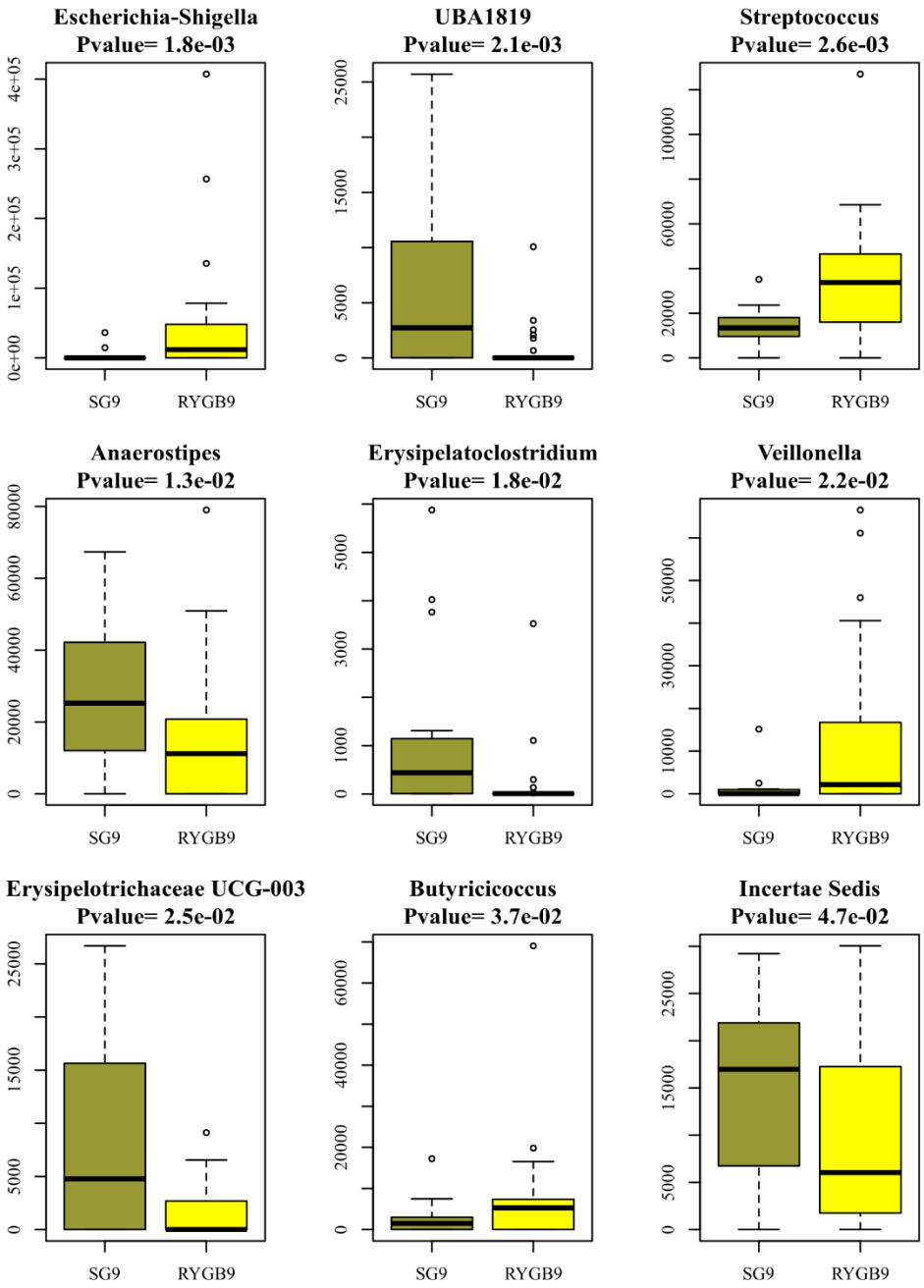

Supplementary Figure 32. Differential microbial taxa on univariate analysis at the genus level between sleeve gastrectomy and Roux-en-Y gastric bypass at 9 months. Raw, non-corrected p-values are displayed.

Supplementary Table 1. Clinical biochemistry results

Blood test mean (sd)	Non-operative controls n = 25			Sleeve gastrectomy n = 18			Roux-en-Y gastric bypass n = 27		
	0 months	3 months	9 months	0 months	3 months	9 months	0 months	3 months	9 months
Hemoglobin (g/L)	139.0 (9.5)	137.6 (8.8)	133.6 (32.6)	134.6 (8.3)	135.9 (8.7)	135.5 (8.2)	140.3 (10.8)	137.8 (10.8)	135.9 (10.5)
White blood cell (10^9/L)	6.8 (1.8)	7.0 (1.7)	6.5 (2.2)	6.0 (1.9)	5.3 (1.0)	5.0 (1.2)	7.4 (2.0)	6.4 (1.9)	5.9 (1.7)
Creatinine (µmol/L)	68.9 (10.6)	71.0 (11.7)	68.9 (13.5)	67.8 (8.9)	69.2 (10.0)	69.5 (9.5)	71.4 (15.1)	65.7 (12.9)	65.6 (13.4)
ALT (U/L)	24.2 (12.6)	25.3 (14.4)	25.4 (13.7)	24.6 (9.1)	28.6 (15.7)	24.8 (11.8)	27.4 (14.1)	22.3 (8.2)	25.3 (12.8)
ALP (U/L)	85.0 (17.7)	86.1 (21.9)	89.3 (26.7)	70.2 (17.)	78.2 (20.9)	72.7 (14.1)	77.7 (18.4)	86.2 (17.7)	93.4 (19.3)
Bilirubin (µmol/L)	9.0 (3.4)	9.3 (3.7)	10.1 (4.7)	9.8 (4.1)	11.3 (4.7)	9.5 (3.1)	10.4 (5.5)	10.9 (4.6)	10.2 (3.7)
Ferritin (µg/L)	101.5 (84.4)	89.4 (79.7)	95.1 (54.5)	74.5 (75.4)	91.8 (61.4)	79.6 (53.0)	103.8 (81.1)	72.7 (70.4)	60 (48.9)
TSH (mU/L)	2.13 (0.97)	2.26 (1.04)	2.00 (0.80)	1.78 (1.16)	1.44 (0.87)	1.81 (1.59)	2.11 (1.01)	1.46 (0.84)	1.65 (0.85)
Free T4 (pmol/L)	14.5 (1.4)	14.8 (1.5)	14.5 (1.2)	15.2 (2.8)	15.1 (3.5)	14.7 (2.2)	14.4 (1.9)	14.9 (2.2)	13.5 (2.9)
Total cholesterol (mmol/L)	4.4 (0.9)	4.5 (0.9)	4.2 (0.8)	4.7 (0.8)	4.6 (0.9)	5.1 (1.1)	4.8 (1.0)	4.2 (1.1)	4.4 (1.1)
Triglycerides (mmol/L)	1.4 (0.6)	1.4 (0.7)	1.2 (0.6)	1.4 (0.9)	1.2 (0.6)	1.2 (0.5)	1..5 (0.7)	1.1 (0.4)	1.0 (0.4)
LDL (mmol/L)	2.5 (0.8)	2.5 (0.8)	2.4 (0.7)	2.7 (0.8)	2.7 (0.8)	3.0 (1.0)	2.8 (0.8)	2.5 (0.9)	2.5 (0.8)
HDL (mmol/L)	1.2 (0.3)	1.3 (0.3)	1.2 (0.3)	1.4 (0.3)	1.4 (0.2)	1.6 (0.3)	1.3 (0.3)	1.2 (0.3)	1.5 (0.4)
Non-HDL (mmol/L)	3.2 (0.8)	3.2 (0.8)	3.0 (0.7)	3.3 (0.8)	3.3 (0.9)	3.5 (1.0)	3.5 90.9)	3.0 (1.0)	2.9 (1.0)
Fasting blood glucose (mmol/L)	5.4 (0.6)	5.5 (0.9)	5.4 (0.9)	5.4 (1.1)	4.9 (0.4)	4.8 (0.3)	5.5 (0.8)	5.1 (0.4)	5.0 (0.6)
Hemoglobin A1c (%)	5.6 (0.3)	5.7 (0.4)	5.6 (0.5)	5.8 (0.5)	5.5 (0.3)	5.5 (0.2)	5.7 (0.8)	5.4 (0.4)	5.3 (0.4)
Insulin (pmol/L)	198.6 (167.3)	191.6 (150.0)	159.8 (97.2)	113.3 (50.5)	66.5 (47.9)	50.4 (18.8)	115.8 (51.3)	64.4 (23.4)	44.4 (14.7)

Supplementary Table 2. C-reactive protein, lipopolysaccharide, and inflammatory cytokines

Blood test mean (sd)	Non-operative controls n = 25			Sleeve gastrectomy n = 18			Roux-en-Y gastric bypass n = 27		
	0 months	3 months	9 months	0 months	3 months	9 months	0 months	3 months	9 months
C-reactive protein (mg/L)	11.2 (9.4)	11.1 (7.7)	16.6 (25.5)	6.0 (6.1)	4.4 (5.9)	3.5 (4.6)	9.5 (6.8)	4.0 (5.4)	2.5 (3.9)
Lipopolysaccharide (EU/mL)	2.4 (2.1)	2.0 (1.5)	2.9 (4.0)	1.6 (0.7)	1.4 (0.7)	1.7 (1.0)	1.7 (1.2)	1.5 (0.7)	1.9 (1.2)
IL-1β (pg/mL)	36.2 (104.1)	44.8 (106.8)	52.8 (151.9)	72.0 (179.4)	81.3 (215.1)	112.4 (224.2)	94.6 (202.0)	143.0 (245.1)	118.6 (221.9)
IL-6 (pg/mL)	41.1 (88.2)	51.4 (103.4)	43.8 (86.4)	87.1 (191.4)	113.4 (214.5)	134.7 (242.8)	83.6 (184.2)	160.1 (300.2)	96.6 (186.1)
IL-8 (pg/mL)	25.7 (56.5)	29.5 (60.3)	32.6 (72.1)	45.7 (85.5)	57.8 (106.9)	105.4 (258.8)	25.5 (46.7)	86.6 (166.3)	48.6 (84.)
IL-10 (pg/mL)	204.0 (415.7)	258.8 (511.5)	261.4 (552.4)	403.5 (718.1)	486.3 (751.0)	632.6 (930.5)	387.3 (680.7)	504.5 (802.8)	577.5 (917.3)
TNF-α (pg/mL)	6.0 (1.2)	6.2 (1.4)	5.9 (1.6)	6.2 (1.5)	7.3 (4.7)	7.3 (4.4)	21.5 (70.1)	44.8 (134.1)	24.8 (79.1)

CHAPTER 5. CONCLUSIONS

Bariatric surgery is an increasingly important modality for the treatment of severe obesity and metabolic syndrome. Despite increasing use of bariatric surgery worldwide, our current understanding of its mechanisms remains poorly understood. In the enclosed thesis, we explored the intestinal physiological changes that occurred with bariatric surgery with a focus on the gut microbiome, metabolome, bile acids, intestinal morphology, gut hormones and L cells.

Increasing evidence supports that bariatric surgery induces complex changes in the gut. Some of the gut hormonal changes that occur after RYGB have been translated into therapeutic strategies including the use of GLP-1, GIP and glucagon. Therefore, it is of vital importance that we study the physiological changes in bariatric surgery to create new targets for the medical treatment of obesity. Additionally, this knowledge may lead to modifications in bariatric surgical techniques, as it is still not known how parameters such as Roux and biliopancreatic limb length or pouch size affect weight and metabolic outcomes.

To answer these questions, we first needed to develop a RYGB surgical model. In Chapter 2, we present a protocol with a published video demonstrating the RYGB procedure in rats. This protocol had excellent survival rates nearing 90% which is higher than comparative protocols. This rat model also had significant weight loss and metabolic effects that are representative of human RYGB.

In Chapter 3, we used this rat model to study the early and late effects of RYGB on the ileum. We found a significant change to intestinal morphology including greater villi height and increased L cell density. There was a dramatic decrease in bile acid concentrations after RYGB. This was correlated with microbial shifts including higher abundances of Escherichia-Shigella and lower abundances of Lactobacillus. Furthermore, Lactobacillus and Escherichia-Shigella were correlated with shifts in conjugated bile acids. Given these findings and supporting studies in the literature, it is highly plausible that these bacterial and bile acid shifts are contributing to the proliferation of L cells leading to improved glucose tolerance.

Lastly, in Chapter 4, we conducted a prospective three-arm clinical trial to study the microbial, metabolomic, and inflammatory changes that occur after RYGB, SG, and CTRL. We conducted integrated microbial-metabolomic analysis which revealed three unique pathways. In RYGB, there was a decrease in the abundance of Romboutsia which was tied to decreases in glycerophospholipids and this was further correlated with lower weight and lower insulin resistance.

In SG, there was enrichment of the aminoacyl-tRNA biosynthesis pathway, which was enriched in both the microbiome and metabolome. A decrease in a specific cluster of Firmicutes (*Butyriciccocus*, *Eubacterium ventriosum* and *Monoglobus*) appeared to drive an increase in five amino acids (arginine, asparagine, lysine, glutamine, threonine) which contributed to this pathway. The loss of this cluster of Firmicutes was correlated with lower weight, decreased

insulin resistance, and decreased systemic inflammation. This appears to be a significant pathway in which SG acts on the gut bacteria to enrich a metabolically beneficial pathway.

When comparing SG to RYGB, the SG cohort had an enriched sphingolipid metabolism pathway. The loss of five Firmicutes genera (*Monoglobus*, *Eubacterium ventriosum*, *Eubacterium hallii*, *Dorea*, and *Lachnospira*) were closely correlated to an increase in sphingomyelins and hydroxysphingomyelins. The loss of these five Firmicutes genera was also linked to improved glucose tolerance. This appears to be a pathway in which SG, but not RYGB, improved glucose homeostasis.

Taken together, these studies contribute to the growing evidence of the complex intestinal physiological changes that occur with bariatric surgery. The early explanations for the effects of RYGB and SG were thought to be strictly malabsorptive or restrictive, but as more research is being conducted, the physiological changes that occur become more complex. However, targeted therapies that go beyond bariatric surgery are needed to better control the obesity epidemic. Future studies are needed to clarify the pathways identified in this thesis and to potentially create non-surgical therapies to induce similar changes to bariatric surgery. These include targeting specific microbial change through prebiotics, probiotics and fecal microbial transplant. There is also potential for combinations of therapies to also target the reduction of bile acids, possibly by using bile acid sequestrants such as colesevelam. Additional targets include dietary changes to increase amino acids to enrich the aa-tRNA biosynthesis pathway, decrease glycerophospholipids or to increase the sphingolipid metabolism pathway.

In summary, this body of work identified various microbial-metabolomic pathways including bile acids, glycerophospholipids, amino acids, and sphingolipids in which SG and RYGB induce weight loss and improved glucose metabolism. Translational work building upon these findings by targeting and inducing shifts in microbial, metabolomic, or bile acid composition may lead to novel therapeutic options to treat obesity and its associated metabolic diseases.

5.1 FUTURE DIRECTIONS

Future directions include study into the mechanisms responsible for the pathways identified in this thesis and translational work targeting these pathways for the treatment of obesity and metabolic disease. These include studies targeted at the gut microbiota, sphingolipids, amino acids, glycerophospholipids, and bile acids.

The microbial changes identified in this research were reductions in abundances of bacteria and this makes translational research difficult. This precludes the use of probiotics to induce increases in specific bacterial groups. However, our study identified that decreases in Firmicutes genera were responsible for many of the positive effects of bariatric surgery. Previous studies have demonstrated that dietary fibers can decrease the abundance of Firmicutes species in the gut. One study using dietary fibers derived from potato starch demonstrated decreased abundances of Firmicutes with the potential to prevent obesity in children[268]. Studies on supplementing patients with diets such as these, especially in conjunction with bariatric surgery, may improve obesity and metabolic outcomes.

Sphingolipid metabolism, another potential target identified in this thesis, can also be modified by constituents of diet[269]. For example, Norris et al. demonstrated that dietary sphingomyelins reduced hepatic steatosis and adipose tissue inflammation with differential effects between egg and milk sphingomyelins. Future studies enriching our understanding of relationships between sphingomyelins, the gut microbiome, and obesity could potentially lead to targeted therapies utilizing sphingolipid metabolism pathways.

There is emerging evidence that high protein intake can enrich the aa-tRNA pathway. Durainayagam et al. performed a randomized study on elderly males receiving the recommended intake of proteins compared to two-times the recommended intake of dietary protein and found that higher protein intake enriched the aa-tRNA biosynthesis pathway[270]. Studying relationships between protein intake, the gut microbiome, and obesity could potentially strengthen our understanding of mechanisms and produce targeted therapies using the aa-tRNA pathway.

Dietary glycerophospholipids come from soybean, egg yolk, milk, and marine life. A double-blinded, randomized trial conducted by Weiland et al. demonstrated that dietary milk phospholipids reduced waist circumference and attenuated γ-glutamyl transferase (GGT), a marker of fatty liver disease, compared to control. Additionally, soybean phospholipids had no metabolic effect when compared to milk phospholipids[271]. This study emphasizes that different phospholipid preparations can have varying effects on obesity. A study on different glycerophospholipids preparations, the gut microbiome, and obesity would be important to understand these mechanisms.

Finally, bile acids play a key role in the effects of bariatric surgery. There are multiple studies demonstrating that longer biliopancreatic limb length increases weight loss and improves diabetic outcomes after RYGB[272]. However, most of these studies do not control for the associated decrease in common channel length that occurs due to the increase in biliopancreatic limb length and this likely contributes to these effects. Despite this, one theory is that longer biliopancreatic limbs lead to greater bacterial overgrowth which consequently increases bile acid deconjugation in that limb. This increase in deconjugation leads to increased bile acid reabsorption in the intestine with resultant changes in bile acid signaling to enteroendocrine cells, causing changes in the secretion gut hormones such as GLP-1. Future animal studies directed at varying biliopancreatic limb lengths after RYGB and determining their effects on the intestinal microbiota and bile acids, would increase our understanding of the mechanisms behind RYGB and potentially modify how surgeons perform RYGB in the future.

REFERENCES

1. World Health Organization. Obesity and Overweight. http://www.who.int/news-room/fact-sheets/detail/obesity-and-overweight (2018).

2. Peeters, A. *et al.* Obesity in Adulthood and Its Consequences for Life Expectancy: A Life-Table Analysis. *Ann. Intern. Med.* **138**, 24 (2003).

3. Aune, D. *et al.* BMI and all cause mortality: systematic review and non-linear dose-response meta-analysis of 230 cohort studies with 3.74 million deaths among 30.3 million participants. *BMJ* i2156 (2016) doi:10.1136/bmj.i2156.

4. Haslam, D. W. & James, W. P. T. Obesity. *Lancet (London, England)* **366**, 1197–209 (2005).

5. Wang, Y. C., McPherson, K., Marsh, T., Gortmaker, S. L. & Brown, M. Health and economic burden of the projected obesity trends in the USA and the UK. *Lancet (London, England)* **378**, 815–25 (2011).

6. Stewart, S. T., Cutler, D. M. & Rosen, A. B. Forecasting the Effects of Obesity and Smoking on U.S. Life Expectancy. *N. Engl. J. Med.* **361**, 2252–2260 (2009).

7. Flegal, K. M., Kit, B. K., Orpana, H. & Graubard, B. I. Association of All-Cause Mortality With Overweight and Obesity Using Standard Body Mass Index Categories. *JAMA* **309**, 71 (2013).

8. Poobalan, A. S. *et al.* Long-term weight loss effects on all cause mortality in overweight/obese populations. *Obes. Rev.* **8**, 503–13 (2007).

9. Sjöström, L. Review of the key results from the Swedish Obese Subjects (SOS) trial - a prospective controlled intervention study of bariatric surgery. *J. Intern. Med.* **273**, 219–234 (2013).

10. Knowler, W. C. *et al.* Reduction in the incidence of type 2 diabetes with lifestyle intervention or metformin. *N. Engl. J. Med.* **346**, 393–403 (2002).

11. Diabetes Prevention Program Research Group *et al.* 10-year follow-up of diabetes incidence and weight loss in the Diabetes Prevention Program Outcomes Study. *Lancet (London, England)* **374**, 1677–86 (2009).

12. Horvath, K. *et al.* Long-term effects of weight-reducing interventions in hypertensive patients: systematic review and meta-analysis. *Arch. Intern. Med.* **168**, 571–80 (2008).

13. Bray, G. A., Kim, K. K. & Wilding, J. P. H. Obesity: a chronic relapsing progressive disease process. A position statement of the World Obesity Federation. *Obes. Rev.* **18**, 715–723 (2017).

14. Wharton, S. *et al.* Obesity in adults: A clinical practice guideline. *Cmaj* **192**, E875–E891 (2020).

15. Mann, J. F. E. *et al.* Liraglutide and cardiovascular outcomes in type 2 diabetes. *Drug Ther. Bull.* **54**, 101 (2016).

16. Sjöström, L. *et al.* Effects of bariatric surgery on mortality in Swedish obese subjects. *N. Engl. J. Med.* **357**, 741–752 (2007).

17. Carlsson, L. M. S. *et al.* Bariatric Surgery and Prevention of Type 2 Diabetes in Swedish Obese Subjects. *N. Engl. J. Med.* **367**, 695–704 (2012).

18. Sjöström, L. *et al.* Lifestyle, diabetes, and cardiovascular risk factors 10 years after bariatric surgery. *N. Engl. J. Med.* **351**, 2683–2693 (2004).

19. WHO. WHO | Obesity and overweight. *World Health Organisation Media Centre Fact Sheet No. 311* 1–2 (2012).

20. National Institutes of Health. Classification of Overweight and Obesity by BMI, Waist Circumference, and Associated Disease Risks. https://www.nhlbi.nih.gov/health/educational/lose_wt/BMI/bmi_dis.htm.

21. WHO | Obesity. *WHO*.

22. Finkelstein, E. A., Trogdon, J. G., Cohen, J. W. & Dietz, W. Annual Medical Spending Attributable To Obesity: Payer-And Service-Specific Estimates. *Health Aff.* **28**, w822–w831 (2009).

23. Shea, J. *et al.* The obesity epidemic. *Clin. Chem.* **58**, 968–73 (2012).

24. Galgani, J. & Ravussin, E. Energy metabolism, fuel selection and body weight regulation. *Int. J. Obes.* **32**, S109–S119 (2008).

25. Schwartz, M. W. *et al.* Is the Energy Homeostasis System Inherently Biased Toward Weight Gain?

26. Ley, R. E. Obesity and the human microbiome. *Curr. Opin. Gastroenterol.* **26**, 5–11 (2010).

27. Bray, G. A. & Perreault, L. Obesity in adults: Health consequences. *UpToDate* http://www.uptodate.com (2017).

28. Mauro, M., Taylor, V., Wharton, S. & Sharma, A. M. Barriers to obesity treatment. *Eur. J.*

Intern. Med. **19**, 173–180 (2008).

29. Look AHEAD Research Group *et al.* Cardiovascular effects of intensive lifestyle intervention in type 2 diabetes. *N. Engl. J. Med.* **369**, 145–54 (2013).

30. Moon, R. C. *et al.* Morbidity Rates and Weight Loss After Roux-en-Y Gastric Bypass, Sleeve Gastrectomy, and Adjustable Gastric Banding in Patients Older Than 60 Years old: Which Procedure to Choose? *Obes. Surg.* **26**, 730–6 (2016).

31. Ara, R. *et al.* What is the clinical effectiveness and cost-effectiveness of using drugs in treating obese patients in primary care? A systematic review. *Health Technol. Assess.* **16**, iii–xiv, 1–195 (2012).

32. Heck, A. M., Yanovski, J. A. & Calis, K. A. Orlistat, a new lipase inhibitor for the management of obesity. *Pharmacotherapy* **20**, 270–9 (2000).

33. Astrup, A. *et al.* Effects of liraglutide in the treatment of obesity: a randomised, double-blind, placebo-controlled study. *Lancet (London, England)* **374**, 1606–16 (2009).

34. Bray, G. A. & Ryan, D. H. Medical therapy for the patient with obesity. *Circulation* **125**, 1695–703 (2012).

35. Burguera, B. *et al.* Critical assessment of the current guidelines for the management and treatment of morbidly obese patients. *J. Endocrinol. Invest.* **30**, 844–52 (2007).

36. Mechanick, J. I. *et al.* Clinical practice guidelines for the perioperative nutritional, metabolic, and nonsurgical support of the bariatric surgery patient-2013 update: Cosponsored by american association of clinical endocrinologists, The obesity society, and american society fo. *Obesity* **21**, S1–S27 (2013).

37. NIH conference. Gastrointestinal surgery for severe obesity. Consensus Development Conference Panel. *Ann. Intern. Med.* **115**, 956–61 (1991).

38. Resources for Optimal Care of the Metabolic and Bariatric Surgery Patient 2016. (2016).

39. DeMaria, E. J. *et al.* High failure rate after laparoscopic adjustable silicone gastric banding for treatment of morbid obesity. *Ann. Surg.* **233**, 809–18 (2001).

40. Patrone, V. *et al.* Postoperative Changes in Fecal Bacterial Communities and Fermentation Products in Obese Patients Undergoing Bilio-Intestinal Bypass. *Front. Microbiol.* **7**, 200 (2016).

41. Federico, A. *et al.* Gastrointestinal Hormones, Intestinal Microbiota and Metabolic Homeostasis in Obese Patients: Effect of Bariatric Surgery. *In Vivo* **30**, 321–30 (2016).

42. Angrisani, L. *et al.* Bariatric Surgery Worldwide 2013. *Obes. Surg.* **25**, 1822–1832 (2015).

43. Hess, D. & Hess, D. Biliopancreatic diversion with a duodenal switch. *Obes. Surg.* (1998).

44. Abdemur, A. *et al.* Morphology, localization, and patterns of ghrelin-producing cells in stomachs of a morbidly obese population. *Surg. Laparosc. Endosc. Percutan. Tech.* **24**, 122–6 (2014).

45. Gribble, F. M. & Reimann, F. Function and mechanisms of enteroendocrine cells and gut hormones in metabolism. *Nat. Rev. Endocrinol.* **15**, 226–237 (2019).

46. Yehoshua, R. T. *et al.* Laparoscopic sleeve gastrectomy--volume and pressure assessment. *Obes. Surg.* **18**, 1083–8 (2008).

47. Basso, N. *et al.* First-phase insulin secretion, insulin sensitivity, ghrelin, GLP-1, and PYY changes 72 h after sleeve gastrectomy in obese diabetic patients: the gastric hypothesis.

Surg. Endosc. **25**, 3540–50 (2011).

48. Deitel, M. A brief history of bariatric surgery to the present. *J. Obes. Eat. Disord.* **03**, 90–92 (2017).

49. Elder, K. A. & Wolfe, B. M. Bariatric surgery: a review of procedures and outcomes. *Gastroenterology* **132**, 2253–71 (2007).

50. Lim, R. B. Bariatric procedures for the management of severe obesity: Descriptions. *UpToDate* https://www.uptodate.com/ (2017).

51. Korner, J. *et al.* Effects of Roux-en-Y gastric bypass surgery on fasting and postprandial concentrations of plasma ghrelin, peptide YY, and insulin. *J. Clin. Endocrinol. Metab.* **90**, 359–65 (2005).

52. Cummings, D. E. *et al.* Plasma ghrelin levels after diet-induced weight loss or gastric bypass surgery. *N. Engl. J. Med.* **346**, 1623–30 (2002).

53. Tritos, N. A. *et al.* Serum ghrelin levels in response to glucose load in obese subjects post-gastric bypass surgery. *Obes. Res.* **11**, 919–24 (2003).

54. Jacobsen, S. H. *et al.* Changes in gastrointestinal hormone responses, insulin sensitivity, and beta-cell function within 2 weeks after gastric bypass in non-diabetic subjects. *Obes. Surg.* **22**, 1084–96 (2012).

55. le Roux, C. W. *et al.* Gut Hormones as Mediators of Appetite and Weight Loss After Roux-en-Y Gastric Bypass. *Ann. Surg.* **246**, 780–785 (2007).

56. Dixon, J. B., McPhail, T. & O'Brien, P. E. Minimal reporting requirements for weight loss: Current methods not ideal. *Obes. Surg.* **15**, 1034–1039 (2005).

57. Nelson, D. W., Blair, K. S. & Martin, M. J. Analysis of obesity-related outcomes and bariatric failure rates with the duodenal switch vs gastric bypass for morbid obesity. *Arch. Surg.* **147**, 847–54 (2012).

58. Hutter, M. M. *et al.* First report from the American College of Surgeons Bariatric Surgery Center Network: laparoscopic sleeve gastrectomy has morbidity and effectiveness positioned between the band and the bypass. *Ann. Surg.* **254**, 410–20; discussion 420-2 (2011).

59. Cottam, D. *et al.* Laparoscopic sleeve gastrectomy as an initial weight-loss procedure for high-risk patients with morbid obesity. *Surg. Endosc.* **20**, 859–863 (2006).

60. van Rutte, P. W. J., Smulders, J. F., de Zoete, J. P. & Nienhuijs, S. W. Outcome of sleeve gastrectomy as a primary bariatric procedure. *Br. J. Surg.* **101**, 661–668 (2014).

61. Magro, D. O. *et al.* Long-term Weight Regain after Gastric Bypass: A 5-year Prospective Study. *Obes. Surg.* **18**, 648–651 (2008).

62. Karmali, S. *et al.* Weight Recidivism Post-Bariatric Surgery: A Systematic Review. *Obes. Surg.* **23**, 1922–1933 (2013).

63. Mingrone, G. & Castagneto-Gissey, L. Mechanisms of early improvement / resolution of type 2 diabetes after bariatric surgery. *Diabetes Metab.* **35**, 518–523 (2009).

64. Mingrone, G. *et al.* Bariatric surgery versus conventional medical therapy for type 2 diabetes. *N. Engl. J. Med.* **366**, 1577–1585 (2012).

65. Ikramuddin, S. *et al.* Roux-en-Y Gastric Bypass vs Intensive Medical Management for the Control of Type 2 Diabetes, Hypertension, and Hyperlipidemia. *JAMA - J. Am. Med.*

Assoc. **309**, 2240–2249 (2013).

66. Courcoulas, A. P. *et al.* Three-Year Outcomes of Bariatric Surgery vs Lifestyle Intervention for Type 2 Diabetes Mellitus Treatment. *JAMA Surg.* **15213**, 1–9 (2015).

67. Salminen, P. *et al.* Effect of LSG vs LRYGB on Weight Loss at 5 Years Among Patients With Morbid Obesity. *Jama* **319**, 241 (2018).

68. Peterli, R. *et al.* Effect of Laparoscopic Sleeve Gastrectomy vs Laparoscopic Roux-en-Y Gastric Bypass on Weight Loss in Patients With Morbid Obesity. *Jama* **319**, 255 (2018).

69. Still, C. D. *et al.* Preoperative prediction of type 2 diabetes remission after Roux-en-Y gastric bypass surgery: a retrospective cohort study. *LANCET Diabetes Endocrinol.* **2**, 38–45 (2014).

70. Wilson, P. W. F., D'Agostino, R. B., Sullivan, L., Parise, H. & Kannel, W. B. Overweight and obesity as determinants of cardiovascular risk: the Framingham experience. *Arch. Intern. Med.* **162**, 1867–72 (2002).

71. Anderson, K. M., Castelli, W. P. & Levy, D. Cholesterol and mortality. 30 years of follow-up from the Framingham study. *JAMA* **257**, 2176–80 (1987).

72. Zhang, N. *et al.* Reduction in obesity-related comorbidities: is gastric bypass better than sleeve gastrectomy? *Surg. Endosc.* **27**, 1273–80 (2013).

73. Tishler, P. V, Larkin, E. K., Schluchter, M. D. & Redline, S. Incidence of sleep-disordered breathing in an urban adult population: the relative importance of risk factors in the development of sleep-disordered breathing. *JAMA* **289**, 2230–7 (2003).

74. Smith, P. L., Gold, A. R., Meyers, D. A., Haponik, E. F. & Bleecker, E. R. Weight loss in

mildly to moderately obese patients with obstructive sleep apnea. *Ann. Intern. Med.* **103**, 850–5 (1985).

75. Sarkhosh, K. *et al.* The Impact of Bariatric Surgery on Obstructive Sleep Apnea: A Systematic Review. *Obes. Surg.* **23**, 414–423 (2013).

76. Telem, D., Greenstein, A. J. & Wolfe, B. Medical outcomes following bariatric surgery. *UpToDate* https://www.uptodate.com (2017).

77. Chiu, S., Birch, D. W., Shi, X., Sharma, A. M. & Karmali, S. Effect of sleeve gastrectomy on gastroesophageal reflux disease: a systematic review. *Surg. Obes. Relat. Dis.* **7**, 510–5 (2011).

78. Sjöström, L. *et al.* Bariatric surgery and long-term cardiovascular events. *JAMA* **307**, 56–65 (2012).

79. Sjöström, L. *et al.* Effects of bariatric surgery on cancer incidence in obese patients in Sweden (Swedish Obese Subjects Study): a prospective, controlled intervention trial. *Lancet. Oncol.* **10**, 653–62 (2009).

80. Adams, T. D. *et al.* Cancer incidence and mortality after gastric bypass surgery. *Obesity (Silver Spring).* **17**, 796–802 (2009).

81. Stenberg, E. *et al.* Early Complications After Laparoscopic Gastric Bypass Surgery. *Ann. Surg.* **260**, 1040–1047 (2014).

82. Leivonen, M. K., Juuti, A., Jaser, N. & Mustonen, H. Laparoscopic sleeve gastrectomy in patients over 59 years: early recovery and 12-month follow-up. *Obes. Surg.* **21**, 1180–7 (2011).

83. Longitudinal Assessment of Bariatric Surgery (LABS) Consortium *et al.* Perioperative safety in the longitudinal assessment of bariatric surgery. *N. Engl. J. Med.* **361**, 445–54 (2009).

84. Chen, S. Y., Stem, M., Schweitzer, M. A., Magnuson, T. H. & Lidor, A. O. Assessment of postdischarge complications after bariatric surgery: A National Surgical Quality Improvement Program analysis. *Surgery* **158**, 777–86 (2015).

85. Nielsen, J. B., Pedersen, A. M., Gribsholt, S. B., Svensson, E. & Richelsen, B. Prevalence, severity, and predictors of symptoms of dumping and hypoglycemia after Roux-en-Y gastric bypass. *Surg. Obes. Relat. Dis.* **12**, 1562–1568 (2016).

86. Mathews, D. H., Lawrence, W., Poppell, J. W., Vanamee, P. & Randall, H. T. Change in effective circulating volume during experimental dumping syndrome. *Surgery* **48**, 185–194 (1960).

87. Eisenberg, D., Azagury, D. E., Ghiassi, S., Grover, B. T. & Kim, J. J. ASMBS Position Statement on Postprandial Hyperinsulinemic Hypoglycemia after Bariatric Surgery. *Surg. Obes. Relat. Dis.* **13**, 371–378 (2017).

88. Gebhard, B., Holst, J. J., Biegelmayer, C. & Miholic, J. Postprandial GLP-1, norepinephrine, and reactive hypoglycemia in dumping syndrome. *Dig. Dis. Sci.* **46**, 1915–1923 (2001).

89. Ukleja, A. Dumping Syndrome: pathophysiology and treatment. *Nutr. Clin. Pract.* **20**, 517–525 (2005).

90. Service, G. J. *et al.* Hyperinsulinemic Hypoglycemia with Nesidioblastosis after Gastric-

Bypass Surgery. *N. Engl. J. Med.* **353**, 249–254 (2005).

91. Rumilla, K. M. *et al.* Hyperinsulinemic hypoglycemia with nesidioblastosis: Histologic features and growth factor expression. *Mod. Pathol.* **22**, 239–245 (2009).

92. Patti, M. E. *et al.* Severe hypoglycaemia post-gastric bypass requiring partial pancreatectomy: Evidence for inappropriate insulin secretion and pancreatic islet hyperplasia. *Diabetologia* **48**, 2236–2240 (2005).

93. Lee, C. J. *et al.* Hormonal response to a mixed-meal challenge after reversal of gastric bypass for hypoglycemia. *J. Clin. Endocrinol. Metab.* **98**, 1–5 (2013).

94. Muskiet, M. H. A. *et al.* GLP-1 and the kidney: From physiology to pharmacology and outcomes in diabetes. *Nat. Rev. Nephrol.* **13**, 605–628 (2017).

95. Umeda, L. M. *et al.* Early improvement in glycemic control after bariatric surgery and its relationships with insulin, GLP-1, and glucagon secretion in type 2 diabetic patients. *Obes. Surg.* **21**, 896–901 (2011).

96. Yoon, H. S. *et al.* Akkermansia muciniphila secretes a glucagon-like peptide-1-inducing protein that improves glucose homeostasis and ameliorates metabolic disease in mice. *Nat. Microbiol.* **6**, (2021).

97. Nauck, M. *et al.* Efficacy and safety comparison of liraglutide, glimepiride, and placebo, all in combination with metformin, in type 2 diabetes. *Diabetes Care* **32**, 84–90 (2009).

98. Astrup, A. *et al.* Effects of liraglutide in the treatment of obesity: a randomised, double-blind, placebo-controlled study. *Lancet* **374**, 1606–1616 (2009).

99. Kushner, R. F. *et al.* Semaglutide 2.4 mg for the Treatment of Obesity: Key Elements of

the STEP Trials 1 to 5. *Obesity* **28**, 1050–1061 (2020).

100. Frías, J. P. *et al.* Tirzepatide versus Semaglutide Once Weekly in Patients with Type 2 Diabetes. *N. Engl. J. Med.* **0**, null.

101. Finan, B. *et al.* A rationally designed monomeric peptide triagonist corrects obesity and diabetes in rodents. *Nat. Med.* **21**, 27–36 (2015).

102. Wahlström, A., Sayin, S. I., Marschall, H. U. & Bäckhed, F. Intestinal Crosstalk between Bile Acids and Microbiota and Its Impact on Host Metabolism. *Cell Metab.* **24**, 41–50 (2016).

103. Sayin, S. I. *et al.* Gut microbiota regulates bile acid metabolism by reducing the levels of tauro-beta-muricholic acid, a naturally occurring FXR antagonist. *Cell Metab.* **17**, 225–235 (2013).

104. Selwyn, F. P., Csanaky, I. L., Zhang, Y. & Klaassen, C. D. Special section on drug metabolism and the microbiome: Importance of large intestine in regulating bile acids and glucagon-like peptide-1 in germ-free mice. *Drug Metab. Dispos.* **43**, 1544–1556 (2015).

105. Sinal, C. J. *et al.* Targeted disruption of the nuclear receptor FXR/BAR impairs bile acid and lipid homeostasis. *Cell* **102**, 731–744 (2000).

106. Lefebvre, P., Cariou, B., Lien, F., Kuipers, F. & Staels, B. Role of bile acids and bile acid receptors in metabolic regulation. *Physiol. Rev.* **89**, 147–191 (2009).

107. Trabelsi, M.-S. *et al.* Farnesoid X receptor inhibits glucagon-like peptide-1 production by enteroendocrine L cells. *Nat. Commun.* **6**, 7629 (2015).

108. Lund, M. L. *et al.* L-cell differentiation is induced by bile acids through GpBAR1 and

paracrine GLP-1 and serotonin signaling. *Diabetes* **69**, 614–623 (2020).

109. Potthoff, M. J. *et al.* Colesevelam suppresses hepatic glycogenolysis by TGR5-mediated induction of GLP-1 action in DIO mice. *Am. J. Physiol. - Gastrointest. Liver Physiol.* **304**, 371–380 (2013).

110. Harach, T. *et al.* TGR5 potentiates GLP-1 secretion in response to anionic exchange resins. *Sci. Rep.* **2**, 2–8 (2012).

111. Kaur, A. *et al.* Loss of Cyp8b1 improves glucose homeostasis by increasing GLP-1. *Diabetes* **64**, 1168–1179 (2015).

112. Li, F. *et al.* Microbiome remodelling leads to inhibition of intestinal farnesoid X receptor signalling and decreased obesity. *Nat. Commun.* **4**, (2013).

113. The human gut microbiome: current knowledge, challenges, and future directions. *Transl. Res.* **160**, 246–257 (2012).

114. Ecological and Evolutionary Forces Shaping Microbial Diversity in the Human Intestine. *Cell* **124**, 837–848 (2006).

115. Turnbaugh, P. J. *et al.* The human microbiome project. *Nature* **449**, 804–10 (2007).

116. NIH HMP Working Group, T. N. H. W. *et al.* The NIH Human Microbiome Project. *Genome Res.* **19**, 2317–23 (2009).

117. Moore, W. E. & Holdeman, L. V. Human fecal flora: the normal flora of 20 Japanese-Hawaiians. *Appl. Microbiol.* **27**, 961–79 (1974).

118. Morgan, X. C. & Huttenhower, C. Chapter 12: Human Microbiome Analysis. *PLoS Comput. Biol.* **8**, e1002808 (2012).

119. Woese, C. R. & Fox, G. E. Phylogenetic structure of the prokaryotic domain: the primary kingdoms. *Proc. Natl. Acad. Sci. U. S. A.* **74**, 5088–90 (1977).

120. Nocker, A., Burr, M. & Camper, A. K. Genotypic Microbial Community Profiling: A Critical Technical Review. *Microb. Ecol.* **54**, 276–289 (2007).

121. Cole, J. R. *et al.* The ribosomal database project (RDP-II): introducing myRDP space and quality controlled public data. *Nucleic Acids Res.* **35**, D169–D172 (2007).

122. DeLong, E. F., Pace, N. R. & Kane, M. Environmental Diversity of Bacteria and Archaea. *Syst. Biol.* **50**, 470–478 (2001).

123. Tilg, H. & Kaser, A. Gut microbiome, obesity, and metabolic dysfunction. *J. Clin. Invest.* **121**, 2126–2132 (2011).

124. Ley, R. E. *et al.* Obesity alters gut microbial ecology. *Proc. Natl. Acad. Sci.* **102**, 11070–11075 (2005).

125. Turnbaugh, P. J. *et al.* An obesity-associated gut microbiome with increased capacity for energy harvest. *Nature* **444**, 1027–1031 (2006).

126. Ley, R. E., Turnbaugh, P. J., Klein, S. & Gordon, J. I. Microbial ecology: Human gut microbes associated with obesity. *Nature* **444**, 1022–1023 (2006).

127. Turnbaugh, P. J. *et al.* A core gut microbiome in obese and lean twins. *Nature* **457**, 480–4 (2009).

128. Maruvada, P., Leone, V., Kaplan, L. M. & Chang, E. B. The Human Microbiome and Obesity: Moving beyond Associations. *Cell Host Microbe* **22**, 589–599 (2017).

129. Sze, M. A., Schloss, P. D. & Arbor, A. Looking for a Signal in the Noise : Revisiting

Obesity and the Microbiome. (2016).

130. Mehal, W. Z. The Gordian knot of dysbiosis , obesity and The Gordian Knot of dysbiosis , obesity and NAFLD. *Nat. Publ. Gr.* **10**, 637–644 (2013).

131. Chassaing, B. *et al.* Dietary emulsifiers impact the mouse gut microbiota promoting colitis and metabolic syndrome. *Nature* **519**, 92–96 (2015).

132. Hotamisligil, G. S. *et al.* IRS-1-mediated inhibition of insulin receptor tyrosine kinase activity in TNF-alpha- and obesity-induced insulin resistance. *Science* **271**, 665–8 (1996).

133. Cani, P. D. *et al.* Metabolic endotoxemia initiates obesity and insulin resistance. *Diabetes* **56**, 1761–72 (2007).

134. Ghoshal, S., Witta, J., Zhong, J., de Villiers, W. & Eckhardt, E. Chylomicrons promote intestinal absorption of lipopolysaccharides. *J. Lipid Res.* **50**, 90–7 (2009).

135. Cani, P. D. *et al.* Changes in Gut Microbiota Control Metabolic Endotoxemia-Induced Inflammation in High-Fat Diet–Induced Obesity and Diabetes in Mice. *Diabetes* **57**, 1470 LP – 1481 (2008).

136. Amar, J. *et al.* Energy intake is associated with endotoxemia in apparently healthy men. *Am. J. Clin. Nutr.* **87**, 1219–23 (2008).

137. Creely, S. J. *et al.* Lipopolysaccharide activates an innate immune system response in human adipose tissue in obesity and type 2 diabetes. *AJP Endocrinol. Metab.* **292**, E740–E747 (2006).

138. Reinhardt, C., Reigstad, C. S. & Bäckhed, F. Intestinal Microbiota During Infancy and Its Implications for Obesity. *J. Pediatr. Gastroenterol. Nutr.* **48**, 249–256 (2009).

139. Cani, P. D., Hoste, S., Guiot, Y. & Delzenne, N. M. Dietary non-digestible carbohydrates promote L-cell differentiation in the proximal colon of rats. *Br. J. Nutr.* **98**, 32 (2007).

140. Samuel, B. S. *et al.* Effects of the gut microbiota on host adiposity are modulated by the short-chain fatty-acid binding G protein-coupled receptor, Gpr41. *Proc. Natl. Acad. Sci. U. S. A.* **105**, 16767–72 (2008).

141. Le Roux, C. W. & Bloom, S. R. Editorial: Why do patients lose weight after Roux-en-Y gastric bypass? *J. Clin. Endocrinol. Metab.* **90**, 591–592 (2005).

142. Miras, A. D. & le Roux, C. W. Mechanisms underlying weight loss after bariatric surgery. *Nat Rev Gastroenterol Hepatol* **10**, 575–584 (2013).

143. Zhang, H. *et al.* Human gut microbiota in obesity and after gastric bypass. *Proc. Natl. Acad. Sci. U. S. A.* **106**, 2365–70 (2009).

144. Ling-Chun Kong Judith Aron-Wisnewsky, Veronique Pelloux, Arnaud Basdevant, Jean-Luc Bouillot, J. T. & Jean-Daniel Zucker and Karine Cle´ment, J. D. Gut microbiota after gastric bypass in human obesity:\rincreased richness and associations of bacterial genera\rwith adipose tissue genes. *Am. Soc. Nutr.* **98**, 16–24 (2013).

145. Graessler, J. *et al.* Metagenomic sequencing of the human gut microbiome before and after bariatric surgery in obese patients with type 2 diabetes: correlation with inflammatory and metabolic parameters. *Pharmacogenomics J.* **13**, 514–522 (2013).

146. Tremaroli, V. *et al.* Roux-en-Y Gastric Bypass and Vertical Banded Gastroplasty Induce Long-Term Changes on the Human Gut Microbiome Contributing to Fat Mass Regulation. *Cell Metab.* **22**, 228–238 (2015).

147. Furet, J.-P. *et al.* Differential adaptation of human gut microbiota to bariatric surgery--induced weight loss links with metabolic and low-grade inflammation markers. *Diabetes* **59**, 3049–3057 (2010).

148. Kong, L. C. *et al.* Gut microbiota after gastric bypass in human obesity: Increased richness and associations of bacterial genera with adipose tissue genes. *Am. J. Clin. Nutr.* **98**, 16–24 (2013).

149. Ward, E. K. *et al.* The Effect of PPI Use on Human Gut Microbiota and Weight Loss in Patients Undergoing Laparoscopic Roux-en-Y Gastric Bypass. *Obes. Surg.* **24**, 1567–1571 (2014).

150. Damms-Machado, A. *et al.* Effects of Surgical and Dietary Weight Loss Therapy for Obesity on Gut Microbiota Composition and Nutrient Absorption. *Biomed Res. Int.* **2015**, 1–12 (2015).

151. Palleja, A. *et al.* Roux-en-Y gastric bypass surgery of morbidly obese patients induces swift and persistent changes of the individual gut microbiota. *Genome Med.* **8**, 67 (2016).

152. Murphy, R. *et al.* Differential Changes in Gut Microbiota After Gastric Bypass and Sleeve Gastrectomy Bariatric Surgery Vary According to Diabetes Remission. *Obes. Surg.* **27**, 917–925 (2017).

153. Ilhan, Z. E. *et al.* Distinctive microbiomes and metabolites linked with weight loss after gastric bypass, but not gastric banding. *ISME J.* **11**, 2047–2058 (2017).

154. Sanmiguel, C. P. *et al.* Surgically Induced Changes in Gut Microbiome and Hedonic Eating as Related to Weight Loss. *Psychosom. Med.* **79**, 880–887 (2017).

155. Patil, D. P. *et al.* Molecular analysis of gut microbiota in obesity among Indian individuals. *J. Biosci.* **37**, 647–657 (2012).

156. Liu, R. *et al.* Gut microbiome and serum metabolome alterations in obesity and after weight-loss intervention. *Nat. Med.* **23**, 859–868 (2017).

157. Cortez, R. V. *et al.* Shifts in intestinal microbiota after duodenal exclusion favor glycemic control and weight loss: a randomized controlled trial. *Surg. Obes. Relat. Dis.* **14**, 1748–1754 (2018).

158. Chen, H. *et al.* Change in gut microbiota is correlated with alterations in the surface molecule expression of monocytes after roux-en-Y gastric bypass surgery in obese type 2 diabetic patients. *Am. J. Transl. Res.* **9**, 1243–1254 (2017).

159. Medina, D. A. *et al.* Distinct patterns in the gut microbiota after surgical or medical therapy in obese patients. *PeerJ* **2017**, (2017).

160. Kumar, R. *et al.* New microbe genomic variants in patients fecal community following surgical disruption of the upper human gastrointestinal tract. *Hum. Microbiome J.* **10**, 37–42 (2018).

161. Kikuchi, R. *et al.* The Impact of Laparoscopic Sleeve Gastrectomy with Duodenojejunal Bypass on Intestinal Microbiota Differs from that of Laparoscopic Sleeve Gastrectomy in Japanese Patients with Obesity. *Clin. Drug Investig.* **38**, 545–552 (2018).

162. Aron-Wisnewsky, J. *et al.* Major microbiota dysbiosis in severe obesity: Fate after bariatric surgery. *Gut* **68**, 70–82 (2019).

163. Campisciano, G. *et al.* Gut microbiota characterisation in obese patients before and after

bariatric surgery. *Benef. Microbes* **9**, 367–373 (2018).

164. Magouliotis, D. E., Tasiopoulou, V. S., Sioka, E., Chatedaki, C. & Zacharoulis, D. Impact of Bariatric Surgery on Metabolic and Gut Microbiota Profile: a Systematic Review and Meta-analysis. *Obes. Surg.* **27**, 1345–1357 (2017).

165. Turnbaugh, P. J., Backhed, F., Fulton, L. & Gordon, J. I. Diet-Induced Obesity Is Linked to Marked but Reversible Alterations in the Mouse Distal Gut Microbiome. *Cell Host Microbe* **3**, 213–223 (2008).

166. Santacruz, A. *et al.* Interplay between weight loss and gut microbiota composition in overweight adolescents. *Obesity* **17**, 1906–1915 (2009).

167. Tanida, M. *et al.* High-fat diet-induced obesity is attenuated by probiotic strain Lactobacillus paracasei ST11 (NCC2461) in rats. *Obes. Res. Clin. Pract.* **2**, 159–169 (2008).

168. Kang, J.-H. *et al.* Anti-Obesity Effect of Lactobacillus gasseri BNR17 in High-Sucrose Diet-Induced Obese Mice. *PLoS One* **8**, e54617 (2013).

169. Ridaura, V. K. *et al.* Gut microbiota from twins discordant for obesity modulate metabolism in mice. *Science* **341**, 1241214 (2013).

170. Bäckhed, F. *et al.* The gut microbiota as an environmental factor that regulates fat storage. *Proc. Natl. Acad. Sci. U. S. A.* **101**, 15718–23 (2004).

171. Pedersen, H. K. *et al.* Human gut microbes impact host serum metabolome and insulin sensitivity. *Nature* **535**, 376–381 (2016).

172. Li, J. V *et al.* Metabolic surgery profoundly influences gut microbial-host metabolic cross-

talk. *Gut* **60**, 1214–23 (2011).

173. Wilson-Pérez, H. E. *et al.* The effect of vertical sleeve gastrectomy on food choice in rats. *Int. J. Obes.* **37**, 288–295 (2013).

174. Nicholson, J. K. & Lindon, J. C. Systems biology: Metabonomics. *Nature* **455**, 1054–1056 (2008).

175. Pan, Z. & Raftery, D. Comparing and combining NMR spectroscopy and mass spectrometry in metabolomics. *Anal. Bioanal. Chem.* **387**, 525–527 (2007).

176. Suhre, K. *et al.* Human metabolic individuality in biomedical and pharmaceutical research. *Nature* **477**, 54–60 (2011).

177. Wang, X. *et al.* Metabolomics Study on the Toxicity of Aconite Root and Its Processed Products Using Ultraperformance Liquid-Chromatography/Electrospray-Ionization Synapt High-Definition Mass Spectrometry Coupled with Pattern Recognition Approach and Ingenuity Pathways Analysis. *J. Proteome Res.* **11**, 1284–1301 (2012).

178. Abu Bakar, M. H. *et al.* Metabolomics – the complementary field in systems biology: a review on obesity and type 2 diabetes. *Mol. Biosyst.* **11**, 1742–1774 (2015).

179. Zhang, A., Sun, H. & Wang, X. Serum metabolomics as a novel diagnostic approach for disease: a systematic review. *Anal. Bioanal. Chem.* **404**, 1239–1245 (2012).

180. Zhang, A., Sun, H., Wang, P., Han, Y. & Wang, X. Modern analytical techniques in metabolomics analysis. *Analyst* **137**, 293–300 (2012).

181. Pang, Z. *et al.* MetaboAnalyst 5.0: narrowing the gap between raw spectra and functional insights. *Nucleic Acids Res.* **49**, 388–396 (2021).

182. Chong, J., Liu, P., Zhou, G. & Xia, J. Using MicrobiomeAnalyst for comprehensive statistical, functional, and meta-analysis of microbiome data. *Nat. Protoc.* **15**, 799–821 (2020).

183. Ni, Y. *et al.* M2IA: A web server for microbiome and metabolome integrative analysis. *Bioinformatics* **36**, 3493–3498 (2020).

184. Delzenne, N. M., Neyrinck, A. M., Bäckhed, F. & Cani, P. D. Targeting gut microbiota in obesity: effects of prebiotics and probiotics. *Nat. Rev. Endocrinol.* **7**, 639–646 (2011).

185. Roberfroid, M. *et al.* Prebiotic effects: metabolic and health benefits. *Br. J. Nutr.* **104**, S1–S63 (2010).

186. Schwiertz, A. *et al.* Microbiota and SCFA in lean and overweight healthy subjects. *Obesity* **18**, 190–195 (2010).

187. Dewulf, E. M. *et al.* Inulin-type fructans with prebiotic properties counteract GPR43 overexpression and PPARγ-related adipogenesis in the white adipose tissue of high-fat diet-fed mice. *J. Nutr. Biochem.* **22**, 712–722 (2011).

188. Cani, P. D., Dewever, C. & Delzenne, N. M. Inulin-type fructans modulate gastrointestinal peptides involved in appetite regulation (glucagon-like peptide-1 and ghrelin) in rats. *Br. J. Nutr.* **92**, 521 (2004).

189. Dewulf, E. M. *et al.* Insight into the prebiotic concept: lessons from an exploratory, double blind intervention study with inulin-type fructans in obese women. *Gut* **62**, 1112–21 (2013).

190. Andreasen, A. S. *et al.* Effects of Lactobacillus acidophilus NCFM on insulin sensitivity

and the systemic inflammatory response in human subjects. *Br. J. Nutr.* **104**, 1831–1838 (2010).

191. Kadooka, Y. *et al.* Regulation of abdominal adiposity by probiotics (Lactobacillus gasseri SBT2055) in adults with obese tendencies in a randomized controlled trial. *Eur. J. Clin. Nutr.* **64**, 636–643 (2010).

192. Borgeraas, H., Johnson, L. K., Skattebu, J., Hertel, J. K. & Hjelmesaeth, J. Effects of probiotics on body weight, body mass index, fat mass and fat percentage in subjects with overweight or obesity: a systematic review and meta-analysis of randomized controlled trials. *Obes. Rev.* (2017) doi:10.1111/obr.12626.

193. Vrieze, A. *et al.* Transfer of intestinal microbiota from lean donors increases insulin sensitivity in individuals with metabolic syndrome. *Gastroenterology* **143**, 913-916.e7 (2012).

194. Kootte, R. S. *et al.* Improvement of Insulin Sensitivity after Lean Donor Feces in Metabolic Syndrome Is Driven by Baseline Intestinal Microbiota Composition. *Cell Metab.* **26**, 611-619.e6 (2017).

195. Ardestani, A., Rhoads, D. & Tavakkoli, A. Insulin cessation and diabetes remission after bariatric surgery in adults with insulin-treated type 2 diabetes. *Diabetes Care* **38**, 659–664 (2015).

196. Casella, G. *et al.* Ten-year duration of type 2 diabetes as prognostic factor for remission after sleeve gastrectomy. *Surg. Obes. Relat. Dis.* **7**, 697–702 (2011).

197. Panunzi, S., De Gaetano, A., Carnicelli, A. & Mingrone, G. Predictors of Remission of

Diabetes Mellitus in Severely Obese Individuals Undergoing Bariatric Surgery. *Ann. Surg.* **261**, 459–467 (2015).

198. Edelman, S. *et al.* Control of type 2 diabetes after 1 year of laparoscopic adjustable gastric banding in the helping evaluate reduction in obesity (HERO) study. *Diabetes, Obes. Metab.* **16**, 1009–1015 (2014).

199. Mingrone, G. *et al.* Metabolic surgery versus conventional medical therapy in patients with type 2 diabetes: 10-year follow-up of an open-label, single-centre, randomised controlled trial. *Lancet* **397**, 293–304 (2021).

200. Thaler, J. P. & Cummings, D. E. Minireview: Hormonal and metabolic mechanisms of diabetes remission after gastrointestinal surgery. *Endocrinology* **150**, 2518–2525 (2009).

201. Arapis, K. *et al.* Remodeling of the residual gastric mucosa after Roux-en-Y gastric bypass or vertical sleeve gastrectomy in diet-induced obese rats. *PLoS One* **10**, e0121414 (2015).

202. Bruinsma, B. G., Uygun, K., Yarmush, M. L. & Saeidi, N. Surgical models of Roux-en-Y gastric bypass surgery and sleeve gastrectomy in rats and mice. *Nat. Protoc.* **10**, 495–507 (2015).

203. Bueter, M. *et al.* Roux-en-Y Gastric Bypass Operation in Rats Protocol. 1–7 (2012) doi:10.3791/3940.

204. Stevenson, M., Lee, J., Lau, R. G., Brathwaite, C. E. M. & Ragolia, L. Surgical Mouse Models of Vertical Sleeve Gastrectomy and Roux-en Y Gastric Bypass : a Review. *Obes. Surg.* (2019) doi:10.1007/s11695-019-04205-8.

205. Hao, Z. *et al.* Reprogramming of defended body weight after Roux-En-Y gastric bypass surgery in diet-induced obese mice. *Obesity* **24**, 654–660 (2016).

206. McErlane, S. Adult Rodent Anesthesia SOP. *UBC Animal Care Guidelines* https://animalcare.ubc.ca/sites/default/files/documents/ACC-01-2017 Rodent Anesthesia.pdf (2017).

207. Sotocinal, S. G. *et al.* The Rat Grimace Scale : A partially automated method for quantifying pain in the laboratory rat via facial expressions. 1–10 (2011).

208. Arora, T. *et al.* Microbial regulation of the L cell transcriptome. *Sci. Rep.* **8**, 1–9 (2018).

209. Sweeney, T. E. & Morton, J. M. Metabolic surgery: Action via hormonal milieu changes, changes in bile acids or gut microbiota? A summary of the literature. *Best Pract. Res. Clin. Gastroenterol.* **28**, 727–740 (2014).

210. Thomas, C. *et al.* TGR5-Mediated Bile Acid Sensing Controls Glucose Homeostasis. *Cell Metab.* **10**, 167–177 (2009).

211. Schaap, F. G., Trauner, M. & Jansen, P. L. M. Bile acid receptors as targets for drug development. *Nat. Rev. Gastroenterol. Hepatol.* **11**, 55–67 (2013).

212. Li, J. V. *et al.* Experimental bariatric surgery in rats generates a cytotoxic chemical environment in the gut contents. *Front. Microbiol.* **2**, 1–9 (2011).

213. Osto, M. *et al.* Roux-en-Y gastric bypass surgery in rats alters gut microbiota profile along the intestine. *Physiol. Behav.* **119**, 92–96 (2013).

214. Chambers, A. P. *et al.* Weight-independent changes in blood glucose homeostasis after gastric bypass or vertical sleeve gastrectomy in rats. *Gastroenterology* **141**, 950–958

(2011).

215. Duboc, H. *et al.* Roux-en-Y Gastric-Bypass and sleeve gastrectomy induces specific shifts of the gut microbiota without altering the metabolism of bile acids in the intestinal lumen. *Int. J. Obes.* 1–4 (2018) doi:10.1038/s41366-018-0015-3.

216. NYU Langone Medical Center. Tisse preparation and cryopreservation with sucrose for frozen tissue sections. https://med.nyu.edu/research/scientific-cores-shared-resources/sites/default/files/frozen-tissue-preparation-with-sucrose.pdf.

217. Abcam. Immunocytochemistry and immunofluorescence protocol. *Abcam* 1–6 (1998).

218. Callahan, B. J. *et al.* DADA2: High-resolution sample inference from Illumina amplicon data. *Nat. Methods* **13**, 581–583 (2016).

219. McMurdie, P. J. & Holmes, S. Phyloseq: An R Package for Reproducible Interactive Analysis and Graphics of Microbiome Census Data. *PLoS One* **8**, (2013).

220. Le Roux, C. W. *et al.* Gut hypertrophy after gastric bypass is associated with increased glucagon-like peptide 2 and intestinal crypt cell proliferation. *Ann. Surg.* **252**, 50–56 (2010).

221. Dudrick, S. J., Daly, J. M., Castro, G. & Akhtar, M. Gastrointestinal adaptation following small bowel bypass for obesity. *Ann. Surg.* **185**, 642 (1977).

222. Hansen, C. F. *et al.* The effect of ileal interposition surgery on enteroendocrine cell numbers in the UC Davis type 2 diabetes mellitus rat. *Regul. Pept.* **189**, 31–39 (2014).

223. Awad, W. A., Ghareeb, K. & Böhm, J. Effect of addition of a probiotic micro-organism to broiler diet on intestinal mucosal architecture and electrophysiological parameters. *J.*

Anim. Physiol. Anim. Nutr. (Berl). **94**, 486–494 (2010).

224. Simonen, M. *et al.* Conjugated bile acids associate with altered rates of glucose and lipid oxidation after Roux-en-Y gastric bypass. *Obes. Surg.* **22**, 1473–1480 (2012).

225. Patti, M. E. *et al.* Serum bile acids are higher in humans with prior gastric bypass: Potential contribution to improved glucose and lipid metabolism. *Obesity* **17**, 1671–1677 (2009).

226. Kohli, R. *et al.* Weight loss induced by Roux-en-Y gastric bypass but not laparoscopic adjustable gastric banding increases circulating bile acids. *J. Clin. Endocrinol. Metab.* **98**, 6–10 (2013).

227. Bhutta, H. Y. *et al.* Effect of Roux-en-Y gastric bypass surgery on bile acid metabolism in normal and obese diabetic rats. *PLoS One* **10**, 1–17 (2015).

228. Kohli, R. *et al.* Intestinal adaptation after ileal interposition surgery increases bile acid recycling and protects against obesity-related comorbidities. *Am. J. Physiol. - Gastrointest. Liver Physiol.* **299**, 652–660 (2010).

229. Smith, C. D. *et al.* Gastric acid secretion and vitamin B12 absorption after vertical Roux-en-Y gastric bypass for morbid obesity. *Ann. Surg.* **218**, 91–6 (1993).

230. Engevik, M. A., Hickerson, A., Shull, G. E. & Worrell, R. T. Acidic conditions in the NHE2 -/- mouse intestine result in an altered mucosa-associated bacterial population with changes in mucus oligosaccharides. *Cell. Physiol. Biochem.* **32**, 111–128 (2013).

231. Celiker, H. A new proposed mechanism of action for gastric bypass surgery: Air hypothesis. *Med. Hypotheses* **107**, 81–89 (2017).

232. Albenberg, L. *et al.* Correlation between intraluminal oxygen gradient and radial partitioning of intestinal microbiota. *Gastroenterology* **147**, 1055-1063.e8 (2014).

233. Liong, M. T. & Shah, N. P. Bile salt deconjugation ability, bile salt hydrolase activity and cholesterol co-precipitation ability of lactobacilli strains. *Int. Dairy J.* **15**, 391–398 (2005).

234. Urdaneta, V. & Casadesús, J. Interactions between bacteria and bile salts in the gastrointestinal and hepatobiliary tracts. *Front. Med.* **4**, 1–13 (2017).

235. Yadav, H., Jain, S. & Sinha, P. R. Oral administration of dahi containing probiotic Lactobacillus acidophilus and Lactobacillus casei delayed the progression of streptozotocin-induced diabetes in rats. *J. Dairy Res.* **75**, 189–195 (2008).

236. Wickens, K. L. *et al.* Early pregnancy probiotic supplementation with Lactobacillus rhamnosus HN001 may reduce the prevalence of gestational diabetes mellitus: A randomised controlled trial. *Br. J. Nutr.* **117**, 804–813 (2017).

237. Foley, M. H. *et al.* Lactobacillus bile salt hydrolase substrate specificity governs bacterial fitness and host colonization. *Proc. Natl. Acad. Sci. U. S. A.* **118**, (2021).

238. Dao, M. C. *et al.* Akkermansia muciniphila abundance is lower in severe obesity, but its increased level after bariatric surgery is not associated with metabolic health improvement. *Am. J. Physiol. Endocrinol. Metab.* **317**, E446–E459 (2019).

239. Yan, M., Song, M.-M., Bai, R.-X., Cheng, S. & Yan, W.-M. Effect of Roux-en-Y gastric bypass surgery on intestinal Akkermansia muciniphila . *World J. Gastrointest. Surg.* **8**, 301 (2016).

240. Zhou, K. Strategies to promote abundance of Akkermansia muciniphila, an emerging

probiotics in the gut, evidence from dietary intervention studies. *J. Funct. Foods* **33**, 194–201 (2017).

241. Roopchand, D. E. *et al.* Dietary polyphenols promote growth of the gut bacterium akkermansia muciniphila and attenuate high-fat diet-induced metabolic syndrome. *Diabetes* **64**, 2847–2858 (2015).

242. Buchwald, H. & Oien, D. M. Metabolic / Bariatric Surgery Worldwide 2011. 427–436 (2013) doi:10.1007/s11695-012-0864-0.

243. Kelly, T., Yang, W., Chen, C., Reynolds, K. & He, J. Global burden of obesity in 2005 and projections to 2030. 1431–1437 (2008) doi:10.1038/ijo.2008.102.

244. Wilding, J. P. H. *et al.* Once-Weekly Semaglutide in Adults with Overweight or Obesity. *N. Engl. J. Med.* **384**, 989–1002 (2021).

245. Welbourn, R. *et al.* Bariatric Surgery Worldwide: Baseline Demographic Description and One-Year Outcomes from the Fourth IFSO Global Registry Report 2018. *Obes. Surg.* **29**, 782–795 (2019).

246. Mocanu, V. *et al.* Fecal microbial transplantation and fiber supplementation in patients with severe obesity and metabolic syndrome: a randomized double-blind, placebo-controlled phase 2 trial. *Nat. Med.* **27**, 1272–1279 (2021).

247. University of Oxford. HOMA2 Calculator. https://www.dtu.ox.ac.uk/homacalculator/.

248. Wemheuer, F. *et al.* Tax4Fun2: Prediction of habitat-specific functional profiles and functional redundancy based on 16S rRNA gene sequences. *Environ. Microbiomes* **15**, 1–12 (2020).

249. Vester-Andersen, M. K. *et al.* Increased abundance of proteobacteria in aggressive Crohn's disease seven years after diagnosis. *Sci. Rep.* **9**, 1–10 (2019).

250. Guo, Y., Liu, C. Q., Liu, G. P., Huang, Z. P. & Zou, D. J. Roux-en-Y gastric bypass decreases endotoxemia and inflammatory stress in association with improvements in gut permeability in obese diabetic rats. *J. Diabetes* **11**, 786–793 (2019).

251. Ferrara, P. J. *et al.* Lysophospholipid acylation modulates plasma membrane lipid organization and insulin sensitivity in skeletal muscle. *J. Clin. Invest.* **131**, (2021).

252. Zeng, Q. *et al.* Discrepant gut microbiota markers for the classification of obesity-related metabolic abnormalities. *Sci. Rep.* **9**, 1–10 (2019).

253. Vazquez-Moreno, M. *et al.* Association of gut microbiome with fasting triglycerides, fasting insulin and obesity status in Mexican children. *Pediatr. Obes.* **16**, (2021).

254. Cui, H. *et al.* Da-Chai-Hu Decoction Ameliorates High Fat Diet-Induced Nonalcoholic Fatty Liver Disease Through Remodeling the Gut Microbiota and Modulating the Serum Metabolism. *Front. Pharmacol.* **11**, 1–17 (2020).

255. Kasai, C. *et al.* Comparison of the gut microbiota composition between obese and non-obese individuals in a Japanese population, as analyzed by terminal restriction fragment length polymorphism and next-generation sequencing. *BMC Gastroenterol.* **15**, 1–10 (2015).

256. Tims, S. *et al.* Microbiota conservation and BMI signatures in adult monozygotic twins. *ISME J.* **7**, 707–717 (2013).

257. Sheppard, K. *et al.* From one amino acid to another: tRNA-dependent amino acid

biosynthesis. *Nucleic Acids Res.* **36**, 1813–1825 (2008).

258. Abbott, J. A., Francklyn, C. S. & Robey-Bond, S. M. Transfer RNA and human disease. *Front. Genet.* **5**, 1–18 (2014).

259. Wei, F. *et al.* Deficit of tRNA Lys modification by Cdkal1 causes the development of type 2 diabetes in mice Find the latest version : Deficit of tRNA Lys modification by Cdkal1 causes the development of type 2 diabetes in mice. *J Clin Invest* **121**, 3598–3608 (2011).

260. Wei, F. Y. & Tomizawa, K. Functional loss of Cdkal1, a novel tRNA modification enzyme, causes the development of type 2 diabetes. *Endocr. J.* **58**, 819–825 (2011).

261. Palmer, C. J. *et al.* Cdkal1, a type 2 diabetes susceptibility gene, regulates mitochondrial function in adipose tissue. *Mol. Metab.* **6**, 1212–1225 (2017).

262. Wang, M. *et al.* A deafness-and diabetes-associated tRNA Mutation causes deficient pseudouridinylation at position 55 in tRNAGlu and mitochondrial dysfunction. *J. Biol. Chem.* **291**, 21029–21041 (2016).

263. Igoillo-Esteve, M. *et al.* tRNA Methyltransferase Homolog Gene TRMT10A Mutation in Young Onset Diabetes and Primary Microcephaly in Humans. *PLoS Genet.* **9**, (2013).

264. Yu, Y. C., Han, J. M. & Kim, S. Aminoacyl-tRNA Synthetases and amino acid signaling. *Biochim. Biophys. Acta (BBA)-Molecular Cell Res.* 118889 (2020).

265. Shao, Y. *et al.* Alterations of Gut Microbiota After Roux-en-Y Gastric Bypass and Sleeve Gastrectomy in Sprague-Dawley Rats. *Obes. Surg.* **27**, 295–302 (2017).

266. Sui, J. *et al.* Sphingolipid metabolism in type 2 diabetes and associated cardiovascular complications. *Exp. Ther. Med.* 3603–3614 (2019) doi:10.3892/etm.2019.7981.

267. Khan, S. R. *et al.* Diminished Sphingolipid Metabolism, a Hallmark of Future Type 2 Diabetes Pathogenesis, Is Linked to Pancreatic β Cell Dysfunction. *iScience* **23**, (2020).

268. Barczynska, R. *et al.* The effect of dietary fibre preparations from potato starch on the growth and activity of bacterial strains belonging to the phyla Firmicutes, Bacteroidetes, and Actinobacteria. *J. Funct. Foods* **19**, 661–668 (2015).

269. Vesper, H. *et al.* Sphingolipids in Food and the Emerging Importance of Sphingolipids to Nutrition. *J. Nutr.* **130**, (2000).

270. Durainayagam, B. *et al.* Impact of a High Protein Intake on the Plasma Metabolome in Elderly Males: 10 Week Randomized Dietary Intervention. *Front. Nutr.* **6**, 1–13 (2019).

271. Weiland, A., Bub, A., Barth, S. W., Schrezenmeir, J. & Pfeuffer, M. Effects of dietary milk- and soya-phospholipids on lipid-parameters and other risk indicators for cardiovascular diseases in overweight or obese men – Two double-blind, randomised, controlled, clinical trials. *J. Nutr. Sci.* **5**, 1–9 (2016).

272. Zorrilla-Nunez, L. F. *et al.* The importance of the biliopancreatic limb length in gastric bypass: A systematic review. *Surg. Obes. Relat. Dis.* **15**, 43–49 (2019).